THE PLATELET STORAGE LESION - NOVEL APPROACHES TO OPTIMISE THE FUNCTION AND QUALITY OF STORED PLATELET CONCENTRATES

BY

JAMIE NASH

A THESIS SUBMITTED FOR THE DEGREE
DOCTOR OF PHILOSOPHY

CARDIFF SCHOOL OF SPORT AND HEALTH SCIENCES
CARDIFF METROPOLITAN UNIVERSITY
2022

II - Acknowledgements

Firstly, I would like to thank my supervisors, Prof Philip James, Ms Amanda Davies, Dr Christine Saunders, and Mrs Chloe George. Your support in setting up the PhD project, and your guidance and support throughout the PhD in both laboratory-based and writing skills have helped shape me into the scientist I am today. Thanks to Gareth Walters and Paul Jones for your hands-on advice and for dealing with my special requests and setups for some interesting novel studies.

I would like to thank the friends I have made in both the PhD office in Llandaff and the laboratory group within the biomedical science department. To Cass Whelan, thanks for putting up with me for the best part of 4 years, working things out together and de-stressing in Kong's on the regular. To Jess Williams, thank you for guiding me through the laboratory and to help shape my academic writing, even if you were a little brutal. Enjoyed our lunch club and numerous rants, which have got me through the PhD process.

A special thanks to Mum and Dad for your encouragement and support through the highs and the lows and for never letting me throw in the towel. Your support for me from such a young age to pursue a career in science is a major reason why and how I am here today.

To all my pals, thanks for helping me through this with copious amounts of booze. To Stacey, thank you for dealing with constant moaning and for the many meals out. To Charlie and Mike, the 10 from Len banter has got me through a lot over the past 3 years, thank you.

Figures within this thesis were created using Servier Medical Art, licensed under a Creative Commons Attribution 3.0 Unported License. Knowledge Economy Skills Scholarships (KESS 2) funded the PhD. KESS 2 is a pan-Wales higher-level skills initiative led by Bangor University on behalf of the HE sectors in Wales. It is part funded by the Welsh Government's European Social Fund (ESF) convergence programme for West Wales and the Valleys.

III - Abbreviations

^{15}NPDT	4-oxo-2,2,6,6-tetramethylpiperidine-d~6-1-oxyl
a2	a2-antiplasmin
AA	Arachidonic acid
ADP	Adenosine diphosphate
ALIX	Programmed cell death 6-interacting protein
APC	Allophycocyanin
APPT	Activated partial prothrombin time
aSMase	Acid sphingomyelinase
ATP	Adenosine triphosphate
AUC	Area under the curve
BC	Buffy coat
Ca^{2+}	Calcium
cAMP	Cyclic adenosine monophosphate
CCI	Correct count increment
CD	Cluster of Differentiation
CD144	VE-cadherin
CD41	GPIIb/IIIa
CD62P	P-selectin
CO_2	Carbon dioxide
CRP	C-reactive protein
CS	Cold Storage
CVD	Cardiovascular disease
DAMPs	Damage-associated molecular patterns
DEHP	Di-2-ethylhexyl phathalate
DNA	Deoxyribonucleic acid
DPBS	Dulbecco's phosphate buffered saline
EDTA	Ethylenediaminetetraacetic acid
EM	Electron microscopy
EPR	Electron paramagnetic resonance
ESC	Extent of shape change
ESCRT 0-III	Endosomal sorting complex required for transport 0-III
EVs	Extracellular vesicles
FBC	Full blood count
FDA	Food and Drug administration
FDP	Fibrin degradation products
Fig	Figure
FITC	Fluorescein isothiocyanate
FSC	Forward scatter
FVa	Factor 5 (activated)
FVII	Factor VII
FX	Factor X
FXI	Factor XI
FXII	Factor XII

FXIIIa	Factor XIII (activated)
g	Centrifugal force
GP	Glycoprotein
GPIbα	Glycoprotein Ibα
GPVI	Glycoprotein VI
Hb	Haemoglobin
HCT	Haematocrit
HSCs	Haematopoietic stem cells
HSR	Hypertonic shock response
HUVEC	Human umbilical vein endothelial cells
ILVs	Intraluminal vesicles
IP_3	Inositol triphosphate
ISEV	International Society for extracellular vesicles
JEV	Journal of extracellular vesicles
LFQ	Label-free quantitation
MCH	Mean corpuscular haemoglobin
MCV	Mean corpuscular volume
MEA	Multiple electrode aggregometry
MISEV	Minimal information for studies of extracellular vesicles
mRNA	Messenger ribonucleic acid
mtDNA	Mitochondrial DNA
MVBs	Multivesicular bodies
NAD	Nicotinamide adenine dinucleotide
NADH	Nicotinamide adenine dinucleotide + Hydrogen
NSF	N-ethylmaleimide-sensitive fusion
NTA	Nanoparticle tracking analysis
O_2	Oxygen
$[O_2]$	Oxygen concentration
OCR	Oxygen consumption rate
ORAC	Oxygen radical absorbance capacity
OS	Oxidative stress
PAI-1	Plasminogen activator inhibitor 1
PAR	Protease activated receptors
PAS	Platelet additive solution
PBS	Phosphate buffered saline
PC	Platelet concentrate
PE	Phycoerythrin
PECAM1	Platelet endothelial cell adhesion molecule
PEV	Platelet extracellular vesicle
PF4	Platelet factor 4
PLTs	Platelets
PO	Polyolefin
PO_2	Partial pressure of oxygen
PPP	Platelet Poor Plasma
PRP	Platelet rich plasma
PS	Phosphatidylserine
PSL	Platelet storage lesion
PT	Prothrombin time

PTE	Polyethene
PVC	Polyvinyl chloride
QC	Quality Control
RBC	Red blood cell
RDW	Red cell distribution width
RNA	Ribonucleic acid
ROS	Reactive oxygen species
RT	Room temperature
SaBTO	Safety of Blood, Tissues and Organs
SD	Standard deviation
SEC	Size exclusion chromatography
SNARE	Soluble NSF attachment protein receptor
SSC	Side scatter
TAFIa	Thrombin activatable fibrinolysis inhibitor
TBST	Tri-buffered saline-tween
TEM	Tetraspanin-enriched microdomains
TF	Tissue factor
TFPI	Tissue factor pathway inhibitor
tPA	Tissue plasminogen activator
TRALI	Transfusion-related acute lung injury
TRAP-6	Thrombin receptor activator protein 6
TSG101	Tumour susceptibility gene 101
TxA2	Thromboxane A2
VAMP7	Vesicle associated membrane protein 7
vWF	von Willebrand Factor
WAS	Wiskott-Aldrich syndrome
WB	Whole blood
WBCs	White blood cells
WBS	Welsh Blood Service

IV – Publications, Presentations and Prizes

Publications

1. A Two-Phase, Single Cohort Study of COVID-19 Antibody Sera-Surveillance. JO Williams; L Watkeys; J Nash; C Whelan; AJ Davies; J Evans; KM Morris; PE James. Journal: Annals of Epidemiology and Public health, 2021. https://meddocsonline.org/annals-of-epidemiology-and-public-health/a-two-phase-single-cohort-study-of-COVID-19-antibody-sera-surveillance.pdf

2. Williams J.O., Whelan C., Nash J., James P.E. (2022) Extracellular Vesicles in Atherosclerosis Research. In: Ramji D. (eds) Atherosclerosis. Methods in Molecular Biology, vol 2419. Humana, New York, NY. https://doi.org/10.1007/978-1-0716-1924-7_22. Used in Chapter 2.6.

Presentations and Prizes

1. May 2019 – 2nd Place Poster Prize "Addressing the Platelet Storage Lesion – New Approaches to Optimising Storage and Function of Donated Platelets". Cardiff Metropolitan University Post Graduate Researchers conference

2. May 2019 – Oral Presentation "Addressing the Platelet Storage Lesion – New Approaches to Optimising Storage and Function of Donated" at Annual School of Health Conference at Cardiff Metropolitan University

3. December 2019 – Invited speaker at British Blood Transfusion Conference "Platelet Storage – Putting biology to the Test". Abstract published in Transfusion Medicine, DOI- 10.1111/tme.12635

4. July 2020 – Poster Presentation "The effects of platelet concentrate storage time on extracellular vesicle interactions associated with fibrin clot formation in-vitro" at International society of extracellular vesicles (online due to COVID-19). Abstract published in Journal of Extracellular Vesicles, DOI - 10.1080/20013078.2020.1784511, Abstract number PF09.03.

5. March 2022 - 28th Scott Murphy Memorial Award Lectureship awarded by The Biomedical Excellence for Safer Transfusion (BEST) Collaborative; lecture entitled "The understated importance of extracellular vesicles in cold-stored platelet concentrates" – Data from chapter 4

V – Abstract

Routinely, Platelet Concentrates (PC) are stored at 22±2^{o}C, constantly agitated, for up to 7 days with constant bacterial monitoring. Storage conditions stemmed from historical studies and have not differed substantially, despite advances in knowledge and technology. Extracellular vesicles (EVs) are small membrane bound vesicles released from all cells and their roles include cell-to-cell communication. EVs are present within PC, however their actions and roles upon reinfusion is unknown. The aim of this thesis was to assess EVs within PC storage and to optimise the external storage environment to improve platelet function and quality overtime, with the potential to increase storage duration. For this purpose, use of cold storage (4±2^{o}C) and differential oxygen environments were investigated. EVs extracted from PC were characterised using Nanosight tracking analysis and flow cytometry. Direct measurements of oxygen concentration within the storage container and oxygen consumption of platelets was assessed by electron paramagnetic resonance oximetry. Impedance platelet aggregometry was used to assess platelet function. Results from cold storage indicated that platelet aggregometry was not significantly improved compared to conventional storage, however a significant increase in pro-coagulant EV numbers was observed during cold storage which could result in a shortened bleeding time if transfused. A significant finding was oxygen availability in the bag was limited even when incubated at 21% oxygen under standard conditions. Applying the direct measurements made to a mathematical model demonstrated large areas of hypoxia at a relatively short distance from the surface of the container. To address this, predicted by the model, two approaches were taken: reducing platelet concentration or increasing external oxygen concentration. Platelet quality was increased, although elevated oxygen levels gave rise to oxidative stress. This work has provided a new understanding of factors which limit PC storage and point the way forward to improving platelet quality.

Table of Contents

1.0 Introduction

1.1 Platelet Physiology

Platelets (PLTs) are small a-nucleated, discoid cells first discovered in 1882 by Giulio Bizzozero (1). The first description of PLT function involved microscopic observation of PLTs in blood, allowing the relationship between adhesion, aggregation, and fibrin clot formation to be determined. The primary function of PLTs is haemostasis whereby PLTs initiate blood clotting and the coagulation cascade. PLTs are generally inactive when circulating in the body and typically become activated when the vasculature is damaged, exposing the sub-endothelium and allowing PLT interaction with von Willebrand Factor (vWF) and collagen. PLT activation leads to PLT aggregation and thus the formation of a blood clot (2).

1.1.1 Primary Haemostasis

Upon vasculature injury, vWF is stretched under the shear flow stress which allows its binding site domain A1 to be exposed. A1 is the binding site for Glycoprotein Ibα (GPIbα) on the PLT surface in the GPIb-IX-V complex (3). Under normal conditions, un-activated vWF does not bind with high affinity to GP1bα, preventing random activation. vWF binding leads to anchoring of PLTs to collagen, known as PLT adhesion and is shown in Fig 1.1 (step 1) (4).

Activation of PLTs occurs through the interaction of collagen and glycoprotein VI (GPVI), whereby the glycine-proline-hydroxyproline sites on the collagen bind directly to GPVI on the PLT surface (5). Without GPVI and GPIb-XI-V, PLTs would not adhere nor activate (6). Strong binding to either collagen or vWF activates PLTs causing the release of both α-granules and dense granules. α-granules contain more vWF, P-selectin (CD62P) and PLT factor 4 (PF4), which further encourages activation and adhesion to the damaged endothelium. Dense granules contain adenosine diphosphate (ADP), serotonin and calcium (Ca^{2+}), leading to further activation and recruitment of PLTs (see Fig1.1, step 3) (7). Granule release can lead to activation of other PLTs through GPIIb/IIIa signalling. GPVI

activation leads to inositol trisphosphate (IP_3) signalling downstream of phospholipase C isoform B, releasing Ca^{2+} from storage and allowing Ca^{2+} to enter PLTs from the plasma by opening calcium channels. A rise in Ca^{2+} leads to expression of phosphatidylserine (PS) giving rise to a charged surface to the PLTs and inducing microparticle shedding (1.3.2.2), critical in coagulation (1.1.3). The binding of collagen leads to PLT shape change through actin-filament mechanisms in the cytoskeleton allowing the damaged endothelium to be repaired. PLTs interact with each other through the GPIIb/IIIa that binds to fibrinogen, which links two PLTs by fibrinogen-GPIIb/IIIa. vWF can also bind to this receptor (8). The vWF-GPIIb/IIIa complex can form a new surface for more PLTs to bind through GPIbα, leading to further anchoring of PLTs. Once the PLT "plug" is formed, collagen is no longer exposed and therefore can no longer activate PLTs. Primary haemostasis has been summarised in Fig 1.1.

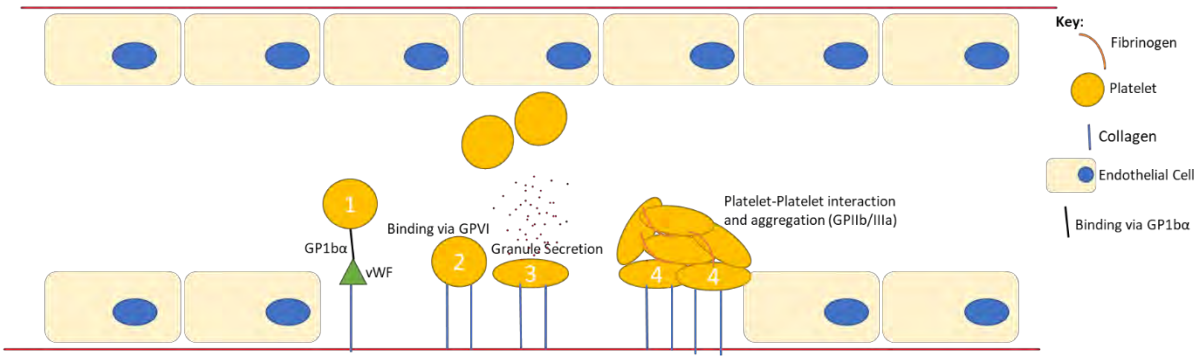

Figure 1.1 – **Primary haemostasis**. When the vasculature is injured, collagen is first exposed. 1 – vWF from the plasma and/or activated endothelial cells binds to the collagen. 2 – After adhesion, the receptor GPVI on the PLT binds to glycine-proline-hydroxyproline (GPO) sites on the exposed collagen. 3 – PLT activation leads a shape change and degranulation of α and dense granules. 4 – Activated PLTs aggregate together through GPIIb/IIIa, being linked together by fibrinogen. Diagram adapted from (9)

1.1.2 PLT Agonist Activation

Independent of collagen and vWF, PLT aggregation can occur through soluble agonists including ADP, thromboxane A2 (TxA2) and thrombin. These agonists can be released by activated PLTs (section 1.1.1). The main mechanism of agonist activation will cause an increase in Ca^{2+} concentration and activates specific downstream pathways (10). Thrombin is the strongest activator of PLTs and is responsible for converting fibrinogen to fibrin to stabilize the PLT "plug" (section 1.1.3)

(10). Thrombin specifically acts through protease activated receptors (PAR), PAR1 and PAR4. PAR1 is stimulated by low concentrations, whereby PAR4 is stimulated by a much higher concentration of thrombin, for example, as seen in cases of trauma (11).

ADP released from dense granules interacts with purinergic receptors known as P2Y1 and P2Y12 (12). Once activated, P2Y1 signalling causes reversible Ca^{2+} mediated shape changes due to cytoskeleton remodelling, compared to irreversible PLT activation caused by P2Y12 activation (12). Activation via this pathway leads to cyclic adenosine monophosphate (cAMP) inhibition and upregulation of Protein Kinase A which causes activation of GPIIb/IIIa. Daniel et al in 1998 showed that signalling through both P2Y1 and P2Y12 was required for the full activation of the PLTs (13). Deficiency in the P2Y12 receptor can lead to mild bleeding disorders and is the main target for anti-PLT drugs such as Clopidogrel (14), highlighting the importance of the P2Y12 pathway.

All activation pathways will converge upon the common functional upregulation of adhesion molecules (3, 11, 15). The most important as mentioned previously (section 1.1.1) is GPIIb/IIIa resulting in the cross-linking of fibrinogen. Fig 1.2 shows a summary of agonist activation. A full review on agonist activation is beyond the focus of this thesis and has been extensively reviewed elsewhere (16) .

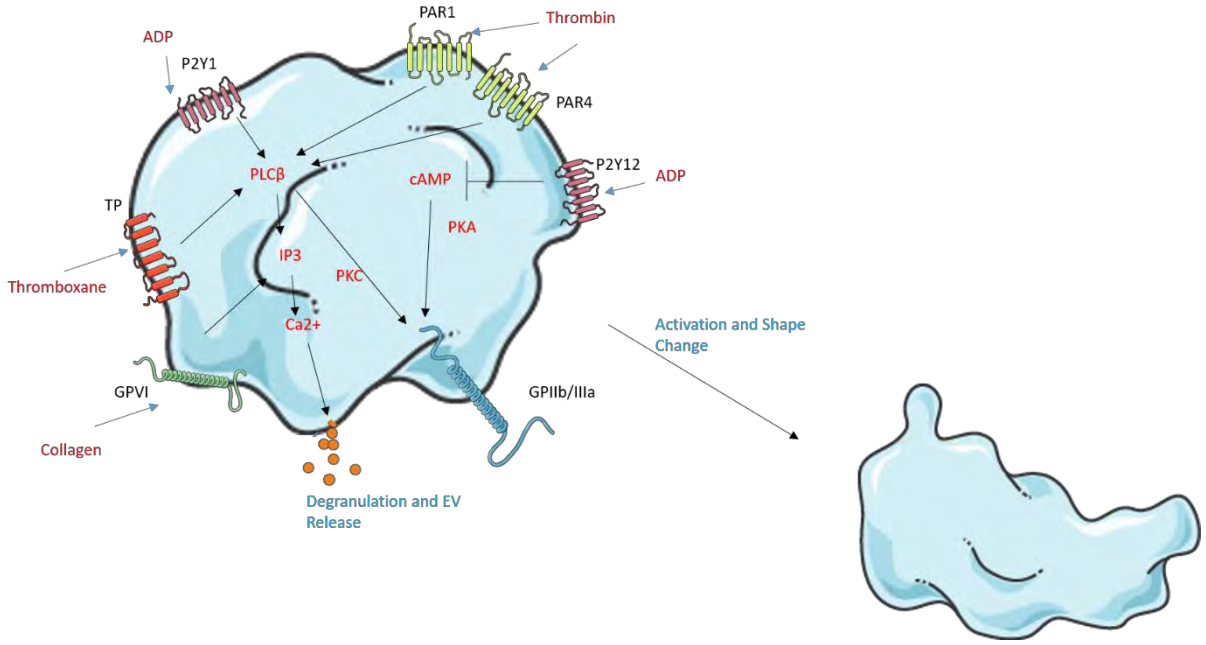

Figure 1.2 – **Agonist activation of PLTs.** PLT receptors include G-protein coupled receptors P2Y1, P2Y12, (Protease activating receptor 1 and 4) PAR1 and PAR4. Initial activation through the ADP receptor P2Y1 results in a reversible shape change and rise in cytosolic Ca^{2+}. If ADP activation occurs through P2Y12 along with P2Y1, full activation of PLTs occurs, decreasing cAMP production leading to an irreversible shape change. Signalling through the thromboxane receptor (TP) occurs in a PLCβ dependent manner. PAR1 and PAR4 receptors are responsible for thrombin based activation, also in a PLCβ dependent manner leading to irreversible PLT activation (17).

1.1.3 Secondary Haemostasis; the Coagulation Cascade

Secondary Haemostasis occurs rapidly after primary haemostasis and involves the "coagulation cascade". The cascade is a well-defined pathway that can be split into the intrinsic and extrinsic pathways, converging to a common pathway to cleave soluble fibrinogen into insoluble fibrin. The extrinsic pathway is activated by tissue factor (TF) which is released and expressed by sub-endothelial tissue. This release occurs at the site of endothelial damage. TF is the receptor for Factor VII (FVII) which leads to the formation of a TF-FVIIa complex, in turn activating factor X (FX) and the common pathway (18). Once activated, FXa along with the cofactor Factor V (FVa), form the prothrombinase complex that functions to cleave prothrombin to thrombin. Thrombin then cleaves fibrinogen to fibrin. Factor XIII (FXIIIa) then cross-links this fibrin, stabilizing the PLT thrombus, as seen in Fig 1.3 (19, 20).

The intrinsic pathway is activated by negatively charged interactions on the PLT surface due to PS expression, caused by an influx of Ca^{2+} into the PLT. The negative charge on the PLTs or collagen

from damaged endothelial cells activates factor XII (FXII) with high molecular weight kininogen. FXIIa then activates Factor XI (FXI), which with Ca^2, activates Factor IX (FIX). When thrombin is initially activated a positive feedback loop occurs, which also activates FVIII, which in turn forms a complex with FIXa. This complex goes on to activate FX, allowing the prothrombinase to be formed and amplification of the common pathway (21). This is summarised in Fig 1.3. The role of activated PLTs is critical to provide a catalytic surface for the assembly of enzyme complexes (22). When anionic phospholipid concentration reaches 30%, the activated PLTs accelerates two distinct reactions: activation of FX by FIXa; and activation of FII by FXa, by providing the surface for assembly (23).

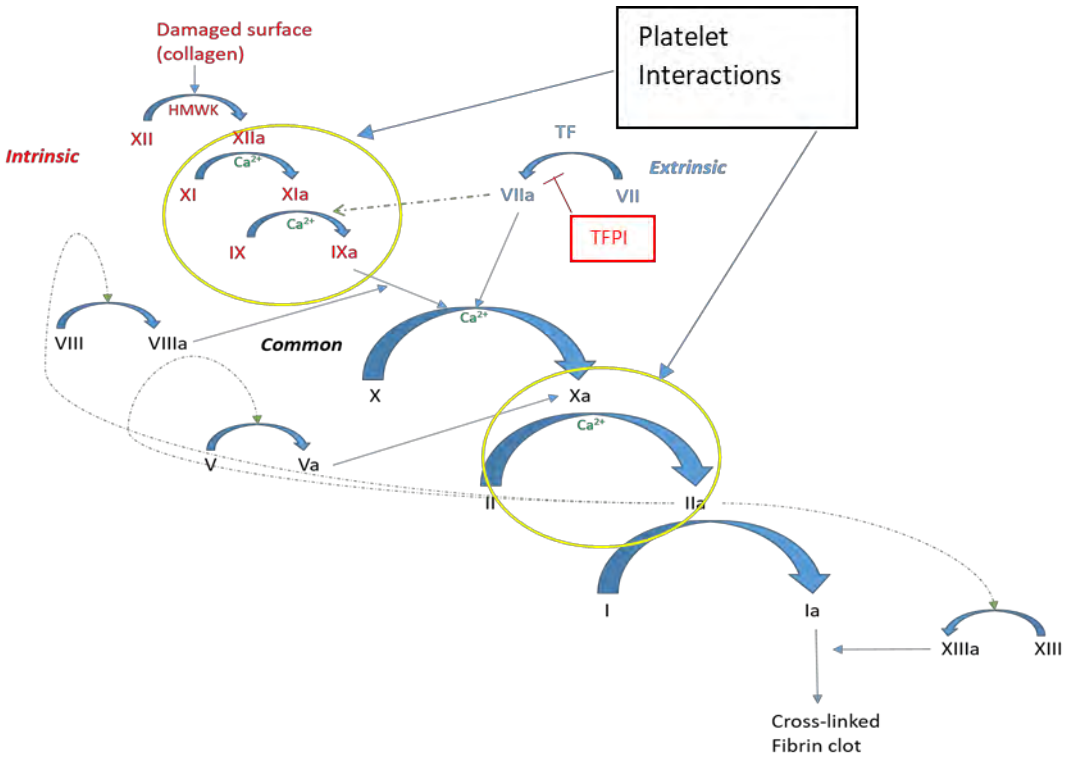

Figure 1.3 – **Coagulation Cascade.** A simplified version of the coagulation cascade involving the Intrinsic, Extrinsic and Common pathways. The green-dashed arrows represent positive feedback loops to continue generating sufficient thrombin and fibrin to produce a stable clot. HMWK-High molecular weight Kininogen. The yellow circle denotes where PLTs are crucial to the cascade. Tissue factor pathway inhibitor (TFPI) inhibits extrinsic coagulation. Diagram adapted from (21).

Inhibitors of coagulation play a major role in haemostasis, stopping random coagulation. The tissue factor pathway inhibitor (TFPI) regulates the initial extrinsic pathway that involves both TF and

FVIIa (Fig 1.3). Circulating TFPI is primarily synthesized by smooth muscle and endothelial cells, with approximately 10% of total TFPI present in PLTs (24). TFPI is found in both the free form (active – 20%) and lipoprotein bound form (inactive – 80%), with an average level in the healthy population of 70ng/mL, enough to maintain homeostasis (25). A detailed review of TFPI can be found in elsewhere (26). Another key anticoagulation mechanism is through the vitamin K dependant glycoproteins Protein C and Protein S, synthesized by the liver (27). In the presence of thrombin, protein C is activated on the endothelial surface. In combination with Protein S, Ca^{2+} and phospholipids from PLTs, activated Protein C inactivates membrane bound FVa and FVIIIa by cleaving arginine regions. A full review can be found elsewhere (28).

1.1.4 Fibrinolysis

A parallel regulatory system to secondary haemostasis known as fibrinolysis acts to stop exponential growth of the blood clot that could lead to downstream blockage. Fibrin is a substrate for the enzyme plasmin. Fibrinolysis is split into the generation of plasmin and the digestion and degradation of fibrin (29). Tissue plasminogen activator (tPA) is the most widely studied activator of plasminogen and is involved in intravascular fibrinolysis. tPA is synthesised by endothelial cells and is rapidly inhibited by a high concentration of plasminogen activator inhibitor 1 (PAI-1) leading to a short half-life of tPA of 4 to 6 minutes (30), briefly discussed in section 1.1.4.2. tPA binds to fibrin through the tPA finger domains with an alternating charge sequence of amino acids, while plasminogen binding relies on C-terminal lysines (31, 32). Binding of tPA to fibrin drastically reduces the effect of inhibitors on tPA activity. The activity of tPA is co-localized with plasminogen on the fibrin surface, forming a ternary complex allowing efficient plasmin generation (33). Increased plasmin production leads to increased levels of binding between fibrin C terminal lysines and plasminogen. It has been proposed that that a positive feedback mechanism known as the kringle domain in plasminogen, binds to fibrin, triggering a conformational change to expose lysine residues that allow tPA and other plasminogen activators to cleave plasminogen into plasmin (29).

The mechanism of fibrin degradation by plasmin is not fully understood. However, it is known that αC-domains within the fibrin molecule are a primary target for plasmin. Secondly, it is thought that E-D domains within the coiled fibrin molecule are cleaved (34). It has been reported that 25% of E-D domains need to be cleaved in order for efficient solubilisation of fibrin (35). Solubilisation is achieved by clustering of plasmin on fibrin molecules which has been demonstrated by atomic force microscopy (35).

1.1.4.1 Profibrinolytic properties of PLTs

PLTs contain tPA and plasminogen, which has been demonstrated in multiple studies (36-38). Plasminogen is released in the alpha granules when activated. Plasminogen can bind to PLTs, as PLTs provide a surface for fibrinolysis which can enhance the activation of plasminogen. This binding is mediated by C-terminal lysine residues (39). Studies mainly indicate that the interaction of PLTs with plasminogen is localised to fibrin that is bound to GPIIb/IIIa (40). When bound to PLTs, plasminogen goes through a conformational shape change allowing a higher affinity for cleavage to plasminogen by activators (41). Studies have shown that PLT-rich thrombi under physiological flow conditions accumulate plasminogen, which supports tPA induced fibrinolysis. Studies indicated that this accumulation was higher on PLTs with a high level of PS (42). PLTs along with the binding of plasminogen can enhance tPA's catalytic capabilities (43). Other profibrinolytic properties of PLTs are discussed elsewhere (44).

1.1.4.2 Inhibitors of Fibrinolysis

Important mechanisms exist to inhibit fibrinolysis and to prevent systemic activation of plasmin. The two most integral inhibitors are PAI1 and a2 antiplasmin (a2). Both inhibitors have a plasma concentration roughly equal to that of tPA (29). When plasmin is bound to fibrin, a2 inhibits at a much slower rate, due to the protection of the C-terminal lysines, allowing plasmin to carry out its function before inhibited (45).

Once a clot has formed thrombin activatable fibrinolysis inhibitor (TAFIa) can inhibit fibrinolysis. In its inactive zymogen form, TAFI circulates until activated by thrombin or

thrombomodulin. It then cleaves the C terminal lysine in fibrin, therefore stopping the binding of plasminogen. TAFIa effects the binding of both plasmin and plasminogen and but has no known effect on the binding of tPA (45, 46). Fibrinolysis has been summarised in Fig 1.4.

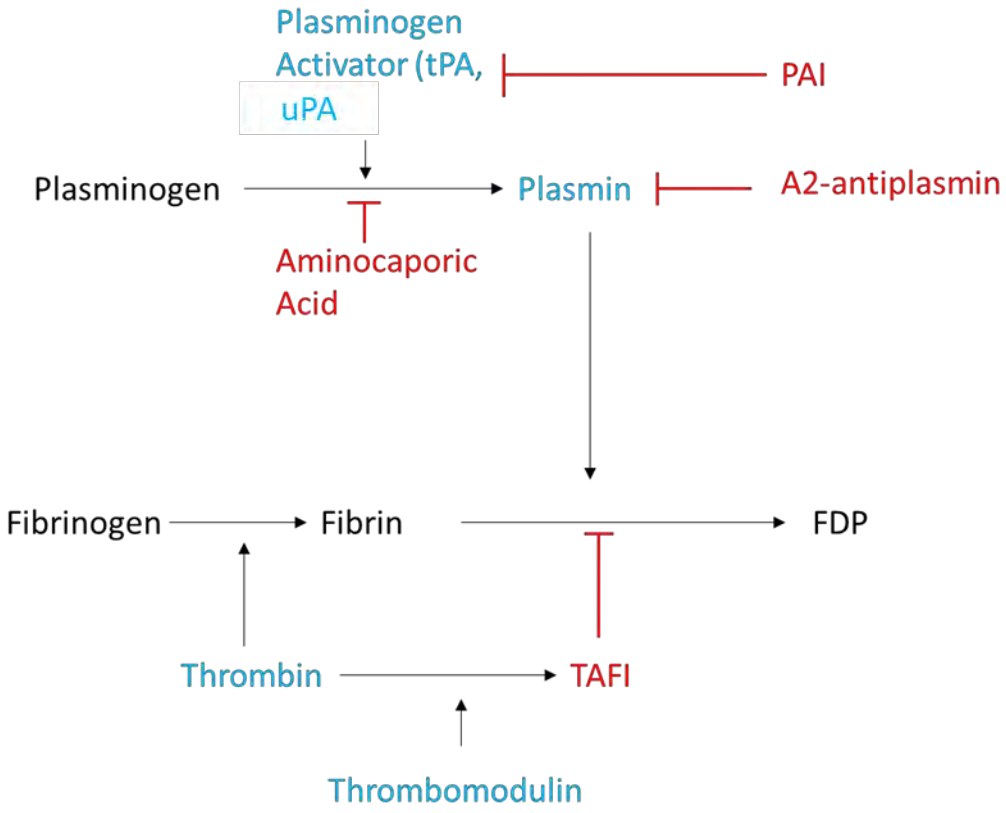

Figure 1.4 – **Fibrinolysis Pathway**. Plasminogen is activated by a plasminogen activator to form plasmin, which then binds to fibrin to degrade the clot to form fibrin degradation products (FDP). Plasminogen activator inhibitor (PAI) and thrombin activatable fibrinolysis inhibitor (TAFI) inhibit this process. Blue indicates activators of fibrinolysis and red indicates inhibitors of fibrinolysis. tPA – tissue factor pathway inhibitor. uPA – urokinase.

1.2 Platelet Concentrates

1.2.1 Preparation

In Wales, ~15,000 PLT components are issued for distribution to hospitals each year, with the number significantly larger across England (~275,000 units). PLTs are donated by healthy individuals following a donor check in accordance with the *Guidelines for the Blood Transfusion Services in the UK* (8th Edition), using either a single component method known as apheresis, or by pooling multiple donations together from whole blood (WB) donations to form a PLT concentrate (PC). There has been, and currently still is an ongoing debate within the transfusion field as to which preparation method is best, and whether the PLT product differs in function and applicability.

In the USA, the preferred method of preparation is from PLT rich plasma (PRP), generated from a gentle WB centrifugation. The PRP is then subjected to a much harder centrifugation, in order to pellet out the PLTs and enable the removal of most of the plasma into a separate pack. The resulting pellet is re-suspended in the remaining plasma (50-70ml) to generate a PC. 4-6 of these are pooled to form one adult dose.

After centrifuging WB, researchers in the 1980s noted that buffy coats (BC) where rich in PLTs, and today, these BC to contain around 30mls of RBCs and Plasma, two thirds of the white blood cells (WBCs) and the majority of all PLTs from the original donation (47). The general approach is to give WB a “hard centrifugation” to generate a BC. BCs must then be rested for a minimum of 3 hours; however, guidance has more recently changed to allowing BC to be rested at least overnight. This was due to finding a higher PLT yield without any storage defects (47). 4 -6 BC are pooled together with PLT additive solution (PAS) in a ratio of 65:35 plasma. The BCs are then subjected to a slower centrifuge separating the PLTs from the RBCs and the majority of the WBC. An inline filter removes the remaining WBCs. This is the favoured method in Europe including the UK and is used throughout the experiments in this thesis.

Apheresis is an automated procedure taking 90-120 minutes. The process involves the separation of WB using centrifugation, with the RBCs being returned to the donor. Up to 3 adult doses can be donated by an individual, at any one time, depending on the PLT number, meaning up to 5 litres of blood can be processed per donation (48). As with BC, an in-line filter removes WBCs. Apheresis is favoured for immunocompromised patients due to the reduced risk of allo-sensitisation as only one donor is used. A review in 2010 was completed comparing apheresis and BC methods (49) and concluded that there is a clear benefit when it comes to patients who are allo-sensitised to receive apheresis matched PCs. However, due to the additional donor risk and costs of apheresis, and that there is no superior haemostatic advantage, BC pooled PCs should be used unless specific clinical needs require a single donor.

The PLTs tested in this thesis are BC derived and use of "PC" refers to BC derived PC throughout unless otherwise stated. Preparation of these units as used in this thesis can be found in section 2.1.

1.2.2 Storage

Optimal storage conditions for all blood products are stated by the red book guidelines. These are nationally adopted transfusion guidelines. For PCs, the current guidelines suggest storage at 22±2^{o}C in a gas permeable bag under constant agitation (an agitator is required to perform an agitation every second) for up to 7 days. These conditions stem from extensive studies undertaken across the 1960s right through to the early 2000s. The entire storage process and conditions will be discussed in detail below.

1.2.2.1 – Storage Packs

It has long been understood that PLTs require a storage container which is able to allow the efficient exchange of oxygen (O_2) and carbon dioxide (CO_2) to allow for PLT metabolism (50). First generation bags were made using polyvinyl chloride (PVC) with the use of di-2-ethylhexyl phathalate (DEHP)(51). The use of these plastic PVC containers allowed a PC life of 3 days, whereby after 3 days a significant drop in pH and poor PLT viability (52). More recently, the PVC bag was redeveloped with

use of polyethene (PE). PE bags have been shown to maintain pH at end of storage better due to the reduction of lactate production by PLTs. The suggested reason was due to PE being more permeable than PVC, therefore allowing a greater O_2 availability to the PLT (53). Greater O_2 availability was determined by a higher PO_2 in PE bags compared to PVC, direct O_2 concentration ($[O_2]$) was not measured. This hypothesis correlated with work showing that PLTs in an anoxic (absence of O_2) container led to a decrease in pH and increase in lactate which resulted in observations of poor viability of PLTs (53).

Bags made with PE also have limitations, mainly associated with the practical side of manufacturing, due the fragile nature of the plastic. Adaptations were made to produce second generation bags made with polyolefin (PO), which maintained gaseous exchange and allowed for mass manufacturing (51). Along with the type of plastic, the wall thickness and bag surface area play a role in maintaining the PC quality. Wllvik and colleagues hypothesised that the oxygen diffusion capacity of a storage container would predict the ability of maintaining a high-quality PC (54). Thinner walled packs with an increased surface area available for gaseous exchange were then developed, with a definition of a max yield to comply with a high O_2 diffusion rate (53, 55). Thus, the need for the container to be able to allow O_2 in for metabolism and allow the release of CO_2 is key to the survival of PLTs. If the bags were unable to allow CO_2 release, a build-up would lead to a reduction in pH, ultimately compromising the PLT function and survival.

1.2.2.2 – Temperature

Transfusion guidelines currently state that PC storage must be at 22°C±2°C (56). Storage at this temperature gives rise to a major risk of bacterial contamination when compared to storage at 2-6°C. Research in 2001 shows that storage at 2-6°C decreases bacterial contamination 50-fold (57). This has been confirmed further with research, showing cold storage (CS) ablates bacterial growth entirely (58), but is dependent on the speed at which PCs are placed at 4°C from time of donation. Another apparent advantage of cold storage would be the slowing of PLT metabolism. Multiple studies using apheresis and BC PC have shown that during cold storage, lactate production and glucose utilisation

is decreased compared to the room temperature controls (59, 60). However, back in the 1970s CS of PCs was abandoned due to the inability of transfused PLTs to remain in circulation in the recipient (61). It was believed that an effective product should show good haemostatic properties and survival in the body, as observed with PC stored at room temperature (RT). The reason for this increased clearance is associated the clustering of GPIbα, leading to hepatic macrophages binding to the N-linked glycans in GPIbα through B-GlcNAc interactions. The interaction causes phagocytosis of the PLTs (62). Minimising the clustering of the glycoprotein may be the key to increasing the recovery and survival of CS PLTs *in vivo.* Other changes including loss of the spherical shape, which translates in practical terms to the loss of the "swirl" effect, is taken to reflect cold-stored induced activation - often termed the "CS lesion".

Recently, there has been a renewed interest into cold storage of PC. The reason for this is the fact that cold stored PC have been demonstrated *in vitro* to have more haemostatic capabilities compared to RT, although adequate clinical data is yet to fully support this. This was first noted by Murphy and colleagues and repeatedly shown in studies today (59, 61). Cap *et al* showed that cold apheresis stored PLTs had better aggregation responses to ADP, a higher clot strength and released less pro-inflammatory markers such as CD40L (59). The increased aggregation response has even been seen at a prolonged storage time >7 days. A 2017 study showed that compared to room temperature, cold storage PCs had better aggregation and function for up to 14 days. At day 14, the cold stored PLTs were still performing better than 5-day old room temperature storage PC (60). However, research has shown not all agonist induced aggregation is increased, with Thrombin receptor activator protein 6 (TRAP-6) (59) and Ristocetin (63) being decreased or equal to that of the room temperature control. The clinical significance of this is not yet fully understood. The increased haemostatic capability can be useful for the treatment of trauma, due to the primary goal of cessation of bleeding and less emphasis on the need for PLTs to last in the circulation. The acute need of these PLTs could improve treatment outcomes, whereby current PC usage has increased in trauma and surgery, now above 30% of all PC transfusions (64). This possibly gives more emphasis on the need for improved haemostasis.

More studies applying cold stored PCs in trauma patients is needed, and this is now a reality given that the FDA approved the use of cold-stored PC for resuscitation (65). A possible reason for the superior acute haemostatic capabilities *in vivo* could be due to the increased levels of microparticles in cold stored PCs (66). These have been found to be 50-100 times more pro-coagulant then the PLTs themselves due to the high levels of PS on the surface (section 1.3.6) and will be investigated within this thesis (Chapter 4.0).

Investigations into 37^{o}C storage of PC were evaluated and quickly shown to not be viable. An increase in ATP usage and O_2 consumption rate (OCR) demonstrated an enhanced metabolism in 37^{o}C compared to conventional 22^{o}C storage (67). A 2003 study also demonstrated the sharp decrease in pH and an increase in apoptosis (68). Therefore, it was concluded that "physiological" temperature storage increases the onset of the storage lesion and aging characteristics.

1.2.2.3 – Agitation

Agitation has been used as a means of maintaining the PC quality. Static PC storage causes a decrease in pH and an increase in activation (69), possibly due to a lack of gaseous exchange. Murphy et al (50) showed that by impeding agitation, a reduction in PLT viability was seen using isotonic labelling of PLTs over a 2-day period (50, 52). This was later confirmed with modern PO containers, showing a fall in pH and rise in lactate over 5 days without agitation compared to the control (70). The decrease in viability is suggested to be the cause of inadequate oxygenation leading to lactic acid production (53) even though the bags are gas permeable. This was paired with the theory that inadequate mixing caused the decrease in function (54). Recently, studies have shown that PLTs can be statically stored up to 24 hours at any point without affecting the quality of PC *in vitro*, allowing for transportation of units without agitation (70, 71).

1.2.2.4 – Bacterial Contamination

Bacterial contamination is a big issue with PC storage, with estimates of 1 in 2000 components having contamination, with 1 in 50,000 PC transfusion recipients being at risk of a severe reaction, far exceeding the risk of the contamination of a screened virus (72). Measures to reduce the risk include

a diversion pouch, sterilisation of the site and bacterial monitoring over the storage period (73). Since March 2010, bacterial testing on day 1 and 4 has allowed the shelf life of room temperature stored PLTs to be extended to 7 days in the UK (74). Since implementation of standard testing procedures no transfusion transmitted infections have been reported, which was covered recently in a detailed report by the advisory committee on the Safety of Blood, Tissues and Organs (SaBTO) (75). The units are also to inactivate lymphocytes and reduce the risk of graft vs host disease, but the dose of irradiation is not high enough to kill pathogens. It is worth noting, some methods of sterilisation such as pathogen reduction can affect storage characteristics and are discussed elsewhere (76).

1.2.3 PLT storage lesion

Taken as a whole, the term PLT storage lesion (PSL) is defined by biochemical and mechanical changes that occur to the PLTs over storage causing a deterioration in quality over time. Although the PSL cannot be distinguished by one single test, an array of tests including decreasing pH, decreasing aggregation responses and increasing basal activation measured by CD62P expression can be used to determine the quality of the PC (77). Some factors influencing the PSL are shown in the Table 1.1.

Collection Techniques	**Sample Collection and Processing**
Anticoagulant Solution	Storage temperature and duration
Blood Drawing flow rate	Type of agitation
Time between whole blood collection and separation	Volume of suspending plasma
Processing temperature	Leukodepletion method
Centrifugation forces	Irradiation

Table 1.1 - **Factors influencing the PLT storage lesion**. Table adapted from Table adapted from Snyder et al 2007. (78)

Blood establishments are organisations that are responsible for blood component collection, processing, and testing. They will routinely use quality control (QC) tests such as pH to determine the

state of the PSL. A low pH is caused by a build-up of lactic acid taken to reflect an increase in anaerobic metabolism; therefore, a pH under 6.4 suggests a poor-quality unit and is discarded. This was developed when PCs were stored in 100% plasma, where a clear correlation was reported with low PC pH and low PLT survival *in vivo* (79). The relationship was not as clear with other tests. Simple QC tests may only reflect a small subset of changes over storage. There are many assays used to evaluate the extent of the PSL in greater depth. More in depth assays evaluate PLT structure, function, metabolic state and activation (80). For example, evidence shows that PCs react poorly to natural agonists by the end of storage, suggesting that the ability of PLTs to aggregate decreases as storage time increases (81), however, there is conflict as to whether this effects PLTs *in vivo*. Other *in vitro* tests are shown in Table 1.2 which are not used routinely but have a rationale when introducing a new component for storage or change to an existing storage component. Some of these assays will be discussed in more detail.

***In-Vitro* tests**
Activation
CD62P surface and supernatant levels
Annexin V binding
PLT Extracellular Vesicle formation
PLT Structure
Swirling Phenomena
Morphology by microscopy
Metabolic Status
pH
Glucose and lactate levels
Functional Tests
Aggregation studies
Hypertonic shock response
Extent of change

Table 1.2 - **In-Vitro tests of PLT Quality**. Table adapted from Snyder et al 2007. (78)

1.2.3.1 – PLT Activation

PLT activation has been associated with PSL for many years, with studies indicating granule release, microparticle formation (82, 83) and conformational changes leading to CD62P expression on the PLT surface (83). Assays can assess the level of basal activation prior to addition of exogenous

stimuli (84). A key marker used to measure activation is CD62P, a marker that reflects alpha granule release. CD62P has been demonstrated consistently to increase over storage time (85). It has been suggested that the increased CD62P is associated with an increase of PLT clearance in the body, due to CD62P binding to P-selectin glycoprotein ligand 1 on leukocytes (86, 87). Increased clearance due to CD62P levels is found with cold stored PC (59). Confirmation of this in the literature is conflicting and has uncovered the lack of standardisation when it comes to *in vivo* studies evaluating PC recovery. The inconsistency could also be due to CD62P being cleaved, as some authors may measure total CD62P while others just look at cell surface levels therefore reflecting different indicators of PLT activation (88). Flow cytometry is used to analyse CD62P expression, along with other glycoproteins like CD42b (GPIba). CD42b has been shown to decrease during the storage (89). The decrease could be associated with the redistribution of glycoproteins, as when PLTs activate the morphology is affected (90) (section 1.1.1).

A relatively novel measure of PLT activation is PLT microparticle generation. This is discussed in section 1.3.6.3. The issue with applying microparticle generation consistently is that flow cytometry is often the method of convenience but is inaccurate and we now know does not capture all microparticles, especially smaller ones. There is also vast inconsistency in isolation and measurement techniques within the transfusion and microparticle field. This thesis will apply current state of art methodology and standards in the microparticle field. However, it is acknowledged that this field is fast moving, and chapters may vary slightly in approach which reflects how new knowledge from evolving literature was applied.

1.2.3.2 – PLT Morphology

Morphological changes in PCs have been linked to a poorer recovery of PLT function and number *in vivo.* The change from a discoid shape to a more spherical shape has been linked to PLT activation (91, 92). Changes in PLT morphology can be assessed using a scoring system under x100 magnification. The system classifies PLTs as discs, spheres, dendritic or ballooned forms. Each classification is given a score between 0-4, and the percentage of each type is multiplied by that score

(93). Using this, studies have demonstrated up to a 45% decrease in the morphological score over PC storage (94). However, the morphology score is highly affected by operator interpretation, therefore not the most reproducible measure.

A second, crude measure of morphology can also be described as the "swirling phenomena" which is widely applied in transfusion centres. Discoid PLTs in a PC refract light in numerous directions giving the appearance of a "foggy supernatant" when held up to a light source. Once PLTs lose their discoid shape to a spherical shape, this swirl is lost (95). This measure is a quicker and easier test than the above morphology test but again can lead to differences within the literature due to imprecise assessment (limited to "excellent" – "poor" – or "no swirl").

Some conflicting evidence using animal models concluded that morphology does not correlate with the effective reduction of bleeding times (96). Others have shown that shape change does not relate to clearance in the body (97). Therefore, the use of morphology within PSL testing needs to be clarified as to what this relates to *in vivo.* Due to the inconsistencies stated, morphology scoring has not been applied when testing PC in this Thesis.

1.2.3.3 – PLT Metabolism

Metabolism is a key contributor to PSL. PLTs utilise aerobic and anaerobic metabolism to maintain energy to stay alive. Part of the routine QC testing, pH measurement is still seen as one of the most robust and effective measures to determine change in metabolic activity and determine PSL. Levels below pH 6.4 are detrimental (50, 52), and is thought to be a result of the PSL, not a cause. The decrease in pH in PC suspended in plasma is due to the switch to glycolysis from oxidative phosphorylation increasing the lactic acid, driving down pH (98). Bicarbonate in the plasma will buffer to approximately 25mmol/L of lactate, and in PAS these levels may be higher. The buffering capacity of the PASs has caused debate within the transfusion community as to whether lactate levels proves a better predictor of PC quality and metabolic measures over traditional pH measures (92).

Most of the ATP generation in the PLTs takes place in the mitochondria (99), whereby 80-95% of ATP generated in PLTs is by oxidative phosphorylation (50, 100). In most studies, aerobic

metabolism is measured using pO_2 and pCO_2, giving an indirect measure of consumption. Low pO_2 and high CO_2 is indicative of an increased OCR and aerobic metabolism and vice versa (101). Careful interpretation is required however as the pressures of gas are relative to the atmospheric conditions and permeability of the bag (102). A direct measure of OCR would be a more accurate reflection. A few studies have measured OCR in stored PLTs, first by Murphy in the 80s with older PC storage technology (100), and more recently studies involving OCR in PLTs using seahorse techniques (103, 104). Recognising the importance of this measure, this PhD will use direct measurement of OCR and $[O_2]$ within the PC bag by applying novel Electron Spin Resonance Oximetry techniques to directly measure metabolic state of PLTs. Section 2.4 describes these techniques as utilised in this thesis in greater depth.

1.2.3.4 – PLT Function

One of the issues with PLT testing is the failure to predict *in vivo* outcomes with *in vitro* tests. Extent of shape change (ESC) has been used successfully, with studies showing a positive correlation with the post transfusion PLT recovery (105). The basis of ESC is the addition of ADP to a PC sample to measure the change in light transmission, due to the PLTs going from a resting to activated state. However, evidence has been shown that ESC reflects PLTs forming micro aggregates, and not due to the PLTs going from a disc to a spherical shape (106).

Hypertonic shock response (HSR) is another assay which measures the recovery of PLTs in a hypotonic solution, where PLTs swell in water and gradually release this water if viable through an ATP-dependent mechanism (107). The refractive index decreases with the uptake of water increasing the light transmission. As the water is then released, light transmission decreases overtime, giving a measurement of light absorbency fluctuation. The results show reasonable correlation with *in vivo* functionality (105) but not as strong as ESC. These tests are usually done in parallel, therefore improving the predictive outcome.

The major question facing transfusion services is whether PCs can perform their primary role after storage. This can be done by looking at the aggregation of PLTs in *in vitro* assays. Traditional

aggregometers work on the basis of light transmission where the light transmission increases as PLT aggregates are formed (108). Improvements to this method involved measuring adhesion along with aggregation, where a company developed an aggregometer to measure impedance between 2 electrodes (Section 2.2). Several studies have shown that over the 7-day storage period, aggregation decreases in response to ADP, collagen, and TRAP (61, 80). ADP, however, induces poor aggregation after only 3 days and throughout storage (109). Studies that have reported poor ADP responses concluded that PLT degranulation in storage causes ADP release leading to desensitisation of the ADP receptors P2Y1 and P2Y12 (81). The exact cause of this phenomenon to ADP response loss in PC is not fully understood and is demonstrated in section 3.4.3. ADP is a potent activator of PLTs *in vivo* and so ADP response defects within PC could cause major problems in functionality once transfused. Some researchers have shown the ability for some responses to recover *in vivo* so have used a WB-based model, adding a concentration of PC to WB before assessing the aggregation, mimicking a more "physiological" response (81). Scott Murphy for example demonstrated many years ago the partial recovery of ADP *in vivo*, therefore suggesting that *in vitro* testing of PCs does not always reflect *in vivo* function (110). This model has shown that TRAP and arachidonic acid (AA) induced aggregation was well preserved over storage.

1.2.3.5 – Recovery and Survival

Once *in* vitro and animal studies had been concluded, recovery and survival of transfused PLTs in the circulation in healthy volunteers is the next step in the study hierarchy of the evaluation of new PC products. Autologous PLTs (PLTs obtained by the intended recipient) labelled with chromium 51 or indium 111 are re-infused in order to determine recovery; however, this method is expensive and technically complex so is not used often. Alternatively, the PLT increment can be calculated after PC transfusion. Correct count increment (CCI) determines the increase in PLT numbers, and the relationship between CCI, survival and recovery is yet to be established (111). The expected increment when all PLTs are viable is 20 x 10^9/L (112). However, increments are often seen at 10-15 x 10^9 units, with older, day 7 PC, decreasing CCI by up to 50% (113). If the CCI is below 7.5 x 10^9/L, the transfusion

is deemed a failure with the patient possibly requiring a second transfusion (114). A publication in 2006 outlined a standardisation of techniques for *in vivo* analysis of PC efficacy (115). Recovery and survival limits of 66% and 50% respectively have been accepted as a good standard to employ (116). It is worth noting that factors such as estimated blood volumes and differences in PLT uptake by the spleen can also be used to determine viability in *in-vivo* studies (112). The problem with these measurements like CCI and recovery of PLT only measures number and does not address PLT functionality.

The final stage of evaluation, and the gold standard, are clinical studies in patients with relevant endpoints dependent on the transfusion goal as the primary outcome. An example of these endpoints can be found in a recent CS study, evaluating the efficacy of CS PCs vs RT PCs in cardiothoracic surgery, using chest drain output as a primary output and platelet function, blood usage and mortality as secondary outputs (117).

Currently, further studies need to be carried out to determine the value of *in-vitro* results as an accurate prediction for *in-vivo* efficacy after transfusion, giving rise to a level of uncertainty on the precise effect of the PSL on the PLT transfusion efficacy. With these limitations in mind, *in-vitro* tests allow the study of complex physiological roles that PLTs perform and allow studies to look at a vast range of parameters not possible *in-vivo* without major complication and difficulty.

1.2.4 – Use of PLT additive solutions (PAS)

PLTs were originally stored in plasma, however multiple PAS's have been developed to better maintain PLT structure and function in storage. PAS's are buffered salt solutions and contain additives including acetate and glucose. Acetate is involved in the citric acid cycle and is thought to reduce lactate production and glucose utilization (118). The use of PAS has reduced the volume of plasma utilised for PLT storage to approximately 35%. This is beneficial and has simultaneously led to a reduction in the incidence of allergic and febrile reactions (119). PAS's are primarily used for BC preparations and have not yet been implemented for apheresis PCs within the UK likely due to the

complicated collection procedure (119). The PAS utilised in this thesis, known as SSP+, is detailed in section 2.1.1, Table 2.1.

1.3 Extracellular Vesicles

Extracellular vesicles (EVs) are submicron particles enclosed in a phospholipid bilayer, with their size ranging from 30nm-1000nm in diameter and are roughly spherical in shape. In recent years, the research interest into EVs has increased exponentially. The term EV is the "umbrella term" for all subtypes of EVs discussed in section 1.3.2.

1.3.1 History

Originally, EVs were regarded as cellular debris and having no "defined" biological function. In 1946, plasma free from PLTs was noted to generate thrombin, and the rate of this generation could be reduced via a high-speed centrifugation (120). Decades later in 1967, Peter Wolf and colleagues identified EVs in plasma, confirming the observations by Chargaff and West in 1946. Wolf found these small, spherical vesicles (<500nm) and described the findings as "platelet dust" (121). From these findings, it took 3 years before Webber showed that these particles could "bleb" from PLTs after activation and enter the circulation, using electron microscopy (2).

A different line of research to the above led to usage of the term "exosomes". The term was first introduced when vesicles were isolated from culture medium of sheep reticulocytes. Exosomes shared many characteristics to the reticulocyte's membrane, including tetraspanin proteins, but did not possess any lysosomal function. This led to the conclusion that shedding of the transferrin receptor was mediated by exosome production (122). In 1992, Johnstone et al showed exosomes are formed within multivesicular bodies (MVBs), and released when the MVBs fuse with the plasma membrane (123). Further studies in 1996, showed B-lymphocytes release antigen presenting exosomes (124), suggesting that exosomes may be involved in the inflammatory process.

In 2005, the first gathering relating to these small particles brought together interested scientists. The following decade saw a large increase of EV related publications. In 2011, the International Society for extracellular vesicles (ISEV) formed, with the Journal of Extracellular Vesicles (JEV) being launched the year after. Due to the interest in EVs and the large number of diverse

publications and methodologies, ISEV in 2014 released a position paper on the minimal set of requirements, standardised methods, and definition of EVs. These standards allow for more comparability across studies and EV research (125). These guidelines were updated in 2018, due to the continued exponential increase in EV knowledge being generated (126) and largely represent the minimal standards and methods applied during the body of work presented in this thesis.

1.3.2 Nomenclature

The terminology "EV research" has been applied to a wide selection of work over the past decade and has caused confusion in the literature with regards to comparability of EVs being studied. Many terms used in the literature reflect the function of EV like "tolerosomes" that induce immunological tolerance to antigens (127). A different method is to term the EV depending on origin like "prostasomes" (prostate) (128) and "oncosomes" (tumour) (129). These are very specific terms; however broader terms are also used to describe EVs. "Exosomes", "microvesicles", "microparticles" and "apoptotic bodies" have been applied throughout the literature, these broader terms are used interchangeably in some cases, which has led to the incorrect use of terminology and more confusion. A letter to the editor in Journal of EVs highlighted the issues (130) and when the position paper was released, it clarified the terminology. The use of "extracellular vesicles" is now widely accepted as a generic term encompassing "exosomes" "microvesicles" and "apoptotic bodies" (125) (Fig 1.5).

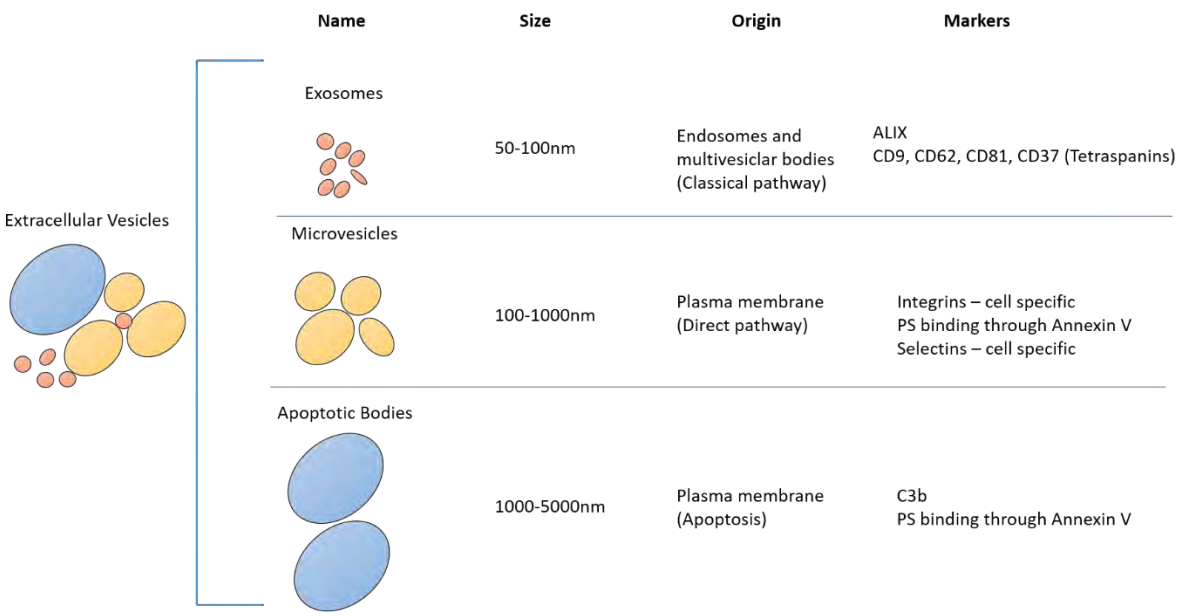

Figure 1.5 - **Extracellular Vesicle Classification**. "EV" is a generic term used to describe the 3 subtypes of secretory vesicles. The main differences are size and origin, giving rise to different markers on the vesicle. Biogenesis of exosomes and microvesicles will be discussed below. PS – Phosphatidylserine

1.3.2 Biogenesis

The main difference characterising each population of EVs is their biogenesis, giving rise to different markers and content to each of the subtypes. Two pathways are recognised; the endocytic pathway (exosomes) and direct pathway (microvesicles) and are summarised in Fig 1.6.

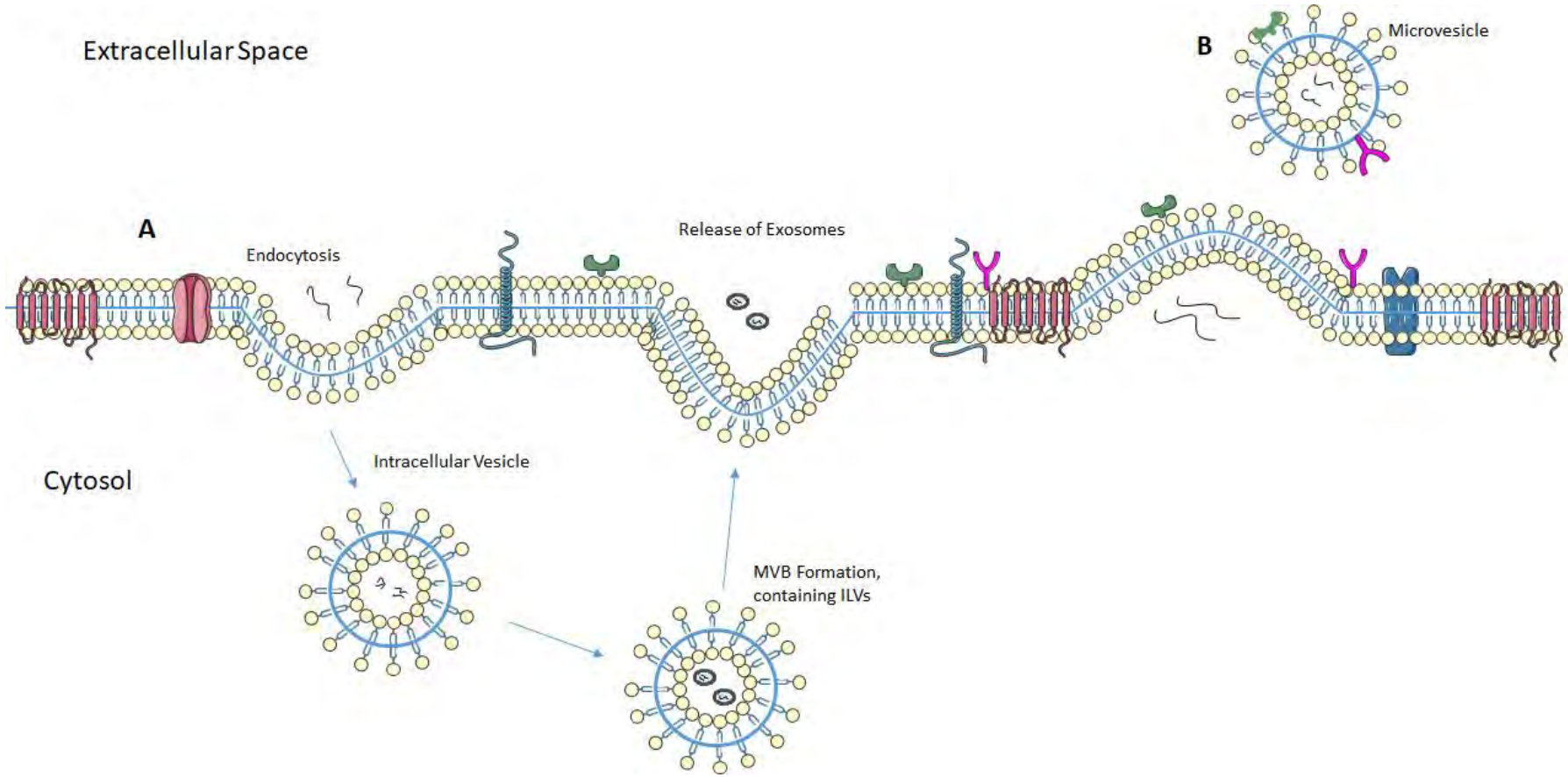

Figure 1.6 – **Overview of Extracellular Vesicle Biogenesis**. A) Biogenesis of exosomes via the endocytic pathway. In brief, endosomes are formed by invagination of the plasma membrane. These mature to late endosomes which contain multiple intraluminal vesicles (ILVs), forming multivesicular bodies (MVBs). MVBs then fuse with the plasma membrane, releasing exosomes. Exosomes share markers from the internal cells, and proteins involved in the biogenesis. B) Direct Pathway of microvesicle production. Microvesicles are formed from the outward budding and fission of the plasma membrane, normally due to the redistribution of phospholipids. Microvesicles share markers found on the parent cell membrane

1.3.2.1 Endocytic Pathway

Exosomes are derived from the endocytic pathway(131). In the early stages, endosomes are formed by invagination of the plasma membrane within the cell, which in turn transform into late endosomes (132). The invagination is mediated by both clathrin- dependent and clathrin-independent pathways (133). Late endosomes contain multiple intraluminal vesicles (ILVs) and are termed MVBs. Release of the exosomes is facilitated by the subsequent fusion of MVBs with the plasma membrane. MVBs may be signalled for lysosomal degradation instead of exosome release (134).

The formation of ILVs involves the endosomal sorting complex required for transport (ESCRT), consisting of around 30 different proteins. Four separate ESCRTs (0-III) are required for MVB formation, vesicle budding and cargo sorting (135, 136). Initiation of the process involves ESCRT0, whereby recognition of ubiquitinated proteins bind to subunits of ESCRT0. Interaction with ESCRTI and II leads to the combined complexes to combine with ESCRTIII. ESCRTIII is involved in promoting budding. Once these buds are formed by ESCRTIII, they are cleaved forming ILVs, allowing ESCRTIII to separate from the now termed MVB using the sorting protein Vps4 (135). Other proteins seen bound in exosomes such as Alix are associated with several ESCRT proteins including TSG101, which has been reported to participate in the endosomal membrane budding process and interacts with syndecan involved in cargo selection (137). Evidence of these proteins reflects an ESCRT dependant manner of exosome biogenesis. Silencing ESCRT leads to a marked decrease in exosome production (138) but does not deplete the production completely, suggesting other mechanisms exist.

Growing evidence has indicated an ESCRT independent pathway of cargo sorting into MVBs, involving multiple microdomains. The microdomains are enriched with sphingomyelinases, from which ceramides are formed which induce lateral phase separation (139). Ceramide's cone like structure can induce budding due to the negative curvature of the endosomal membrane (140). Tetraspanins have also been shown to be key in exosomal development (141). Tetraspanin-enriched microdomains (TEM) are responsible for signalling proteins within the plasma membrane. Proteins like cluster of differentiation (CD)81 are key to sorting intracellular components and receptors in

exosomes (142, 143). Other mechanisms independent of ESCRT proteins involve CD63, which has been shown to be highly enriched in ILVs within HeLa cells when ESCRT function is absent (144). Depending on the cell type, other mechanisms have been eluded to be ESCRT independent (145).

After MVBs are formed, fusing with the plasma membrane is required to release the exosomes into the extracellular space. This process is mediated by multiple Rab GTPases. Inhibition of Rab35 leads to a decrease in exosomal production in oligodendrocytes (146), Rab27A/B release is linked to exosomes enriched in late endosomal proteins like CD63 (147), and responsible for direction of the MVBs to the membrane. It was shown that inhibiting Rab27A leads to impairment of exosomal secretion (148). Other Rab GTPases led to high amounts of ALIX protein (149). Therefore, it has been concluded that the Rab protein pathway is dependent on the cell type.

Soluble NSF (N-ethylmaleimide-sensitive fusion) attachment protein receptor (SNARE) proteins are involved in the final stages of MVB fusing with the plasma membrane to release exosomes via exocytosis. Generally, it has been shown that one R-SNARE and 3 Q-SNAREs form a complex required for membrane fusion (150). It has been shown that vesicle associated membrane protein 7 (VAMP7), an R-SNARE, is needed for exosomal release in K562 cells (151). Overexpression of VAMP7 inhibits SNARE complex formation which inhibited exosome release. MVBs were enlarged in this experiment, showing that MVB formation wasn't affected, just the release and fusion of MVBs (151). SNAREs are folded to facilitate fusion, which provides thermodynamic energy to pull apart the membrane (151). However, the current hypothesis is still poorly understood. Other research has shown that exosome release can be controlled by Ca^{2+}. Increased Ca^{2+} using the ionophore A23187 increased exosome production (152).

Whether MVBs are released or degraded can depend on a cell's homeostatic status. Multiple studies have shown that as cellular stress increases, the number of exosomes increase (153-156). Stresses include irradiation of cells or exposure to hypoxia. On the contrary, research conflicting the theory has shown that an increase in autophagy (nutrient supply during starvation) decreases exosome release (157). However, the pathways controlling stress-induced exosomal release are not

clear from the current research available. Fig 1.7 summarizes the endocytic pathway of EV biogenesis as we currently understand it.

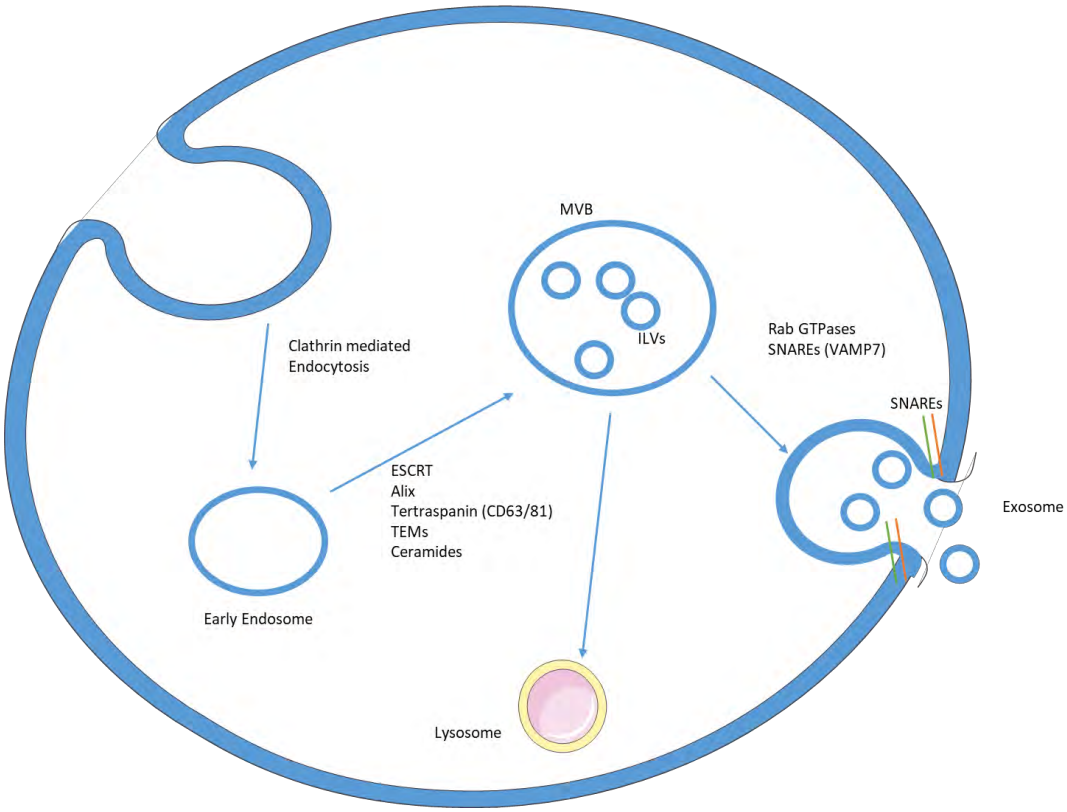

Figure 1.7 – **Classical pathway of exosome biogenesis**. Endosomes are formed from invagination of the plasma membrane, mediated by the clathrin pathway. ILVs are formed from ESCRT dependent or independent pathways involving multiple proteins such as Alix, TEMs and tetraspanins. The MVBs are then assisted by Rab GTPases to the plasma membrane, with SNARE proteins involved in the docking and fusion with the membrane, leading to release of exosomes. ESCRT – endosomal sorting complex required for transport. ILV – intraluminal vesicle. MVB – multivesicular body. SNARE - Soluble NSF (N-ethylmaleimide-sensitive fusion) attachment protein receptor. VAMP7 – vesicle-associated membrane protein 7.

1.3.2.2 Direct Pathway

The direct pathway for microvesicle production is less well defined, with different mechanisms thought to be responsible for the shedding of these typically larger EVs. Generally, it is accepted that microvesicles are formed by outward budding and fission of the plasma membrane, due to several factors including the redistribution of phospholipids, mainly PS. The outer membrane of cells in usually dominated by phoshatidylcholine and sphingomyelin, while the inner is dominated by PS and phosphatidyletholamine (158). The asymmetry and regulation of these phospholipids is maintained

by translocase enzymes within the membrane. Flippases translocate PS from the outer surface to the inner half of the lipid bilayer while floppase has the opposite effect. Both enzymes are ATP dependent and are members of the ATP binding cassette family (149). Scramblase is an enzyme that causes bidirectional transport of PS and is ATP-independent unlike the other enzymes mentioned. In resting conditions, flippase's rate of work is far greater, leading to an asymmetric balance of PS (158).

When activated, a Ca^{2+} influx inhibits flippase while activating floppase and scramblase, disrupting the PS asymmetry due to a profound increase in PS externalisation (159). High cystolic Ca^{2+} leads to actin cytoskeleton disruption, which normally modulates cell stability by membrane interactions (160). When PS is translocated, the covalent links between the membrane and the cytoskeleton are disrupted, triggering Ca^{2+} dependent enzymes like u-Calpain (161). U-calpain is a protease which can cleave the actin cytoskeleton, causing cytoskeletal remodelling. There is evidence of this enzyme having a major role in aggregating PLTs and EV release (161). Calpain has also been shown to be a key enzyme in the blebbing of EVs from neutrophils (162). Due to a loss in cell membrane surface area, a plasma volume reduction is required, which facilitates membrane budding due to the stress of a surface area mismatch (163) (Fig 1.8). The microvesicles are shed from the cell, with a size between 100-1000nm.

Apoptotic bodies are typically much bigger, have different character, and are generated as part of the cycle of programmed cell death. A detailed review of the biogenesis and properties of apoptotic bodies can be found elsewhere by Akers et al 2013 (163) and He et al, 2018 (164).

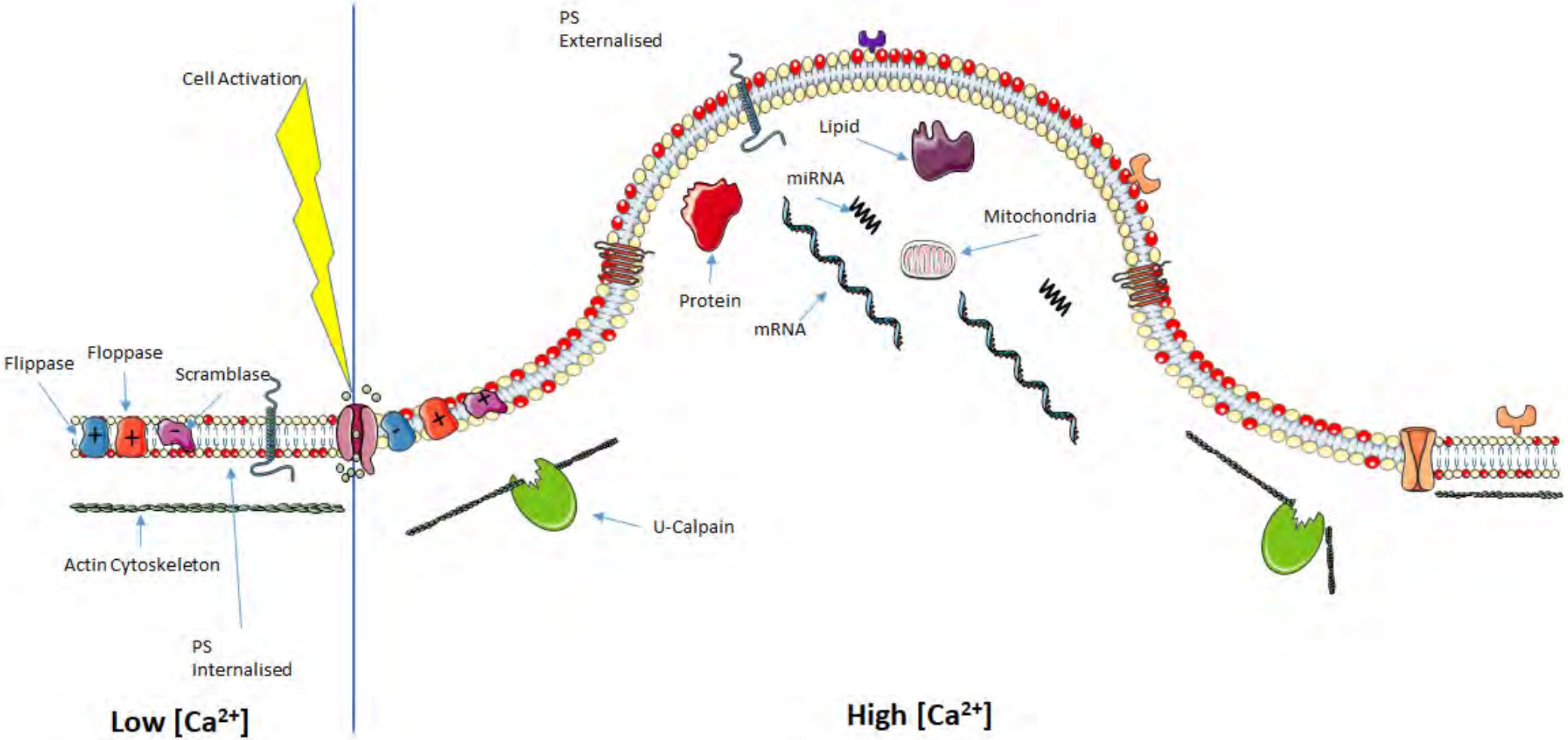

Figure 1.8 – **Biogenesis of Microvesicles**. Microvesicles are formed via the direct pathway, involving budding of the plasma membrane caused by an increased in cystolic calcium. Calcium influx into the cell leads to loss of membrane asymmetry and disrupting cytoskeletal arrangement. PS – Phosphatidylserine

1.3.3 EV Composition

Markers of EVs are highly dependent on the cell of origin, for example GPIIb/IIIa (CD41/61) will be present on PLT EVs (PEVs) (165), VE-cadherin (CD144) on endothelial EVs (166). They also differ dependant on the mechanism of production, for example ESCRT proteins will be observed in exosomes (125). There is however overlapping of these markers, for example CD9 once thought to be indicative of exosomes has also been shown to be present on certain microvesicle populations (167). A challenge in EV research is that there is no exosome/microvesicles specific markers to distinguish the two populations. The exact composition of each EV formed varies greatly, as they are composed of numerous lipids, proteins and nucleic acids. The process of packaging EVs in thought to be a carefully controlled mechanism, discussed in detail elsewhere (168). As proteomic technology improves, identifying EV specific markers is a realistic future aim (169).

Exosomes generally consist of proteins from the tetraspanin family, major histocompatibility (MHC) molecules and proteins such as TSG101 (170). Exosomes have also been shown to harbour and transport RNA. Valadi and team showed that exosomes contain functional mRNA and miRNA. The mRNA was capable of supporting protein synthesis, and the miRNA was expressed at higher levels than the parent cells, suggesting purposeful packaging (171). Examples from endothelial cells grown in a hypoxic (1% O_2) environment showed mRNA encoding N-myc downstream related gene 1, which is heavily involved in the endothelial stress response (168), showing that exosomes can reflect the activation status of the parent cell. Microvesicles also contain RNA which can mediate cell-cell communication. Pancreatic cancer cell lines that lead to the release PEVs contained mRNA and miRNA (171, 172). The nucleic acid content of EVs is still a rapidly growing area of EV research. Some research has shown that RNAs are selectively packaged into EVs to be translated by target cells (171). EV RNA, as previously mentioned, has been demonstrated to be highly enriched in comparison to the parent cell, suggesting a function of EVs is related to RNA transport (173).

Lipids are vital to the EVs structure as well as being found contained within the EV. PS for example is a vital component of EVs generated through the direct pathway (1.3.2.2). Cholesterol has

been found to be enriched within EVs increasing the stability of the lipid bilayer (174). Lipids have also been shown to exhibit a functional role. Prostaglandins bound to EVs has led to activation of certain signalling pathways in leukaemia cells (175). PEVs have also been shown to have different sub-sets of lipids within populations of EVs (176).

1.3.4 EV Internalisation

For EVs to affect and alter the target cell, it's content must first be internalised. This mechanism is not as well studied as the biogenesis and composition and is highly dependent of the cell target and the EV subtype. Due to the high variation, numerous mechanisms of internalisation have been suggested – the broad concepts and examples are outlined here.

Before internalisation of an EV, it must be recognised by the target cell, which is mediated via interaction between the EV and membrane receptors. Research into EV recognition has demonstrated the implication of tetraspanins, whereby blocking CD81 reduces EV uptake by dendritic cells (131). Blocking of CD9 also demonstrated a similar effect. EVs also interact with integrins, and inhibition of CD11a binding site reduces uptake of EVs significantly. The presence of α4β1 on EVs has been demonstrated to be essential for recognition and uptake of endothelial EVs within target endothelial cells (177).

Once recognised, internalisation ensues. The mechanism of EV internalisation has been described as an active pathway, which has been shown to be severely affected in lower temperatures (173), with the most widely studied pathway being clathrin-mediated endocytosis. This involves the formation of clathrin-coated vesicles within the cell which causes invagination of the membrane, leading to endocytosis (178). When the pit formation is inhibited, EV uptake is reduced (179). Endocytosis can also be clathrin-independent, mediated by caveolae, forming small chasms in the membrane (180). Knockdown of caveolin-1, a key protein in caveolae, caused a reduced EV uptake (181). Lipid rafts are another example of clathrin-independent endocytosis, as studies indicated that these rafts effect membrane fluidity, and inhibiting sphingolipids (enriched in these rafts) reduces EV internalisation (182).

Phagocytosis has been reported to be involved in EV uptake, especially uptake of microvesicles (183). Exosome internalisation by phagocytosis has also been demonstrated through MØ (184). PS has been shown to mediate phagocytosis, due to being an apoptotic signal on cells. EVs, predominately microvesicles, have a high level of PS on the surface as discussed in 1.3.2.2. In macrophages, a PS receptor Tim-4 was blocked, leading to a reduction in EV phagocytosis (184). Staining EVs with Annexin V (blocking PS) has also shown to reduce cellular uptake (185).

The final mechanism considered are non-endocytic, direct membrane fusion, like that of the MVB fusion with the membrane. Fusion of the EVs with the membrane will lead to EVs not to be intact when internalised. Researchers found that EVs fuse with PLTs, leading to the transfer of TF, inducing coagulation (186). Others have shown that EVs can fuse with the target cell membrane to deliver functional miRNA (187).

Several mechanisms are involved in EV internalisation, with the endocytic pathways thought to be the primary mechanism. The pathway of choice may be dependent on both the EV subtype, EV contents and the interaction of the ligands and receptors exhibited by the EV and target cell.

Apart from direct fusion, EVs are intact when internalised. This has been confirmed with studies using fluorescence and confocal microscopy (188).

1.3.5 EV Processing

Across the EV field, there is still a fundamental lack of consistency when comes to isolation, characterisation, and quantification of EVs from biological/extracellular fluid. No “gold standard” method exists, leading to a considerable level of complexity when comparing across studies. Guidelines set by ISEV inform the researcher of the minimal requirements for isolating and defining a pure EV population from fluids (125, 126). As the field expands, it is expected that isolation and purification will need to become more standardised.

1.3.5.1 Sample Collection

EVs have been isolated from almost all biological fluids including blood, sweat and urine (189, 190) to cell culture media and even from processed blood products such as PCs (1.3.6.3). Isolation of

EVs from WB offers a number of challenges primarily associated with PLT activation and to EV release during sample manipulation, potentially effecting concentration and characteristics (191). WB sampling has been recommended with a 210-gauge butterfly needle (192), with the first few millilitres discarded to avoid surplus activation. Following collection, in sodium citrate vacutainers, samples should be immediately processed (193). With PC, sampling is usually undertaken very slowly under gravity, if possible, to avoid shear stress. When isolating from PC no anti-coagulant is needed due to the WB being collected into sodium citrate.

The choice of anticoagulant however is important; with ISEV suggesting anticoagulants like heparin should be avoided due to evidence of simulation of EV release (194). The downstream assay should also be considered, with anticoagulants such as EDTA causing interference with polymerase chain reaction measures (195).The Scientific Standardisation Committee of the International Society on Thrombosis and Haemostasis recommend sodium citrate (196), however ISEV recommend more research be required to resolve the question.

1.3.5.2 EV Isolation

Many studies of EVs collected from biofluids or cell culture (including the EVs isolated in this thesis) have employed differential centrifugation, due to the simplicity and short time taken. Initial steps involve clearing the fluid of cells. Removal of cells is usually undertaken at 200-1500 x g, followed by the removal of cellular debris at 10,000 x g, before a final centrifugation at 100,000 x g to pellet EVs. EVs can be further isolated by size using differential centrifugation. Using 20,000x g, this should pellet larger microvesicles, while 100,000-120,000 x g should pellet smaller exosomes, however absolute separation is not possible by this method due to contaminants such as lipoprotein particles (197). Resuspending in phosphate buffered saline (PBS) and washing may aid in removing some contaminants but will affect EV yield. Due to the carryover of contaminates, such as soluble proteins, protein concentrations of EV samples isolated by centrifugation alone are unreliable and largely do not reflect EV recovery from the source (198). Other issues with centrifugation includes EV aggregation, extra vesicular protein complexes, and increased PS exposure (142, 199, 200).

EVs can be separated based on their size using filters or chromatography. For example, use of a 0.8um pre sized filter will exclude any particle larger than 0.8um (800nm). In the literature, 0.8um filters are used to remove large cell fragments and PLTs prior to EV isolation (199) and 0.2um may be used when smaller EVs are required (201). These are usually "pre-isolation" methods before centrifugation (190). A more efficient method of size exclusion chromatography (SEC) has emerged, with the ability of removing contaminating lipoproteins and proteins (202). However, some studies dispute the efficiency of excluding lipoproteins (203). Pilot observations from our lab show good protein separation, but not full exclusion (Fig 1.9). The major concern with SEC is the dilution of EV sample (typically upward of 10-20 times), leading to debated subject of quantity vs purity, largely dependent on the downstream application. Other methods based on size/density includes density gradient centrifugation, however a study published in JEV demonstrated HDL contamination in EV isolation via this method, suggesting that like SEC, the method is prone to limitations (204). Size exclusion still needs more research of removing lipoproteins before being a "Gold Standard" recognised by ISEV.

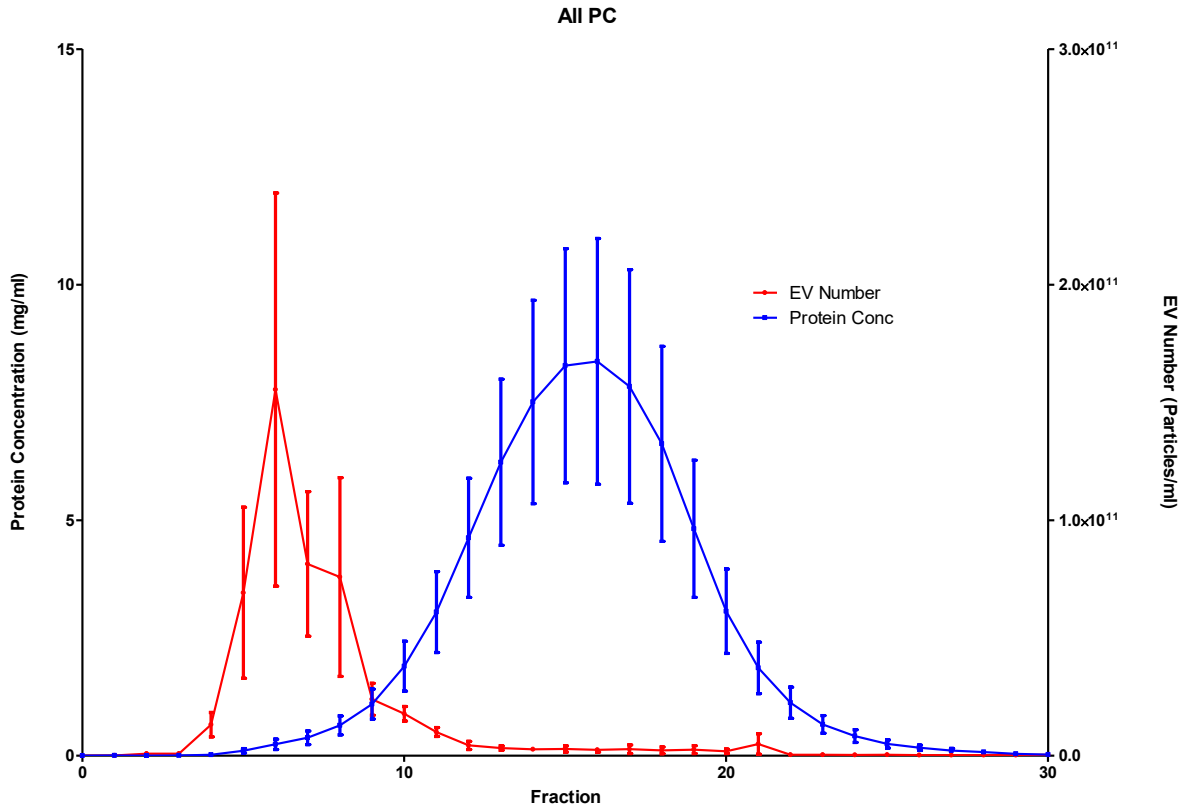

Figure 1.9 – **EV concentration vs Protein Concentration**. PC samples collected and EVs isolated using a size exclusion column. Number was calculated using nanoparticle-tracking analysis (red), protein concentration via the Nanodrop (blue). Error bars denote SD.

Surface proteins on the EV surface (e.g., CD41 on PEVs) allow for immunoaffinity isolation with the use of antibodies (205, 206). The methods can be positive or negative selection based on selecting the desired or unwanted EV populations, respectively. Antibodies are bound to beads and can be separated by magnetic properties of the attached bead (207). This process is rapidly being improved with commercial kits available from manufacturers such as Miltenyi Biotech with specific CD9 isolation using positive selection.

Finally, a more recent method that has gained popularity involves microfluidics. Chen et al in 2010 showed rapid recovery of small EVs using an antibody coated microfluidic device, using cell cultured media (208). A recent development (2017) involves using undiluted WB in an automated microfluidics chip to isolate exosomes with a yield of 110nm particles of 99% (209). Microfluidics is very promising, although expensive, with a potential for automated high yield, but still needs developing and optimising before widespread use.

To summarise, multiple methods are available for EV isolation, however there is currently no "gold standard", so methodologies must be stated with full detail to allow accurate comparisons to be drawn across the EV field. Details of the methods used in this thesis are described in section 2.5.

1.3.5.3 Measurement of EV concentration and size

As interest in EV increases, the technology to evaluate quantitatively and qualitatively is improving. Quantification methods include transmission electron microscopy, flow cytometry and the most common method of nanoparticle tracking analysis (NTA). NTA is the most widely used for size and concentration analysis (210). For a deeper analysis of EV surface components and cargo, proteomics, genomics and lipidomic are employed (211). The methods have been extensively reviewed elsewhere and will not be discussed in this thesis (211).

NTA was used throughout the thesis for the measurement of EV concentration and size. NTA combines laser scattering microscopy with a charged coupled device camera to visualize and record EVs (212). The software is able to identify and track particles moving under Brownian motion and calculate the particle size according to the Stokes-Einstein equation, as described in detail in section 2.5.3. It was decided that flow cytometry for concentration analysis was not going to be used due to the limit of detection being 150-190nm for specialised machines compared to NTA's 30nm-1000nm (213). Due to exomes being smaller than 150nm, counts will (and have been shown) to be significantly reduced on flow cytometry compared to NTA, up to 15 times lower (214). Issues with protocol set up and complex gain control can lead to large variations in data collection using flow cytometry for concentration analysis.

1.3.5.4 Storage of EVs

Samples should be analysed on the day of isolation; however, is not always possible, especially in a large clinical study with multiple parameters of assessment. The majority of studies store EVs at -80^{o}C in 0.2µm filtered PBS (190), with studies demonstrating no EV decrease with multiple freeze thaw cycles (215). However, unpublished data from our group shows that EV surface characteristics degrade over time during storage even when frozen, and that ideally EV can be stored at 4^{o}C for 5-7

days without significant losses. Research has shown that refrigeration best preserves EV characteristics short term (193). However, longer term storage is best achieved via slow freezing (as adopted with cells) and storage at -80'C.

1.3.6 PLT-Derived EVs

PEVs mechanism of biogenesis is in large via the direct pathway (1.3.2.2). Formation of PEVs relies on a rise in intracellular Ca^{2+} and can be induced by PLT activation or cell death (216). On average, ~104 PEVs/µl circulate in the blood of a healthy individual, characterised by the presence of CD41 (217). PEVs are known to be pro-coagulant and can support secondary haemostasis (1.1.1) even in the absence of PLTs (121). PLTs support coagulation through the anionic PS suggesting PEVs act via a similar mechanism due to an abundance of PS on their surface. Indeed, PEVs are thought to be 50-100 times more pro-coagulant than the parent PLT because of PS exposure.

PEVs contain more than 40 glycoproteins shared with the parent cell, including CD62P, GPIIb/IIIa and GP53 (218, 219). Research has showed that PEVs formed after activation showed many characteristics of α-granules, containing PF4 and thrombospondin (220). PEVs also contain metalloproteinases within the membrane, which are able to promote cancer progression and tumour growth. This has been shown with high levels of metalloproteinase positive PEVs in different tumour types, including lung cancer (221, 222).

1.3.6.1 PEVs Physiological Roles in-vivo

Today EVs are recognised as signalling molecules allowing cell to cell communication via the transfer of cargo. The message relayed by the EV is both specific to the parent and recipient cell, as well as the composition of the EV (1.3.3 & 1.3.4). This section will focus on the roles established for PEVs.

PEVs have been reported to be involved in haemostasis and have a procoagulant effect. This has been reported since the first research published on EV in 1946 by Wolf, when EV were referred to as "PLT dust" (121). Recently, PEVs have been shown to enhance the generation of thrombin (223). PS on PEVs provides FVII and FX with a surface for assembly during the clotting cascade (224).

However, it is worth noting, that not all PEVs display PS (225). PEVs have been shown to alter clot stability and have been incorporated within the fibrin network (226). Another theory as to why PEVs are procoagulant is TF, however a study by Yáñez-Mó and colleagues (227) showed low levels of TF present in PEVs, suggesting that TF is expressed on other EVs, mainly endothelial derived (227). Patients with Scott syndrome have lower levels of PEVs due to a mutation in the scramblase enzyme (228). Individuals with Scotts' suffer from bleeding complications, due to the lower levels of PS on PLTs and number of PEVs, suggesting, PEVs are vital for normal haemostasis. PEVs are also involved in angiogenesis. containing pro-angiogenic lipids which are implicated in endothelial cell proliferation (229).

Inflammation is another physiological process in which PEVs are implicated in. PEVs promote leukocyte adhesion and chemotaxis of monocytes (230). PEVs also contain AA when released during activation, which in turn can form pro-inflammatory TxA_2 (231), further recruiting more WBC cells to the site of injury. Clinical studies with patients experiencing hypertension showed higher levels of PEVs containing PLT and endothelial cell adhesion molecule 1 (232), suggesting an increase in leukocyte adhesion. CD62P positive PEVs can interact with PSGL-1 on leukocytes leading to activation and aggregation (233). PEVs that cause inflammation in a normal response to infection can cause serious issues and implications in certain pathophysiological conditions, discussed below.

1.3.6.2 PEVs Pathophysiological Involvement

Cardiovascular Disease (CVD) is the leading cause of mortality worldwide (234) and is an umbrella term for diseases such as heart failure and coronary artery disease. Obesity has been long associated with an increased risk of CVD, and recently associated with a difference in EV profile. Comparing healthy lean and obese individuals, PEVs (235, 236) and endothelial EVs (237, 238) were significantly increased in obesity. PEVs along with endothelial EVs have shown to be reduced after fat-loss along with the loss of pro-coagulant markers (239) suggesting that weight loss in obese individuals without overt CVD, shows health benefits. More work on the effects of PEVs in obesity is required to determine the risks of PEVs numbers to determine a possible biomarker risk calculation for CVD.

Associations between high PEVs and risk of thromboembolic events have been reported in conditions such as type I diabetes (240). The study showed an increase in PEV numbers in patients who have type I diabetes compared to their matched controls, but no significant increase was seen in type 2 diabetes compared to the controls. This disputes previous evidence (241), from research into more complicated forms of diabetes. When total microparticle numbers were considered, both showed an increase and showed that type 1 diabetes was associated with a high level of procoagulant EVs compared to type 2, characterised by thrombin generation and PS exposure, however the mechanism was not fully understood (241).

Elevated levels of PEVs and endothelial EVs have been reported in patients who have had a stroke, the second-leading cause of death world-wide (242). To date, studies have found PEVs increase in the acute phase of a stroke, with the prothrombic nature of PEVs likely to contribute to the cerebral infarction (243, 244). Other studies report this increase in PEVs in stroke is associated with increased annexin V binding (245, 246). A further reported difference between healthy controls and stroke patients was the significant increase in PEVs originating from activated PLTs displaying CD62P (245, 246). Paired with more recent PEV research, the data suggests the highly prothrombotic nature of these PEVs (247, 248). When EVs from this acute stroke insult are applied to immune cells, a significant increase in cytokines and chemokine expression is reported, implying EV reflect the proinflammatory nature of the stroke (249). Endothelial EVs have been demonstrated to be linked to stroke severity (250), possibly alluding to EVs being used as a severity biomarker in the future.

PEVs have a role within physiological inflammation, with implications in certain inflammatory diseases, including rheumatoid arthritis (RA). RA is a chronic autoimmune disease characterised by inflammation within the joints. PEVs have been associated with RA, with high numbers of plasma PEVs compared to matched controls, and the concentration of PEVs has been correlated with disease severity (251). These PEVs were not predominately found within the synovial fluid of effected joints, taken to imply more of a systemic inflammatory effect (252). Leukocyte EVs were the dominant subtype in the synovial fluid, enhancing the release of interleukin (IL) 8, IL6 and other proinflammatory

cytokines (253). PEVs are also implicated in systemic inflammation from sepsis. PEVs are increased significantly in these patients and injecting these EVs into mice led to an increase of cytokine production and oxidative stress (OS) (254). The association of PEVs and inflammation leads to a possible implication in PC transfusions high in PEVs (1.3.6.3).

An increase in PEVs has been associated with a number of clinical disorders. For example, Wiskott-Aldrich Syndrome (WAS) is an inherited disorder causing patients to suffer from severe bleeding from thrombocytopenia and small PLT size. The cause of this is due to a mutated WAS protein involved in cytoskeleton remodelling and WAS PLTs expose a large quantity of PS (255). These PLTs release many PEVs which can lead to increased inflammation (256).

1.3.6.3 PEVs in Transfusion

PEVs have been confirmed in PCs in multiple studies (82, 83, 257-259). The current understanding of PEVs in PCs is that they might be linked to the PSL, due to being produced after PLT activation and/or apoptosis during storage. The largest contributor to PC heterogeneity is considered to be the presence of PEVs (257, 260). Black et al in 2015 (83) looked to use PEVs as a QC approach (83). Using flow cytometry and various markers of PLT activation, they showed over time in storage as functionality decreased, PEVs increased. This increase of PEVs correlated with the increase in TRAP-6 functionality impairment, but more research is needed to confirm this as a QC measure. With the increased interest surrounding PEVs within transfusion, Elisabeth Maurer led a team which developed the ThromboLUX. ThromboLUX uses dynamic light scattering to measure particles moving in suspension, and relies on the phenomenon the faster the movement, the smaller the particle. ThromboLUX can measure microparticles, PLTs and microaggregates at the same time (92). She evaluated that high PEV counts correlated with high ESC, and therefore would lead to poor recovery due to pre-activation of PLTs (257). ThromboLUX score also correlates with the morphology of PLTs, as low PEV number correlates with a high number of discoid PLTs (82). The research is pointing towards “personalised medicine”, whereby a high PEV number is reflecting PLTs are pre-activated, therefore will have a low recovery upon transfusion. Patients who are thrombocytopenic will not

benefit from this type of PC, whereas it is hypothesized a trauma patient might benefit due to the superior pro-coagulant capabilities of PEVs. This theory is supported by Maurer and more research using ThromboLUX and other PEV characterisation methods are being tested to support or reject this hypothesis.

Studies have assessed PEVs in relation to the method of PC production. Different production methods where different centrifugal forces were used alters PEV production. It is important to note that PEVs have been detected in both apheresis and buffy coat PCs (261, 262). A study by Noulsri et al investigated the number of PEVs using flow cytometry from different PEV production methods. Results showed higher PEVs in apheresis compared to BC PCs, however this was dependent on the apheresis machine used (263). The data also suggests that BC PC are less activated compared to PC produced by apheresis. PCs are irradiated to increase safety of the unit. Irradiation is mainly used to prevent the proliferation of WBCs (264), therefore reducing the incidence of graft vs host disease post transfusion. It has been shown that irradiation increases EV production 4-fold using lung cancer cell lines compared to the control (265). When investigated with PCs however, there was no significant increase in the PEVs produced over the storage period, suggesting that irradiation of PLTs does not induce microvesicle production (83).

PEVs have been indicated to have a role in adverse reactions from transfused PCs. Sub-populations of PEVs have been shown, initially by Boudreau et al (217), to contain respiratory-competent mitochondria. These mitochondria can be transferred to other cell types causing inflammation by means of damage-associated molecular patterns (DAMPs). Mitochondrial DNA (mtDNA) released from the hydrolysis of mitochondria can lead to leukocyte activation and inflammatory responses. PEVs harbouring mitochondria have been confirmed in PCs (266, 267). Cognasse and colleagues showed that PC cause adverse reactions that are associated with higher level of mitochondria positive PEVs. The PEVs increase mitochondrial DAMPs and therefore increase inflammation after transfusion and can be a suggestive cause of lung injury (268). It suggests a higher

level of PEVs in PC leads to a worsened outcome in transfused patients, especially those who are already severely compromised.

The current question therefore with PEVs in transfusion is “are PEVs detrimental or advantageous to the recipient?” PCs high in PEVs may lead to an increased risk of venous thrombosis and embolism after transfusion (269). If paired with a possible hypercoagulative state this could negatively impact the patient, and this is usually seen when PEVs are at the highest (older PCs).Clinical trials have observed the haemostatic advantage of older PCs, which could be due to a high PEV level (270), suggesting benefits to patients in trauma. The use of PEVs as a functional infusible product has been indicated by numerous studies (271, 272). These PEVs when injected into mice reduced bleeding time without increasing PLT count (273). A review on these methods of infused PLT membranes can be found elsewhere (274).

1.4 Thesis Hypothesis and Aims

1.4.1 Hypothesis

Storage condition guidelines were tested and established in 1980s, with old PC technology and a lesser understanding of the role of EVs within transfusion. I therefore hypothesise that optimisation of the external storage environment used for PC, will improve PLT function, PC longevity and alter EV character, to improve transfusion outcomes.

1.4.2 Aims

In order to investigate this hypothesis, several objectives were determined and were split into individual results chapters, each containing specific aims. Broadly, the overarching thesis aims were as follows:

1. Define haematological and EV measures in a healthy donor population and fresh PC currently not measured within the transfusion sector.
2. To investigate the effect of temperature of PC storage on PC function, EV concentration and pro-coagulant potential of PC EV.
3. Assess whether optimising O_2 to a physiological level improves PC quality.
4. Optimise the O_2 availability within PCs to minimise areas of hypoxia.

2.0 Methods

2.1 Platelet Concentrate Preparation

2.1.1 Background

In Wales, 56% PCs are prepared by the BC method compared to apheresis (see section 1.2.1). Preparation is in-line with the red book guidelines (275). PCs are diluted with a PAS:Plasma ratio of 65:35, which has been extensively researched to provide the optimal storage media for the current generation of PAS (see section 1.2.4). The current components of the PAS used are shown in the table 2.1 below.

Component	***mmol/L***
Na_3 citrate $\cdot 2H_2O$	*10.8*
Na acetate $\cdot 3H_2O$	*32.5*
NaH_2PO_4	*6.7*
Na_2HPO_4	*21.5*
$MgCl_2 \cdot 6H_2O$	*1.5*
KCl	*5*
NaCl	*69*
pH – 7.2	*N/A*

Table 2.1 **- Current components of SSP+ Platelet additive solution.**

2.1.2 Experimental Method

WB were donated by healthy individuals that have been screened by the WBS for suitability and were used under IRAS approval number 251196. PCs were prepared by standard methodology employed by the WBS (276, 277). BC obtained from WB donations were held overnight at 22^{o}C+/-2^{o}C without agitation. Four ABO identical BC were connected and pooled using 280 mL of SSP+™ PAS (Table 2.1), providing a PAS to plasma ratio of 65:35. BC were then centrifuged at 500xg for 5 minutes, followed by separation of PC by a blood component separator (CompoMat G5, Fresenius Kabi, Canada). Leukoreduction occurred at the time of separation through a reduction filter (Autostop™;

Pall Medical, Portsmouth, UK). A pool and split study design (Fig 2.1) was used to eliminate donor variability and increase the statistical power of the analysis (JPAC, Chapter 8.3, 2013). 2 ABO specific PCs were pooled into a 2:1 Transfer Pack (Termumo Europe, Leuven, Belgium) which was then split into 2 PC storage packs by weight, creating two identical PC units. PLT count was completed on a haematology analyser (ABX 80). Approximately 3 mL of PC was stripped and aseptically sampled into an EDTA tube before agitation for 30 minutes prior to PLT count. A sample site couple with needle injection site (Fresenius Kabi Limited, Cheshire, UK) was aseptically inserted into the transfusion port. A 20mL sample was taken under gravity each testing day to avoid excessive PLT activation and therefore falsely elevated EV numbers.

PCs were stored at 22°C+/-2°C under constant agitation (60 cycles/min, 1Hz/min) and shipped to Cardiff Metropolitan University under official WBS guidelines unless otherwise stated.

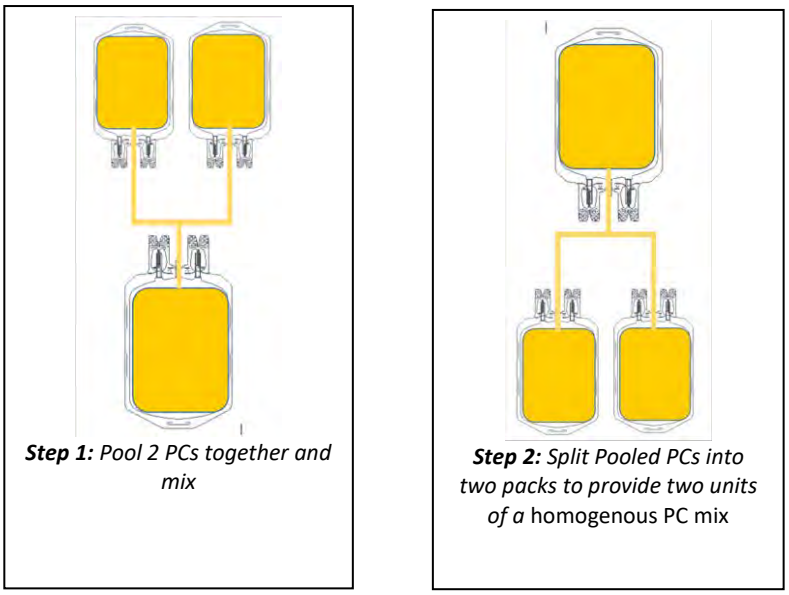

Figure 2.1– **Experimental Design.** Simplified depiction of a 'pool and split' design for creating homogenous PCs for paired experimentation.

2.2 Platelet Aggregation

2.2.1 Background

Multiple electrode aggregometry (MEA) (Multiplate®, Roche Diagnostics Ltd, Switzerland) is a measurement of the platelets ability to adhere to an artificial surface, based on the 1980 impedance aggregometry method (278). The principle is that resting platelets are non-aggregatory, however when activated by an agonist, surface receptors are exposed allowing the platelets to bind to artificial and vascular surfaces. The MEA test cell (Fig 2.2) contains two pairs of silver coated electrodes and a Teflon coated stirring bar. The impedance of current is measured across the electrode pair, recorded over 6 minutes. When platelets are activated and adhere to the electrode, the impedance is increased (Fig 2.3). Quality control is maintained by simultaneous measurements over the two pairs of electrodes. The change in impedance over 6 minutes relates to the magnitude of platelet adhesion.

Figure 2.2- **MEA Test Cell.** Two pairs of electrodes allow a current to be passed across, which when platelets activate and bind, impedance is increased. A Teflon coated stirring bar is used to keep the sample homogenous without increasing platelet activation.

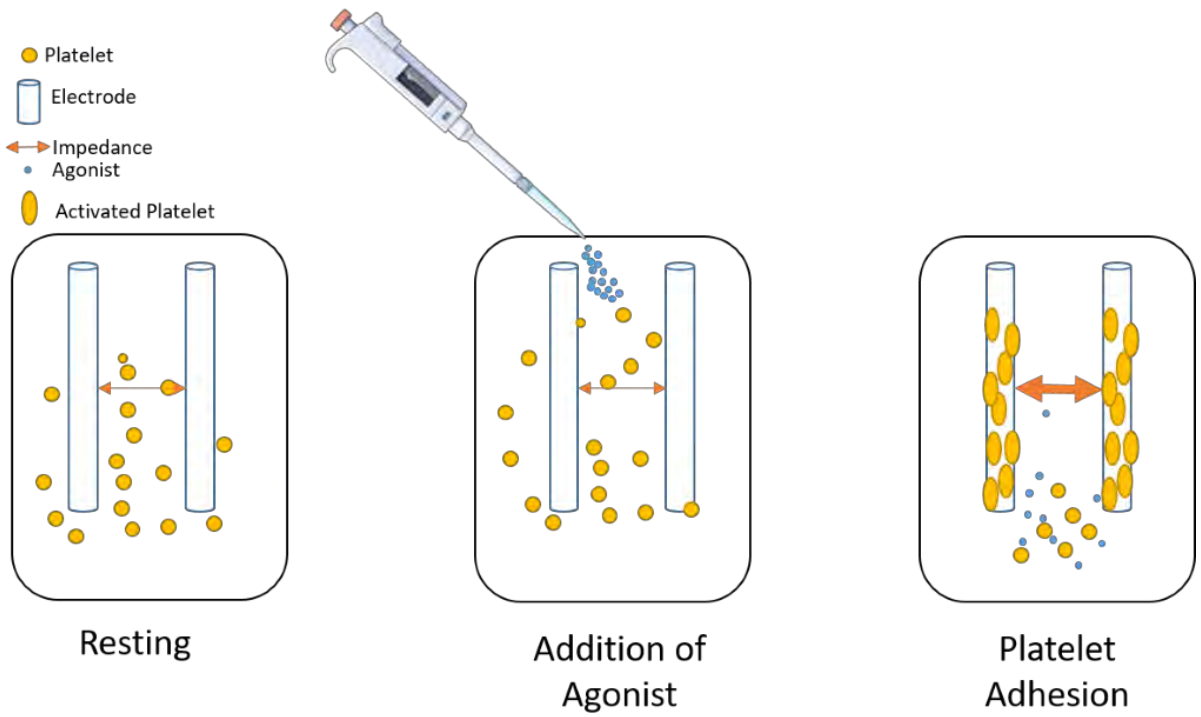

Figure 2.3 - **MEA procedure depicted**. At resting state platelets do not adhere to the electrode therefore making the impedance between those electrodes low. Once activated by an external agonist, the platelets then adhere to the electrodes, making the electrical impedance higher.

2.2.2 Experimental Methodology

MEA utilises a Multiplate ® (Roche Diagnostics Ltd, Switzerland) which measures electrical impedance across electrodes to reflect PLT aggregation in real time (279). PC (200 µL) were diluted 2:1 with SSP+™ PAS. Diluted PCs were further diluted to the manufacturer's instructions of 1:1 with 0.9% NaCl (Ristocetin) or 0.9% NaCl with 3mM $CaCl_2$ (TRAP-6) preheated to 37°C, dependent on the agonist used. A Teflon coated stirring bar kept the sample uniformly mixed. PLT activation was initiated by addition of an agonist, either Ristocetin (50 µL, 0.77mg/mL final concertation) or TRAP-6 (20 µL, 32 µM final concentration) (Roche Diagnostics Ltd, Switzerland). A panel of agonists were initially tested, however ADP did not show aggregation past day 2, so was not used in this thesis. TRAP-6 and Ristocetin had the greatest response on fresh PLTs. Electrical impedance was measured over 6 minutes and expressed as area under the curve (AUC).

2.3 Flow Cytometry

2.3.1 Background

Flow Cytometry utilises a 488nm laser to measure size and granularity of cells in solution. With the addition of fluorescent dyes, stains or conjugated antibodies, the laser can excite the fluorescence and give off a wavelength of light.

2.3.1.1 Forward vs Side Scatter

Size and granularity (density) of cells and particles can be measured without the need of fluorescent staining. As the 488nm laser hits the cell, light is scattered, and lenses detect this light. The first lens is positioned in the forward direction, (forward scatter, (FSC)), where light collected by the lens is focussed onto a photodiode. A blocker is placed in front stopping the original laser from hitting the photodetector but allowing scattered light to pass. The light scattered and measured by the detector gives a representation of the cell diameter. This is known as forward scatter. Larger cells will refract more light thus giving a higher read out.

A second lens located at a 90-degree angle relative to the laser, known as the side scatter (SSC). Side scatter measurement gives an indication of the cellular granularity. For example, a densely packed cell such as a WBC will scatter more light than a RBC.

Together these measurements can discriminate against a heterogeneous population within a blood sample or can be used to discriminate live vs dead populations. FSCvsSSC is summarised is Fig 2.4.

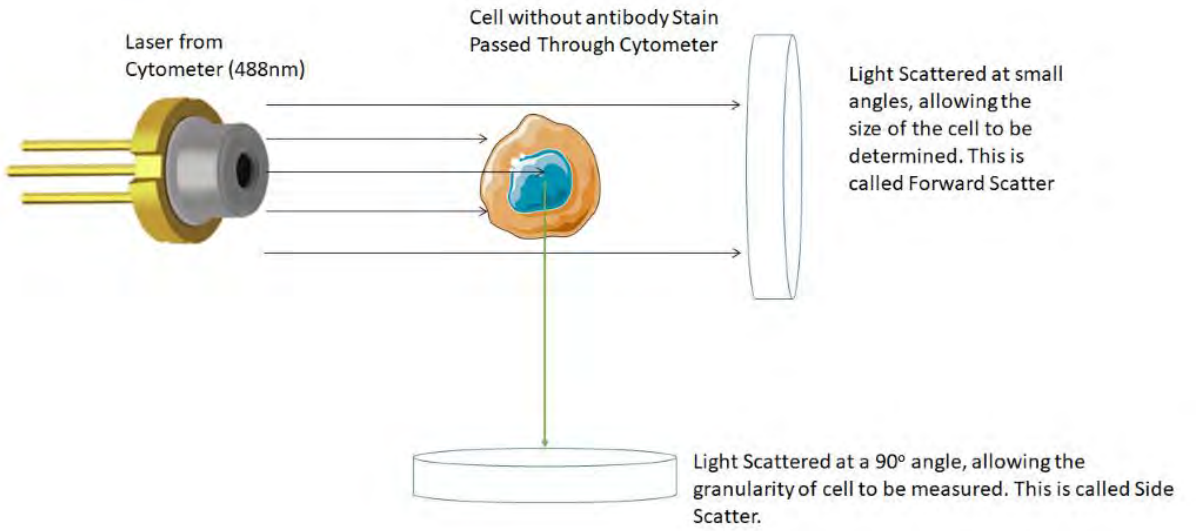

Figure 2.4 - **Basic schematic of forward and side scatter**. As a cell is passed through the cytometer, the 488nm laser hits the cell. Some light is scattered in a forward direction (FSC), based on the cells size. Light is also scattered at a 90° angle (SSC) giving a measurement on the cell's granularity.

2.3.1.2 Violet Side Scatter (405nm)

As previously eluded to in section 1.3.5.3, flow cytometry for EV visualisation has been a problem due to conventional flow cytometers struggling to separate particles under 150nm in size (280). This can lead to all exosomes and some microparticles to be missed in analysis based on size. When the particles size is smaller than the wavelength of light used, the difficulty increases to achieve a clear resolution. This is due to the light scattered being directly proportional to cells diameter and inversely proportional to the wavelength of light used. The relationship can be seen in the Mie Theory used for calculating theoretical light scattering by particles either similar or much smaller than the light used to detect said particle (281).

Based on a physical property first discovered by Newton which states entering a medium of a different refractive index, the light waves are refracted by the new medium are inversely proportional to the wavelength of the light. The smaller wavelengths of light therefore have a higher refraction (282). The use of violet 405nm over the conventional 488nm wavelength will help amplify differences in refractive indexes between EVs and media, allowing for a better resolution for detection. As previous research has shown EVs (Exosomes and microvesicles) have different refractive indexes (283).

From this point forward, when using flow cytometry for cells, 488nm was used. When analysing EVs, Violet 405nm was used unless otherwise stated.

2.3.1.3 Fluorescence Antibody Staining

Fluorescence can be used analyse the cell surface. Detecting fluorescence is similar to side scatter with the major difference being the use of wavelength specific filters and mirrors. These dichroic mirrors transmit and reflect certain wavelengths of light (Fig 2.5). The light then hits a certain photodetector where the light is measured, and the amount is converted to electrical energy. This can be done by using an antibody that is directly conjugated with a fluorochrome, which has bound to a surface marker of a cell. These fluorochromes are summarised in Table 2.2.

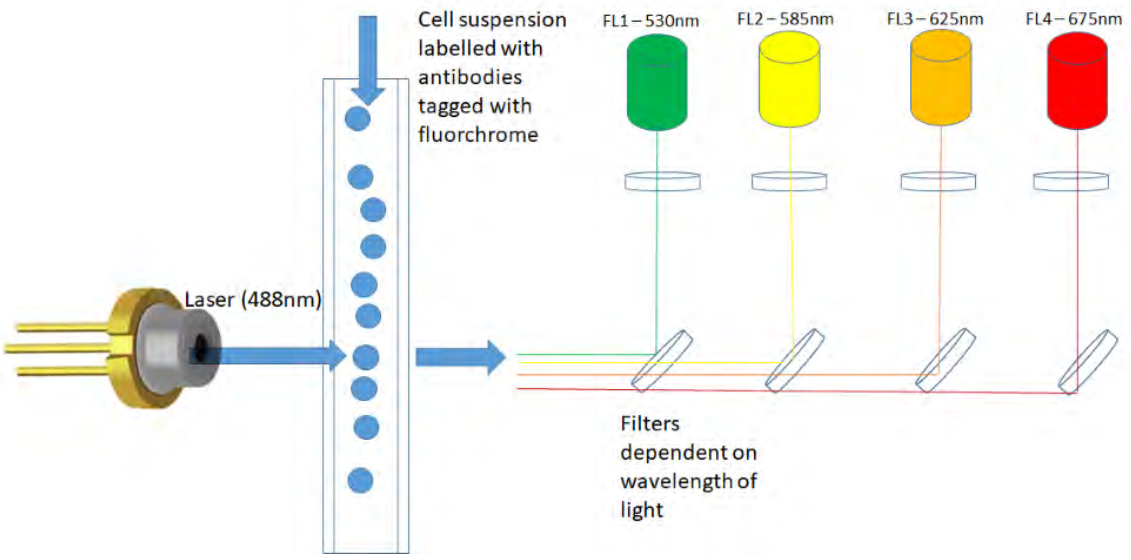

Figure 2.5 - **A basic schematic of a flow cytometer utilising four different fluorescent filters**.

Flurochrome Chart (Information form BD Bioscience)		
Flurochrome	**Fluorescence emission colour**	**EM-Max (nm)**
Pacific Blue ™	Blue	452
Alexa Fluor® 488	Green	519
FITC	Green	519
PE	Yellow	578
BD Horzon PE-CF594	Orange	612
APC	Red	660
Alexa Fluor® 647	Red	668
PE-Cy™5	Far Red	695
PE-Cy™7	Infrared	785
APC-Cy™7	Infrared	785

Table 2.2 - **The Specific wavelength of different fluorochromes commonly used for flow cytometry.** This thesis utilised FITC, PE and APC unless otherwise indicated.

2.3.2 Experimental methodology

2.3.2.1 Platelet Gating

Dulbecco's phosphate buffered saline (DPBS) was initially run for 5 minutes without cells to ensure no events were apparent in the buffer solution. Following this, EDTA anti-coagulated whole blood was centrifuged at 120xg for 20 minutes. Resulting PLT-rich plasma (PRP) was diluted 1:10 in Dulbecco's phosphate buffered saline. PRP was labelled with an allophycocyanin (APC) isotype to gate a negative APC population. PRP was subsequently labelled with APC-conjugated anti-CD41, and 20,000 events were collected. CD41 positive events were gated, and "back-gated" onto a FSC-SSC plot, allowing a PLT population to be selected and gate made. RBC isolated from WB, diluted 1:1000 was then analysed with APC isotype and APC anti-CD235a to make sure the RBC population did not fall within the PLT gate. The gating strategy is demonstrated in Fig 2.6 and 2.7.

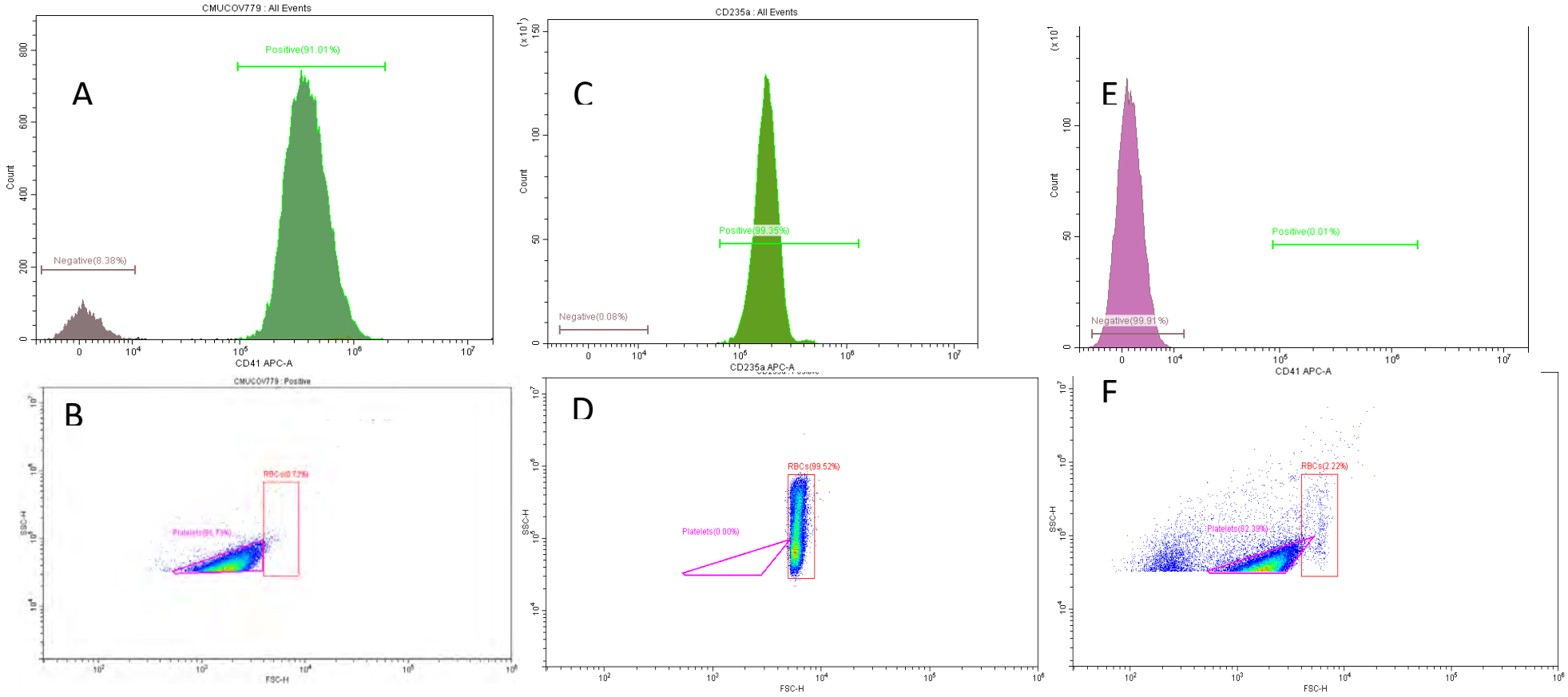

Figure 2.6 - **Gating strategy used for platelets.** A – PRP was stained with anti-CD41, where 91% of the population was positive. This population was selected and "back gated" onto a FSC-SSC plot (B), allowing a platelet population to be gated. C – RBC were stained with anti-CD235a, whereby 99% of the population were positive. The positive population were selected and "back gated" to give a RBC population on a FSC-SSC plot (D). E – PRP run with no antibody stain (99% negative) to check that the platelet gate was in the correct position based on FSC and SSC properties only (F).

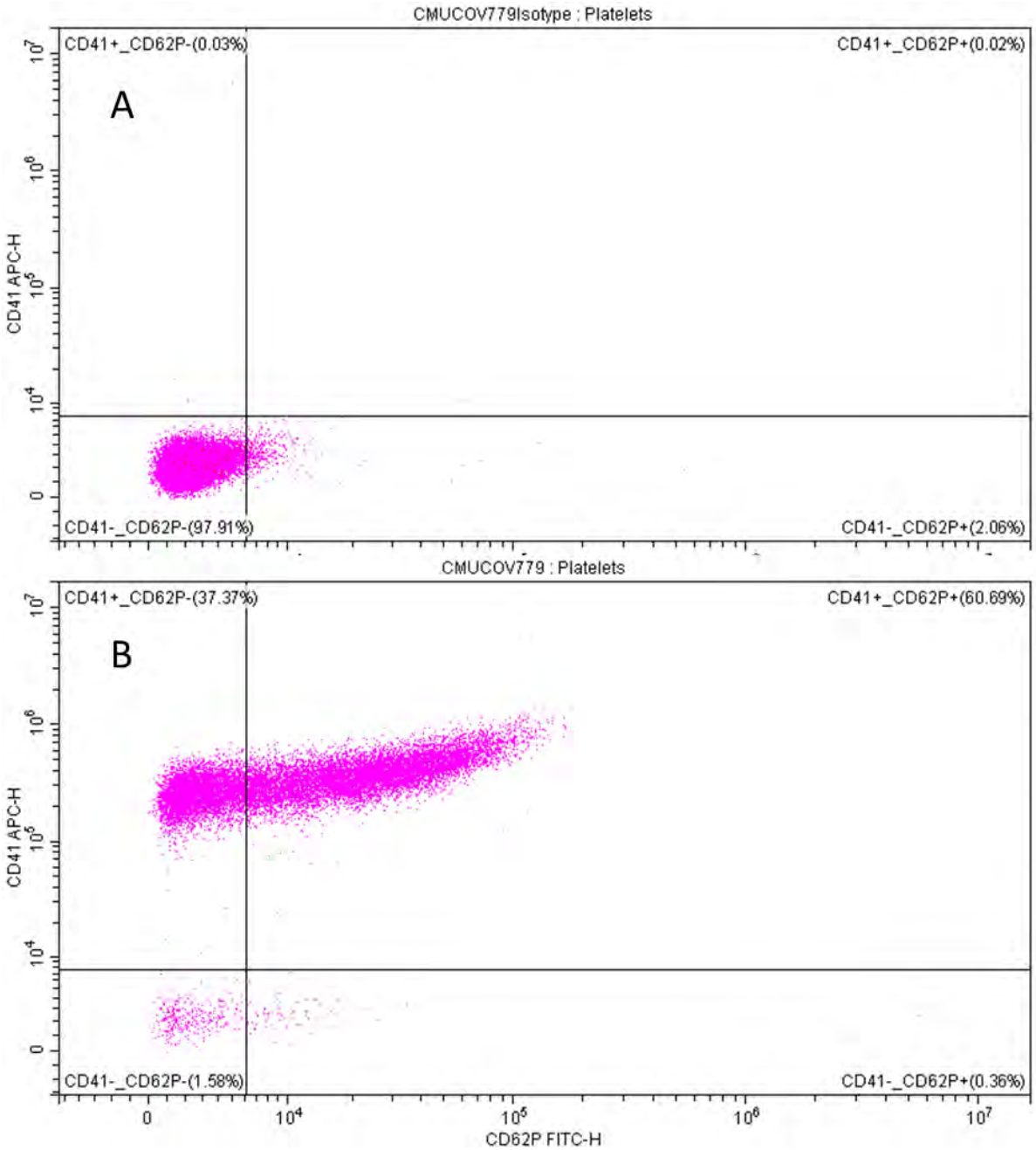

Figure 2.7 - **CD62P staining of platelets.** Based on the gating strategy (Fig 2.6), samples were labelled with APC and a FITC Isotype to determine the negative dual population before running a dual labelled anti-CD41 and anti-CD62P sample. Results were taken as the amount of CD41+CD62P+ events.

2.3.2.2 Platelet Staining for CD62P

PC was diluted 1:10 in DPBS and labelled with APC-conjugated anti-CD41 and Fluorescein isothiocyanate (FITC)-conjugated anti-CD62P (BD Biosciences) for 30 minutes at room temperature. Isotype-matched controls were used to monitor non-specific binding with each sample. 20,000 PLT

gated (See Gating strategy, Figure 2.6) events were collected and analysed on a Cytoflex flow cytometer (Beckman Coulter) for CD62P+ expression (%) (Fig 2.7).

2.3.2.3 Gating Strategy – CD9 positive selection of EVs

DPBS, filtered through a 0.2µm filter, was initially run for 5 minutes to ensure no events were apparent in the buffer solution. EVs, isolation described in section 2.5.1) were initially analysed without antibody labelling, to determine if EV populations could be distinguished from other particulates. EVs were then stained with Phycoerythrin (PE) Isotype. A PE threshold was then set to eliminate all events. EVs were labelled with PE anti-CD9 and 20,000 events were collected. These were gated as CD9+EVs. An unstained EV sample was then run to check that no events were present if PE anti-CD9 was not used. Subsequent analysis of EVs required PE-anti-CD9 plus a second antigen marker of interest conjugated to a different fluorophore (APC). Fig 2.8 shows the gating strategy, with Fig 2.9 depicting the EV gate. PE-anti-CD9+ labelled EVs were also mixed with a detergent for 15 minutes to check disappearance of events due to the lysis of EVs. This confirms the presence of EVs.

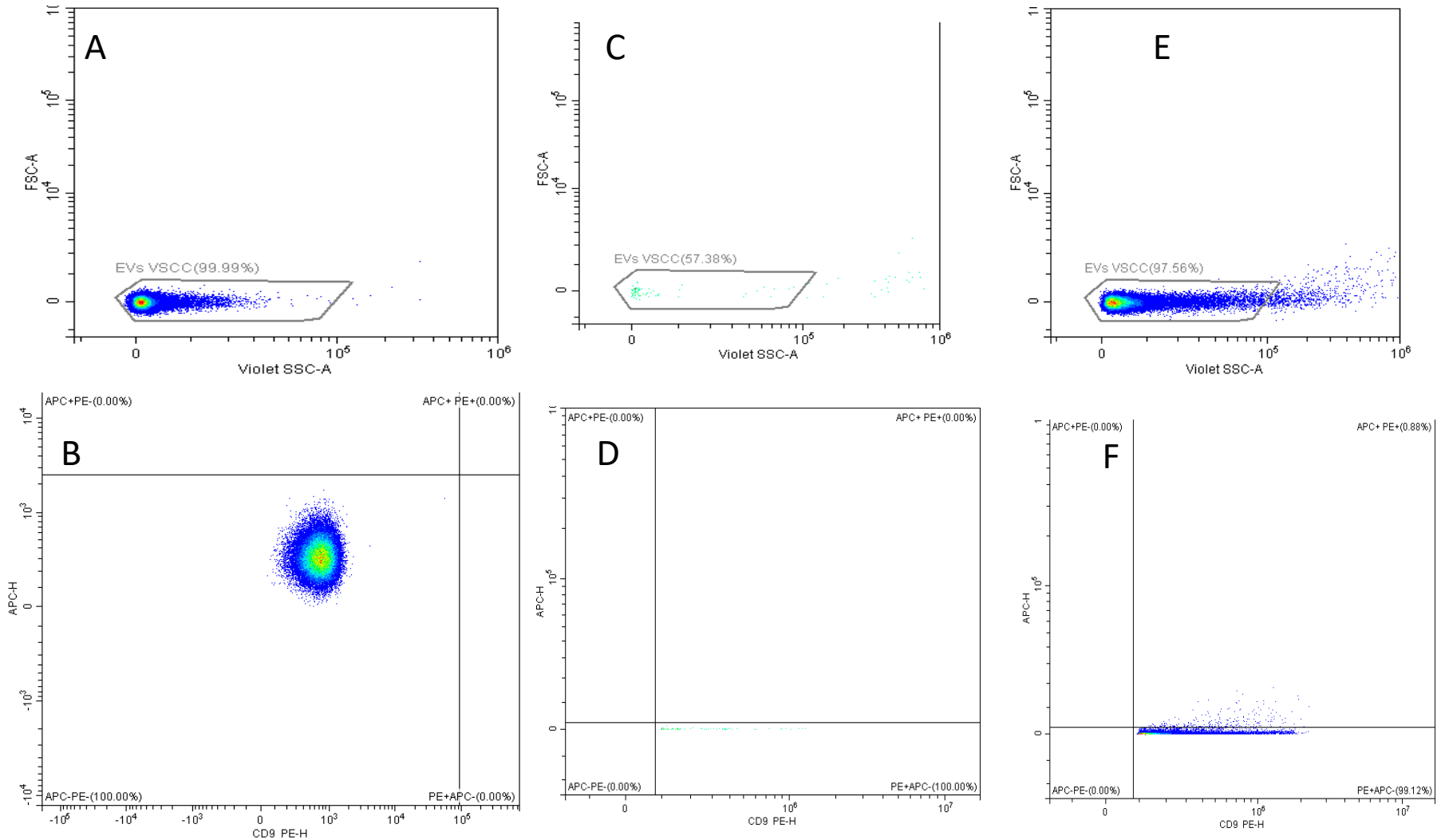

Figure 2.8 - **EV Gating**. A&B - EVs were analysed with no label and plotted onto a violet SSC-FSC plot and a dual PE vs APC plot. This could not discriminate between "non-EV sized particles". C&D – EVs were labelled with a PE Isotype and a threshold on PE was set until no PE events were seen in the quadrant PE+APC-. After 5 minutes, only 120 events were recorded, this was taken as a negative result. E&F – EVs were labelled with PE anti-CD9 and events were collected up to 20,000.

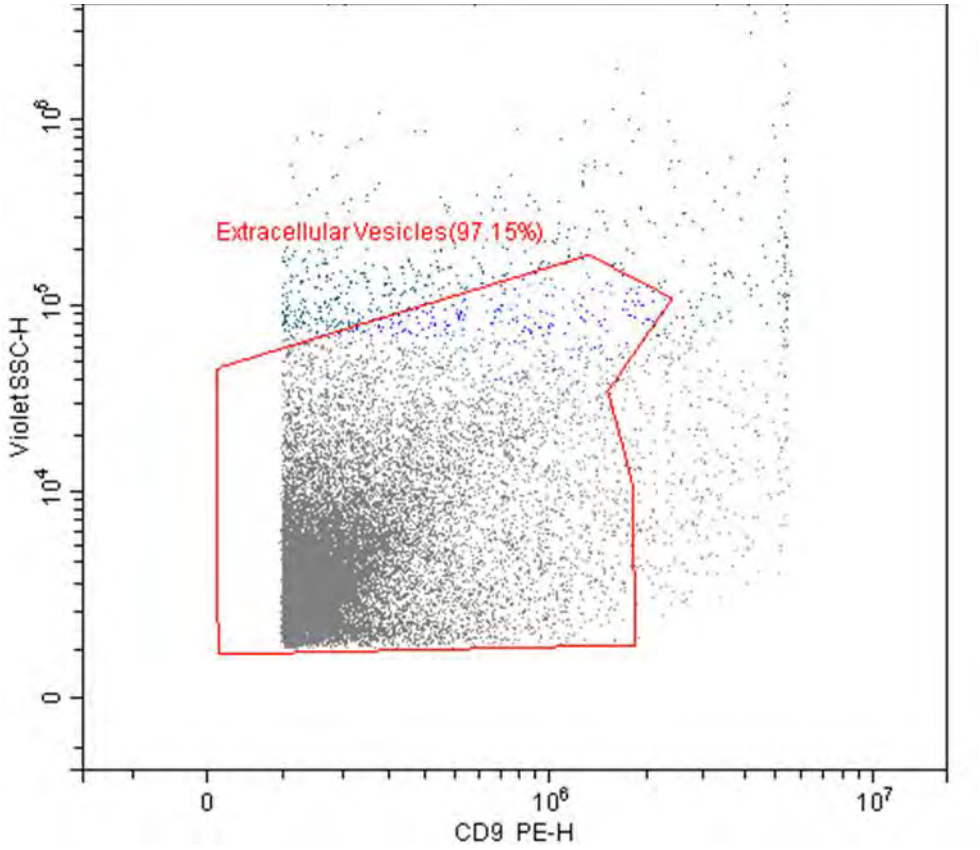

Figure 2.9 - **EV gate**. Based on figure 2.8 gating strategy, an EV gate was set up based on CD9 positivity and VSC which determines size. This gate was used to select EVs which were dual stained when analysing further antigenic markers.

2.3.2.4 EV subtype analysis

EVs (80 µL) were labelled with PE-anti CD9 (20 µL) and subtype antigenic marker (5 µL); either APC anti-CD41 (PLT), APC anti-CD144 (endothelial), APC anti-CD235a (RBC) or APC anti CD11b (WBC). These were incubated for 20 minutes in the dark and diluted using DPBS to a final volume of 250 µL. 20,000 events or total sample volume was collected and analysed on a Cytoflex Cytometer (Beckman Coulter) for dual antigen positive expression (Expressed as a percentage).

2.4 Electron paramagnetic resonance (EPR) Oximetry

2.4.1 Background

EPR Oximetry is a well-established method applied extensively to measure [O_2] in vivo and ex-vivo (284-286). The principles of EPR oximetry involves a free radical based chemical (which can be soluble or particulate in nature). The probe utilised in this thesis has a neutral nitroxide, 4-oxo-2,2,6,6-tetramethylpiperidine-d~6-1-oxyl (^{15}N PDT). ^{15}NPDT is soluble, therefore addition to a cell suspension results in distribution throughout the extracellular and intracellular space of the sample. The EPR spectral line width of nitroxide is sensitive to environmental parameters leading to signal broadenings due to immobilisation of the nitroxide probe. O_2 is a paramagnetic molecule that can affect the EPR spectral linewidth (287), and therefore can be used to measure concentration and consumptions in cellular preparations (287, 288). Spin-label oximetry measures O_2 based on broadening of the nitroxides, arising from interactions associated with the unpaired electron with protons and within the nitrogen atom. This sensitive interaction has allowed total and intracellular concentration of O_2 to be measured ranging from 0 to super saturation (287)

The probe used ^{15}NPDT contains a free radical (Fig 2.10).

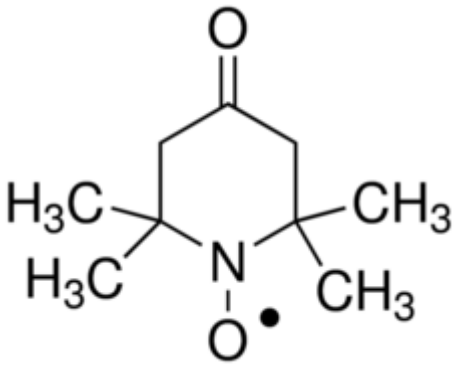

Figure 2.10 - **^{15}N PDT chemical structure.**

2.4.2 Calibration

EPR calibration was performed using 0.2mM PDT in PAS drawn into a gas permeable Teflon® tube and inserted into a quartz capillary tube open at both ends. The tube was perfused with either Nitrogen (0% O_2) or ambient air (21% O_2) to determine the spectral line width at the minimal and maximal [O_2] (Fig 2.11, $[O_2]_{nitr}$ and $[O_2]_{air}$, respectively). [O_2] measured in the experimental sample ($[O2]_{sample}$) can then be calculated according to the equation 2.1.

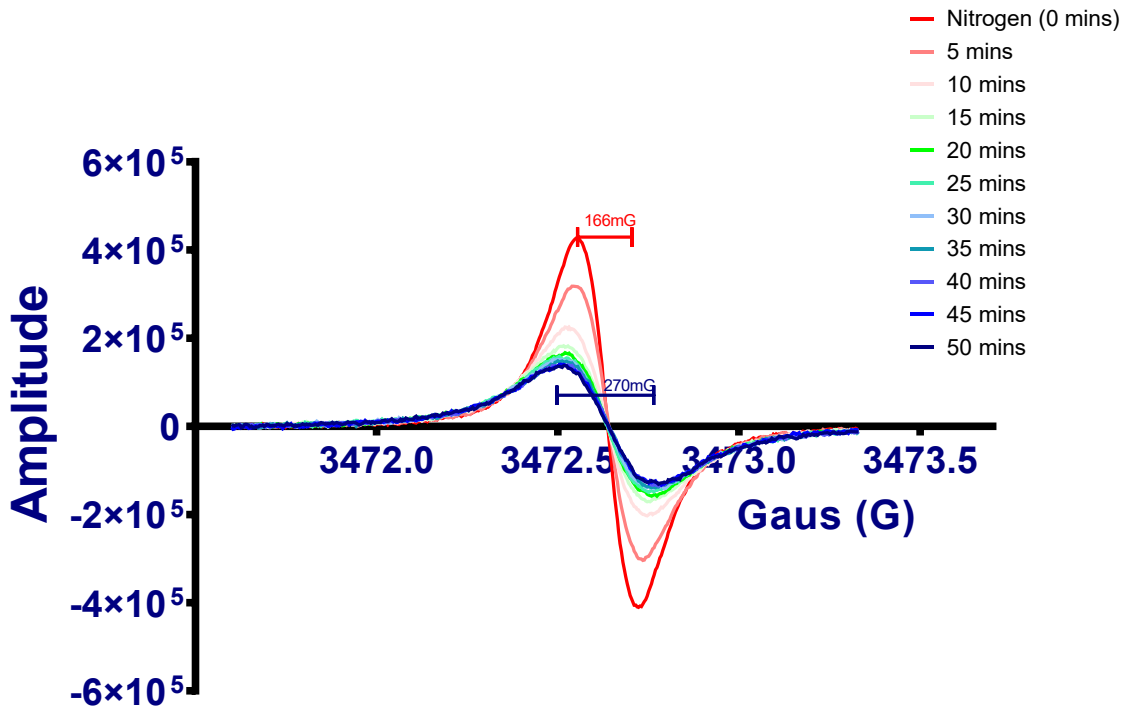

Figure 2.11 - **PDT signal broadening with oxygen exposure.** As the nitrogen is stopped and atmospheric air is introduced to the probe, the signal from the PDT begins to broaden. Over time, this signal will reach the same width as the calibration curve shown in the above figure. This demonstrates that within the same sample, the line width will change relative to the amount of oxygen present.

Using the calibration, the equation 2.1 below is used to determine oxygen concentration.

$$\frac{[O2]_{sample} - [O2]_{nitr}}{[O2]_{air} - [O2]_{nitr}} \times 210_{\mu}M$$

Equation 2.1 – **Calculation of [O] using EPR.**

2.4.3 Oxygen Consumption Rate

OCR can be measured by utilising the change in $[O_2]$ over a set time. As O_2 is utilised the EPR signal will narrow (Fig 2.11). Taking measurements at one-minute intervals allows a rate to be calculated over time. Fig 2.12 shows multiple line width measurements to give delta line width over 30 minutes.

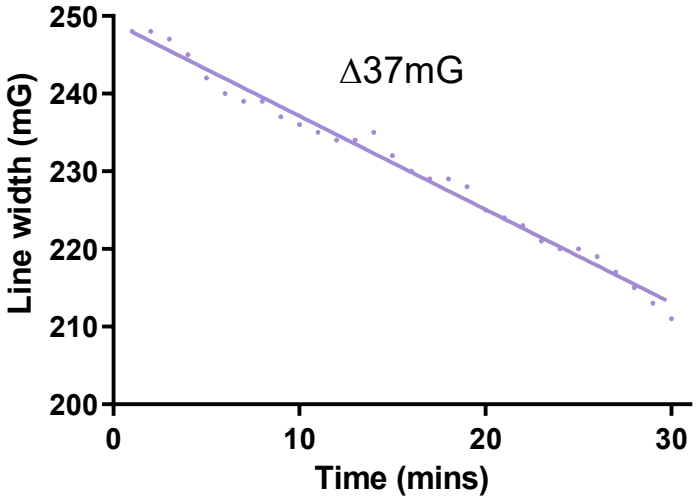

Figure 2.12 - **Oxygen consumption rate.**

The delta over time can be utilised to calculate the OCR rate per minute for x number of cells. This will be described for PCs used in this thesis. The protocol used is detailed below.

1. Calculate the change in line width over the 30 minutes.
2. Convert this line width to [O] using a modified equation 2.1.
    a. $\frac{\Delta[O2]_{\text{sample}}}{[O2]_{\text{air}} - [O2]_{\text{nitr}}} \times 210\mu M$
3. µM is µmoles/L, for PC, sample used is 100µl. Converting to 100µl allows the PLT concentration to be used. This was based on an average PLT count derived from all units tested within the thesis.
    a. $\frac{2a}{10{,}000}$ (100µl PC = ~1x10^8 PLTs)
4. Then convert µmoles/1x10^8 PLTs to nmoles/1x10^8 PLTs
    a. $3a \times 1000$

5. To get the rate, divide by time taken, which was 30 minutes
    a. $\frac{4a}{30}$
6. This gives an oxygen consumption rate as nmoles/1x10^8 PLTs /min.

The OCR as calculated above was plotted as a single point in the results throughout the thesis and was compared to other measures at different storage times and conditions.

2.4.4 Experimental Methodology

100µl of undiluted PC (typically 1x10^8 PLTs) and ^{15}N PDT (0.2mM) were mixed and drawn into a glass capillary tube, then sealed at both ends using Critoseal to create a closed system. The EPR spectra were recorded for 30 minutes at 1-minute intervals to generate a linear plot of spectral linewidth against time to calculate the rate of linewidth change. This was converted to O_2 using the $[O_2]_{nitr}$ and $[O_2]_{air}$ reference points as above. The starting O_2 was taken to reflect the direct concentration of O_2 inside the bag. In-bag $[O_2]$ measures were recorded at day 2 for PC and a PAS only control.

Spectra were recorded on a Bruker ER 220DSRC ESR spectrometer. The sealed capillary sample was placed into the ESR cavity and maintained at 22^{o}C throughout.

Typical spectrometer conditions applied were –

Amplitude of modulation – 0.07G

Modulation Frequency – 86kHz

Attenuator – 30dB

Centre Field – 3472.4G

2.5. Extracellular vesicles

2.5.1 Isolation

EVs cannot be isolated via normal centrifugation methods, and requires centrifugation at 100,000xg to pellet EVs out of a sample (section 1.3.5.2). PC (~4 mL) samples were centrifuged at 800xg for 20 minutes to separate the PLTs. The supernatant was subsequently centrifuged at 3000xg for 10 minutes at 22^{o}C, twice, to achieve platelet poor plasma (PPP), which was acellular. PPP was then subjected to a final ultracentrifugation of 100,000xg for 60 minutes at 4^{o}C to pellet the EVs. The EV pellet was re-suspended in 0.2µm filtered DPBS. EVs were re-suspended in 50µl of DPBS for every 1ml of PPP ultracentrifuged. EV isolation was based on a standardised protocol used in multiple clinical studies (289) and applied in our research laboratory when the source sample is a single cell type, following ISEV guidelines (126).

2.5.2 Storage

EVs were stored at 4^{o}C±2^{o}C for a maximum of 7 days before analysis, or were slow frozen at -1^{o}C a minute, to –80^{o}C using a Mr. Frosty ™ (ThermoFisher, UK) if storage was for longer than 7 days, which is a protocol used extensively within our laboratory group.

2.5.3 Nanosight Tracking Analysis

2.5.3.1 Background

Nanoparticle tracking analysis (NTA) is a well-accepted and documented method for the analysis of EV. Previous methods have included flow cytometry and electron microscopy. These can confirm the presence of EVs but have limitations. For example, flow cytometry has a limit of detection between 150-200nm, unless a highly sensitive cytometer is used. Electron Microscopy is non-quantitative and requires significant preparation, highlighting an additional issue (290).

NTA allows rapid, accurate analysis of the concentration and size distribution of particles sized 10-1000nm in diameter, covering the EV spectrum. Particles are suspended in DPBS and passed through the Nanosight, where the particles interact with a 405nm laser, causing light to scatter (Fig 2.13). The particle size is determined from the displacement of light within a time frame due to

Brownian motion (291). This is viewed via a 20x magnification microscope onto which a camera is mounted, capturing 30 frames a second.

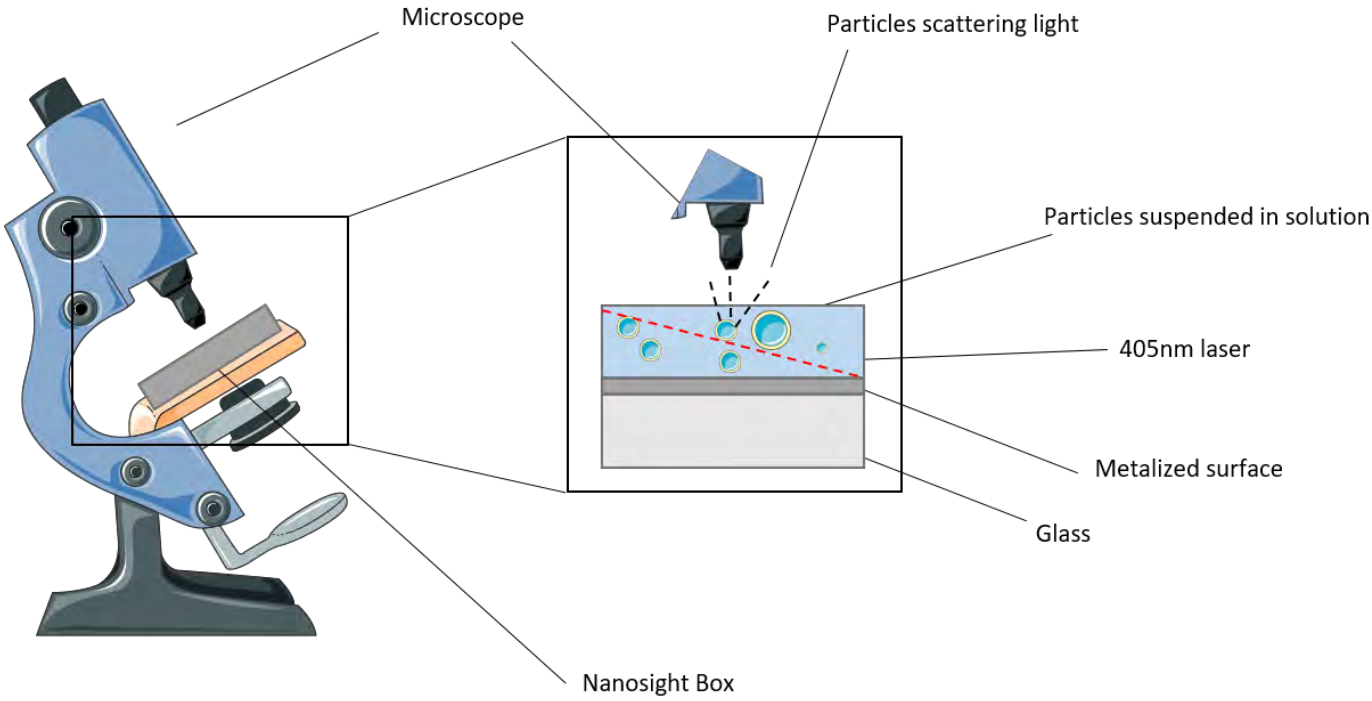

Figure 2.13 - **Basic depiction of the Nanosight**

The NTA software tracks the particles individually, which is then inputted to the Stokes-Einstein equation to generate the hydrodynamic properties. The Stokes-Einstein equation is shown below (Equation 2.2):

$$\frac{D = KbT}{6\pi\mu R0}$$

Equation 2.2; **Stokes Einstein Equation.** Whereby D – Diffusion constant, μ - solvent viscosity, R_0 – solute radius, K_B – Boltzmann's constant and T – temperature (Kelvin). The analysis gives the mean size distribution of the particles in solution on a graph.

2.5.2.2 Experimental methodology

Concentration and size distribution of EVs were determined using NTA, based on tracking movement of EV illuminated by a 405nm laser source as previously described (289). Briefly, EV samples were diluted in DPBS to range from 10^6-10^9 particles per mL (p/mL), prior to being measured and NTA software used to analyse the results.

2.6 Turbidimetric Clotting and Lysis Assay

2.6.1 Background

The basic principle of this method is based on secondary haemostasis (for detail see section 1.1.3) where the introduction of thrombin in plasma containing all of the clotting factors starts the coagulation cascade inevitably forming a fibrin clot. Due to the structure and light properties of the fibrin clot, when formed the amount of light being able to pass is decreased, leading to an increase in turbidity measured at an absorbance of 340nm. This property allows “real-time” analysis of the fibrin clot formation.

Based on the same principle, when the clot has lysed the turbidity of the plasma decreases due to the amount of light measured by the detector increasing. Using tPA, the most potent activator of fibrinolysis, a “real time” measure of fibrinolysis can be measured. When used *in vitro* together, thrombin and tPA can allow the analysis of fibrin clot formation and lysis using the properties of turbidometry. This was originally developed without the addition of EV and applied to patient cohorts by other teams (292).

I have developed the method to assess EV procoagulant capabilities by adding a fixed number of EVs to the assay to assess the impact EVs have on the formation and lysis of a clot (Fig 2.14) , which has been published (293).

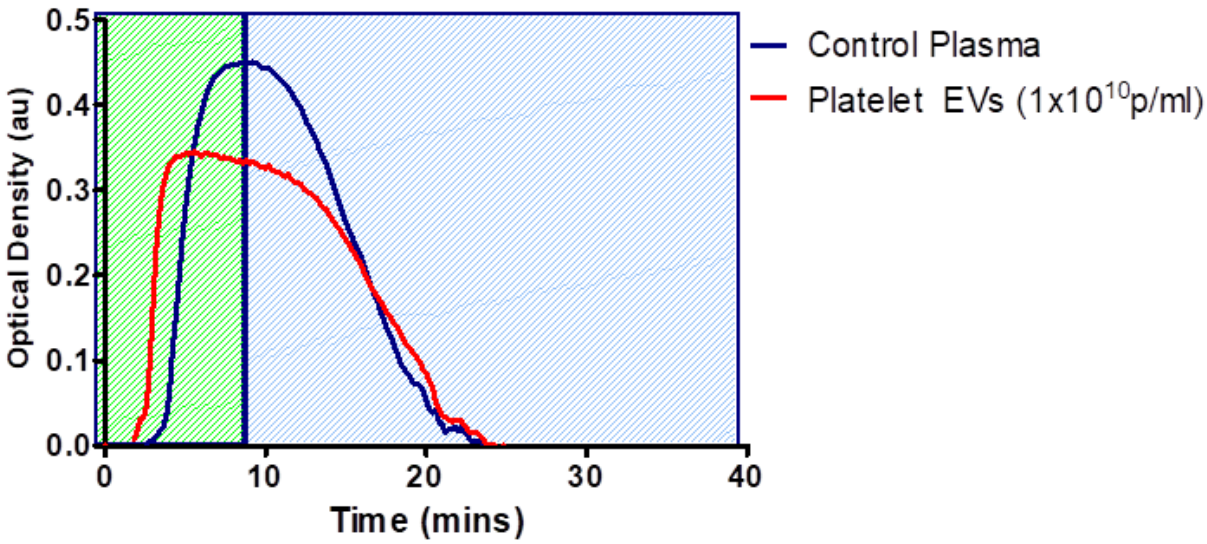

Figure 2.14 - **An example turbidometry trace;** of fresh frozen plasma without (Blue) and with the addition of Platelet Derived EVs (red) at a final concentration of 1x1010p/ml. The green area represents the formation of the clot. The blue area represents the lysis of the formed clot, relative to the control. The graph demonstrates clot formation and lysis is complete within 1 hour.

2.6.2 Experimental Method

Human donor pooled citrated plasma (25 µL) was added to assay buffer (0.05 mol/L Tris-HCl, 0.1 mol/L NaCl, pH 7.4) (65 µL) in a 96 well-plate. $1x10^{10}$ EVs were then added to the plasma for 10 minutes. 12.5 ng of tPA (Technoclone, Austria) was added to the assay buffer (83 ng/mL final concentration) before adding the activation mix (final concentrations: 0.03 U/mL thrombin (Merck, Germany) and 7.5 mmol/L calcium (30 µL). Plates were read every 12 seconds at 340nm absorbance for 1 hour at 37°C. The reaction caused fibrin clot formation and complete lysis within an hour. Clot lysis was defined as the time taken to reach 50% lysis.

2.6.3 Optimisation

Due to using different suppliers than Leeds University where training for the assay was completed, a range of concentrations of thrombin and tPA were tested to ensure the correct concentration was being used. As Fig 2.15 shows, 83ng/mL of tPA showed a 50% lysis of ~10 minutes, which when increasing the concentration did not significantly improve. Fig 2.16 shows 0.03 U/mL of thrombin showed a lag-time of ~255seconds, which when increasing did not improve. Therefore, the optimisation demonstrated that appropriate concentrations of thrombin and tPA were selected.

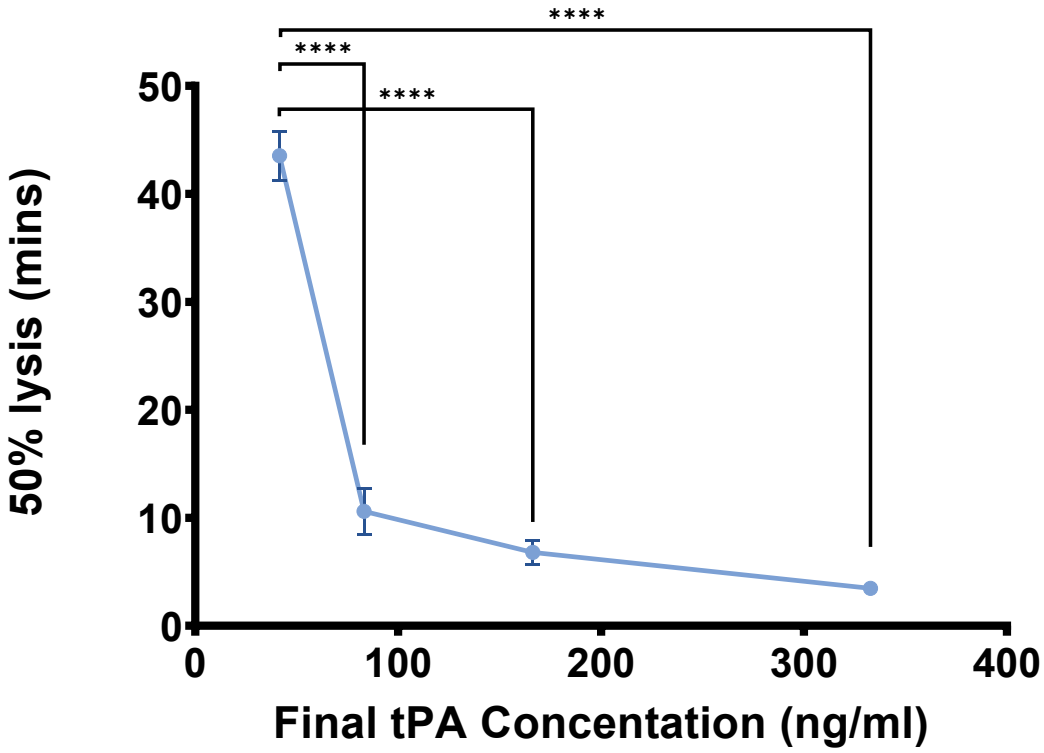

Figure 2.15 - **Optimisation of tPA**. ****p<0.0001, error bars denote SD.

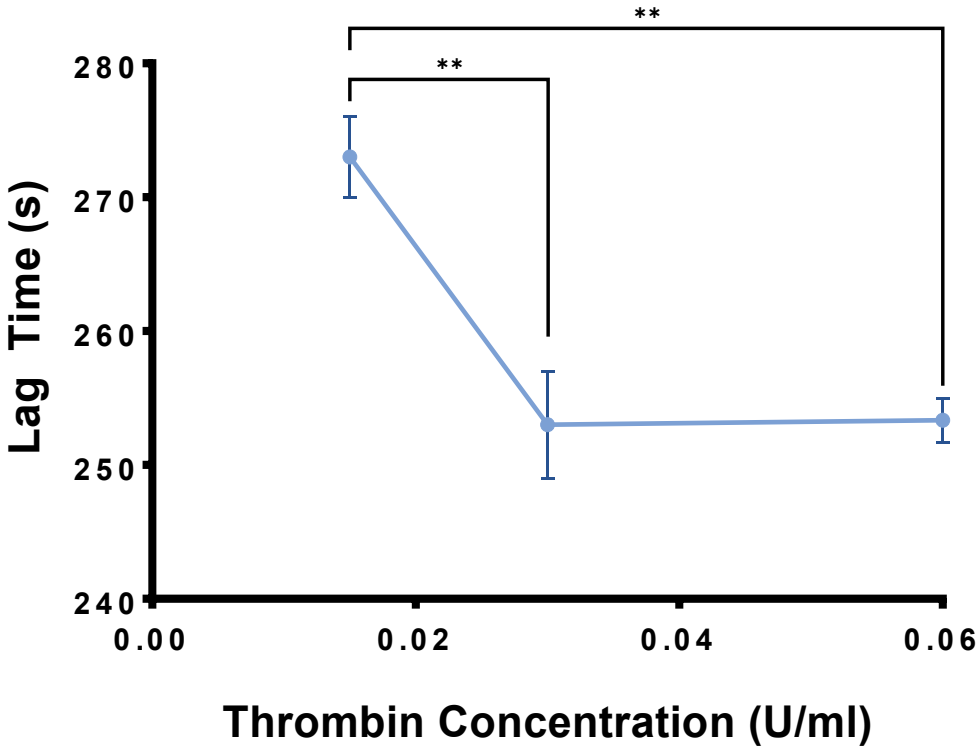

Figure 2.16 - **Optimisation of Thrombin.** **p<0.01, error bars denote SD.

2.7 Western Blotting

2.7.1 Background

Western Blotting is used to detect specific protein in a sample utilising primary antibodies. The process involves using denatured proteins applied to gel electrophoresis allowing separation of the protein by molecular weight. The proteins are transferred to a nitrocellulose membrane. The membrane is probed by antibodies specific to the protein, for example CD41 for platelets, before chemiluminescence detection. This process will be described here.

2.7.2 Sample preparation

PCs were sampled and washed in in SSP+. 100uL of Ice-cold RIPA Buffer with added protease inhibitors was added to washed PLTs. PLTs were kept on ice for 30 minutes before centrifuging at 13,000g for 20 minutes at 4^{o}C to pellet cellular debris. The supernatant was taken and stored in a sterile Eppendorf at -80^{o}C until further analysis.

For EV lysis, 200uL of ice-cold RIPA buffer with added protease inhibitors was added directly to an EV pellet isolated from a PC via ultracentrifugation (see section 2.5.1). EV lysates were kept on ice for 10 minutes before transferring to a sterile Eppendorf and stored at -80^{o}C until further analysis.

2.7.3 Gel Electrophoresis (Nu-PAGE)

Polyacrylamide gels (8%) were obtained from ThermoFisher. The gels were placed into the electrode assembly unit and flooded with running buffer (Table 2.3). 20-60µg of protein was mixed with loading buffer and reducing agent (ThermoFisher, UK). Protein samples were denatured at 95^{o}C for 10 minutes. Once denatured, protein was loaded onto the gel and separated by electrophoresis (Fig 2.17). A pre-stain protein ladder (ThermoFisher, UK) was also added to the gel for reference. Proteins were resolved at 180V for 1 hour in running buffer.

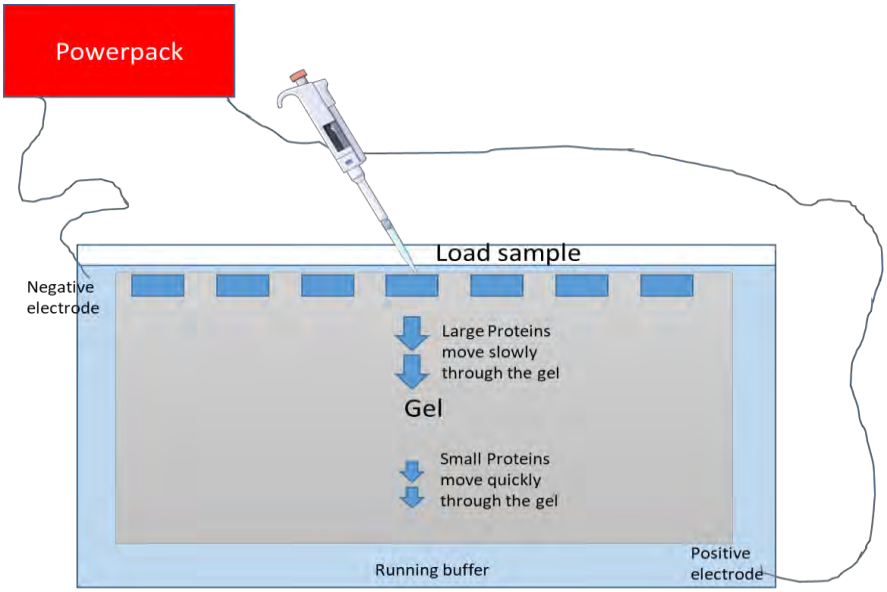

Figure 2.17 – **Gel Electrophoresis set up for the seperation of protein.**

Component	**Weight (g)**
Tris	30
Glycine	144
SDS	10

Table 2.3 - **Running Buffer 10X used in the electrophoresis separation of protein.**

2.7.4 Electroblotting

0.45µm nitrocellulose membrane was soaked in methanol for 1 minute and "sandwiched" between blotting paper and foam pads within a blotting cassette. Proteins were transferred at 100V for 1 hour in ice-cold transfer buffer, components in table 2.4 (Fig2.18).

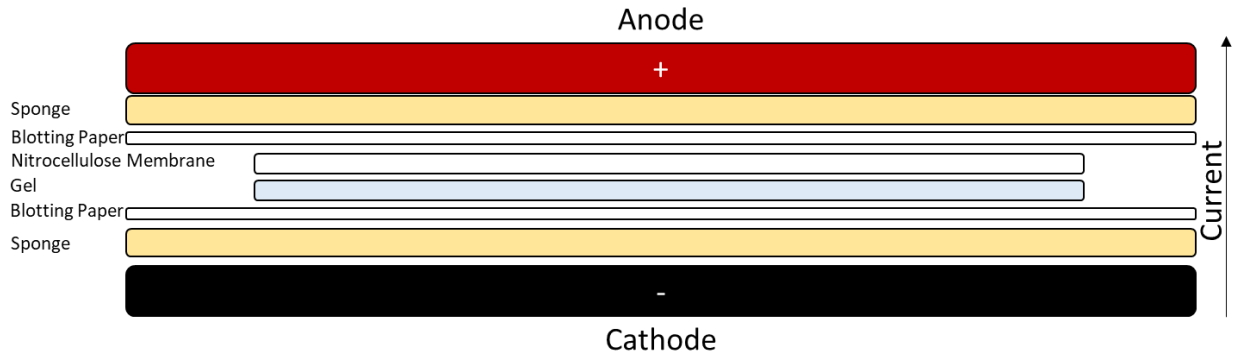

Figure 2.18 - **Transfer of proteins via electroblotting**. Schematic showing the arrangement of components for transfer in Western blotting.

Component	Weight (g)
Tris	3.025
Glycine	13.66

Table 2.4 – **Transfer buffer used in electroblotting**

2.7.5 Target Antibody probing

The nitrocellulose membrane was washed 3 times in tri-buffered saline-tween (TBST) for 5 minutes on a plate shaker. TBST was produced by diluting 10X TBS and adding 500ul of tween (Table 2.5).

Component	Weight (g)
Tris	60.6
NaCl	87.6
HPLC Grade Water	1L (1000)

Table 2.5 - **10X tri-buffered saline used to formulate tri-buffered saline-tween.**

Using 5% skimmed milk powder with TSBT, the nitrocellulose membrane was blocked for 1 hour, stopping non-specific binding. The membrane was then incubated with the monoclonal antibody (Table 2.6) in 1% milk-TSBT overnight at room temperature. The membrane was washed 3 times in TSBT for 5 minutes before ECL peroxidase secondary antibody labelling (1:2000) donkey anti-rabbit IgG HRP-linked. Secondary antibody dilution was in 1% milk-TSBT for 1 hour.

Antibody	Clone	Supplier	Dilution
Rabbit monoclonal Anti-CD41	EPR4330	Abcam, UK	1:1000
Rabbit monoclonal Anti-CD9	D8O1A	Cell Signalling, UK	1:1000
Donkey Anti-Rabbit ECL IgG, HRP Linked	N/A	Cytiva, UK	1:2000

Table 2.6 - **Antibodies utilised for western blots within this thesis**. The dilution, clone and supplier has been detailed.

2.7.6 Photographic film development

Western Blot detection reagents were mixed in an Eppendorf, before 250µl was added to the membrane. The membrane was then exposed to photographic film in a dark room. The film was then soaked in developer until the formation of band appeared, then was soaked in water, and finally soaked in fixer. The films were then thoroughly washed, and air dried before analysis.

2.8 Statistical Analysis

Graphs are presented as mean ± SD, generated using GraphPad Prizm 9 software. One-Way and Two-Way ANOVA with a Bonferroni's post Hoc test was applied to determine significance in normally distributed data between groups.

In storage-time studies, a paired T-test was applied to determine significance over time when comparing day 2 to end of storage. Statistical significance was taken where $P<0.05$.

3.0 Results I – Defining a healthy population compared to fresh platelet concentrates.

3.1 Perspective

Healthy individuals eligible to donate blood are currently not screened for haematology or coagulation disorders and may display large variances in EV heterogeneity that could influence the PC characteristics and therefore have downstream implications on the recipient. This chapter

investigates multiple haematological and coagulation markers that define the healthy population, deemed as suitable donors. The chapter assesses the plasma EVs isolated from this population, which are not currently measured prior to transfusion. Findings will be compared to a fresh PC, investigating the effects of standard transfusion service processing.

3.2.1 Introduction

Eligibility of blood donation within the UK is considered a very crude process, with only a basic questionnaire and haemoglobin (Hb) test performed prior to donation. The WBS refer to the donor criteria of weighing above 50kg, having no series illness including heart disease, cancer or stroke and must be feeling generally well. However, none of these are directly tested or checked against medical records. The only test prior to donation is a non-quantitative Hb measure using copper sulphate to determine Hb levels. A gravity of 1.053 corresponds to a haemoglobin of 12.5g/dL, which is equal to the specific gravity of the copper sulphate solution. If the specific gravity of blood is higher than 1.053, the blood will sink, indicating a haemoglobin higher than 12.5g/dL (294). If failed, a Haemacue® test will be performed to check if levels are above 12.5g/dL for females and 13.5g/dL in males (56). These individuals would be deemed "healthy" and therefore eligible for blood donation in Wales. The Hb level of "healthy" may differ in different blood organisations. The work in this chapter and more widely throughout this thesis mirrors those deemed "healthy" to donate blood. As the measures taken are so crude, the current chapter will explore a full range of haematological indices and coagulation screen, looking in-depth at these healthy donors.

The two overarching goals depending on the patients need of a PLT transfusion is to a) return the PLT level back to a healthy range (above a defined threshold) or b) to stop active bleeding (64). Currently, when donating blood for PLT usage, the function of these PLTs is not currently tested, nor is the PLT function in PCs. The only measure of PC quality in storage is pH, whereby pH above 6.4 is deemed acceptable according to the JPAC guidelines (275).

EV concentration and characteristics in the donor or recipient are not considered within a transfusion context. A high proportion of variability in EV is observed within the general population due to multiple factors including variations in height, weight, and any underlying conditions in which all impact EV populations. Within the last decades, research on EVs has intensified and it is now clear that EVs are reflective of diseased states, such as, cardiovascular disease and stroke (section 1.3.6.2). Similarly, diabetes and obesity lead to an EV number increase (189). Adipocyte derived EVs are upregulated in obesity and have been shown to stimulate monocyte differentiation and pro-inflammatory cytokine secretion (295). If "healthy" donors have undiagnosed underlying health issues, blood donations may include increased populations of pathophysiological EV. The downstream effect of EVs on the recipient is largely unexplored. If a recipient is transfused with a donation containing a large number of EVs stimulated from an underlying disease in the donor, these EVs may lead to downstream inflammation and increased PLT coagulability in the recipient. Increased levels of PEVs in inflammatory based conditions can lead to a hyper-coagulative state due to the high pro-coagulant activity of PEVs (296). If the recipient is at risk of deep vein thrombosis, for example, a large influx of pro-coagulant EVs may exacerbate this risk leading to possible life-threatening complications. Increased pro-coagulant potential however is not always a disadvantage. In trauma, related patient groups with severe bleeding an increased coagulation potential would be desirable. Thus, this chapter characterises "healthy" donor EVs and fresh processed PC EVs to determine baseline levels of variability and their potential benefit/disadvantage for the recipient. Thus, in later chapters, the impact of those EVs isolated over PC storage on the recipient will be assessed.

When ISEV was formed in 2014, to minimise the confusion of nomenclature and an effort to standardise isolation, they released MISEV (126). The guideline reflects both isolation requirements for WB, single cell preparations and characterisation of EV populations. MISEV requirements include evidence of tetraspanin expression (CD9, CD81, ALIX etc) utilising 2 or more different methods. EVs in WB are generated from all cell types, with the majority of EVs originate from four major cell types: PLT, RBC, WBC and endothelial cells. EVs characteristics largely depends on the cellular origin. PLT EV

structure and function are described in detail (section 1.3.6). RBC EVs are produced normally in the RBC ageing process and production is therefore indicative of RBC ageing. RBC EV express high level of PS on their surface and are therefore could be deemed pro-coagulant (297), however RBC EV are rapidly cleared from circulation (298). WBC derived EVs can either be anti-inflammatory or pro-inflammatory based on the resting or active states on the leucocyte that has produced them (299). Endothelial cells line all blood vessels, dysfunction of endothelial cells is often an early indicator of disease states, such as, in cardiovascular pathology and stroke. Endothelial EVs have been shown to be upregulated in these pathologies, making them a potential biomarker of early disease (232, 300). More information on EVs in pathophysiological states are detailed in section 1.3.6.2. The "healthy" proportion of EV subtypes, how this proportion shifts in disease and the downstream effects in transfusion are largely unexplored. This thesis mainly focuses on PC derived EVs. PC are produced from WB collections, and it is unclear if all other subtypes of EV are removed in PC isolation. Therefore, the PC may contain residual EV subtypes from WB which will in turn be transfused to the recipient patient, making EV characterisation before and after processing vital.

The full extent of haematological indices and EV measures in healthy donors are not characterised, and therefore will be characterised in this chapter. It is not known how the ratio of EV subtypes is altered in PCs compared to circulating WB. This chapter therefore addresses these important points, with the working hypothesis of EVs in WB compared to PC will have significantly lower PLT EVs, but increased EVs of other cell types (RBC, WBC and endothelial).

3.2.2 Aims

1. Define the healthy population in terms of haematological indices and PLT function.

2. Establish PLT function, activation, EV concentration and EV subtypes within the healthy population and fresh PCs.

3. Fully characterise a representative PC-derived EV sample within ISEV guidelines, defining the character of EVs investigated in this thesis herein.

3.3.0 Methods

The methods described in this chapter build on those described in detail in Chapter 2 and are used specifically to generate the results described in this chapter.

3.3.1 Platelet Concentrate Preparation

PC were prepared as outlined in section 2.1 and stored at standard blood banking conditions of 22^{o}C +/- 2^{o}C under constant agitation.

3.3.2 Whole Blood Collection ethics

All full-time Cardiff Metropolitan Staff were invited to participate in a multi-phased antibody screening programme in July 2020 (ethics ID; Sta-2860) described in detail in a previous publication by our group (301). From the cohort, COVID-19 Antibody positive participants, and a pool of matched negatives, were asked to provide a venous blood sample. The matched negatives represented a healthy cohort and were used within this thesis.

3.3.3 Whole Blood Collection

Venous blood was collected from 20 donors from median-cubital vein aseptically via a butterfly 20-gauge needle into Na-citrate vacutainers. The first 5 mLs of blood before sampling was discarded to avoid excessive platelet activation. Mean age of participants was 43.9 +/- 11 years.
To note, these donors were not the same as the PC donors, these were 2 different pools of donors eligible to donate blood.

3.3.4 Haematological Analysis

Blood samples were analysed at the University Hospital Wales haematology and biochemistry laboratories. A standard clinical coagulation screen was requested on a Na-citrate sample, including D-Dimer and CRP levels as a non-specific marker to exclude underlying pathologies. All samples were tested within 4 hours of bleeding. A full blood count (FBC) was completed an EDTA sample.

PC PLT number was assessed in an EDTA sample utilising a FBC test.

3.3.5 Platelet aggregation

WB (300uL) collected in a hirudin vacutainer was diluted 1:1 with saline and incubated at 37^{o}C for 3 minutes. Following incubation, aggregation capabilities were assessed as in section 2.2

3.3.6 EV isolation

WB EV isolation was conducted as described in section 2.5.1. PC were also isolated via size exclusion chromatography allowing for direct comparison of samples. 5 mL of PC was centrifuged at 800xg, followed by 2 centrifugations at 3000xg, to render the sample acellular. 1 mL of acellular PC

supernatant was applied to the size exclusion column and allowed to pass through. 500µL of filtered PBS was added to the top of the size exclusion column and sequential 500µL fractions were collected. Fractions 5-10 were pooled and analysed. EVs were analysed using NTA software as described in section 2.5.3.

3.3.7 Western Blot

Western blot methodology is described in section 2.7. The specific proteins of interest for the data presented in this chapter were CD41 (PLT) and CD9 (exosomal marker). Identification of exosomal marker CD9 satisfies part of the MISEV for characterisation of EV samples.

3.3.8 Mass Spectrometry

An optimized mass spectrometry-based method for the unbiased assessment of proteins in cells and EV. Quantitative nUPLC-OrbiTrap mass spectrometry analysis was undertaken using the core facility (Professor Benedikt Kessler, Oxford) to confirm the presence of EV specific proteins such as CD9 and ALIX. This satisfies the requirements of EV classification according to ISEV guidelines.

3.3.9 Statistical analysis

Statistical analysis was performed as described in section 2.8 with the following difference. Unpaired T-tests was applied to determine significance in normally distributed data between the healthy population vs PC population.

3.4 Results

Cohort Characteristics for the 20 participants are detailed in Table 3.1.

Whole Population	***Male***	***Female***
Number	*11*	*9*
Mean ages (years)	*43.52*	*42.3*
Number of Asthmatics	*2*	*3*
Number of type 1 diabetics	*1*	*0*
Number of Hypertensive	*0*	*0*
Number of Type 2 diabetics	*1*	*0*

Number of Cardiomyopathy	*0*	*0*
Number of Chron's Disease	*1*	*0*
Number of Hyperthyroidism	*0*	*1*

Table 3.1 - **Cohort Characteristics**. Descriptive characteristics of all participants who underwent a venous blood sample

3.4.1 Haematology assessment

FBCs and coagulation screens were investigated in healthy individuals. Results detailed in table 3.2 report no measurement was deemed outside the haematology reference ranges set by National Health Service (NHS) (302). CD62P% is not routinely screened within the NHS, therefore does not have a reference range.

Parameter	Average ± SD	Reference Ranges
WBC ($x10^9$/L)	5.18±1.36	3.6-11.0
Hb (g/L)	147.11±8.37	115-180
RBC ($x10^{12}$/L)	4.77±0.24	3.8-6.5
PLT ($x10^9$/L)	262.47±58.78	140-400

HCT (L/L)	0.44±0.02	0.37-0.54
MCH (pg)	30.87±1.25	27-32
MCV (fL)	92.32±3.87	80-100
RDW (%)	14.28±1.20	11.5-15
D-Dimer (ng/mL)	459.6±382.79	<500
PT (s)	11.58±0.67	10-14
APPT (s)	32.27±3.18	22-36
Fibrinogen (g/L)	2.74±0.50	1.50-4.50
CRP (mg/L)	1.26±1.50	<3.0
CD62P (%)	10.32±10.71	**Not Applicable**

3.4.2 PLT number

PLT number was determined in healthy individuals via a FBC analysis. As expected, PLT number when compared to the PLT number of a fresh PC (defined as 2 days old) is significantly lower ($262.5\pm13.49 \times 10^9$/L vs $1266\pm17.28 \times 10^9$/L, $P<0.0001$, Fig 3.1).

Table 3.2 – **Full blood count and Coagulation Screen**. A pool of healthy individuals was screened utilising a coagulation panel and FBC to assess if the measures were within the reported healthy ranges. No measures fell outside these reference ranges. WBC – White blood cells, Hb – Haemoglobin, RBC – Red blood cell, PLT – Platelet, HCT – Haematocrit, MCH – Mean corpuscular haemoglobin, MCV – Mean corpuscular volume, RDW – Red cell distribution width, PT – Prothrombin Time, APPT – Activated partial prothrombin time, CRP – C-reactive protein. N=20

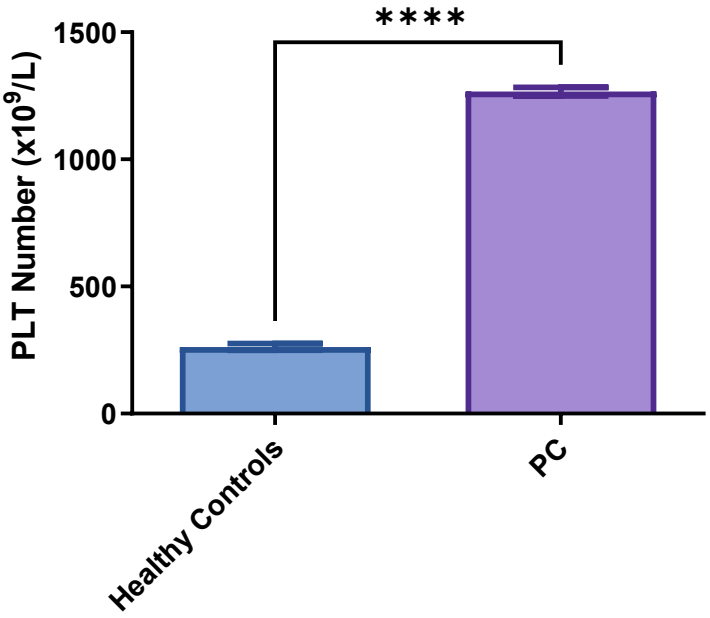

Figure 3.1 – **Platelet Number.** PLT number of healthy individuals reported from a full blood count compared to the PLT number reported in PCs at 2 days old, deemed as fresh. Error bars denote SD, ****p<0.0001. N=20 fresh WB, N=9 PCs.

3.4.3 Platelet Aggregation

PLT aggregation was assessed in fresh PC and fresh WB (Fig 3.2). Trap-6 induced aggregation is significantly lower in PC compared to fresh WB (103.9±3.2U vs 56.19±3.78U, P<0.0001, Fig 3.2a). ADP-induced aggregation is significantly lower in PC compared to fresh WB (2.143±0.83U vs 59.58±2.818U, P<0.0001, Fig 3.2b). Ristocetin induced aggregation was not significantly different in PC when compared to fresh WB (109.6±25.75U vs 110.5±7.776U, Fig 2C). The limitation however of PCs not containing RBC, WBC and minimal plasma is discussed in section 3.5.3.

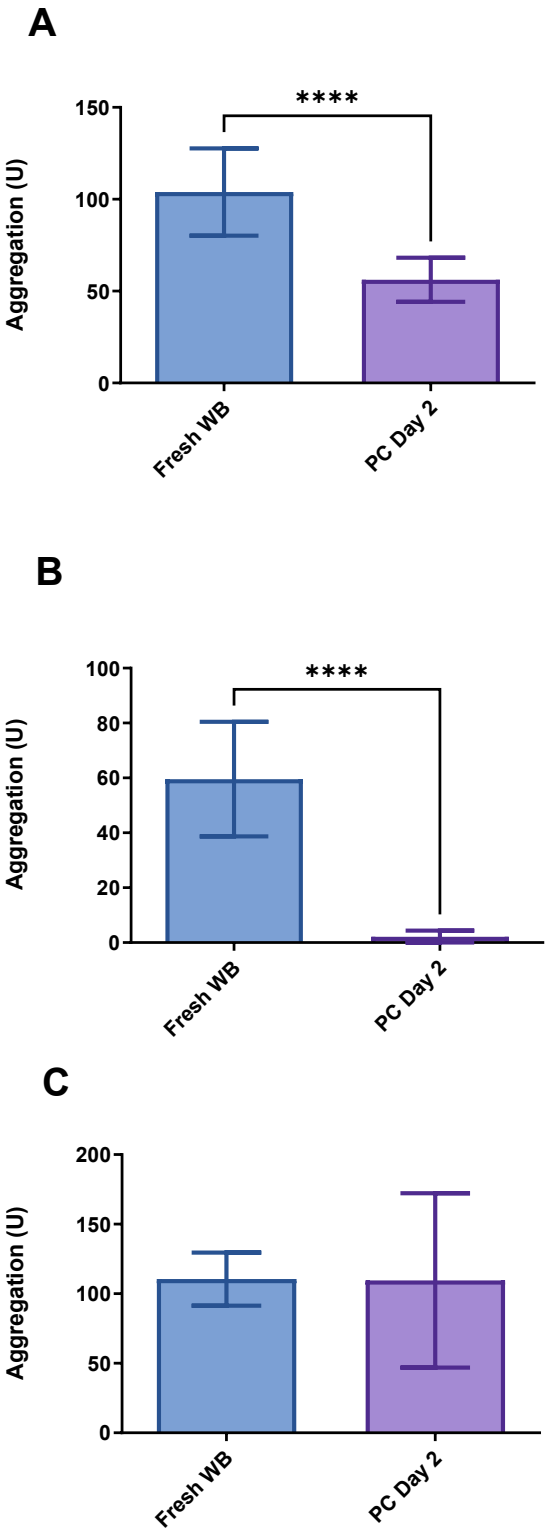

Figure 3.2 - **Platelet aggregation**. A - TRAP-6 induced aggregation. B- ADP-induced aggregation, C – Ristocetin-induced aggregation. Error bars denote SD, ****p<0.0001. WB – whole blood. PC platelet concentrate. WB n=20 (apart from Ristocetin, N=7). PC N=9

3.4.4 Platelet Activation

PLT activation assessed by CD62P expression was demonstrated not to be significantly different in fresh WB compared to Fresh PC (14.02±3.06% vs 6.593±0.54%, p=0.178 Fig 3.3).

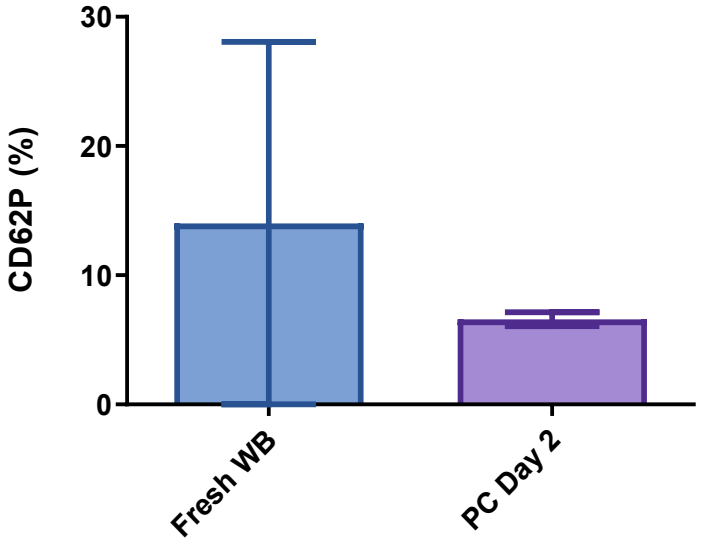

Figure 3.3 - **Platelet activation.** CD62P% expression of PLTs in fresh WB vs fresh PC at day 2 of shelf life. Error bars denote SD, WB – Whole blood, PC – Platelet concentrate. WB N=20, PC N=7

3.4.5 EV Concentration and size

EV concentration is not significantly different in fresh PCs compared to fresh WB ($2.5x10^{10}$±$2.9x10^{9}$ p/ml vs $2.97x10^{10}$±$1.02x10^{9}$p/ml, Fig 3.4). EV size however was reported to be significantly smaller in fresh PCs compared to fresh WB (188.9±3.38nm vs 165.0±5.35nm, P<0.01, Fig 3.5).

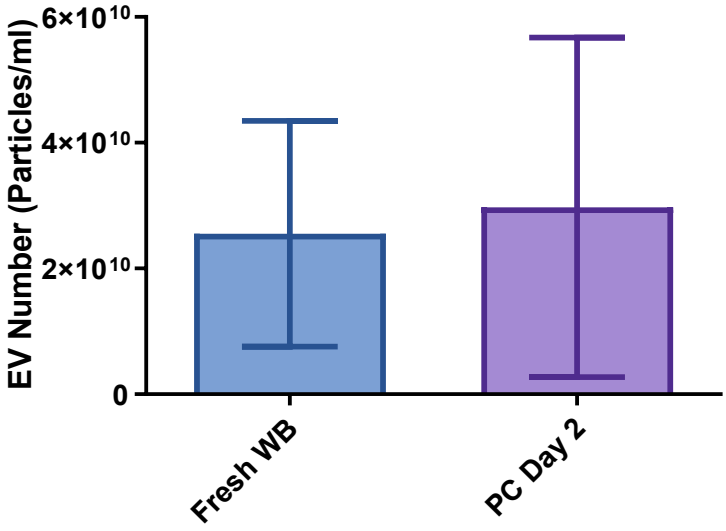

Figure 3.4 – **EV concentration**. EV concentration assessed by NTA in fresh WB compared to Fresh PC at storage day 2. Error bars denote SD, WB – Whole blood, PC – Platelet concentrate. WB N=20, PC N=6

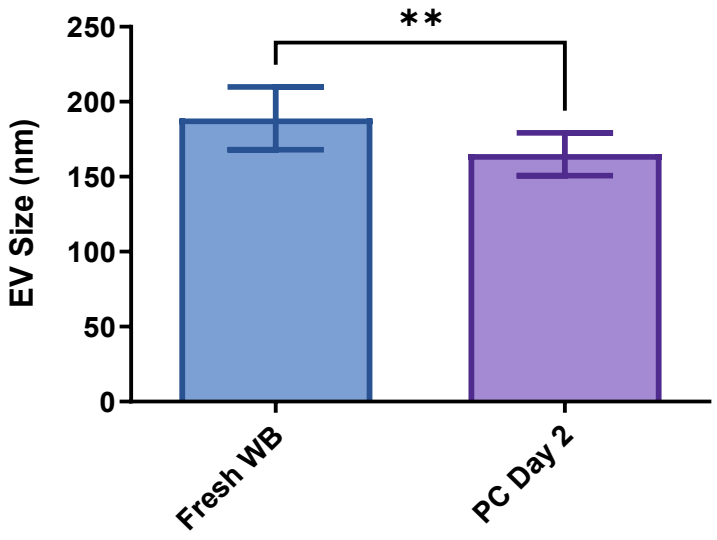

Figure 3.5 – **EV Size**. EV size assessed by NTA in fresh WB compared to Fresh PC at storage day 2. Error bars denote SD, **p<0.01. WB – Whole blood, PC – Platelet concentrate. WB N=20, PCN=6

3.4.6 EV Characterisation

EVs from WB and PC were characterised using flow cytometry to assess expression of parental cellular origin on EV (Fig 3.6), using a CD9 positive gating method. EVs in PC had a significantly higher percentage of PEV (classified by CD41+ binding) compared to fresh WB (46.7% vs 79.76%, P<0.001). No other EV subtypes (Endothelial (CD144+), RBC (CD235a+) and WBC (CD11b+) were significantly different.

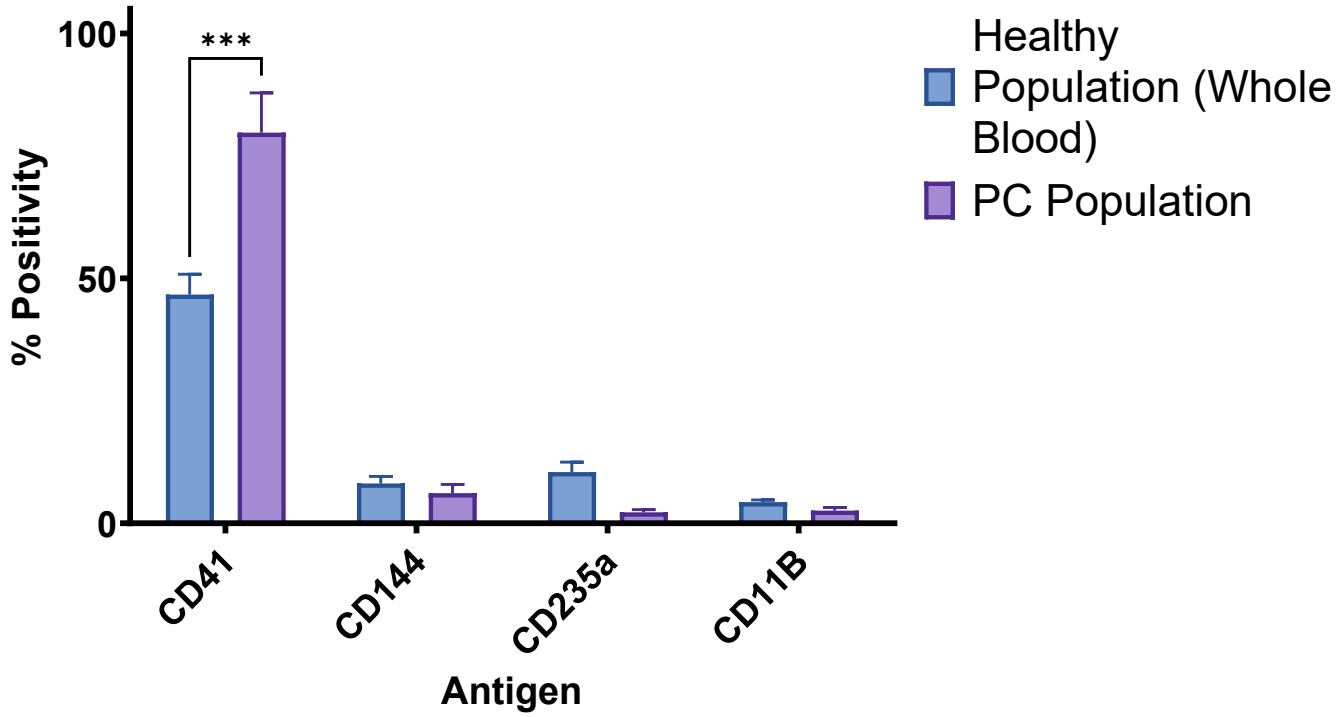

Figure 3.6 – **EV Origin**. EV family characterisation by flow cytometry. EV populations were positively selected based on CD9 positivity and size and were dual stained for a specific family marker. Family markers are: CD41-Platelet; CD144-Endothelial cell; CD235a-red blood cell; and CD11B-White blood cell. Error bars denote SD, ***p<0.001, N=15

To meet ISEV criteria, EVs isolated form PC were characterised further. Fig 3.7 represents a western blot gel image from two separate western experiments of 2 distinct EV samples and a PLT sample. The western blot shows a band for all samples, at ~113kDa, indicative of CD41 expression. CD9 expression is shown in all samples by the presence of a dual band, at ~20kDa, and ~35kDa. This confirms the EVs express both CD9 and CD41. To confirm the presence of other tetraspanins, a non-selective protein analysis approach was used via Mass spec. Representative raw label-free quantitation (LFQs) are reported, confirming the protein presence. (Table 3.3).

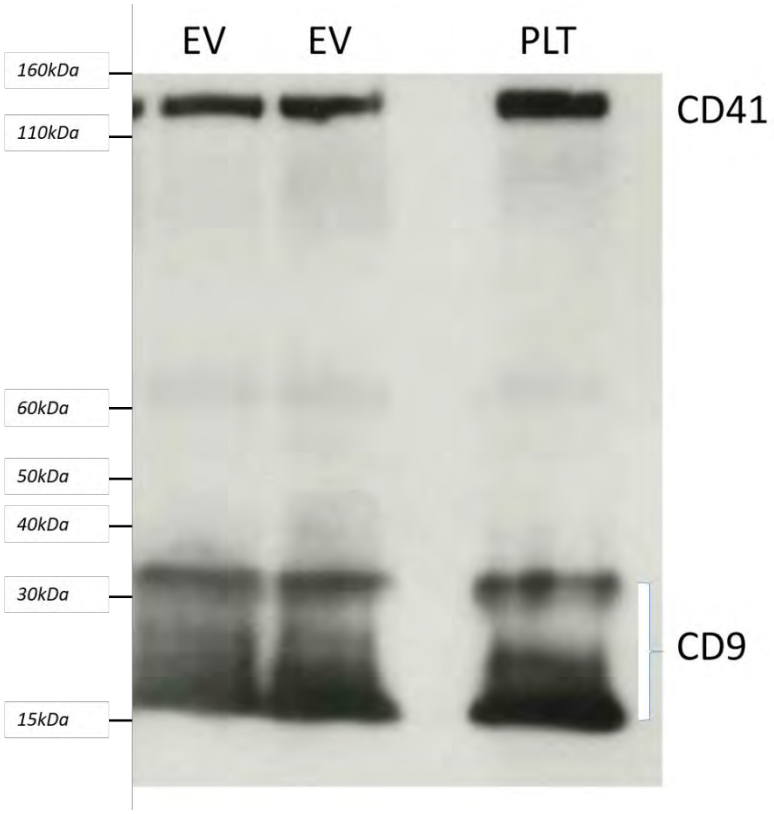

Figure 3.7 - **EV Western Blot**. Western blot images of EV lysates from RT stored PCs to confirm the presence of an exosomal marker, CD9 (tetraspanin), and a PLT origin marker, CD41. These were compared to a PLT cell lysate. CD41 represented by the top band at ~113kDa. CD9 has a dual band, at ~20kDa, and ~35kDa. Data derives from two separate western blots. EV – Extracellular Vesicle. PLT – Platelet.

Gene	***Protein***	***Raw LFQ Intensity Platelets***	***Raw LFQ Intensity EV***
ITGA2B (CD41)	GPIIb	8.15534	8.55367
CD9	CD9 Tetraspanin	-0.135499	7.25995
PDCD6IP (ALIX)	Programmed cell death 6-interacting protein	2.29246	2.00588

Table 3.3- **Confirmation of "exosomal" proteins**. Mass-spectrometry protein analysis of PLTs and EVs of known EV markers, represented as raw LFQ values, (Log2). Proteins present in both samples include CD9, CD41 and ALIX that fulfils the ISEV requirements of EV identification.

3.5 Discussion

3.5.1 Key Findings

- PLT aggregation to TRAP-6 and ADP significantly decreases in PCs compared to Fresh WB.
- PLT activation, measured by CD62P expression and EV concentration was not significantly different in Fresh WB compared to fresh PCs
- EV subtypes, specifically PLT-derived EVs, significantly increase in PCs compared to fresh WB.

3.5.2 Main Discussion

The data presented within this chapter describes the healthy population, able to become blood donors, utilising haematological indices and a coagulation screen that is not currently used by transfusion services to screen donors. Further to this, agonist induced PLT aggregation is demonstrated to be reduced when PLTs are processed and stored as PCs. Finally, the data adds to the knowledge of EVs within the healthy population and fresh PCs defined as 2-days-old, with comprehensive characterisation confirming the nature of the particles isolated from PCs within this thesis herein.

Table 3.1 reports that the haematological indices and coagulation screen for the population sampled were within the normal range for all tests, therefore supporting the analogy that the population is deemed healthy (302). The PLT number, as expected, is significantly higher in PCs compared to WB (Fig 3.1). As previously described (section 1.2.1), buffy coat derived PCs are formed from a pool of 4 donors, therefore explaining the large increase of 4x the PLT count in PC, demonstrating the efficacy of PLT isolation processes and formation of PCs from WB.

TRAP-6 induced PLT aggregation is significantly lower on day 2 compared to fresh WB (Fig 3.2A). Previous data reported suggested TRAP-6 measured by impedance aggregometry in fresh PC resulted in similar observations to those reported here (303, 304) . Others have noted that there was a trend of lower results when comparing baseline (fresh PLTs from WB) to stored PCs (304) . The decrease could be due to the loss of PAR1 and PAR4 receptors during initial processing leading to

decreases of PAR4-mediated aggregation (305). These receptors could be downregulated or shedded in processing of PLTs into a PCs, however the direct mechanism is currently unknown. PAR receptor expression was not measured in this thesis, therefore the full explanation as to why TRAP-6 response is reduced is unknown. An alternate explanation could be that WB aggregometry is resultant from a combination effect of, PLT, RBCs and WBCs. As previously explained (section 1.1) during aggregation PLTs and formation of the PLT plug will entrap RBC within the GPIIb/IIIa mesh network, interlinked with fibrin. Thus, increasing the aggregation potential in comparison to only PLT seen in PC sample potentially leading to a lower electrical impedance during aggregation.

Platelet aggregation to ADP in PC was significantly lower than WB at day 2 (Fig 3.2B). As outlined in section 1.2.3.4 it has been reported that ADP aggregation is decreased in PC following day 2 of storage. (109). There are two potential explanations for a decrease in platelet aggregation following processing and storage. Firstly, desensitisation of the ADP receptors; purogenic P2Y1 and P2Y12 (81). PLT activation by ADP requires simultaneous ADP binding to both receptors (306). In this context, receptor desensitisation occurs when ADP is continuously present in the local environment. A study in 2000 suggested that P2Y1 became completely inhibited to ADP after previous incubation with ADP in medium to high (1mM) concentrations, which may have occurred if ADP was released by activated PLTs during processing. The P2Y1 receptor became internalised, over stimulation time therefore decreasing availability for ADP binding (307). PLTs continuously release granular ADP during storage and ADP is released from residual RBCs, therefore contributing to desensitisation(308). Furthermore, previous evidence suggests PLTs undergo lysis and apoptosis during storage causing granular release of ADP (309). Secondly, extended storage of PLTs has been shown to result in a significant loss of both P2Y1 and P2Y12 receptor expression (310). The level of ADP release and therefore desensitisation can be dependent on the amount of plasma present in the PC. This is due to plasma, containing ADPase that degrades autocrine released ADP. (311). Due to the removal of 65% of plasma, the protective levels of ADPase is decreased, possibly causing a build-up of ADP within the PC. Reports conclude that the autocrine release of ADP during storage leads to rapid P2Y

desensitisation. The data presented in this chapter suggests if desensitisation is occurring it is not related to excessive PLT activation during processing. This is shown by CD62P% (Fig 3.3) and EV concentrations being comparable with fresh WB (Fig 3.4). The data shown in Fig 3.2B is supported by a large body of evidence, therefore ADP aggregation was not assessed further in this thesis when assessing PC functionality over storage time.

Ristocetin induced aggregation was comparable between PC and WB suggesting processing does not significantly impact the Ristocetin induced aggregation pathway in PLTs. Ristocetin induced aggregation utilises the vWF-GP1b pathway, (312, 313). The data presented suggests that GP1b levels are stable throughout the processing of WB to PC, consistent with a protein expression study into PSL, whereby GP1b receptor expression were not significantly different to fresh or throughout storage levels (314).

CD62P% is not significantly different in WB compared to PCs (Fig 3.3), suggesting that there is no excessive PLT activation during processing. The average CD62P% expression in a healthy population range from 3% - 16% (315-318). The large discrepancy within the literature is likely due to differences in sample collection, storage and flow Cytometric analysis leading to different expression levels. For example, a needle with a small diameter (high gauge) would lead to a higher sheer force which has been proven to increase PLT activation (319), giving a false representative of the true basal CD62P expression. This may explain the results here, which reports a high variance, as the needle gauge used by the blood transfusion service would have a much larger diameter than the one used on our healthy population.

EV concentration is not significantly different in WB compared to PC (Fig 3.4). A definitive EV blood concentration within the literature is heavily conflicted, with numbers ranging from $1x10^{8}$-$1x10^{11}$p/ml of plasma (320, 321), with some reporting as low as $1x10^{7}$p/ml (322). The large variation of EV concentrations within the literature is due to differences in collection, storage, and method of processing (section 1.3.5), and can vary largely within a population. A recent meta-analysis study states an average predicted of $1x10^{10}$p/ml of plasma (323), agreeing with the current data. As outlined

in section 1.3.6, PEVs are generated mainly through PLT activation. Due to EV number not being significantly raised in fresh PC in comparison to WB, it would suggest that the impact of processing WB to create PCs does not significantly activate PLTs to EV. Thus, suggesting that processing is not a major cause of the PSL regarding activation, which is paired with CD62P% levels on PLTs, agreeing with a 2012 study showing low activation on day 0 and 1 (324). However, apheresis PLTs have been shown to be more activated, as measured by CD62P expression, after isolation due to the different centrifugal process (325), therefore it is speculative to suggest that a higher number of EVs would be present in apheresis PCs compared to BC PCs.

Although EV concentration does not significantly change in PCs compared to WB, EV size does significantly decrease in PCs compared to WB (Fig 3.5). There are several explanations for a population of smaller EVs within a PC. The main explanation is in reference to the variation of EV size when EV are produced from different cell types. For example, average EV sizes have been reports as ; PEVs 161±5.9nm, RBC EVs 140±13 (a different study suggests average is up to 190nm (326), WBC EVs from cultured monocytes 186±6.7nm (327), and cultured endothelial cells 203±4nm (328). Despite EV being present from all cell types in WB and these EV not being fully removed during processing to PC (Fig 3.6), only PLT remain to continue to produce EV. PEV are smaller than WBC EVs and Endothelial EVs therefore reducing the mean size of EV seen in a PC.

When EV were characterised to determine cellular origin a significantly higher proportion of PEVs (CD41+) within the PC compared to WB was observed (Fig 3.6). Regardless of EV source investigated in this thesis, PEVs are the most abundant of all EV subtypes. This is widely reported with PEV in WB, accounting for between 50-80% of all EV (217). The processing of WB to PC removes the majority of other cell types, leaving only PLTs and minimal RBCs. Therefore, as expected, the resulting EVs produced post-isolation should be PLT-derived and RBC, with PEVs being the major contributor over storage. WB contains all cell type EV as reflected in the WB levels reported in fig 3.2. The data suggests that during PC processing by differential centrifugation and WBC filtration (section 1.2.1) EVs

are not selectively filtered. This is due to the relatively small size of EV and explains why all EV subtypes are present in the final PC product from the inclusion of plasma in the PC.

Due to the non-standardised way of EV isolation and characterisation within the field, ISEV devised guidelines which should be followed for all work published in regards to EV. These guidelines dictate a set of commonly expressed EV markers, which are required to be identified on any particle isolate in order to deem the particles EVs. The data presented in Fig 3.7 and table 3.3 satisfy the guidelines regarding the PC EV used throughout this thesis. The tetraspanin, CD9 is ubiquitously expressed in all EV populations (126) and thus was first identified by western blotting and later used as a housekeeping gene. Detailed untargeted mass spectrometry was used to characterise EVs. Mass spectrometry was chosen due to greater linearity, reproducibility and removes some of the specificity issues with antibody based methods (329). This methodology also confirmed the presence of CD9 and further EV specific markers including ALIX (126). The proteins set out in the ISEV guidelines should be expressed on EV due to the specific biogenesis process outlined in section 1.3.2. ALIX has been previously positively identified as a marker of EV found within the PC (11). PLT glycoprotein marker CD41 was chosen due to being a specific abundant marker on the parent PLT and has been extensively used to identify PEVs within the literature (300, 330), and will be used throughout this thesis alongside CD9 in order to identify PEV.

3.5.3 Limitations

The healthy population were screened for general co-morbidities and regular medication usage. However, similarly to in a blood donor scenario there was no confirmation of this data using medical records. Therefore, the results collected may not be fully representative. Furthering this the study data was collected from a cohort of Cardiff Metropolitan staff, potentially creating a bias in the cohort to not be fully representative of underlying health conditions. This presents as a limitation, due to certain medications effecting PLT activity and possible EV release. Medications such as Aspirin which inhibits the COX-1 receptor has been shown to cause a decrease in larger PEVs (331), which could have led to a lower PEV prediction within the healthy population. A further example would be

imipramine, an anti-depressant that has inhibitory activity on acid sphingomyelinase (aSMase). aSMase enzymes are key to exosomal release as it increases membrane fluidity (332). If using this drug, the mean EV size would appear to be larger due to less exosomal production. Pantetheine, a cholesterol lowering drug, showed similar effects (333). However, these drugs are not screened by the WBS, therefore the assumption is based that the participants are deemed healthy.

Using impedance aggregometry to compare WB vs PC has limitation due to WB containing RBCs and WBCs as well as PLTs. When PLTs aggregate to the electrodes and form a "PLT Plug", some RBCs and WBCs may become entrapped within the aggregate mesh. This may lead to an increase in impedance resistance across the electrodes, possibly leading to a higher result. Another potential issue is the extra plasma in WB, therefore possibly having more coagulation factors again effecting the result.

Flow cytometry for EVs is a widely debated subject amongst the EV community and has been detailed in section 1.3.5. Due to the limits of size and light scattering properties of EVs, traditional flow cytometry (without 405nm side-scatter capacity) is unable to detect particles under 150nm (214). This can lead to large under-representation of the true EVs populations present if the majority of particles are under 150nm. The potential pitfalls of using flow cytometry for EV analysis is explored in detail in the following chapter. However, as detailed in section 2.3.1.2, the flow cytometer used in this study utilises 405nm violet side-scatter, greatly improving the detection range. To further improve selection, a CD9 positive gating strategy was used, so while some EVs not expressing CD9 will be missed, using a positive selection minimises false events like particulates in buffer from skewing the results.

3.6 Conclusions

The current chapter defines a healthy donor population, including PLT functionality, EV concentration, size and subtype characteristic, forming a baseline of fresh WB measures before PLTs are stored as PCs. These measures are further compared to a fresh PC bag, detailing minimal effects of processing on PLT activation and EV generation, but a profound effect on PLT function. The aim for future chapters is to investigate alternative, novel storage environments to improve PC quality, returning the levels closer to the normal, healthy range.

4.0 Results II – The effect of prolonged cold storage on platelet concentrates

4.1 Perspective

Following a detailed analysis of healthy population PLT and EV characteristics (Chapter 3, Results I), a further question was whether storage of PLTs as PCs can be prolonged past 7-days, or changes in the quality of PCs could be identified during the storage period. Thus, this chapter investigates altering the environmental temperature for CS of PCs over a prolonged storage, utilising functional aggregation assessments and experiments relating to EV concentration and effect on coagulation in order to fully assess the impact of CS on PC health.

4.2.1 Introduction

As outlined in section 1.2.2, PC storage has not been altered in sometime. Current transfusion guidelines in the UK indicate that PC should be stored for a maximum of 7-days at 22^{o}C+/-2^{o}C with continuous gentle agitation.

Advances in transfusion has led to the understanding of the supposed aggregation improvement reported when PC are stored at 4^{o}C (59). Evidently, if PLTs are activating and aggregating faster and more efficiently, patients could benefit, especially those who are bleeding as a result of trauma. However, clinical studies evaluating this effect are sparse, with many taking place when older PC storage containers were used (61). Valeri et al reported in 1970s that cold storage (CS) of PCs for 24 hours corrected aspirin induced thrombocytopenia, whereas maintaining PC at room temperature (RT) did not (334). Other more recent studies have shown that bleeding times are reduced when using CS compared to RT as outlined in section 1.2.2.2, leading to the FDA approving the use of CS PC for resuscitation (65). However, its use was limited to a 3-day shelf life in the majority of the USA and has not yet approved in the UK. In February 2020 the FDA granted the first licence for CS with a 14-day shelf life to the South Texas Blood & Tissue centre "when conventional platelet products are unavailable, or their use is not practical" (335). However, this is only for apheresis PCs, not buffy-coat derived PCs explored here.

Another cited benefit of CS is a perceived preservation of quality beyond the conventional 7 day storage period (60). A 2019 study reported CS increased *in-vitro* aggregation responses compared to RT, with some functional measures at day 21 for CS improved or equal to that observed in day 7, RT stored, PC. This suggests CS could prolong the PC shelf life (336). A pilot clinical study, completed in December 2020, examined the feasibility of CS for a 14 day period for use in patients undergoing complex cardiothoracic surgery (117). The study analysed PLT dysfunction before and after transfusion, finding a significant increase in aggregation response in CS PC stored for up to 14 days and that 14-day-old PLTs retain functionality.

PEVs are highly procoagulant, outlined in section 1.3.6, more so if released from activated PLTs. PEVs from active PLTs demonstrate enhanced denser fibrin networks due to GPIIb/IIIa on their surface as compared to PEVs from resting PLTs (337). When injected into mice, tail bleeding time and blood loss was greatly reduced compared to PC. Another study evaluated PEV transfusion vs PC and a vehicle control in a rat haemorrhage model. The reported transfusion of PEVs led to a significantly improved outcome compared to the vehicle control in regards to reduction in abdominal bleeding which fresh PLTs failed to improve (338). Finally, a recent study found that PEVs were equivalent to PLTs at attenuating vascular endothelial growth factor-A-induced vascular permeability (339).

EVs have been shown to increase significantly in CS compared to RT (340), possibly due to the PLT activation that occurs in the cold, as outlined in section 1.2.2.2. As Studies analysing PLT aggregation and activation have not typically assessed PLTs in the absence of EVs, the potential of PEV must be determined in isolation. Translating this to a transfusion context, the reduction in bleeding times induced by administration of a given CS PC unit could be in part attributable to the presence of EVs and not due to the improved haemostatic properties of the donated PLTs.

Taken together, it can be hypothesized that i) CS would generate more EVs with a more pro-coagulant phenotype compared to RT storage and ii) CS would increase aggregation response over a prolonged storage time.

4.2.2 Aims

The aims of this chapter were to:

1. Investigate the influence of CS on PC quality.
2. Investigate the effect CS has on the production and pro-coagulant function of EVs.
3. Determine if CS can pro-long the storage duration of PC compared to conventional RT storage.
4. Evaluate whether CS PCs would be better suited to a prophylactic or acute clinical situation.

4.3 Methods

The methods described in this chapter build on those described in detail in Chapter 2 and are used specifically to generate the results described in this chapter.

4.4.1 PLT Preparation

Platelet concentrates were prepared as outlined in section 2.1 and stored at standard blood banking conditions of 22 +/- 2^{o}C under constant agitation and are termed RT. Each PC consists of 4 blood donors, pooled into one unit. Two PC units were combined and split into two to allow identical experimental bags. CS PCs were stored at 4^{o}C+/-2^{o}C within 24-36 hours of production without agitation, reflective of standard conditions applied by blood establishments.

4.4.2 Oxygen consumption

OCR was used to determine the metabolic activity of PLTs, measured by EPR oximetry, outlined in section 2.4.4.

4.4.3 EV isolation

EVs were isolated from PCs using differential centrifugation outlined in section 2.5.1. An exemplar ISEV-based characterisation of these EVs isolated from PCs can be found in Chapter 3, section 3.4.3.

4.3.4 EV Concentration

EV concentration was determined using NTA, fully described in section 2.5.2.2.

4.3.5 Turbidimetric Clot formation and lysis

Thrombin induced Fibrin clot formation and tPA -induced clot lysis was assessed using a standard turbidometric assay with the addition of a fixed number of EVs 1x10^{10}p/ml as outlined in section 2.6.2.

4.3.6 PLT Aggregation

To determine the functionality of the platelets, TRAP-6 and Ristocetin induced aggregation was assessed as described in section 2.2.2.

4.3.7 pH measurements

An important QC measure of platelet storage is pH, ensuring that the pH does not drop below 6.4. 1mL was taken aseptically from the PC and sampled on a pH metre, which was calibrated (2-point) prior to use.

4.3.8 CD62P% Assessment

CD62P expression on PLTs is suggestive of activation and granular release. CD62P% was assessed by flow cytometry, detailed in section 2.3.2.2

4.3.9 Statistical analysis

Statistical analysis was performed as described in section 2.8.

4.4 Results

4.4.1 Oxygen Consumption Rate

OCR does not significantly change over 20 days storage when comparing CS to RT PCs neither does the OCR when compared to day 2vs20 in CS (Fig 4.1). RT OCR over the 20day storage does significantly decrease (0.17nmoles/min/10^8PLTs vs 0.057nmoles/min/10^8PLTs, P=0.0381).

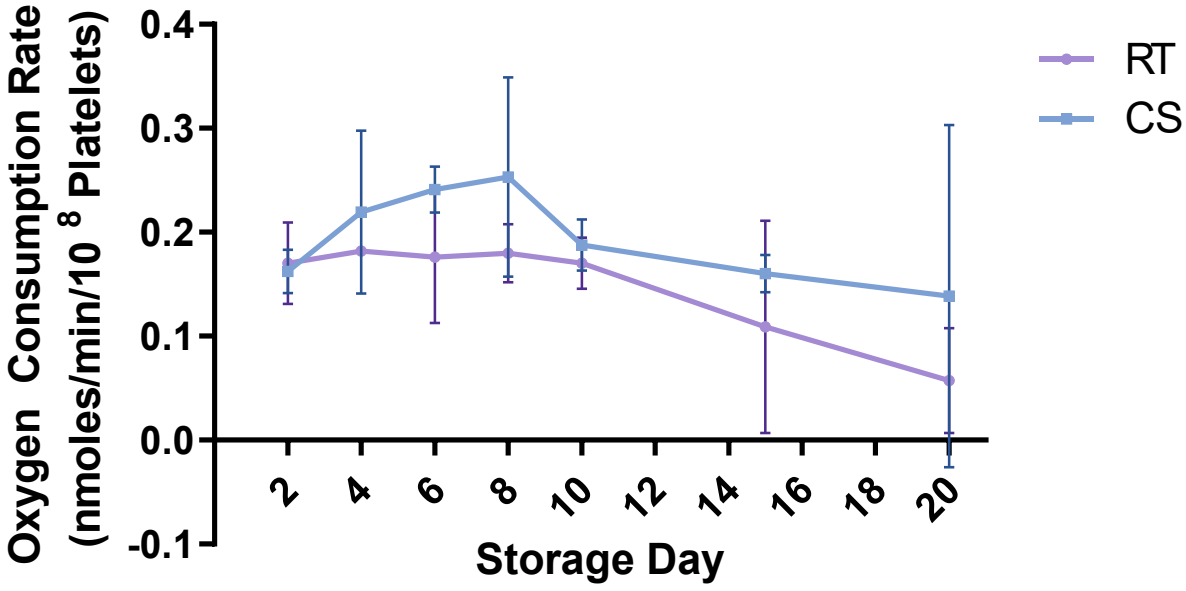

Figure 4.1 – **Oxygen Consumption rate of PLTs**. Oxygen consumption rate of PLT over a 20-day storage period measured by EPR oximetry. Error bars denote ±SD. RT – Room Temperature. CS – Cold Storage. N=3

4.4.2 EV concentration

EV concentration (p/mL) increased throughout the storage time, with CS showing significantly greater EV at day 15 (P<0.01) and 20 (P<0.0001) compared to RT (Fig 4.2). EV concentration over storage time increased in RT (1.4x10^{11}p/ml Day 2 vs 1.2x10^{12}p/ml Day 20, P=0.05) and demonstrated a similar trend in CS (2.3x10^{11}p/ml Day 2 vs 3.5x10^{12}p/ml Day 10, P=0.06).

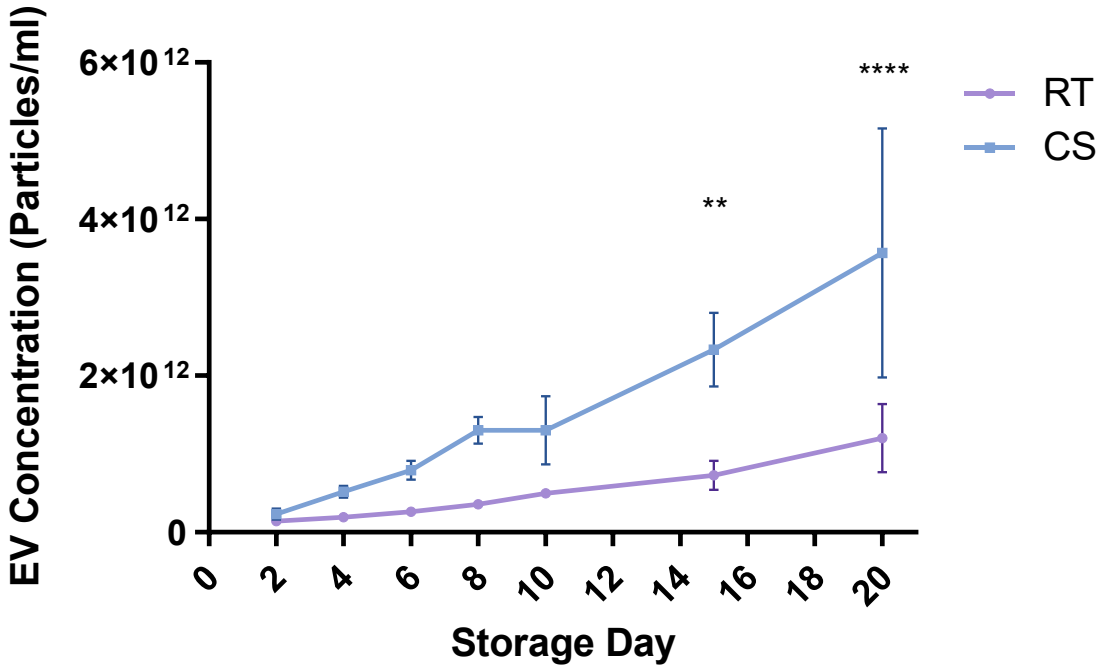

Figure 4.2 **– EV concentration in stored PC**. EV generation over the 20-day storage period determined by NTA. Error bars denote ±SD, **p<0.01, ****p<0.0001. RT – Room Temperature. CS – Cold Storage. N=3

4.4.3 EV size distribution

Mean EV size (nm) was significantly greater in CS compared to RT from day 4 onwards (4-6 P<0.0001, 8-10, P<0.001. 15-20 P<0.01), with a significant increase in EV size over the storage period (204.5nm vs 258.73nm, P=0.0338) (Fig 4.3A). EV size did not significantly change in RT over the storage time (174.67nm vs 213.5nm, P=0.1538). Further analysis indicated CS produced significantly more EVs in the size range 201-300nm (P<0.0001) and 301-350nm (P<0.01) (Fig 4.3B). This significance was evident on all sampling points thereafter, except day 20, where 301-350nm as compared with RT was P<0.05 (Fig 4.3C).

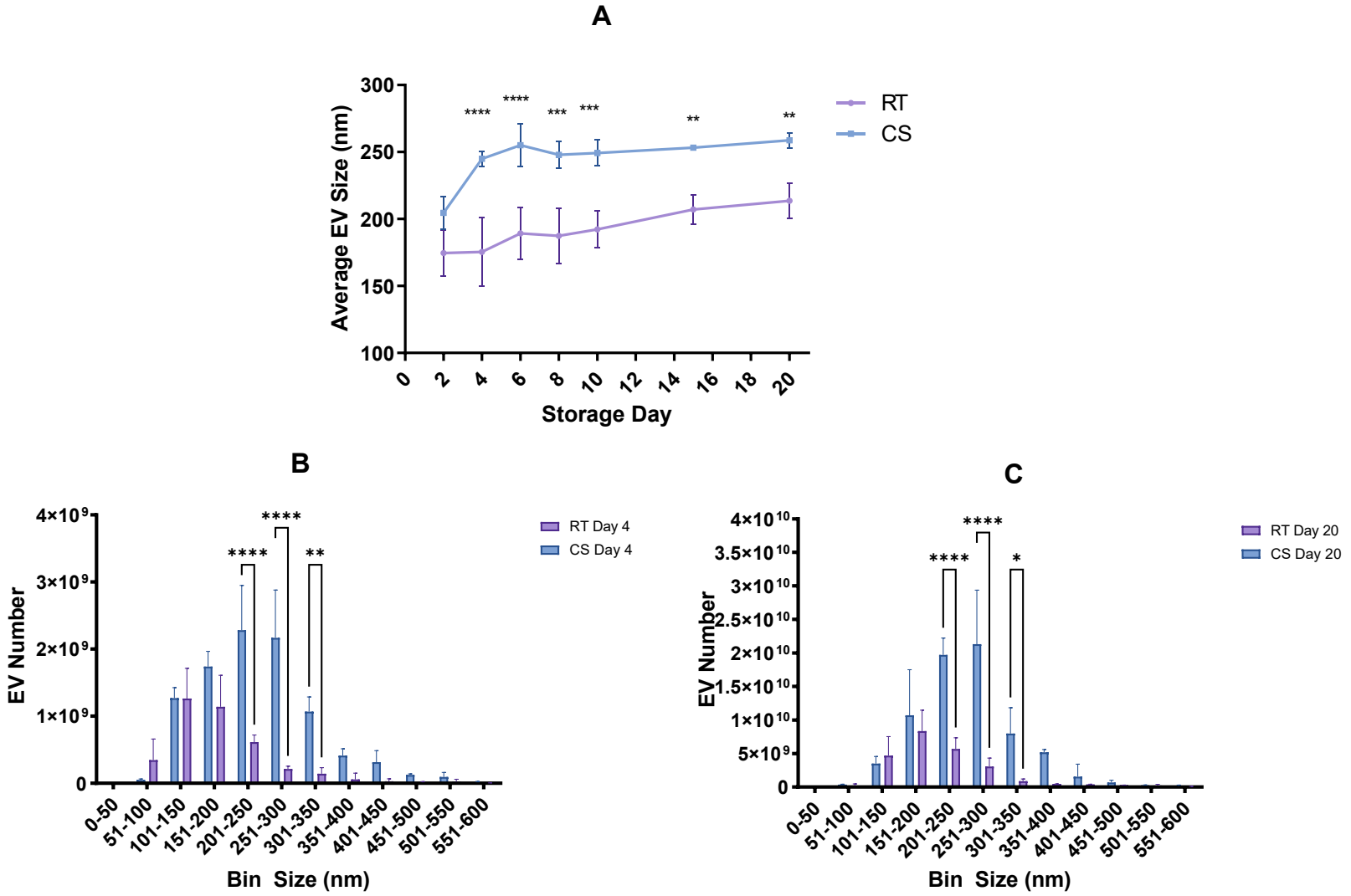

Figure 4.3 **– EV size distribution in stored PC**. (A) Average EV size distribution over 20-day storage period. (B) Size distribution analysis of day 4 PCs in 50nm size ranges (bin sizes) up to 600nm. (C) Size distribution analysis of day 20 PCs in 50 nm bin sizes up to 600nm. Error bars denote ±SD, *p<0.05, **p<0.01, ***p<0.001 ****p<0.001. RT – Room Temperature. CS – Cold Storage.

4.4.4 Normalised EV influence on fibrin clot formation and lysis

EV counts were normalised to $1x10^{10}$p/ml to assess the pro-coagulant characteristics of the EVs. EVs isolated from both RT and CS PCs showed a significantly lower time to maximum clot formation (Fig 4.4A) and maximum clot size (Fig 4.4B) when compared to the "no EV" plasma control. RT isolated EVs exhibited a significantly faster time to maximum clot formation (Fig 4.4A) compared with the plasma "no EV" control on all days ($P<0.001$, day 8 $P<0.01$) as also seen for EVs arising from CS (Days 4, 6 and 10 $P<0.001$, Day 2 $P<0.05$, Days 8, 15 and 20 $P<0.01$). No significant difference in fibrin clot formation was reported comparing RT to CS EVs. RT isolated EVs exhibited significantly decreased maximum clot size at days 6 & 15 ($P<0.01$) and days 8, 10 &20 ($P<0.05$) (Fig 4.4B), whereas CS reported significant difference compared to the control on days 4 ($P<0.01$) 10 and 20 only ($P<0.05$). There was a significant decrease in lag time in CS day 2 isolated EVs compared to the plasma control ($P<0.05$, Fig4.4D). EVs alone without the addition of an activator did not stimulate clot formation, leading to no results and therefore data is not shown.

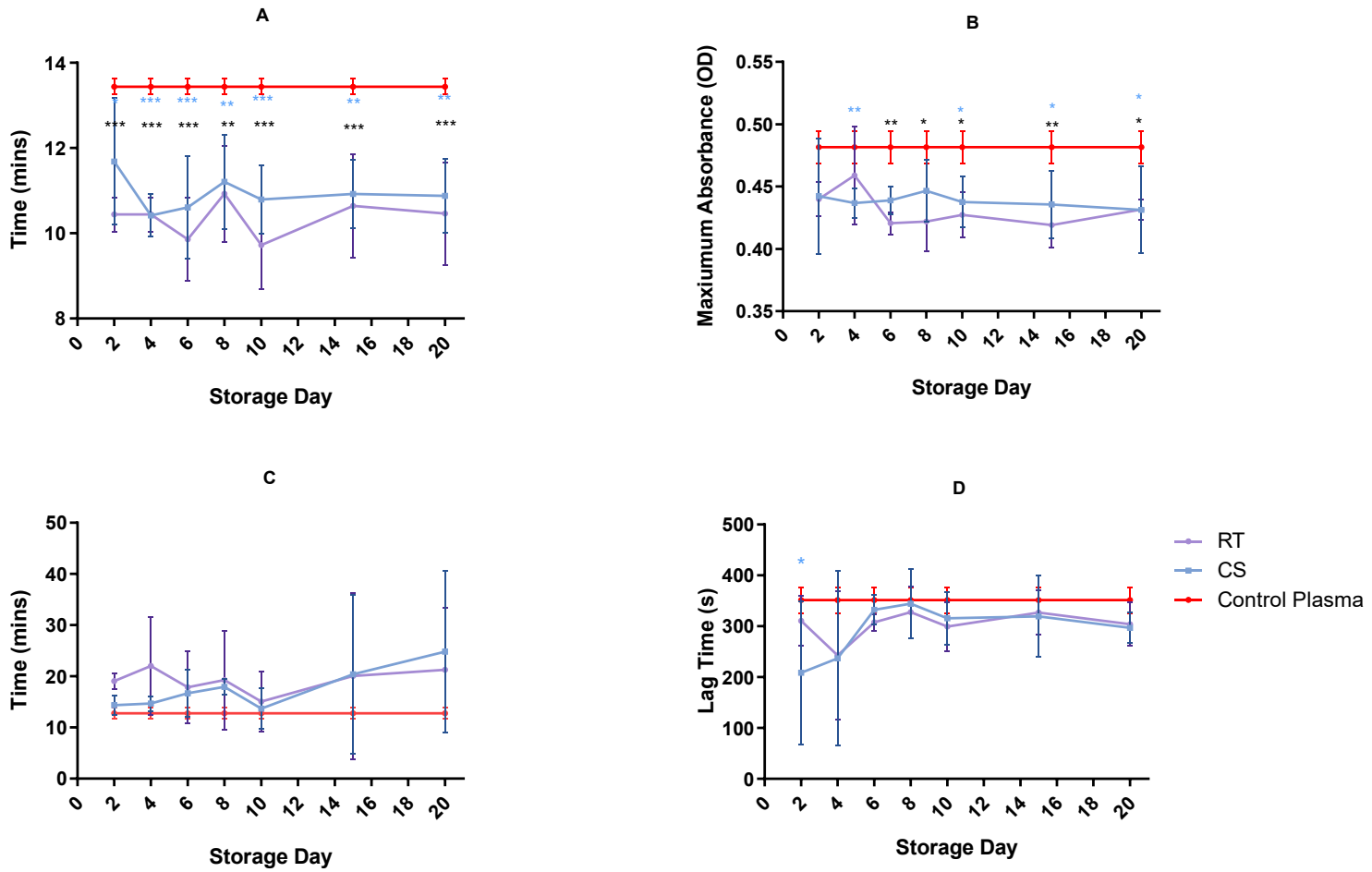

Figure 4.4 **– EV effect on fibrin clot formation and lysis.** EVs at 1x10^{10}p/ml were applied to a turbidity and lysis assay using a control fresh frozen plasma to assess the EV influence on the fibrin clot, compared to a "no EV" control. (A) Time to maximum fibrin clot formation. (B) Maximum fibrin clot size measured by maximal turbidity of plasma. (C) Time taken to achieve 50% lysis. (D) Time taken to initiate fibrin clot formation. Error bars denote ±SD. *p<0.05, **p<0.01, ***p<0.001. Black stars denote control plasma vs RT. Blue stars denote control plasma vs CS. At no point was there statistical difference comparing EV from RT vs CS. RT – Room Temperature. CS – Cold Storage. N=3

4.4.5 Differential EV concentrations on fibrin clot formation and lysis

A range of EV concentrations was applied to the assay to assess the effect of EV concentration on the coagulation induced. A significant decrease was reported in time to maximum clot formation (Fig 4.5A) with the highest concentration of EVs $1x10^{11}$p/mL when compared to no EVs and to the lowest EV concentration tested, $1x10^{8}$p/mL ($P<0.01$). A significant decrease was also seen with $1x10^{10}$p/mL when compared with the control ($P<0.05$) as seen in Fig 4.4A. A significant decrease was reported in maximum clot size (Fig 4.5B) induced in the presence of $1x10^{11}$p/ml compared to the no EV control ($P<0.05$). No significance difference was reported in 50% lysis times (Fig 4.5C) or the lag times (Fig 4.5D).

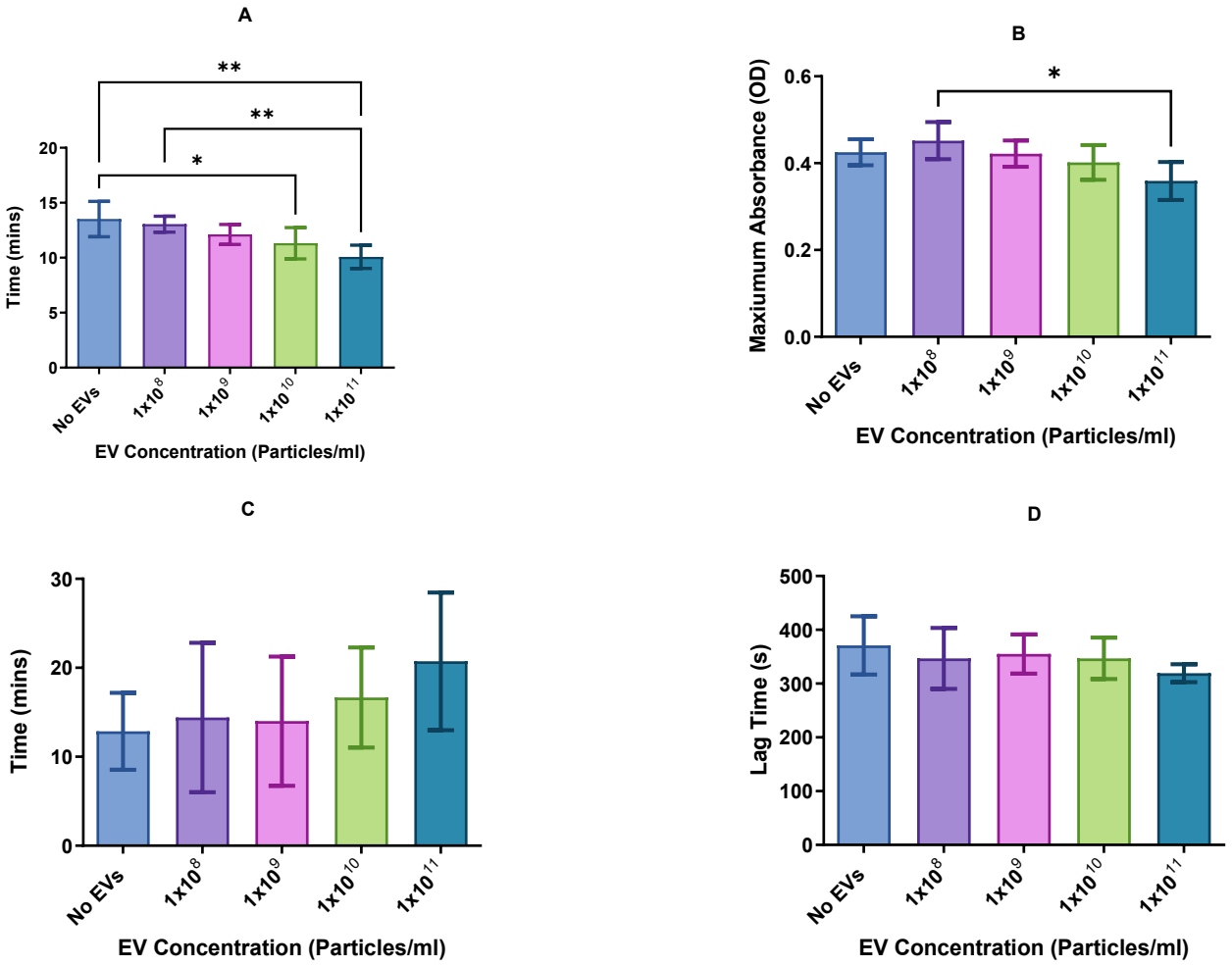

Figure 4.5 **-Concentration effect of EVs on fibrin clot formation and lysis.** EVs from RT were applied at a range of concentrations to fresh frozen plasma utilising the Turbidity and lysis coagulation assay. (A) Time to maximum fibrin clot formation. (B) Maximum fibrin clot size measured by maximal turbidity of plasma. (C) Time taken to achieve 50% lysis. (D) Time taken to initiate fibrin clot formation. Error bars denote ±SD. *p<0.05, **p<0.01. N=4

4.4.6 PLT Aggregation

PLT aggregation in response to TRAP-6 (Fig 4.6A) and Ristocetin (Fig 4.6B) are shown below. No significant difference in TRAP-6 aggregation was reported between RT PC and CS PC at any storage point. RT and CS PC both displayed a significant decline in TRAP-6 responsiveness over the 20-day storage period by comparing day 2 vs. day 20 (60.4U vs 3.2U, P=0.005 & 64.1U vs 0U, P=0.001, respectively). Aggregation response to Ristocetin was significantly lower in CS PC on days 2 to 8 compared to RT PC (P<0.01). There was no significance reported between RT and CS PC response from day 10 onwards. Over the 20 days storage, there was a significant decline in Ristocetin induced aggregation for RT PC (55.0U vs 9.6U, P=0.034) however no significant drop over storage was observed for CS PC (25.2U vs 24.1U, P=0.86).

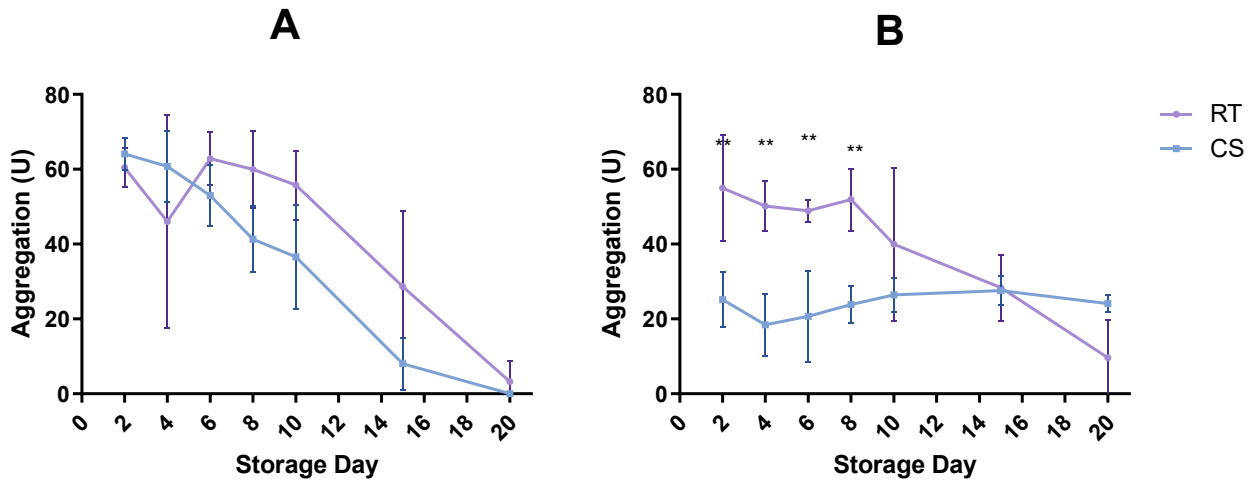

Figure 4.6- **PLT aggregation in stored PC.** (A) TRAP-6 induced PLT aggregation over a 20-day storage period. (B) Ristocetin-induced PLT aggregation over a 20-day storage period. Error bars denote ±SD, **P<0.01, n=3. RT= Room Temperature. CS=Cold storage N=3

4.4.7 Effect of temperature on PC pH

PC pH is a standardised quality control measure as mentioned in section 1.2.3.3. pH was significantly lower in CS from day 6 onwards (Fig 4.7), however this remained above the transfusion quality threshold of pH 6.4 therefore deemed acceptable. Over the 20 days storage, there was a significant increase in pH RT PC (7.19 vs 7.60, P=0.0287) and decline in CS PC (7.19 vs 6.87, P=0.0391).

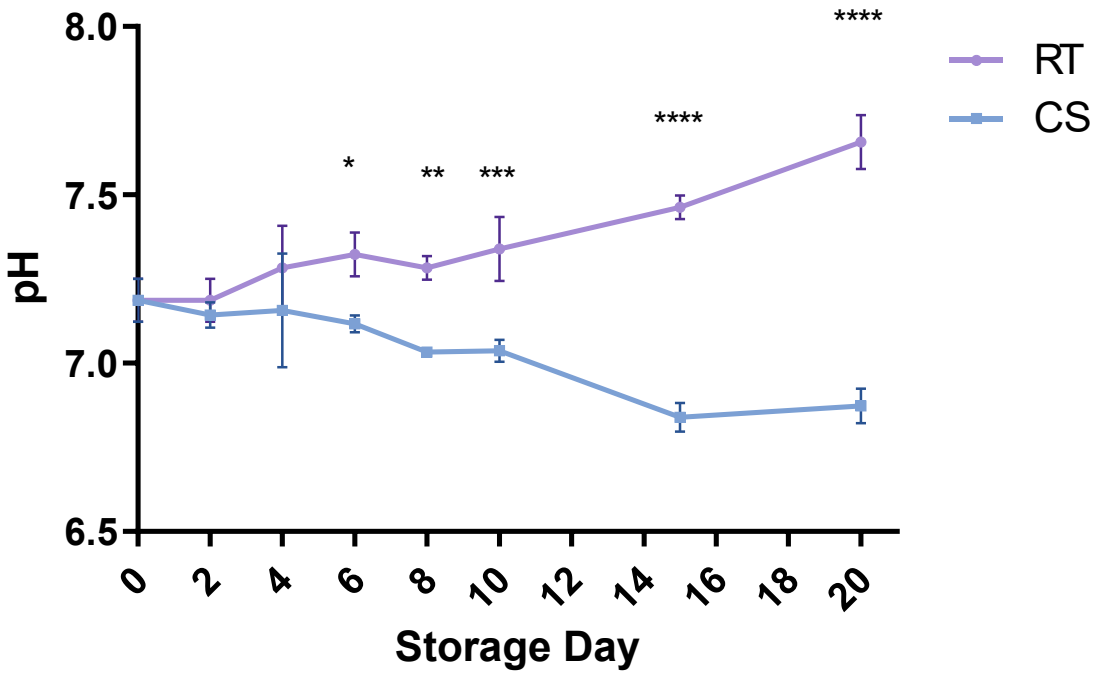

Figure 4.7 – **pH level of stored PCs.** pH measured at day 1(before pool splitting) and periodically throughout the 20-day storage period. Error bars denote ±SD, *p<0.05, **p<0.01, ***p<0.001, ****p<0.0001. RT – Room Temperature. CS – Cold Storage

4.4.8 Effect of temperature on PLT CD62P expression

CD62P% expression is indicative of PLT activation and granular release. CD62P expression is significantly higher in CS compared to RT stored PCs on day 7 ($P<0.05$). Both RT and CS increased over the 20-day storage period when comparing day 2 to day 20 (6.71±1.17% vs 45.3±5.0%, $p=0.0087$, 15.99±5.06% vs 54.8±7.1%, $p=0.0019$ respectively, Fig 4.8).

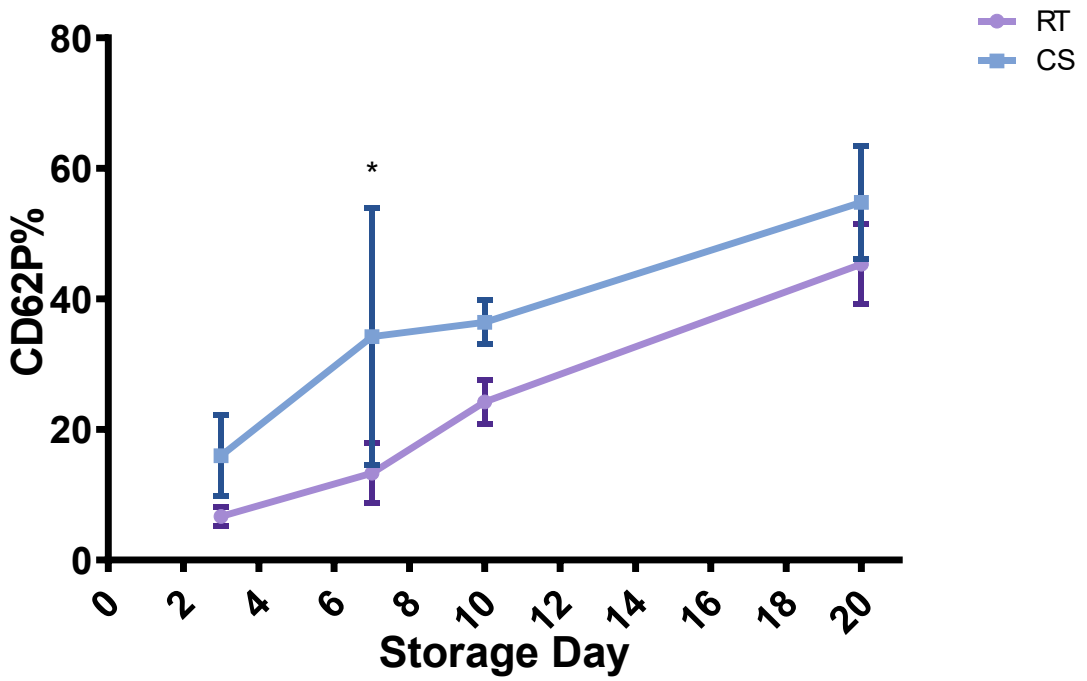

Figure 4.8– **CD62P% Expression on PLTs**. Percentage of PLTs expressing CD62P on the PLT surface assessed by flow cytometry dual staining with CD41. *p<0.05, error bars denote ±SD, N=3. RT – room temperature, CS – cold storage.

4.5 Discussion

4.5.1 Key Findings

- CS generates significantly more EVs on day 15 & 20 compared to RT.
- CS EVs are significantly larger than EVs generated in RT, specifically EVs sized 201-350nm in range.
- EVs decrease the time to maximum fibrin clot formation and maximum clot size significantly compared to a no EV control, which was further exacerbated with an increase in EV concentration. However, no significant difference between RT and CS EVs was reported regarding fibrin clot formation, suggesting an EV concentration effect not a storage condition effect.
- CS PC showed significantly decreased Ristocetin – mediated PLT aggregation on days 2 to 8 and did not significantly increase TRAP-6 – induced PLT aggregation when compared to conventional RT storage.

4.5.2 Main Discussion

This chapter adds to the current understanding of the role and impact of PLT-derived EVs within a transfusion context. The study explored the pro-coagulant effects of EVs isolated from RT and CS PCs over a prolonged storage period. CS induces PLT derived EV that are larger, and prolonged CS produces a higher concentration of EVs compared to RT storage. In combination with coagulation data, a possible haemostatic advantage to CS PC is suggested.

OCR does not significantly change in cold storage compared to RT (Fig4.1). This however could be due to a methodological limitation of EPR spectroscopy being conducted at RT and not 4^{o}C, therefore PLTs will potentially warm over the measurement time. The warming of cells may explain the current result, as it has been demonstrated that platelet ATP linked OCR, decreases when PLTs are stored in the cold (341). Over the 20-day duration of this study, OCR did significantly drop in RT as PLTs age and possibly lyse but did not significantly decrease in the first 7 days of storage and agreeing

with other reports utilising different techniques such as PO_2 to determine OCR (101). CS does not decrease OCR over 20 days, suggesting the potential to maintain metabolic processes over the 20-day storage period.

EV concentrations significantly increased during CS as compared to RT (Fig 4.2), in agreement with data published by Feys et al (66). Cap et al 2013, showed no significant increases of microparticles within the initial 5 days of storage, which also agrees with the data presented, as the significant increase in EV concentration is evident only after prolonged storage (post 7-days) (63). However, with the use of NTA technology to determine the EV concentration in CS and RT PCs, it can be argued that the data presented herein may be a more accurate representation of the EV number as compared to conventional flow cytometry. Flow cytometry has been more commonly applied to EV concentration analysis throughout the transfusion literature (outlined in section 1.3.5.3). Due to the limits of size and light scattering properties of EVs, flow cytometry can fail to detect the majority of particles under 150nm, which if applied to the RT and CS samples used in this study, would equate to 42% of EVs isolated from RT and 14% of EV isolated from CS at day 4. This implies that data derived using flow cytometry must be interpreted with care, as it could lead to a potential underrepresentation of the EVs present and overrepresentation of significant difference (280). Black et al have shown EVs at RT do significantly increase over storage time using NTA (83), which is consistent with the RT data presented here. The increase in EVs in CS documented here could be due to a possible increase in PLT activation evident at lower temperatures as reported previously (342, 343) that used %CD62P expression as a marker for PLT activation. As PLTs activate, they express CD62P and degranulate, generating a large number of PS expressing EVs, which correlates to the CD62P% expression data shown in Fig 4.8. The primary function of PS expressing EVs is to provide a negatively charged surface for haemostasis, which also serves to recruit immune cells and activate further PLTs. Therefore, there is a potential for a PC high in PS positive EVs to activate the patient's circulating "healthy PLTs" in the context of patients who are receiving PC due to trauma (344).

EV concentration does increase over the 20-day storage period in both RT and CS, although due to being p=0.05 and p=0.06 respectively, the data is deemed not significant according to the 95% confidence intervals set within this thesis. However, it could be postulated that overlooking this "borderline significance" may constitute a type II error, causing a false negative. This could be due to the lack of statistical power in the N=3, and so clearly this issue requires further investigation: if the N number were to be increased, the data would then be expected to be more reliable. Nevertheless, the chosen statistical significance was $p<0.05$, so the data in question must be considered to be not statistically significant.

EVs produced under CS conditions are significantly larger than at RT, suggesting more microparticles are being generated during the CS process. Microparticles are classically described as EVs larger than 150nm, and are associated with high PS levels on the EV surface (163), outlined in section 1.3.2. When performing a more detailed analysis of these EVs at day 4, CS is associated with the production of significantly more microparticles, particularly of those sized between 201-350nm (Fig 4.3B). This increase in microparticles was observed throughout 20-day CS period of this study. PS has been used to identify and count EVs derived from PCs previously and may explain the higher number of EVs classically reported in CS, due to these larger EVs displaying high levels of PS (1.3.2.2). A higher percentage of EVs displaying PS on the outer leaflet may lead to a more procoagulant capability (224), however when the EV concentration was normalised and these EVs applied to a turbidometric clot assay, there were no significant differences in procoagulant activity observed between the EVs generated in CS vs RT. The larger EVs in CS may express different markers and therefore change downstream effects when transfused. These effects could involve inflammatory effects, which has been suggested in aged PC due to release of biological response modifiers such as CD40L (268). Further research into the pro-inflammatory effects of EVs from PCs and the impact CS may have is needed. The EVs increase in size at day 4 but do not continue to increase over the remainder of the study, possibly reflecting that CS PLTs activate over the initial days of storage, backed

up by a significant increase in CD62P% expression (Fig 4.8), or alternatively might reflect the initial shape change in PLTs known to occur in CS.

When exposed to lower temperatures (<15^{o}C) PLT lose their discoid shape for a more spherical shape (345) leading to the classical loss of the swirl phenomena, described in section 1.2.3.2. The cooler temperature causes microtubules to depolarise and dissolve in PLTs (346), which is paired with an increase in intracellular calcium concentrations. In normal resting PLTs, increasing calcium is a normal process of early activation and aggregation, and is therefore presumed that a calcium rise is the beginning of CS-induced aggregation (346). Other work investigating the mechanisms of CS activation has implicated phosphoinositide-mediated actin assembly (347). Hoffmeister et al demonstrated that chilling activates phosphoinositide-induced barbed end assembly independently of phospholipid synthesis and GTPase activation (348). This activation and shape change leads to further integrin activation (349) and therefore PEV release. As suggested earlier, PEVs released by stimulation are more procoagulant, however we did not find this in the present study (Fig4.4). The major reported finding was CS generated more EVs.

PLT EVs are known to be up to 50-100x more procoagulant then the parent cell (350). EVs derived from both CS and RT are equally procoagulant. Our results show that the time taken for a clot to form was significantly reduced in the presence of EV compared to the plasma (no EV) control. This data confirms that PLT EVs have a direct influence on agonist–induced clot formation. However, it is also noteworthy that application of EVs without thrombin stimulation did not stimulate clot formation directly (data not shown). Previous research has shown an inhibition of thrombin generation with PLT-EVs when corn trypsin was used, which inhibits FXIIa of the contact pathway, concluding that an initiator is required to be present and that PLT EVs are involved in this pathway (247). A follow-up study in 2020 later confirmed this finding (248). Additionally, Tripisciano had shown that EVs derived from RT PCs do not interact with the clot through a TF mediated pathway by utilising an anti TF antibody to block TF on the EV surface (247, 248). In the presence of EVs the use of anti-TF did not cause a decrease in thrombin generation. Tripsiciano also showed that when PS-expressing EVs are

blocked with annexin V, thrombin generation returned to the no EV level, suggesting that EVs interact through PS-mediated pathways (247, 248). In our studies, the procoagulant effect was seen for EVs derived in both CS and RT, with no difference between the two storage conditions. From these findings, it can be predicted where PLT EVs interact with the coagulation cascade, depicted in fig 4.9.

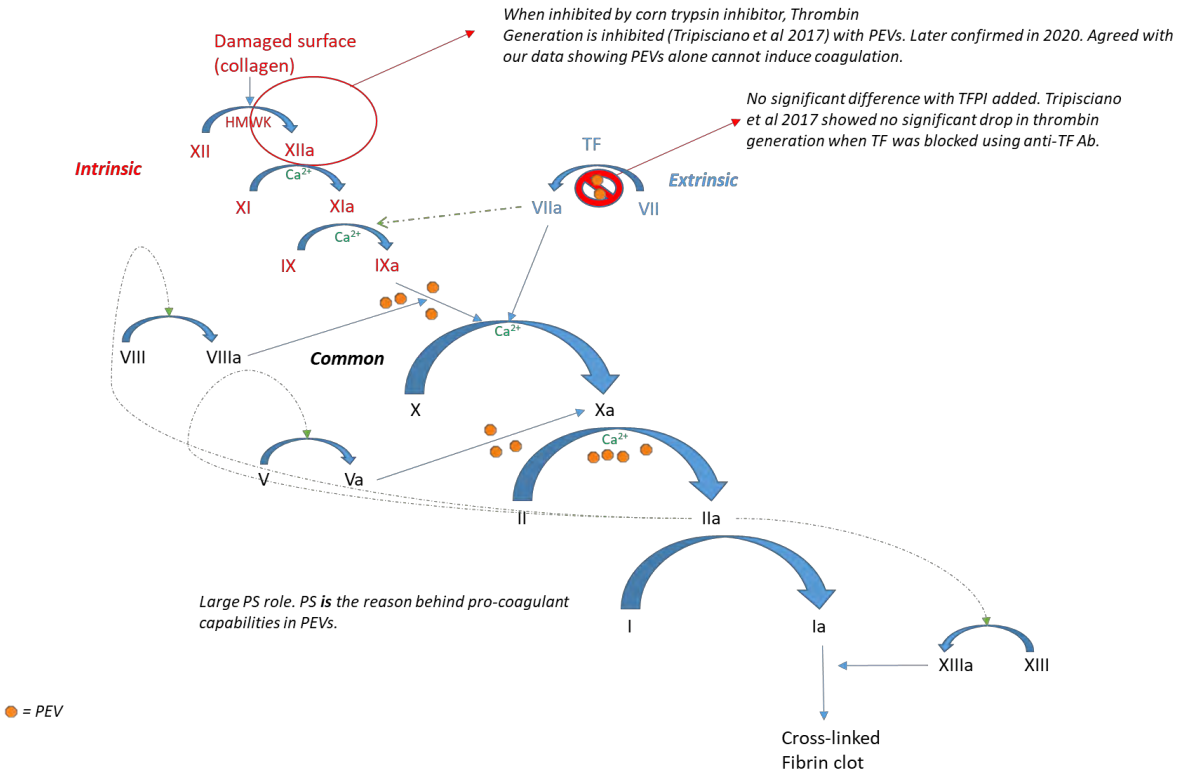

Figure 4.9 - **Proposed EV interaction with fibrin clot formation.** The proposed mechanism of PLT-derived EVs interaction with a simplified coagulation cascade. From the current study and previous work (247, 248), EVs interact with VIIIa-IXa complex and Va-Xa complex to generate thrombin through PS interactions. EVs do not interact through a TF mediated process. PEV=Platelet EVs.

Maximum clot formation was significantly lower in the presence of EVs, more so in RT, possibly due to the rapid formation of the clot. One explanation could be due to the area under the curve not changing, therefore when clot formation increases the maximum peak decreases, a possible limitation of the assay. Why significance was seen at more time points in RT compared to CS is unknown and may be a statistical artefact; however, RT and CS had the same overall effect. Time to 50% lysis showed no significant difference between CS, RT and the no EV control, suggesting PLT EVs in general enhance the speed of formation but do not affect the "strength" of the resulting clot (reflected by the comparable resistance to lysis by plasminogen activator in the second phase of the assay). More

investigations into cross-linking of fibrin within these clots is needed to determine the effects of PLT-EVs on clot structure and stability.

Pro-coagulant capability was directly proportional to the number of EVs present. In addition to the data showing CS increased EV concentration compared to RT (Fig 4.2), it strongly implies an apparent haemostatic advantage of CS PCs. The haemostatic advantage could be down to the enhanced clot formation caused by a high EV level, and this would be observed clinically as a reduction in the bleeding time. Another advantage could be due to an increased level of healthy PLT activation caused by the interaction of PC derived EVs interacting with the circulating patient PLTs. However, this needs further investigation. Microparticles are commonly reported to be increased in CS PC (351-354), but due to differences in sampling and measurement of microparticles, the drawing comparisons is challenging. Utilising ISEV standards, this chapter reports a higher proportion of EVs in CS. Use of ISEV guidelines within transfusion is currently underused and would allow more clarity within transfusion EV research. EV number and character clearly has an important influence on PC function and transfusion outcome.

PLT aggregation within PC is not significantly increased in CS (Fig 4.6), as previously published data suggested (60), however this could be due to the agonists and methods chosen within this thesis. The biggest reported improvement when comparing aggregation between RT and CS stored platelets is related to ADP (60), however ADP was not used in this study due to our observation that ADP was not able to induce aggregation from day 3 onwards (Data in section 3.4.3). CS induced-TRAP-6 aggregation does not significantly differ from RT, in agreement with others (59), suggesting that protease activated receptor mediated PLT aggregation is unaltered in CS. Response to Ristocetin however is significantly worse in CS in the early days compared to RT, conflicting with previous storage studies (342). This could be due to others using apheresis PCs suspended in 100% plasma as the source of samples in their studies. As previously mentioned, chilling PLTs stored below 15^{o}C, leads to extensive shape changes (355). This change rearranges the surface configuration of GP1bα, which is the major receptor for binding vWF. Ristocetin induced aggregation relies on forming a complex with

vWF, causing a conformational change, and leading to binding of GP1b, causing aggregation (356). Montgomery et al 2013 showed a decrease in GP1bα expression in the cold leads to a reduction in Ristocetin induced agglutination (357), providing a possible explanation for our results. This clustering also can explain enhanced clearance once transfused, outlined in section 1.2.2.2. Shedding of GP1bα also increases in CS, providing another possible explanation for the drop in Ristocetin response being caused by a loss of GP1b receptor (358).

As eluded in 1.2.3.3, pH is a routine QC measure seen as the most robust way to determine the PSL state. The cut off is defined as 6.4, as Fig. 4.7 reports, neither RT nor CS of PCs caused the pH to drop below 6.4, therefore essentially passing the standard QC measurement. CS did have a significantly lower pH compared to RT which has been noted by others (359). The difference is more likely due to the phenomena of full glucose utilisation in RT stored PCs that is associated with an increase in pH levels described in previous reports (360). It could be speculated that as the pH begins to rise, OCR decreases, suggesting the level of O_2 increases and CO_2 decreases with no more lactate being produced due to glucose utilisation. However, acetate, a component of SSP+ PAS, could still be metabolised in the absence of glucose, which creates bicarbonate (361, 362). The rise in pH therefore could be due to the rise in bicarbonate levels, which is basic, while no lactate is being produced. However, this hypothesis has not been experimentally tested, and so this issue warrants further investigation.

4.5.3 Limitations

This chapter had a small sample size (N=3) at each time point. However, the study design allowed a direct comparison of the same PC unit held under two different storage conditions over the whole investigation period. With this small sample number, I understand that application of ANOVA has limited power and it is possible the study in retrospect is underpowered given the variance measured.

A second limitation that is noteworthy is that *in vitro* data does not always reflect *in vivo* outcomes, with some evidence of PLT aggregation recovery *in vivo* (92, 111). Clinical significance of

the PLT aggregation data is limited and future work should address this issue to fully understand the *in vivo* effect. PLT EV can induce negative effects, including inflammation and possible causes of transfusion-related acute lung injury (section 1.3.6.3) were not investigated here and should be investigated to understand the implications of transfusing a high number of EVs.

4.6 Conclusions

The chapter concludes that CS of PCs generates a significantly greater EV number over a 20-day storage period compared to conventional RT storage. Although the pro-coagulant potential of these EVs is not significantly different, the higher number of pro-coagulant EVs and larger sized EVs suggests platelets derived from CS conditions may exhibit a haemostatically superior capacity compared to RT storage. Research into the possible side effects of transfusing a higher EV number is needed, as well as clinical trials to evaluate the potential clinical benefits of a higher EV number within a PC unit in the limited clinical context of active bleeding.

5.0 Results III – The effects of a reduced environmental oxygen on platelet storage

5.1 Perspective

A parameter of PC storage that has not been fully investigated is the influence of O_2. Studies in the 1980s reported that PLT function rapidly deteriorates in reduced O_2 conditions (hypoxia), suggesting that PCs should be stored in atmospheric O_2 (21% O_2) for the preservation of function. However, within the body, PLTs in the circulation typically encounter O_2 in the range 40-100mmHg (equivalent to O_2 of 4-13.5%) and are rarely exposed to 21% [O_2]. Maintenance of PLTs in relative "hyperoxia" might contribute to the PSL. Therefore, this chapter addresses the impact of reducing storage [O_2] conditions on PLT character and function, hypothesizing optimisation of [O_2] will mimic *in vivo* like conditions and therefore improve PC quality.

5.2.1 Introduction

The ability of efficient gaseous exchange of O_2 and CO_2 is considered highly important in regard to maintaining a good quality PC, due to the constant metabolism of PLTs in storage (50, 53, 100, 363). Murphy et al, uncovered using PC stored in old containers made from polyvinyl chloride, resulted in a hypoxic environment, detrimental to PC survival (51, 53, 363). This discovery led to the advancement in PLT storage with new storage containers typically made of PTE. The rationale was based on PTE being more gas permeable than PVC. The surface area of new storage containers was also increased, thereby increasing gaseous exchange potential for a given PLT concentration range (53). Storage containers are discussed in detail in section 1.2.2.1. However, the true [O_2] inside the storage container, kept under standard conditions, is not routinely tested, or reported and therefore still largely unknown.

The literature describes the average [O_2] in peripheral tissues as ~5% O_2 (364). Clearly, this will depend on the tissue and cell type, the O_2 requirement (consumption), and anatomical distance from the O_2 source i.e., blood. Arterial [O_2] is typically~13.5% O_2, venous ~6.5% O_2 and peripheral tissue ranges from ~7.5-4% O_2, depending on the tissues (365). Over the last decade, the use of optimised (often-lower) perfused O_2 has been applied to cell culture systems in order to mimic *in vivo* conditions –termed "physioxia". Lowering the [O_2] to a level a cell will typically experience *in vivo* leads to favourable growth conditions. Lower [O_2] has been successfully applied to culture of mouse embryonic fibroblasts which showed no senescence at 3% oxygen, compared to 20% O_2 where DNA damage is displayed at an early stage (366). Culturing of haematopoietic stem cells (HSCs) also benefits from a low [O_2], decreasing proliferation, favouring quiescence and decreasing cellular stresses (367).

Optimisation of [O_2] conditions for storage has already been investigated for RBCs. A major concern with RBC storage is haemoglobin oxidation (368, 369) and reactive O_2 species (ROS) generation (370), resulting in depleted ATP, loss of cell surface area and eventual haemolysis during storage (371). RBCs use glycolytic pathways for metabolism; therefore, O_2 is not a requirement for RBC survival (372). RBCs stored in a hypoxic environment, have lower O_2 availability, discouraging

haemoglobin oxidation. Therefore, RBCs kept in hypoxia produce less ROS by-products, resulting in a decrease in RBC damage (372). It was reported that hypoxic storage also counteracted metabolic impairments (373). Previously, it has been demonstrated a reduction in CO_2, results in a neutralisation of pH which therefore maintains 2,3-diphosphoglyceric acid levels, critical for the glycolytic pathway in RBC metabolism (373, 374). The investigations concluded that improved energy generation and decreased OS in RBCs resulted in enhanced post transfusion recoveries in patients (375). This confirms O_2 storage conditions can be highly influential on the viability and function of blood products.

In this chapter, EPR oximetry techniques and reduced [O_2] conditions were applied to stored PC to firstly, directly measure the [O_2] within the storage container experienced by PLTs and O_2 consumption by PLTs over storage time, and secondly, the influence of lowering ambient [O_2] on these parameters. The hypothesis was that PCs at a reduced [O_2], reflecting conditions PLTs typically experience *in vivo*, would lead to a higher quality PC compared to current conventional storage at atmospheric [O_2].

5.2.2 Aims

1. To measure the [O_2] and PLT O_2 consumption directly within the PC storage container.
2. To investigate the influence of an altered O_2 environment on PC quality and function.

5.3 Methods

The methods described in this chapter build upon those previously described in detail in Chapter 2 and are specific to the work carried out in this chapter.

5.3.1 Platelet Concentrate Preparation

Platelet concentrates were prepared as outlined in section 2.1 and stored at standard blood banking conditions. Each PC consists of 4 blood donors, pooled into one unit. Two PC units were combined and split into two to allow identical experimental bags.

5.3.2 Variation in the ambient [O2] during storage

PCs in ambient air (at 21% O_2) are defined as the control. s. In order to investigate the influence of modulating the [O_2], identical PC samples were kept under hypoxic conditions (10% O_2 or 5% O_2), agitated as set out by standard blood baking conditions using an In VivO_2 chamber (Ruskin Ltd) with access ports for sampling. This allowed PC aliquots from the bag to be collected over the investigation period whilst retaining the desired [O_2]. PAS only was utilised to measure [O_2] within the bag without PLTs present to determine the effect the container and solubility of O_2 has on internal [O_2].

5.3.3 O_2 Oximetry

OCR was used to determine the metabolic activity of PLTs, measured by EPR oximetry, outlined in section 2.4.4. [O_2] measured in the experimental sample was calculated according to the equation shown in section 2.4.2. [O_2] was measured in PAS only (without PLTs) to determine the maximal O_2 capacity of the storage container. A 24-hour stabilisation was applied in order for equilibration at the set [O_2], so the first PC sampling point was day 2.

5.3.4 EV isolation

EVs were isolated from PCs using differential centrifugation outlined in section 2.5.1. An exemplar ISEV-based characterisation of these EVs isolated from PCs can be found in Chapter 3, section 3.4.3.

5.3.5 EV Concentration

EV concentration was determined using NTA, fully described in section 2.5.2.2

5.3.6 Turbidimetric Clot formation and lysis

Thrombin induced fibrin clot formation and tPA -induced clot lysis was assessed using a standard turbidometric assay with the addition of a fixed number of EVs $1x10^{10}$p/ml as outlined in section 2.6.2.

5.3.7 PLT Aggregation

To determine to functionality of the platelets, TRAP-6 and Ristocetin induced aggregation was assessed as described in section 2.2.2

5.3.8 pH measurements

An import ant QC measure of platelet storage is pH, ensuring that the pH does not drop below 6.4. 1mL was taken aseptically from the PC and sampled on a pH metre, which was calibrated (2-point) prior to use.

5.3.9 Statistical analysis

Statistical analysis was performed as described in section 2.8.

5.4 Results

5.4.1 O_2 Consumption Rate

OCR, (Fig 5.1), was consistently higher in the control compared to 5% [O_2] and 10% [O_2] stored PCs. However, this was significantly higher only on day 4 of storage ($P<0.05$). There was no reported significant difference between 5% [O_2] and 10% [O_2] storage throughout the 10-day study. OCR did not significantly alter in control, 10% [O_2] stored PC and 5% [O_2] stored PC over the 10-day storage period (day 2 vs day 10, P=0.073, P=0.33, P=0.58, respectively).

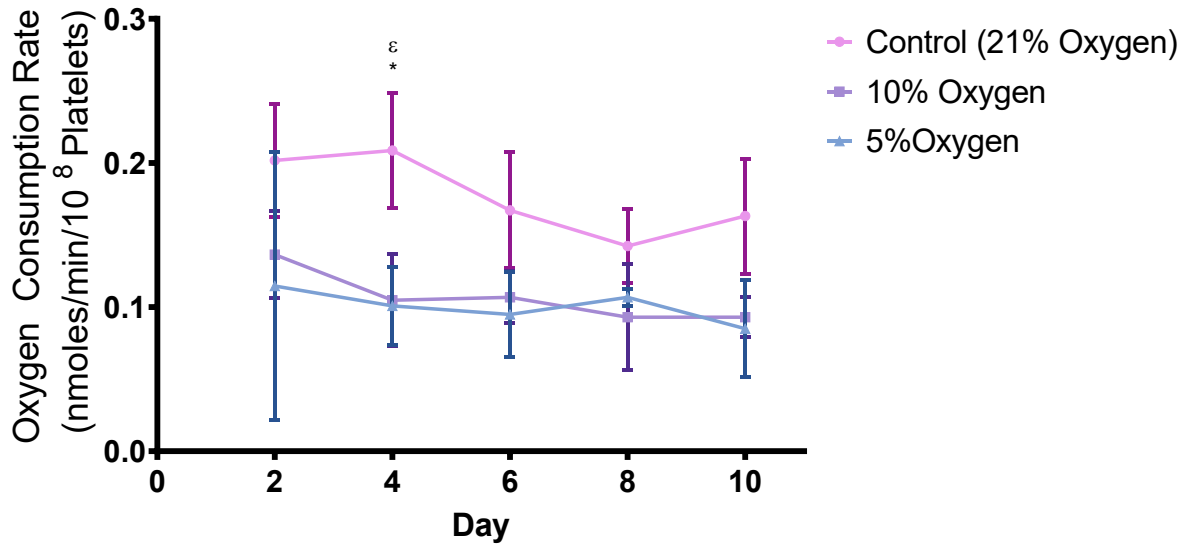

Figure 5.1 – **OCR of PLTs over storage.** O_2 consumption rate of PLTs over a 10-day storage period measured by EPR oximetry. *p<0.05 Control vs 10% O_2. Ɛp<0.05 Control vs 5% oxygen. Error bars denote ±SD, N=3 (N=6 control).

5.4.2 Direct [O_2] measurement with and without PLTs

[O_2] was measured in PAS only and PC samples on day 2 of storage to assess the [O_2] in the bag at the beginning of the investigation period (Fig 5.2). There was a significantly higher [O_2] when comparing PAS to PC at 21% [O_2] ($P<0.01$). The [O_2] was significantly higher in 21% [O_2] PAS compared to all other conditions irrespective of content ($P<0.0001$). 21% O_2 stored PC reported significantly higher [O_2] compared to 10% [O_2] stored PAS only ($P<0.001$); 10% [O_2] PC, 5% [O_2] PAS only and 5% [O_2] PC ($P<0.0001$). 10% [O_2] stored PAS only was not statistically different to 10% [O_2] PC, 5% [O_2] PAS only or 5% [O_2] PC.

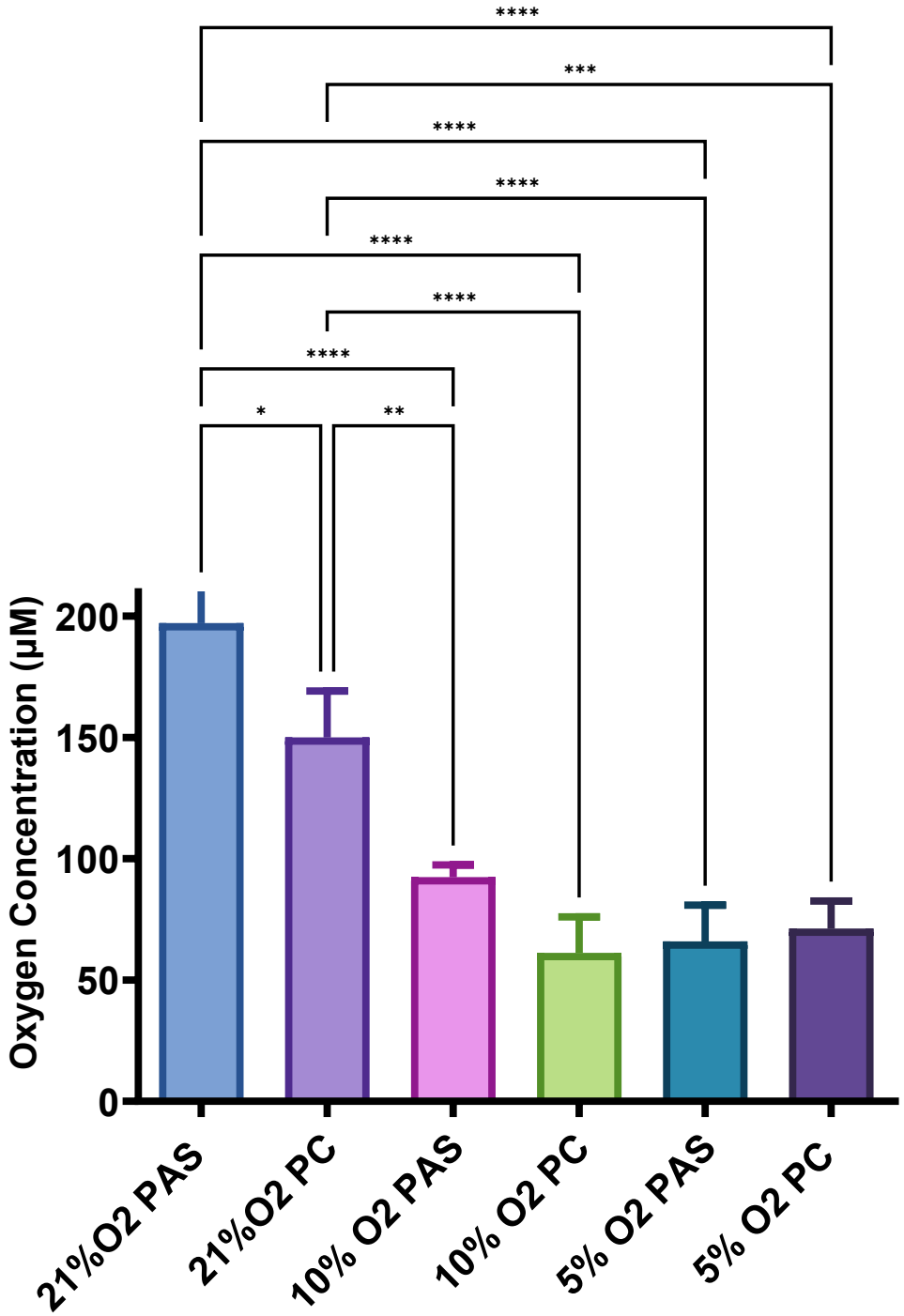

Figure 5.2 – **[O_2] with PC storage containers**. [O_2] within day 2 PCs. PAS related measures represent PAS without the addition of PLTs. *p<0.05, **p<0.01, ***p<0.001 ****p<0.0001. Error bars denote ±SD. N=3 (N=6 Control).

5.4.3 EV Concentration

EV concentration (Fig 5.3) did not significantly change comparing day 2 to day 10 and is the same in control (P=0.0641), 10% [O_2] stored PCs (P=0.2866) and 5% [O_2] stored PC (P=0.5134). There is also no significant difference in EV concentrations at any time point comparing control to 10% [O_2] stored PCs or 5% [O_2] stored PCs.

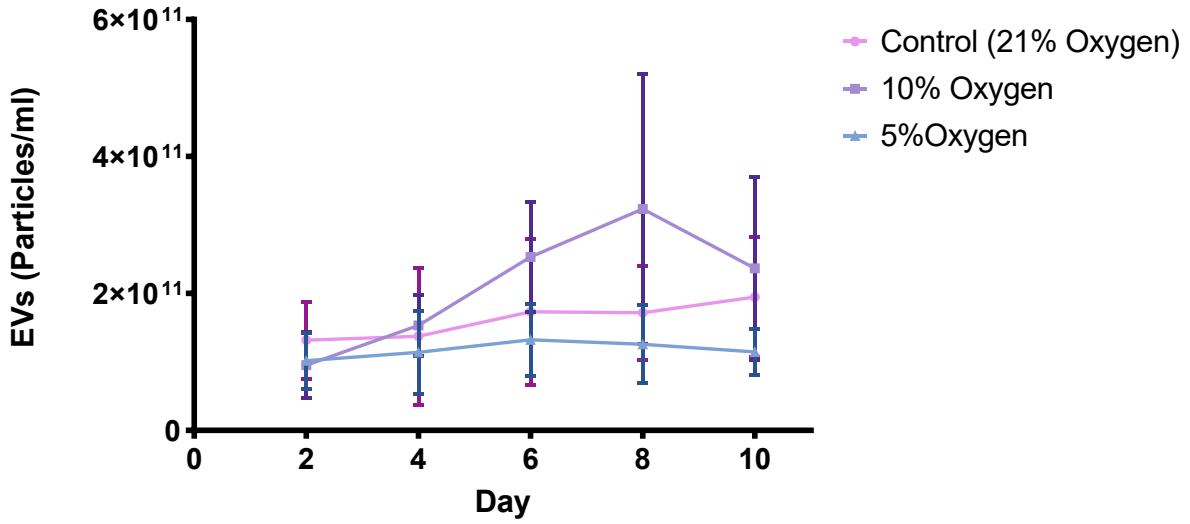

Figure 5.3 – **EV Concentration isolated from PC storage.** EV concentration over the 10-day storage period determined by NTA. Error bars denote ±SD, N=3 (N=6 Control).

5.4.4 EV induced Coagulation

EV concentrations were normalised, as in previous chapters, to assess the EV procoagulant potential. EVs isolated from 21% (P<0.001) [O_2] and 5% [O_2] stored PCs showed significantly reduced lag time compared to the no EV control plasma (P<0.01 except day 20 p<0.05) (Fig 5.4A). A significantly shorter lag time is reported when comparing 21% [O_2] vs 10% [O_2] stored PCs on day 8 (p<0.05) and day 10 (p<0.01). A significantly shorter lag time is also noted when comparing 5% [O_2] to 10% [O_2] stored PC on day 10(p<0.05).

There is no reported significant difference in maximum clot size across all conditions (Fig 5.4B). EVs isolated from 21% [O_2] and 5% [O_2] storage significantly reduced time to maximum clot formation at all-time points when compared to the no EV control (p<0.001) (Fig 5.4C). 10% [O_2] storage significantly reduced time to maximum clot formation on day 4 (p<0.05) compared to the control

plasma. There was also a reduction in time to maximum clot formation when comparing EVs from 5% [O_2] and 10% [O_2] ($P<0.05$).

Time to 50% lysis was significantly longer in 10% [O_2] stored PC derived EVs on days 4 ($P<0.05$) and 8 ($P<0.01$) compared to the no EV control plasma (Fig 5.4D). A significant difference in time to 50% lysis on day 8 was reported when comparing 10% [O_2] to 5% [O_2] stored PC derived EVs ($p<0.05$).

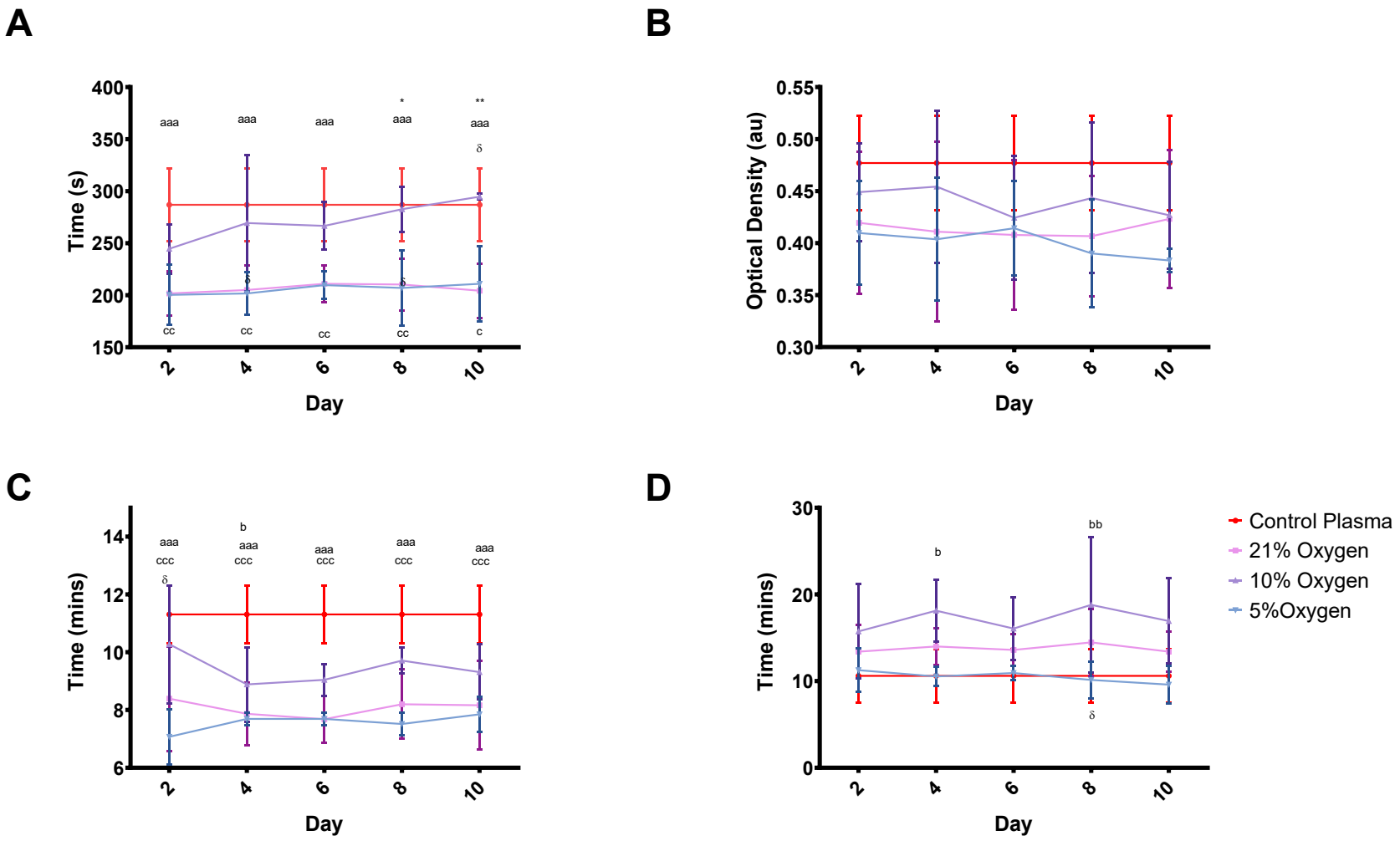

Figure 5.4 – **EVs isolated from PCs effect on fibrin clot formation and lysis**. EVs at $1x10^{10}$p/ml were applied to a turbidity and lysis assay using a fresh frozen plasma to assess the EV influence on the fibrin clot, compared to a "no EV" control. (A) Time taken to initiate fibrin clot formation. (B) Maximum fibrin clot size measured by maximal turbidity of plasma. (C) Time to maximum fibrin clot formation. (D) Time taken to achieve 50% lysis. Error bars denote ±SEM. aaa-p<0.001 Control Plasma vs 21% oxygen; b-p<0.05, bb-p<0.01 Control plasma vs 10% oxygen; cc-p<0.01, ccc-p<0.001 control plasma vs 5% oxygen. *p<0.05, **p<0.01, 21% O_2 vs 10% oxygen. δ-P<0.05 10% O_2 vs 5% oxygen. N=3 (N=6 Control).

5.4.5 PLT Aggregation

PLT aggregation in response to TRAP-6 (Fig 5.5A) and Ristocetin (Fig 5.5B) are shown in Figure 5. A significantly lower TRAP-6 response was reported in 5% [O_2] vs 21% [O_2] stored PCs from day 4 onwards (Day 4 & 6 $p<0.0001$, day 8 & 10 $p<0.001$). A significantly lower TRAP-6 response was also reported in 10% [O_2] stored PCs vs the control on day 6 ($p<0.0001$). A significantly lower TRAP-6 responsiveness was reported on day 10 in 5% [O_2] stored PCs compared to 10% [O_2] storage ($p<0.01$). TRAP-6 responsiveness does not significantly change comparing day 2 to day 10 in the control ($P=0.156$), 10% [O_2] stored PCs ($P=0.230$), however a significant decline in TRAP-6 is reported in 5% [O_2] stored PC ($P=0.0045$).

Aggregation in response to Ristocetin was significantly lower in 5% [O_2] stored PCs on days 2 compared to the control (D4, $P<0.01$) and compared to 10% [O_2] stored PCs ($p<0.0001$). Ristocetin response significantly declines over time when comparing day 2 to day 10 in the control ($P=0.0388$) and 10% [O_2] stored PCs ($P=0.0132$), however is not significantly different in 5% [O_2] stored PCs ($P=0.1289$).

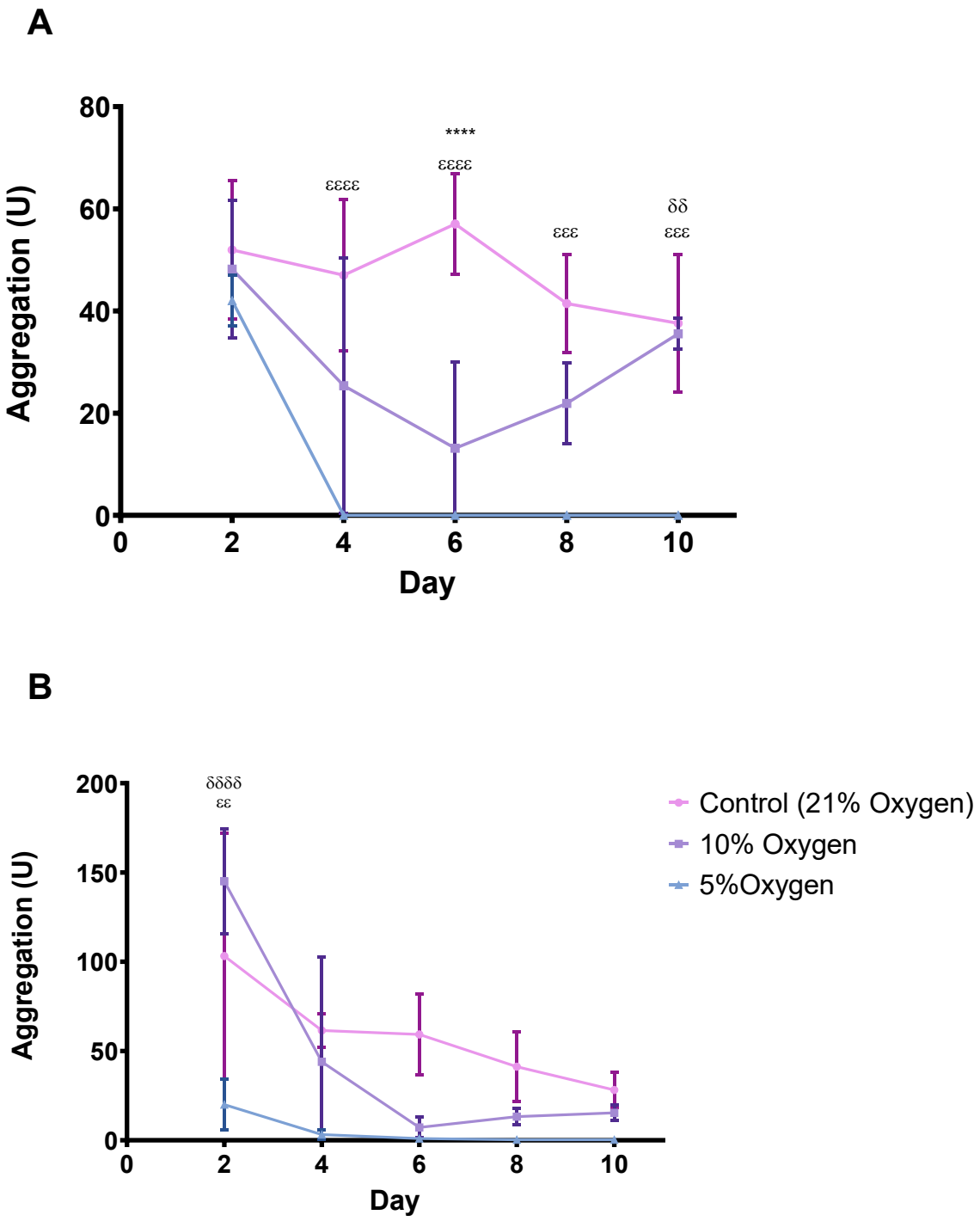

Figure 5.5 – **Aggregation of PLT over storage.** (A) TRAP-6 induced PLT aggregation over a 10-day storage period. (B) Ristocetin-induced PLT aggregation over a 10-day storage. Error bars denote ±SD, **+*p<0.0001 Control vs 10% oxygen. ΕΕ- p<0.01, ΕΕΕ-P<0.001, ΕΕΕΕ-P<0.0001 Control vs 5% oxygen. δδ- p<0.01, δδδδ- p<0.0001 10% O_2 vs 5% oxygen.

5.5.6 pH levels of PCs

pH was significantly lower in 5% [O_2] stored PCs from day 2 onwards compared to the control (P<0.0001) and was significantly lower than 10% [O_2] stored PCs on day 2 only (p<0.0001, Fig 5.6). 10% [O_2] stored PCs also reported a significantly lower pH from day 4 onwards compared to the control (p<0.0001). pH significantly increases in the control over time when comparing day 2 to day 10 (P=0.002). A significant decline in pH is also reported in 10% [O_2] stored PCs (P=0.0347) and 5% [O_2] stored PCs (P=0.01).

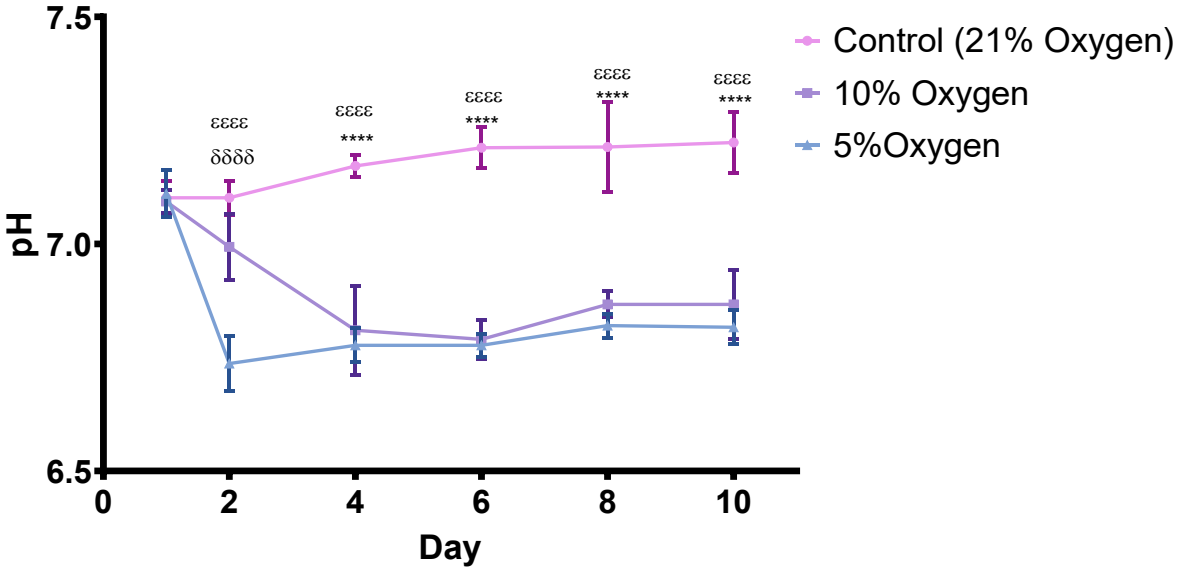

Figure 5.6 – **pH of PCs**. pH measured at day 1 and periodically throughout the 10-day storage period. Error bars denote ±SD, ****p<0.0001 Control vs 10% oxygen. ΕΕΕΕ-P<0.0001 Control vs 5% oxygen. δδδδ- p<0.0001 10% O_2 vs 5% oxygen.

5.5 Discussion

5.5.1 Key Findings

- Direct measurement shows the mean [O_2] experienced by PC within the storage bag is significantly lower than 21% (210uM) O_2.
- Despite an apparent high O_2 outside the bag and constant mixing, these results confirm PCs within the bag experience an inhomogeneous O_2 environment with areas of hypoxia, that is progressively worse the lower the [O_2].
- Reducing storage [O_2] causes a significant decrease in PLT agonist-induced aggregation responses when compared to the conventionally stored PCs.
- EVs generated by PC in storage did not change concentration; however, EVs from PC at 10% O_2 exhibited significantly reduced time to maximum clot formation and lysis time compared to no EV control.

5.5.2 Main Discussion

The reported results provide new knowledge on the importance of [O_2] during storage of PC and show the important consequences on both PC function and quality. The chapter presents, for the first time, direct [O_2] measurement inside the bag does not reflect the [O_2] outside. When storage [O_2] was decreased to levels akin to those experienced by PLTs *in vivo* (Physioxia; 5%-10% [O_2]), consequent reduction in [O_2] experienced by PLTs, resulted in lower OCR and rapid deterioration of PLT aggregation. Thus, data supports the rejection of the initial hypothesis that reduction of [O_2] would protect the PC from PSL.

When [O_2] was reduced, a significant reduction in PLT OCR was reported when compared to the control at storage day 4 (Fig 5.1). These results were not expected, due to the prediction of O_2 being plentiful even under conventional storage conditions. From day 6 onwards, the control PLT OCR decreased. This occurred similarly in both 10% and 5% [O_2]. A possible explanation for the decrease in OCR of the control PLTs could be due to the exhaustion of PC glucose. Glucose has long been regarded

as an important additive of PAS used in PC storage (119, 276). Exhaustion can be linked to the increase in pH noted in Fig 5.6. However, PC OCR when compared to other cells such as human umbilical vein endothelial cells (HUVECs) is much lower, with the average OCR of HUVECs being 1800nmol/min/10^8cells, 9,000x greater than PLTs OCR measured at 0.2nmols/min/10^8cells (376). Therefore, the O_2 requirement of PLT in storage should not be very high.

As previously mentioned, PC arriving at day 1 had 24hrs to equilibrate, so day 2 became the default starting point of the study. [O_2] in PC incubated at 21% O2 was significantly lower than PAS incubated under the same conditions (Fig 5.2). In the presence of healthy PLTs O_2 is constantly being consumed by cellular respiration and where the rate of O_2 consumption exceeds the rate of O_2 replenishment from outside the bag, a lower mean internal [O_2] of 150µM inside the storage container is observed. This data confirms that PLTs stored at 21% O_2 do not experience 21% [O_2] inside bag. Previous reports within the literature and modelling assumptions (based *in silico*, not tested *in vitro*) to predict O_2 in mmHg suggested an average of pO_2 of 95mmHg inside the PC under conventional storage conditions (377). If an assumption of linearity on the percentage of O_2 and mmHg is made and that 21% [O_2] is ~ pO_2 158mmHg, 95mmHg is equivalent to ~12.7% [O_2]. Despite being lower than the results presented, the data supports the finding that at typical PLT concentrations used for storage, the [O_2] inside the storage containers is significantly lower than outside. This difference between PAS only and PC was mirrored at 10% [O_2] although no significance was reported but was not reflected at 5% [O_2].

The lower OCR measured for PLTs stored at 10% and 5% O_2 is unexpected. Mitochondrial respiration should proceed at maximal rate at O_2 concentrations above 0.08µM O_2 (378), which reflects the Km of cytochrome oxidase for O_2 and the rate limiting step in the respiratory chain. This suggests that at O_2 tensions considerably lower than the mean O_2 measured inside the PC should not affect OCR due to progressive reduction of cytochrome C, essentially leading to a constant OCR (378). This therefore raises the question why PLTs exhibited a lower OCR. A possible explanation is that although the mean O_2 measured within the bag remained relatively higher than that required for

respiration, the rate of O_2 supply from outside was not sufficient to maintain homogenous distribution within the storage container, and consequently PLTs at a certain distance from the outside may have been depleted (further explained in 5.5.3). It must also be considered that the bag is constantly agitated to assist with mixing. However, if the scenario above is drawn out, it implies PLTs within the container experience cycles of high O_2, low O_2 and possible zero O_2 depending on their location (and distance from the outside O_2 supply). Consequently, when OCR is measured for a fixed number of platelets in our experiment, there is a progressive decline in OCR at 10% and 5% O_2. This also suggests that the extent of the "no oxygen" zone (Fig 5.7) within the PC is progressively increased when comparing 21% < 10% < 5% O_2.

[O_2] is not the only controller of OCR. Important for respiration is the availability of reducing substrate which determines the level of mitochondrial NAD^+/NADH and the cellular energy supply (ATP/ADP). If this is in short supply, OCR will be decreased. PLTs are highly metabolically active when resting, with a high ATP turnover compared to other resting cells (379). 50-80% of PLT ATP is produced by glycolysis, compared to oxidative phosphorylation providing 20-40% (380). Along with a decrease in cytochrome C oxidase and ATP over storage (381), OCR may decrease at much higher [O_2] than expected due to other OCR factors mentioned.

EV concentration in different storage [O_2] did not significantly differ when comparing 21% to 10% and 5% O_2, possibly reflecting minimal excess PLT activation (165, 258, 259). It is recognised that a consistently higher EV is reported in 10% [O_2] storage, suggesting more activation, but this did not reach statistical significance and decreases at day 10. The reason for this was not investigated and it would require more repeats to determine the reasons behind the decrease.

The procoagulant capability of EVs measured by the turbidometric assay resulted in similar observations to Chapter 4 (CS of PCs) where EVs have an overall effect in reducing the lag time to clot formation (Fig 5.4A) and time to maximal clot formation (Fig 5.4C), which agrees with PEVs being pro-coagulant (337, 382, 383). The data in Fig 5.4B suggests that the maximum clot size is lower than control, in agreement with data reported in the thesis (Chapter 4). 21%and 5% [O_2] PC-derived EVs do

not significantly alter the lysis time compared to the control plasma sample. 10% [O_2] PC-derived EVs significantly increases the lysis time compared to the control plasma and 5% [O_2] isolated EVs. Along with no significant difference in the lag time from 10% [O_2] EVs suggests that the EV character could potentially be different, effecting the clot strength but not the speed of clot formation, which warrants future investigation.

Culturing cells at a "physiological-like O_2" has been reported to increase speed to confluence and decrease metabolic stress, resulting in an overall better quality cell culture (384). However, in the experiments reported in this chapter, as [O_2] decreased, TRAP-6 and Ristocetin induced PLT aggregation decreased significantly compared to conventional 21% O_2 stored PC (Figure 5.5A & 5.5B). At 5% [O_2], a significant loss of PLT function was observed in TRAP-6 induced aggregation from day 4 onwards and Ristocetin-induced aggregation from day 2 onwards. A possible explanation for the decline could be due to impairment of GPIIb/IIIa, demonstrated previously when PLTs experience hypoxia (385). When stored at 10% [O_2] the loss of function was not as severe. There was no significant loss in Ristocetin induced aggregation, but by day 6, TRAP-6 induced aggregation was significantly lower than at 21% O_2. The aggregation recovery observed in PC stored at 10% [O_2] when induced by TRAP-6 at day 8 and 10 was not further investigated due to PLT function not increasing beyond the level of the control PC.

5.3 Modelling O2 Conditions

The reasons why the reduction in [O_2] did not improve PC quality can potentially be explained when applying a mathematical model formulated around cell culture systems (386). The model can determine the O_2 availability within a cell culture vessel and applies a number of assumptions. The first assumption is that mitochondria will utilise any available O_2 that is present, implying that the O_2 gradient at 21% [O_2] concentration will be 210µM if we assume a minimal point within the PC where O_2 is zero. This gradient would be 100µM at 10% [O_2] and 50µM at 5% [O_2]. A diffusion constant equal to cell culture media was applied, as in the model (386), suggested as a conservative coefficient, of $2.86 \times 10^{-5} cm^2/sec$ (387). If lower diffusion constants are used (for example if PAS exhibits lower

coefficient of diffusion), a more dramatic prediction of oxygen limitation will be calculated. The simplified equation (equation 5.1) and re-arranged equation (equation 5.2) are detailed below.

$$F = D \times \frac{\Delta Ox}{\Delta y}$$

Equation 5.1 **– Simplified equation**. Whereby F-Flux, essentially OCR, D-Diffusion Constant, Ox – Maximum gradient of oxygen, y – maximum distance to zero O_2.

$$\Delta y = D \times \frac{\Delta Ox}{F}$$

Equation 5.2 **– Re-arranged equation.** Whereby F-Flux, essentially OCR, D-Diffusion Constant, Ox – Maximum gradient of oxygen, y – maximum distance to zero O_2.

Rearranging the equation allows "y" to be calculated, the distance at which O_2 becomes limiting within the container i.e., zero O_2. Applying the OCR measured in these studies on day 2 (minimising the PSL effect), table 5.1 demonstrates "y" in mm for each storage condition, with Fig 5.7 depicting the model. The width/depth of a PC storage container when filled with a volume of 300ml PC lying flat on its surface is 10.6mm (5.3mm from each surface is we assume equal supply). The model predicts when storing at 21% [O_2], O_2 is limited at a depth of 1.79mm from each surface. The model therefore predicts that the majority of the PLTs within the PC are experiencing hypoxia or even anoxia (whereby cells experience 0% oxygen, depicted in Fig 5.7 as the black region). In other words, the km 0.08µM is for a singular mitochondria, PLTs have 5-8 mitochondria per cell (388). When in such high concentration, the PLTs furthest away from the O_2 source will experience hypoxia, the basis of how hypoxic regions form based on the Krogh cylinder model (389). The majority of previous research suggests hypoxia is detrimental to PC storage (50, 53, 363). Although PC are agitated, causing PLTs to constantly circulate between anoxic, hypoxic and oxygen rich regions, will likely impact on PLT cellular stresses. When the external [O_2] was reduced further to 5%/10%, the reduction of O_2 availability was further exacerbated, reducing the maximal distance O2 was received by PLTs. This is in agreement

with the overall reduction in OCR measured under these conditions and potentially explains the reported observations regarding poor functionality at lower [O_2].

Environmental oxygen (Moles/mL)	*OCR (Moles/sec/mL)*	*Diffusion Constant (cm^2)*	*Oxygen limitation Depth (mm)*
$2.10x10^{-7}$	$3.361x10^{-11}$	$2.86x10^{-5}$	1.79
$1.00x10^{7}$	$2.27333x10^{-11}$	$2.86x10^{-5}$	1.26
$5.00x10^{8}$	$1.91167x10^{-11}$	$2.86x10^{-5}$	0.75

Table 5.1 **– O_2 Modelling calculations**. O_2 limiting calculations utilising the rearranged equation shown as equation 2. Environmental oxygen was supplied by atmosphere or specific gaseous concentration supplied in the experiment and changed from µM to Moles/mL. OCR, represented by Flux in the model, was obtained in this chapter, Fig 5.1 day 2. The resulting "y" was converted to mm and compared to the bag which is 5.3mm.

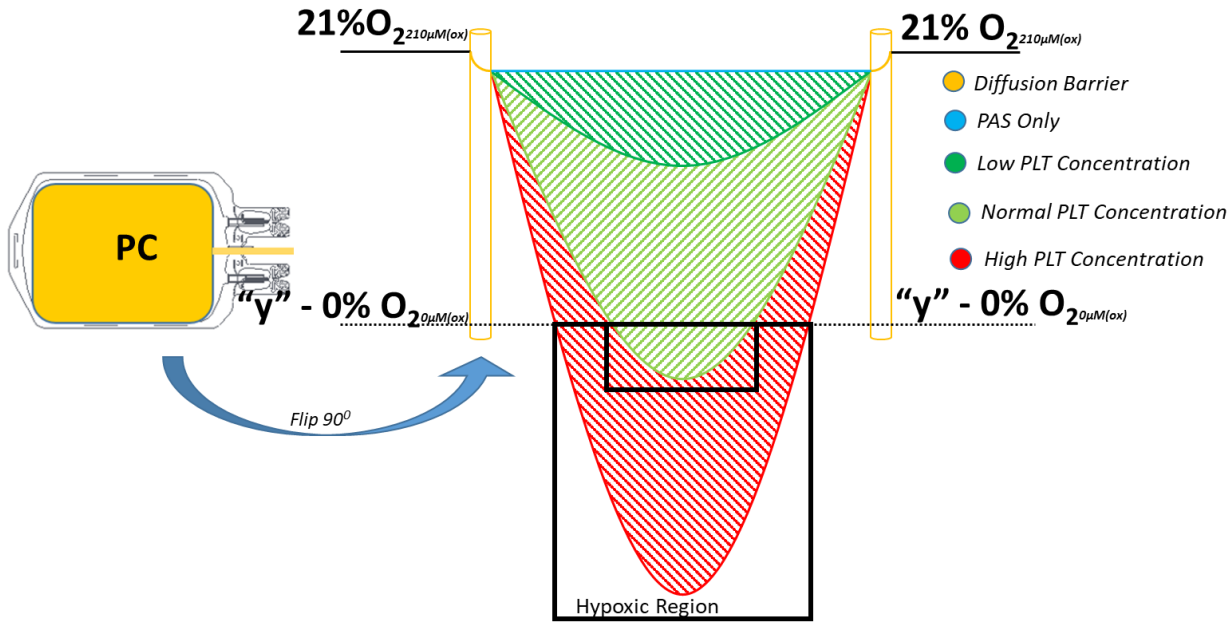

Figure 5.7 **– Schematic of Oxygen Model at 21% O2.** As oxygen diffuses into the bag, a small gradient is present leading to a lower oxygen. The [O2] at PAS only is only affected by this diffusion gradient due to no PLTs respiring O2. A PLTs are introduced to the system at low concentrations oxygen begins to be utilised, dropping the mean oxygen of the bag, leading to an oxygen gradient where cells closest to the source will have more oxygen. As the PLT concentration increases, the equation allows "y" to be calculated which is the distance at which O2 becomes zero, leading to a hypoxic region in the bag. The higher the concentration of PLTs the larger this hypoxic region, so the smaller "y". Therefore, although a mean O2 measured within the bag might be relatively higher than that required for respiration, the rate of O2 supply from outside may not be sufficient to maintain homogenous distribution within the bag as depicted in red, and consequently PLTs at a certain distance from the outside will experience hypoxia, and possible cellular death.

This confirms current PC storage conditions are not optimized for O_2. The main factors that influence the O_2 availability is OCR or the maximal gradient of O_2. The denominator in the equation

and therefore having the greatest influence on "y" is OCR. Modification of these conditions in regard to PLT storage may improve the O_2 availability and hence, improve the function of the PCs compared to conventional storage conditions.

5.5.4 Limitations

This chapter utilised a small sample size (N=3) at each time point. However, the study was designed to minimise donor variability within the small sample by allowing direct comparison of the "same PC" held at different storage parameters significantly increasing the statistical power (paired analysis). However due to the small sample size, it is acknowledged that the application of ANOVA has limited power. It is important that each N represents PC from 8 donors (1 PC is 4 donors, 2 units were combined and split), therefore minimising the donor variation compared to the use of single donor apheresis PCs.

5.6 Conclusion

PC stored under standard conditions of 21% O_2 and a PLT count of $1200x10^9$/L experience lower [O_2] inside the bag, leading to large areas becoming hypoxic. Put another way, O_2 demand by PLTS exceeds the rate of supply form outside. If the external [O_2] is decreased to a more "physiological-like" level, the O_2 availability is further decreased, leading to a higher proportion of PLTs experiencing anoxia, influencing PLT function and overall PC quality. This implies that if O_2 availability is improved (thus minimising the areas of anoxia), PC quality could be improved. The focus of these studies was then shifted to consider improving O_2 availability in the next chapter.

6.0 Results IV – Increasing the O_2 availability in PCs: investigation of the O_2 model

6.1 Perspective

The previous chapter demonstrated that the O_2 availability in the bag at 21% O_2 is limiting causes large areas of hypoxia within the PC container. Consequently, when the external O_2 was decreased to physiological concentrations experienced *in vivo*, the hypoxic region was exacerbated as determined by the O_2 model, resulting in poor PLT function. To address this directly, this chapter investigates the effect of increasing the O_2 availability in the PC container by using the O_2 model to predict the conditions required for homogeneity, based on the hypothesis that increasing O_2 availability will improve PLT function. The O_2 model predicts decreasing the OCR or increasing external O_2 will have the greatest effects on O_2 availability.

6.2.1 Introduction

O_2 availability has been assumed to be homogeneous at 21% O_2 under standard storage conditions, with the ideology of hypoxic conditions being detrimental to PC quality and PLT function (51, 53, 363). However, this thesis has established that O_2 availability at 21% O_2 generates large regions of hypoxia within the storage container, leading to the possible promotion of the PSL. Applying the mathematical model developed, the point at which O_2 becomes limiting can be predicted when parameters are altered (detailed in section 5.3).

To increase oxygen availability, two factors can be altered without changing the storage container itself. These are, decreasing the OCR, by changing the cell concentration, or increasing the supply of O_2 by increasing the external [O_2]. Table 6.1 details that as PLT concentration decreases by 50% (with consequent 50% decrease in OCR) the O_2 availability increases to a depth of 3.57mm from the container surface. Further decrease in PLT concentration to 25% leads to no O_2 limitation in the bag (a depth of 7.15mm). This is particularly relevant given the bag has a practical depth of only 5.3mm. Torres *et al* in a short report to Vox Sanguinis indicated PLT concentration has the biggest effect on internal partial pressure of oxygen, (377) in agreement with the model applied here. Evidence has suggested that patients require approximately 7100PLT/µL per day to maintain homeostasis, (390) which leads to the question whether a product with lower PLT count can achieve the same clinical efficacy (391). It is also apparent that if the quality of PCs can be improved, a reduction in PLT concentration may counteract the effect of reduced PLT count and could be applied.

The optimal PLT dose required for prophylactic or acute need is highly controversial within the transfusion field, reviewed elsewhere (391), with limited randomised clinical trials on lower PLT doses. A 2004 clinical trial assessing 111 acute leukaemia patients needing prophylactic PLT transfusions concluded that a lower dose (3 pooled WB derived PC compared to 5 pooled WB PCs) did not significantly increase incidents of major bleeds and lead to an increase PLT stock (392). A second study, in 2009, used standard and half doses of PLT for transfusions. The study reported 119 patients presenting with thrombocytopenia and therefore the study was concluded early due to 5% of patients

in the low dose arm presenting with clinical grade 4 bleeds. However, the authors could not conclude if this was by chance or represented a real difference (393). The most recent clinical trial with over 1300 patients concluded low dose transfusion in hypoproliferative thrombocytopenia patients resulted in no significant difference in bleeding incidence, but due to a lower PLT number, some patients required more transfusions (394). Larger clinical trials are required to assess effective PLT dose, and to further clarify why lower PLT doses were not significantly different to the standard dose. A possible explanation could be the increased O_2 availability resulting in increased PLT quality. This phenomenon will be explored within this chapter.

The second factor to be modified is external O_2. Given the storage container dimensions it can be confirmed that the mid-point (furthest distance from the external surface) is 5.3mm. Assuming bilateral gaseous exchange, according to the tested model, it was predicted that an [O_2] of ~62% is required to eliminate heterogeneity of O_2 within the bag and eliminate hypoxic regions within the storage container (table 6.1). It is not known how PLTs will react to the higher O_2, as a proportion of cells will experience 22-60% O_2 when close to the container surface which may in turn cause OS. It has been reported that PC PLTs in storage at 21% O_2 are more sensitive to OS compared to fresh PLTs (395). Evidence for other cell types, have shown normal growth up to 36% O_2, where >38% O_2 caused increased cell turnover and cellular swelling (396). The effects of high O_2 on PC has not been previously investigated.

Environmental oxygen (Moles/mL)	***Platelet Concentration (PLTs/ml)***	***OCR (Moles/sec/mL)***	***Diffusion Constant (cm^2)***	***Oxygen limitation Depth (mm)***
$2.10x10^{-7}$	$1x10^9$	$3.361x10^{-11}$	$2.86x10^{-5}$	1.79
$2.10x10^{7}$	**$5x10^8$**	$1.681x10^{-11}$	$2.86x10^{-5}$	3.57
$2.10x10^{7}$	**$2.25x10^8$**	$0.8046x10^{-11}$	$2.86x10^{-5}$	7.15
$6.22x10^{-7}$	$1x10^9$	$3.361x10^{-11}$	$2.86x10^{-5}$	5.30

Table 6.1 – **Predicted oxygen limitation depth**. Parameters investigated within this chapter to improve O_2 availability in PC storage. The assumption made is that as PLT concentration decreases, the OCR remains constant, hence dropping by ½ or ¼ when the concentration is decreased respectively. The bold parameter on each line is the investigated parameter.

From the predictions in table 6.1, the hypothesis is that by increasing the O_2 availability by either reducing OCR, by a reduction in PLT concentration, or increasing external O_2 will have a positive effect on PC quality and PLT function. This will reduce the PSL and possibly result in a prolonged storage time. To investigate both mechanisms of improving O_2 availability, the study was split into two arms.

6.2.2 Aims

1. To improve O_2 availability by reducing the PLT concentration, therefore reducing the OCR.
2. Increase external O_2 to improve the O_2 availability within the PC.

6.3 Methods

The methods described in this chapter build on those described in detail in Chapter 2 and are used specifically to generate the results described in this chapter.

6.3.1 Platelet Concentrate Preparation

PC were prepared as outlined in section 2.1 and stored at standard blood banking conditions. Each PC consists of 4 blood donors, pooled into one unit. For the hyperoxic (60% O_2) study arm, two PC units were combined and split into two to allow identical experimental bags – one held at 60% O_2 and the control held at 21% O_2. For the variation in PLT concentration, see 6.3.2

6.3.2 Variation in the PLT Concentration, study arm 1

To alter the PLT concentration, 3 PC units were combined and split into 3 to allow identical bags. A 65:35 PAS to plasma unit was created by pooling 325mLs of SSP+ PAS to 175mL of autologous plasma. For the reduced PLT concentration, a waste pack was sterilely docked and either 50%, or 75%, of the PC was removed as required, before being replaced with equal volume (weight) of 65:35 PAS plasma solution. A sample was taken for a PLT count on a haematology analyser to ensure the reduced PLT concentration was correct for the given dilution (standard dose, 50% and 25% PLT concentrations).

6.3.3 Variation in the ambient [O_2] during storage, study arm 2.

PCs in ambient air (defined as the "control" at 21% O_2) were stored at standard blood banking conditions as outlined in 5.3.1. In order to investigate the influence of modulating the [O_2] in the chamber, identical PC samples were kept under hyperoxic conditions (60% O_2) using a custom gas mix (60% O_2, 1% CO_2, 39% N_2), on an agitator, using an In VivO_2 chamber (Ruskin Ltd) with access ports for sampling. This allowed PC aliquots from the bag to be collected over the investigation period whilst retaining the desired storage conditions. PAS alone was also stored to measure [O_2] within the bag without PLTs present to determine the effect of the container and solubility of O_2 on internal [O_2].

6.3.4 O_2 Oximetry

OCR was used to determine the metabolic activity of PLTs, measured by EPR oximetry, outlined in section 2.4.4. [O_2] measurements in the experimental sample were calculated as described

in section 2.4.2. [O_2] was measured in PAS only to determine the maximal O_2 capacity of the storage container. A 24-hour stabilisation was applied in order for equilibration at the set [O_2], so the first PC sampling point was day 2. Cyanide (5mM) was added to duplicate samples prior to EPR oximetry to determine the oxidative phosphorylation independent OCR, associated with OS (397). This was only assessed in the 60% [O_2] study arm.

6.3.5 EV isolation

EVs were isolated from PCs using differential centrifugation outlined in section 2.5.1. An exemplar ISEV-based characterisation of these EVs isolated from PCs can be found in section 3.3.

6.3.6 EV Concentration

EV concentration was determined using NTA, fully described in section 2.5.2.2

6.3.7 Turbidimetric Clot formation and lysis

Thrombin induced fibrin clot formation and tPA -induced clot lysis was assessed using a standard turbidometric assay with the addition of a fixed number of EVs $1x10^{10}$p/ml as outlined in section 2.6.2

6.3.8 PLT Aggregation

To determine the functionality of PLTs, TRAP-6 and Ristocetin induced aggregation was assessed as described in section 2.2.2.

6.3.9 pH measurements

An important QC measure of PLT storage is pH, ensuring that the pH does not drop below 6.4. 1mL was taken aseptically from the PC and sampled on a pH metre, which was calibrated (2-point) prior to use.

6.3.10 CD62P% Assessment

CD62P expression on PLTs is suggestive of activation and granular release. CD62P% was assessed by flow cytometry, detailed in section 2.3.2.

6.3.11 Oxygen radical absorbance capacity (ORAC)

The principle of the ORAC assay is to measure the antioxidant potential of a sample by measuring fluorescent quenching. With the use of a free radical, the duration of inhibition of free radical induced fluorescent quenching by antioxidants is measured. PC supernatant was obtained by 800xg centrifugation. PLT samples were also collected and were lysed as previously described in section 2.7.2. Each well had a final volume of 200uL. The blank wells contained 25ul DPBS while the samples received 25ul of PLT lysate or supernatant. In addition, all wells received 150uL of sodium fluorescein (70mM). The plate reader was set with excitation filter 485 nm and emission filter 535 nm. Immediately before measurements began, 25ul of AAPH (240uM) was added to each well. Plates were shaken before each reading and were read each minute for 1 hour. Results were calculated based on differences of the AUC between sodium fluorescein decay and a sample, expressed as radical induced fluorescent drop (398, 399).

6.3.12 Statistical analysis

Statistical analysis was performed as described in section 2.8.

6.4 Results

6.4.1 Study arm 1 – Variation in PLT concentration

6.4.1.1 O_2 Consumption Rate

OCR was normalised to PLT number (Fig6.1). OCR does not significantly change over 10 days storage when comparing the control to 50% OCR at any time point. There is a significant increase in OCR in 25% PLT concentration compared to both 50% PLT concentration and the control ($p<0.0001$). When comparing day 2 vs day 10, the control and 50% PLT concentration did not significantly change over storage (0.197±0.043 vs 0.165±0.012nmmoles/min/10^8PLTs, P=0.2609, 0.154±0.026 vs 0.152±0.082nmmoles/min/10^8PLTs, P=0.9634, respectively). 25% PLT concentration OCR significantly decreased over storage (0.295±0.094 vs 0.008±0.012nmmoles/min/10^8PLTs, P=0.013).

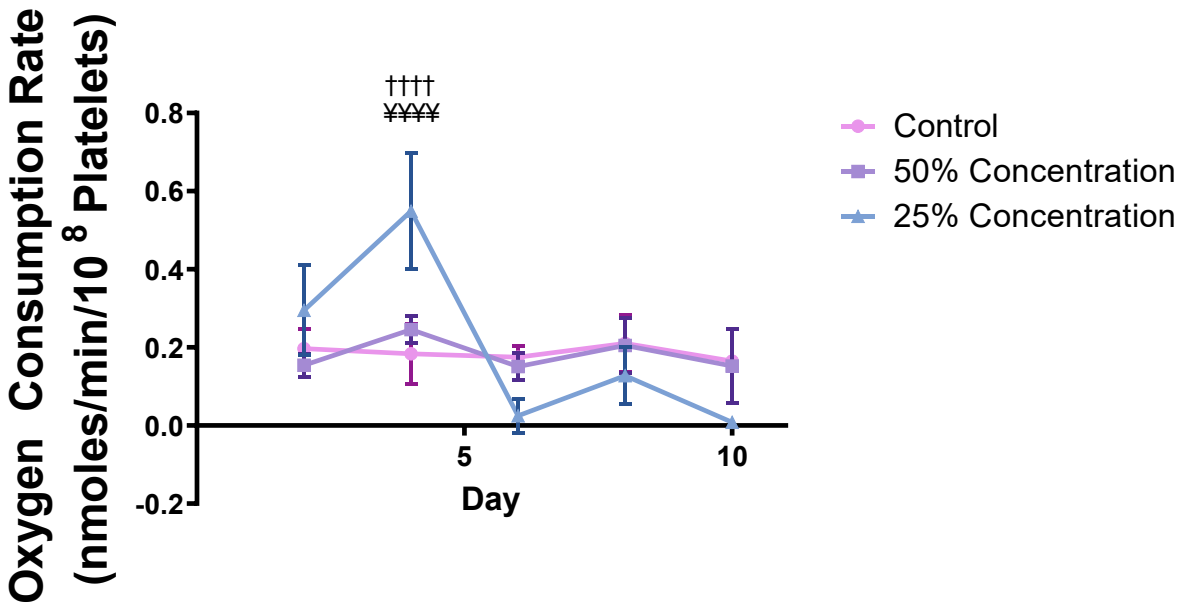

Figure 6.1 – **OCR of PLTs over storage.** O_2 consumption rate of PLTs over a 10-day storage period measured by EPR oximetry. †††† p<0.0001 control vs 25% PLT concentration. ¥¥¥¥p<0.0001 50% PLT concentration vs 25% PLT concentration. Error bars denote ±SD, N= 4 (N=3 25% PLT Concentration units).

6.4.1.2 Direct [O_2]

[O_2] was measured in PC samples on day 2 of storage to assess the [O_2] in the bag at the beginning of the investigation period (Fig 6.2). There was a significantly lower [O_2] in PC at 21%

compared to PC stored at both 50% concentration and 25% PLT concentration ($p<0.05$), as well as PAS only ($p<0.01$). There was no significant difference in the $[O_2]$ within the PC at 50% PLT concentration compared to 25% PLT concentration or PAS only.

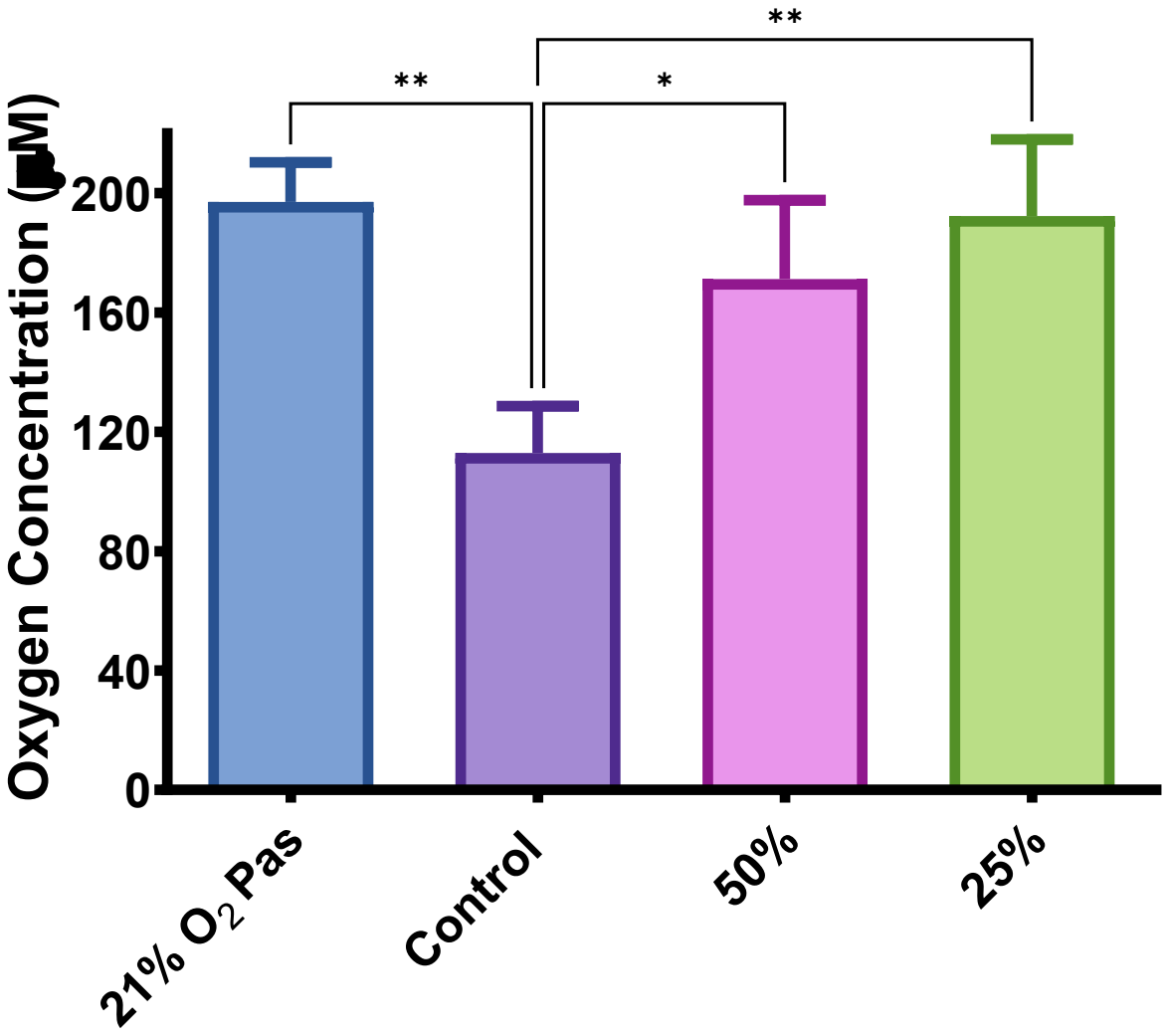

Figure 6.2 – **Direct Oxygen Concentration.** $[O_2]$ within the PC on day 2 of storage measured by EPR oximetry. *p<0.05.*p<0.01. Error bars denote ±SD, N= 4 (N=3 25% PLT Concentration units).

6.4.1.3 EV Concentration

EV concentration (Fig 6.3) does not significantly change when comparing the different concentrations of PLTs used throughout the investigation. Comparing day 2 vs day 10, a significant increase in EVs is reported in the control unit ($4.58x10^{10}±2.2x10^{10}$p/ml vs $1.61x10^{11}±4.24x10^{10}$p/ml, P=0.0062). There was no reported significant difference in EV concentration over storage in both 50% PLT concentration and 25% PLT concentration units ($1.23x10^{11}±3.81x10^{10}$p/ml vs

$1.88x10^{11}\pm1x10^{11}$p/ml, P=0.3354; $9.35x10^{10}\pm5.94x10^{10}$p/ml vs $2.31x10^{11}\pm1.57x10^{11}$p/ml, P=0.3131; respectively).

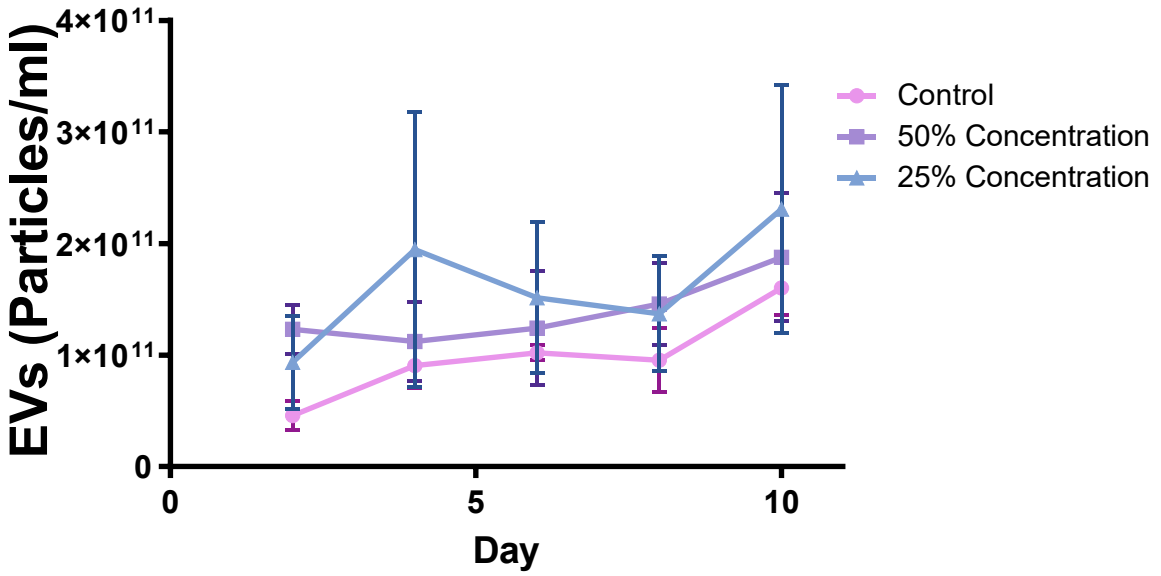

Figure 6.3 – **PC derived EV concentration over storage.** EVs were isolated from PCs via ultracentrifugation over a 10-day storage period. Error bars denote ±SD, N= 4 (N=3 25% PLT Concentration units).

6.4.1.4 EV Induced Coagulation

EV concentrations were normalised, as in previous chapters, to assess the EV procoagulant potential. EVs isolated from all PLT concentrations exhibited similar lag time (Fig 6.4A), maximum optical density (Fig 6.4B) and 50% lysis time (Fig 6.4D) that was not significantly different to the plasma only control. The EVs isolated from the control PC caused a significant decrease in time to maximum clot formation on days 4 ($p<0.05$), 6 ($p<0.01$) and 10 ($p<0.05$). EVs isolated from the 50% PLT concentration units had a significant reduction in time to maximum clot formation on all days except day 6 (day 2 and 8 $p<0.05$, day 4 and 10 $p<0.01$). EVs isolated from the 25% PLT concentration unit only had a significant effect of time to maximum clot formation on day 10 ($p<0.05$, Fig 6.4C).

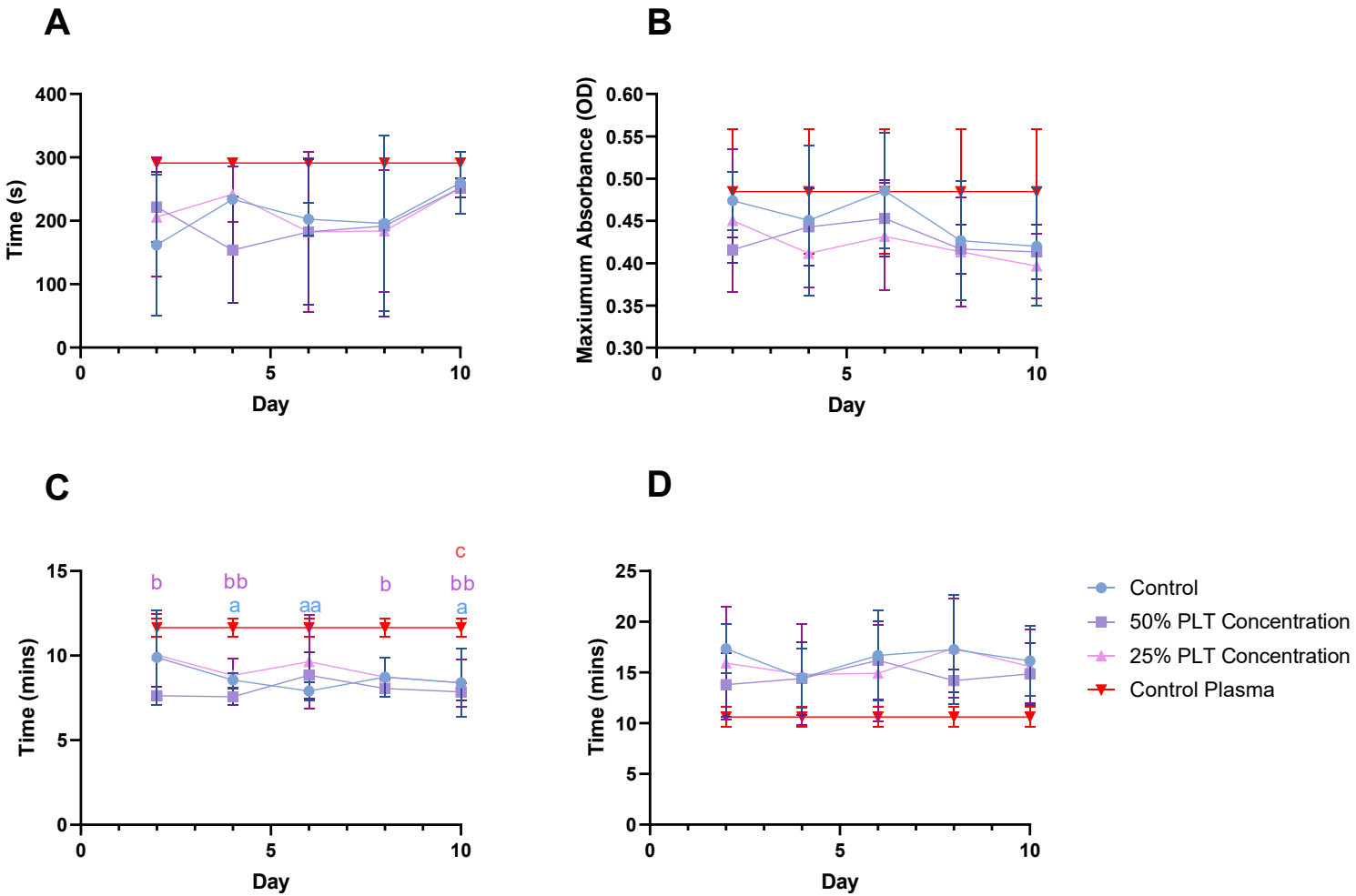

Figure 6.4 **– EVs isolated from PCs effect on fibrin clot formation and lysis**. EVs at 1x10^{10}p/ml were applied to a turbidity and lysis assay using a fresh frozen plasma to assess the EV influence on the fibrin clot, compared to a "no EV" control. (A) Time taken to initiate fibrin clot formation. (B) Maximum fibrin clot size measured by maximal turbidity of plasma. (C) Time to maximum fibrin clot formation. (D) Time taken to achieve 50% lysis. Error bars denote ±SD. a-p<0.05 aa-p<0.01 Control Plasma vs control PC; b-p<0.05, bb-p<0.01 Control plasma vs 50% PLT concentration c-p<0.05, control plasma vs 25% PLT concentration. N=4 (N=3 25% PLT concentration

6.4.1.5 PLT Aggregation

PLT aggregation was normalised for PLT number to therefore allow direct comparison of PLT quality. Trap-6 induced PLT aggregation (Fig 6.5A) was significantly increased in 50% PLT concentration compared to the control on day 4 of storage ($P<0.05$) and the 25% PLT Concentration unit on days 6 and 8 ($p<0.05$, $p<0.01$, respectively). The control also reported a significantly increased Trap 6 aggregation compared to the 25% PLT concentration on day 8 and 10 ($p<0.05$). Over storage, the control did not significantly change comparing day 2 vs day 10 (57.1±6.48U vs 51.8±6.73U, P=0.3636). Both the 50% PLT concentration unit and 25% PLT concentration unit reported a significantly decreased response to trap-6 over the storage duration (85±3.87U vs 40.9±17.99U, P=0.0067; 69.3±31.02U vs 6.3±4.07U, P=0.0464; respectively).

No significant difference was reported in Ristocetin response between the control and 50% PLT concentration unit (Fig 6.5B). The 25% PLT concentration reported a significantly increased Ristocetin response compared to the control on day 6 of storage ($p<0.01$). Over storage, the control showed a significant decline in Ristocetin responsiveness (47.1±13.22U vs 22.4±10.89U, P=0.0465). 50% PLT concentration and 25% PLT concentration reported no significant decline in Ristocetin response (53.7±14.27U vs 45.9±12.57U, P=0.5021; 76.6±14.27U vs 53.6±1.82U, P=0.0771; respectively).

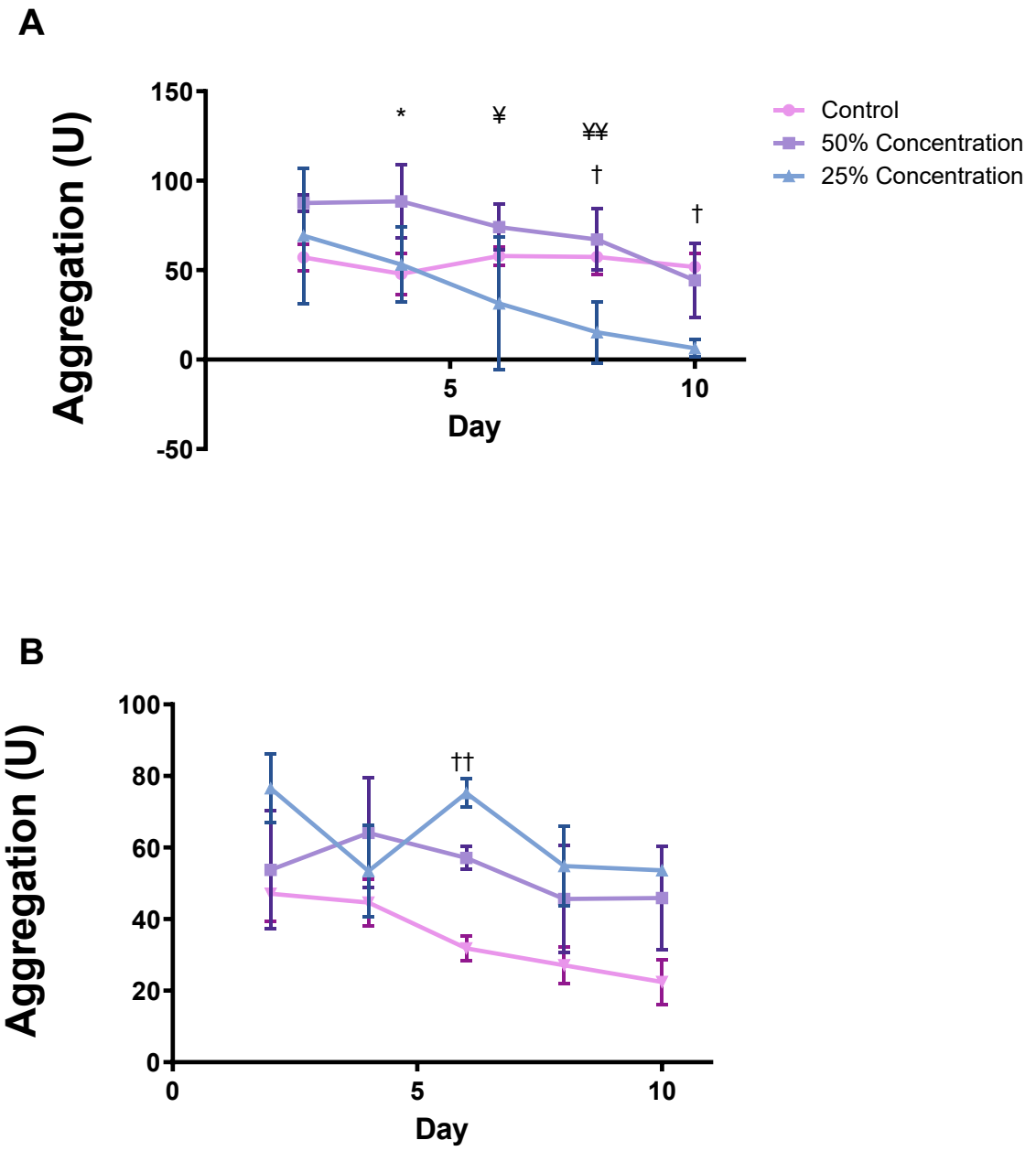

Figure 6.5 – **Aggregation response of PLTs over storage.** PLT aggregation was normalised for PLT number, therefore assessing PLT quality. A) PLT aggregation response to TRAP-6 over a 10-day PC storage. B) PLT aggregation response to Ristocetin over a 10-day storage period. *p<0.05 control vs 59% PLT concentration, †p<0.05, ††p<0.01 control vs 25% PLT concentration, ¥p<0.05, ¥¥p<0.01 50% PLT concentration vs 25% PLT concentration. Error bars denote ±SD, N= 4 (N=3 25% PLT Concentration units).

6.4.1.6 pH levels

pH levels over the study do not fall below pH 6.4 (Fig 6.6), the QC cut-off value used by blood establishments. From day 4 onwards, 25% PLT concentration reports a significantly higher pH compared to the control (Day 4,8-10 $p<0.001$, day 6 $p<0.0001$). On day 6, 50% PLT concentration is significantly higher compared to the control ($p<0.01$). There is no reported significance between 50% PLT concentration and 25% PLT concentration. Over storage, the control pH does not significantly alter (7.2±0.05 vs 7.32±0.05, P=0.0538). Both 50% PLT concentration and 25% PLT concentration show a significant increase in pH over the 10-day storage period (7.2±0.05 vs 7.4±0.07, P=0.0112; 7.2±0.05 vs 7.54±0.05, P=0.0008, respectively).

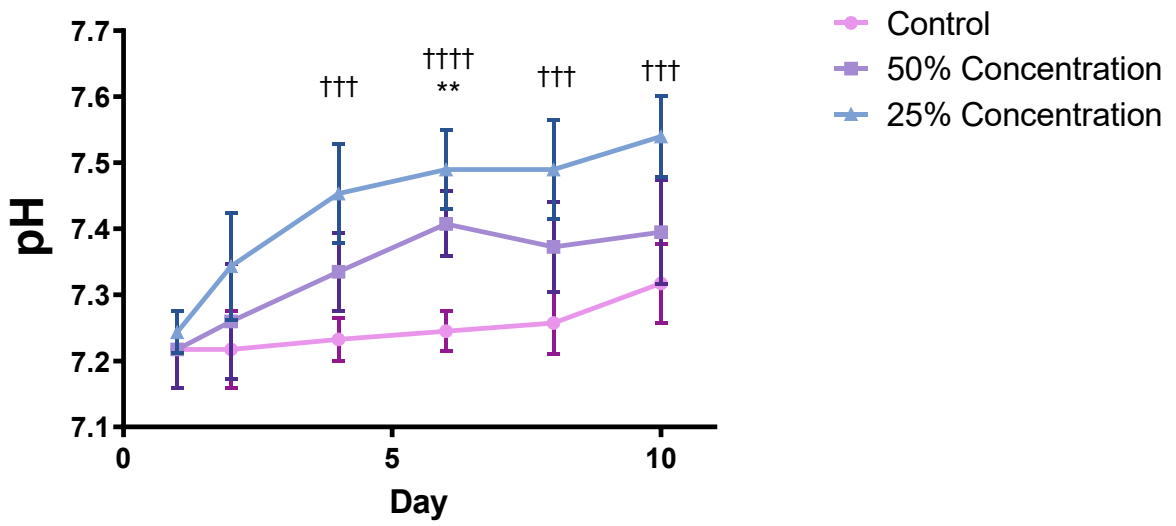

Figure 6.6 – **pH Level of PCs.** QC measures of PCs throughout the 10-day storage period to ensure units do not drop below the 6.4 cut-off value. **p<0.01 control vs 59% PLT concentration, †††p<0.001, ††††p<0.0001 control vs 25% PLT concentration, ¥p<0.05. Error bars denote ±SD, N= 4 (N=3 25% PLT Concentration units).

6.4.1.7 CD62P expression

CD62P% expression measured by flow cytometry (Fig 6.7) was significantly higher in 25% PLT concentration by day 7 of storage compared to the control (day 7 $p<0.05$, day 10 $p<0.0001$). By day 10, 50% PLT concentration also reported a significantly higher CD62P expression compared to the control ($p<0.0001$). All units tested (control, 50% PLT concentration and 25% PLT concentration) demonstrated a significant increase in CD62P% expression over storage (6.51±1.42% vs 20.5±1.73%, P=0.0001; 8.62±1.07% vs 30.07±3.89%, P=0.0001; 9.73±0.877 vs 31.41±3.38, P=0.0009; respectively).

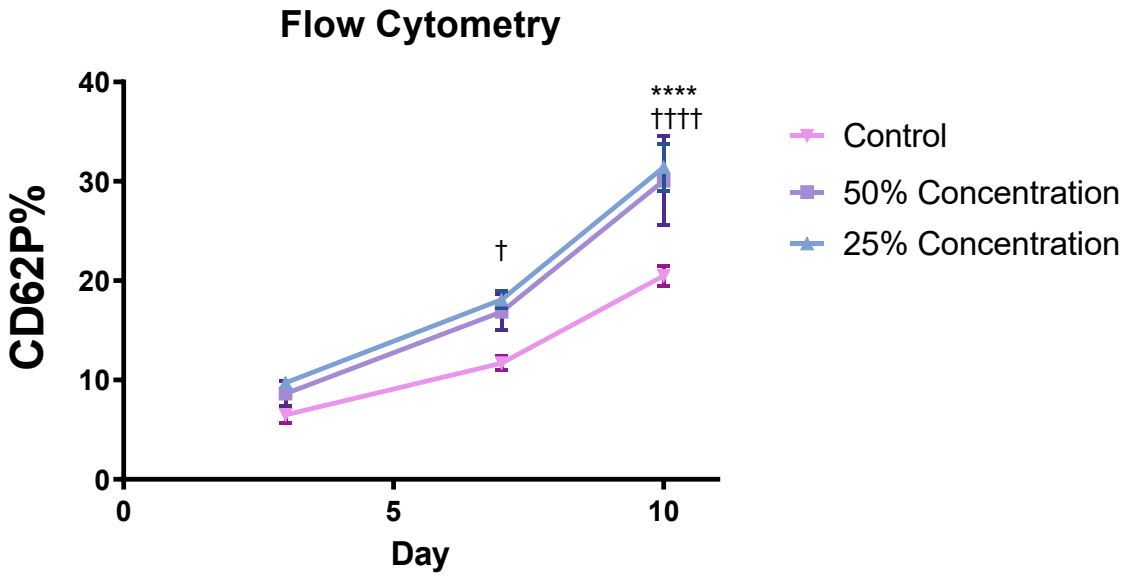

Figure 6.7 – **CD62P% expression on PLTs.** CD62P% surface expression on PLTs isolated throughout storage measured by flow cytometry. ****p<0.0001 control vs 59% PLT concentration, †p<0.05, ††††p<0.0001 control vs 25% PLT concentration, ¥p<0.05. Error bars denote ±SD, N= 4 (N=3 25% PLT Concentration units).

6.4.2 Study arm 2 – Variation in external [O_2]

6.4.2.1 O_2 Consumption Rate

OCR was not significantly different when comparing the control to 60% [O_2] (Fig6.8). Over storage, the OCR of PLT in the control does not significantly change (0.258±0.045 vs 0.157±0.059 nmmoles/min/10^8PLTs, P=0.1269). When PCs are stored at 60% [O_2], the OCR significantly decreased over the storage duration (0.289±0.048 vs 0.0036±0.034nmmoles/min/10^8PLTs, P=0.0035).

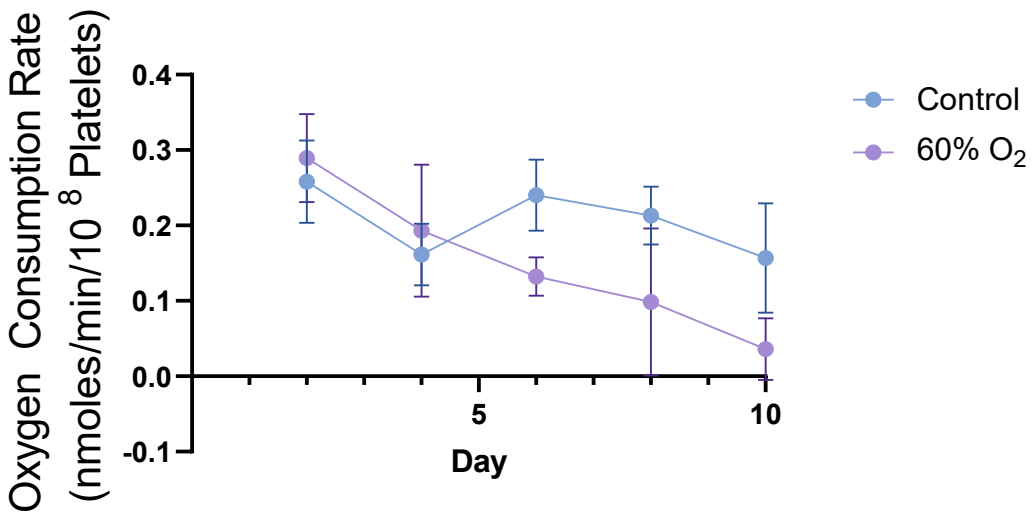

Figure 6.8 – **OCR of PLTs over storage.** O_2 consumption rate of PLTs over a 10-day storage period measured by EPR oximetry. Error bars denote ±SD, N= 3

6.4.2.2 Cyanide-based residual O_2 Consumption Rate

To assess if the increased [O_2] caused additional OS, respiration was blocked using cyanide to assess O_2 consumption independent of oxidative phosphorylation. Fig 6.9A shows at all timepoints except day 4, total PLT OCR in 21% [O_2] PC is significantly higher than the cyanide inhibited OCR (Day 2 and 10 $p<0.001$, day 6-8 $p<0.01$). PC stored at 60% [O_2] (Fig 6.9B) reports that only on day 2 is the oxidative phosphorylation OCR is significantly higher than the cyanide OCR in 60% [O_2] ($p<0.05$). The statistical analysis however is only performed on N=2.

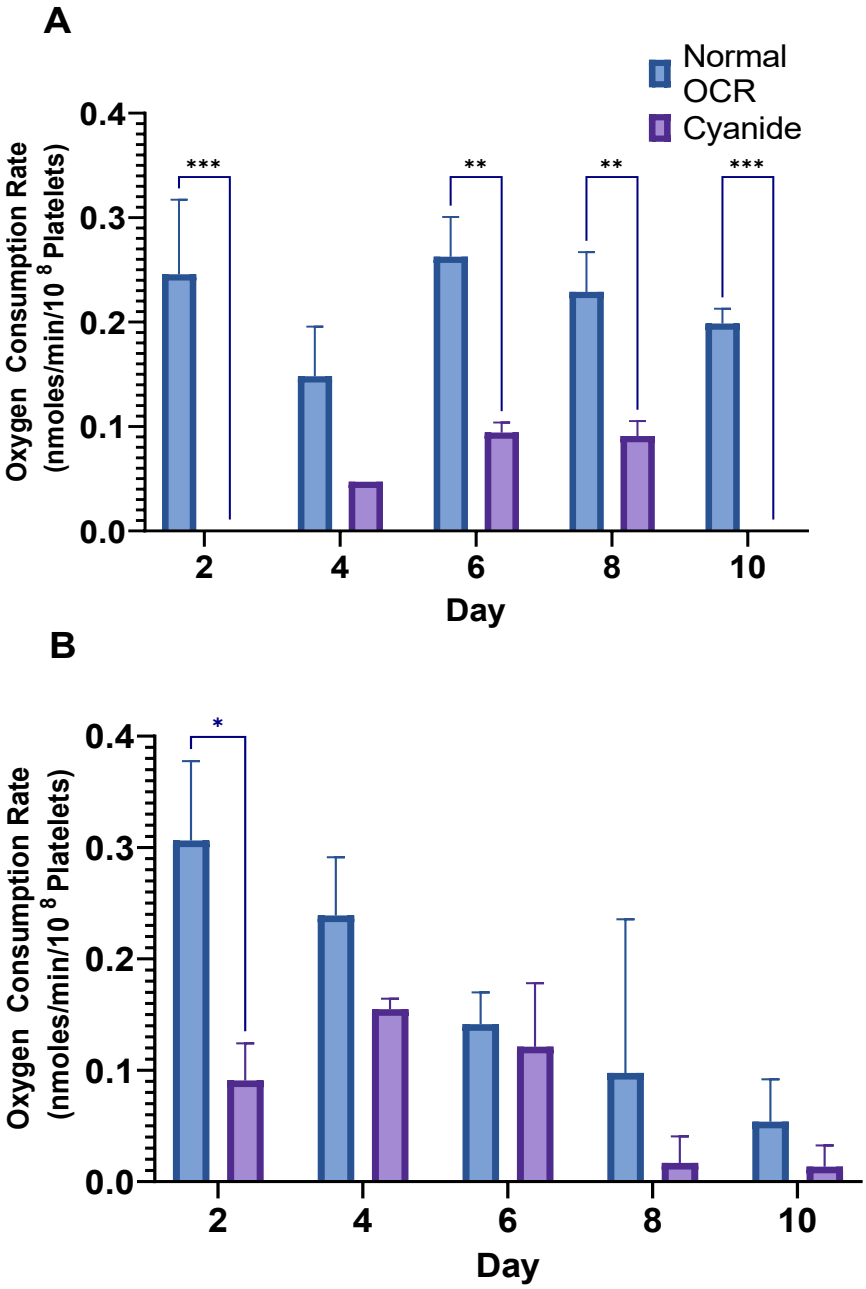

Figure 6.9 – **Assessment of mitochondrial independent O_2 usage.** Cyanide blockage of PLT mitochondrial oxidative phosphorylation to assess O_2 consumption independent of the electron transport chain. A) 21% [O_2] B) 60% [O_2]. *p<0.05, **p<0.01, ***p<0.001. Error bars denote ±SD, N= 2

6.4.2.3 Direct [O_2] measurement in PC

[O_2] was measured in PC samples on day 2 of storage to assess the2 [O_2] in the bag at the beginning of the investigation period (Fig 6.10). As previously reported, there was a significantly lower [O_2] in control PCs compared to PAS at 21% [O_2] ($p<0.01$). This effect was mirrored in 60% [O_2] when PAS only was compared to PCs ($p<0.001$). As expected, the [O_2] in PCs stored at 60% [O_2] was significantly higher than PCs stored at 21%[O_2] ($p<0.0001$).

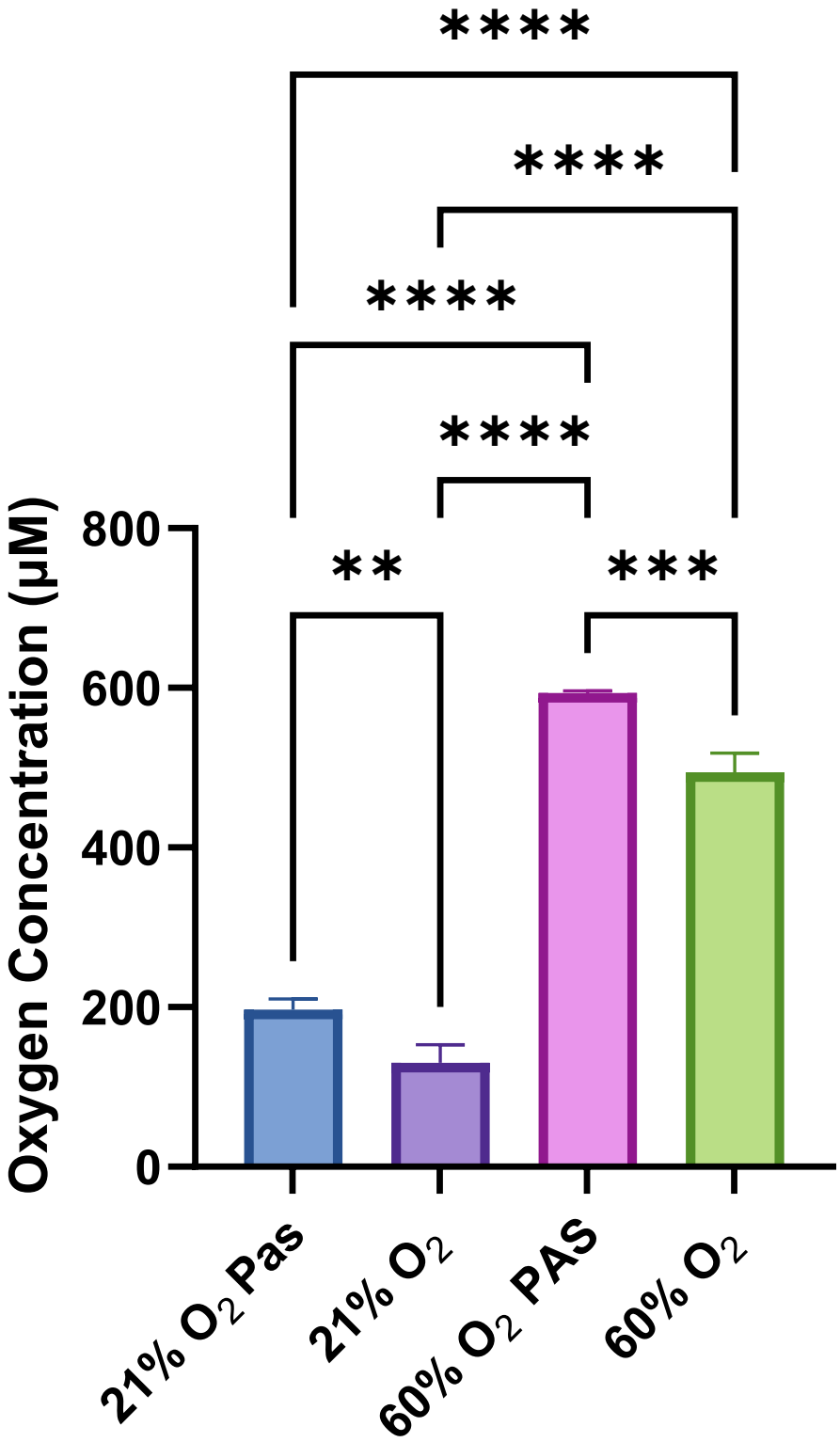

Figure 6.10 – **Direct Oxygen Concentration.** [O_2] within the PC on day 2 of storage measured by EPR oximetry. **p<0.01, ***p<0.001, ****p<0.0001. Error bars denote ±SD, N= 3.

6.4.2.4 EV Concentration

EV concentration (Fig 6.11) does not significantly change when comparing the different concentrations of external O_2. Comparing day 2 vs day 10, there was no significant increase in EV concentration in either storage condition (Control – $8.93x10^{10}$±$4,29x10^{10}$p/ml vs $1.78x10^{11}$±$2x10^{11}$p/ml, P=0.5739; 60% [O_2] - $4.67x10^{10}$±$3.86x10^{10}$p/ml vs $5.13x10^{11}$±$6.27x10^{11}$p/ml, P=0.3532).

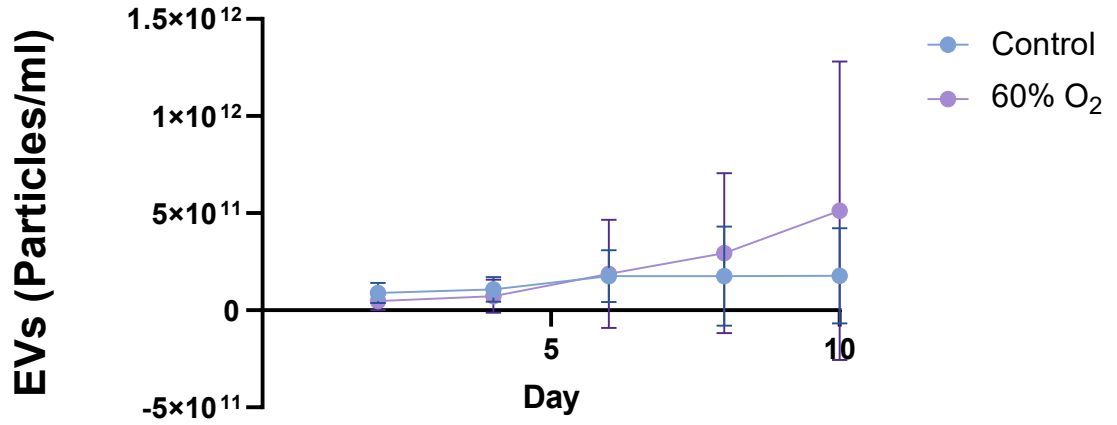

Figure 6.11 – **PC derived EV concentration over storage.** EVs were isolated from PCs via ultracentrifugation over a 10-day storage period. Error bars denote ±SD, N= 3.

6.4.2.5 EV induced coagulation

EV concentrations were normalised, as in previous chapters, to assess the EV procoagulant potential. EVs isolated from either [O_2] had no significant difference from each other or the control plasma regarding maximum optical density (Fig 6.12B) and time to maximum clot formation (Fig 6.12C). However, there was a significant higher maximum optical density and maximum clot formation in the 60% [O_2] stored PC compared to the control ($p<0.05$). The EVs isolated from the 60% [O_2] PC caused a significant decrease in lag time on days 4 and 6($p<0.05$, Fig 6.12A). EVs isolated from the control PC exhibited a significant increase in time to 50% lysis on all days except day 6 (day 2 and 4 $p<0.05$, day 8 and 10 $p<0.01$, Fig 6.12D). EVs isolated from the 60% [O_2] PC unit only had a significant effect on time to 50% clot lysis on day 2 ($p<0.01$).

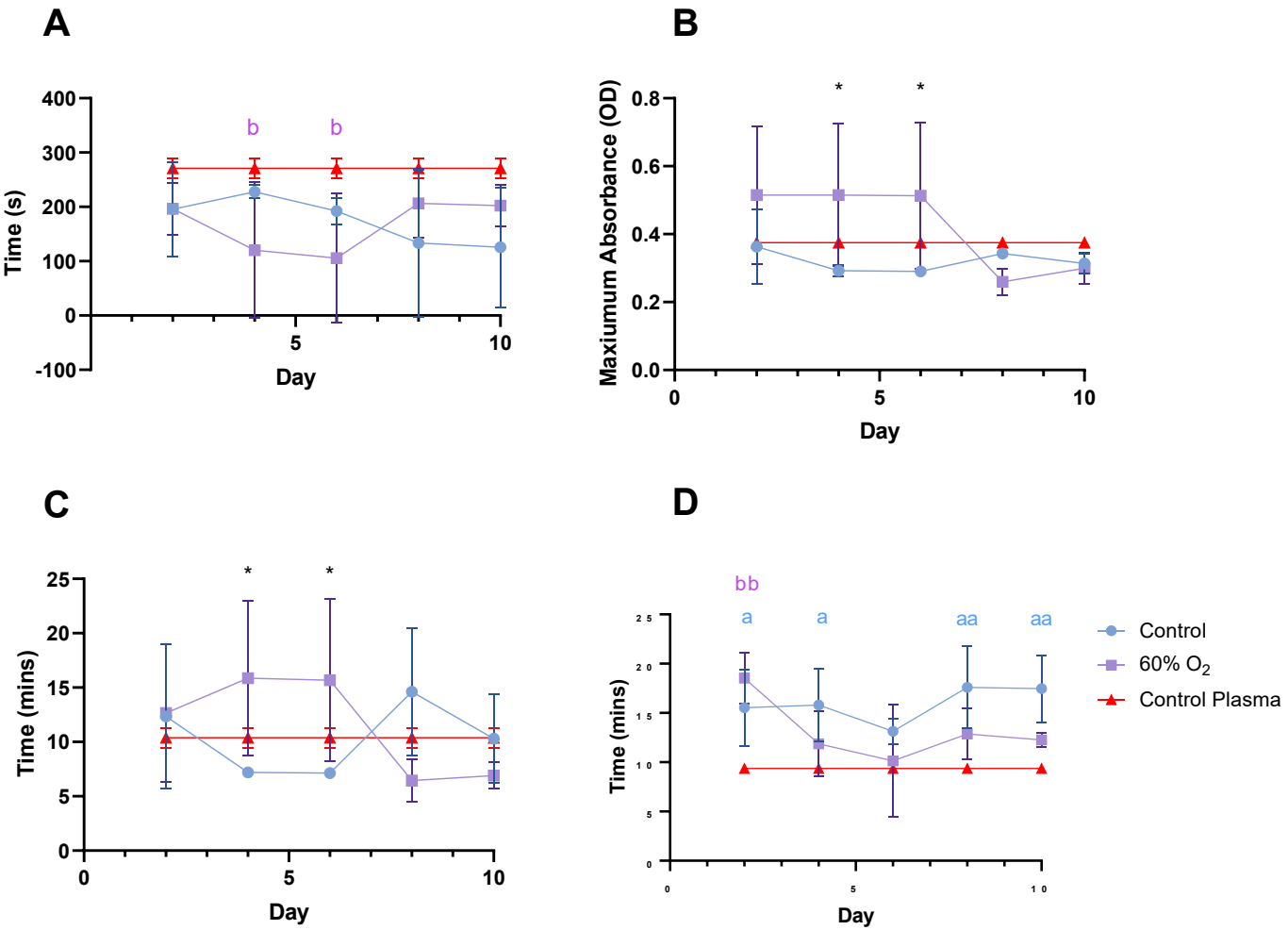

Figure 6.12 – **EVs isolated from PCs effect on fibrin clot formation and lysis**. EVs at $1x10^{10}$p/ml were applied to a turbidity and lysis assay using a fresh frozen plasma to assess the EV influence on the fibrin clot, compared to a "no EV" control. (A) Time taken to initiate fibrin clot formation. (B) Maximum fibrin clot size measured by maximal turbidity of plasma. (C) Time to maximum fibrin clot formation. (D) Time taken to achieve 50% lysis. Error bars denote ±SD. a-p<0.05 aa-p<0.01 Control Plasma vs control PC; b-p<0.05, bb-p<0.01 Control plasma vs 60% O_2, *p<0.05 control vs 60% O_2. N=3

6.4.2.6 PLT aggregation

Trap-6 induced PLT aggregation (Fig 6.13A) was significantly decreased in 60% [O_2] PCs compared to the 21% [O_2] from day 4 onwards (day 4 $p<0.001$; day 6-10 $p<0.0001$). Over storage, both the 21% [O_2] and 60% [O_2] storage showed a significant decline in Trap-6 induced aggregation (63.1±2.1U vs 50.1±4.2U, P=0.0.018; 66.37±5.00U vs 0±0U, P=0.0001; respectively).

60% [O_2] storage of PCs reported a significantly lower Ristocetin (Fig 6.13B) responsiveness on day 8 onwards compared to 21% [O_2] ($p<0.001$). Both 21% [O_2] and 60% [O_2] reported a significant decline in Ristocetin responsiveness when comparing day 2 to day 10 results (48±4.69U vs 30.47±5.41U, P=0.0257; 51.5±14.62U vs 0±0U, P=0.0076; respectively).

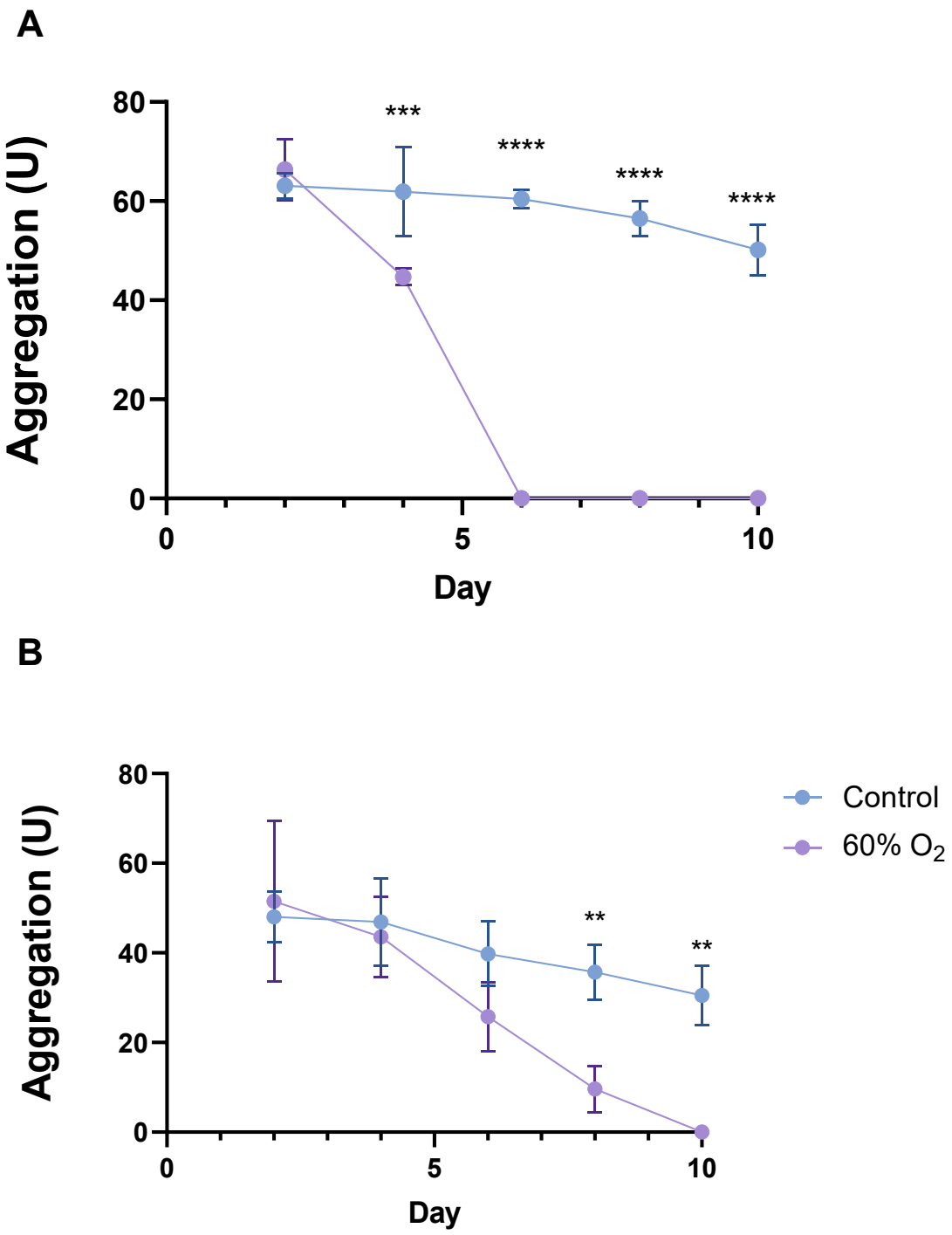

Figure 6.13 – **Aggregation response of PLTs over storage.** A) PLT aggregation response to TRAP-6 over a 10-day PC storage. B) PLT aggregation response to Ristocetin over a 10-day storage period. **p<0.01, ***p<0.001, ****p<0.0001. Error bars denote ±SD, N= 3.

6.4.2.7 pH

pH levels over the study do not fall below the 6.4, the QC cut-off value, used by blood establishments. From day 6 onwards, 60% [O_2] reports a significantly lower pH compared to 21% [O_2] (day 6 and 10 $p<0.01$, day 8 $p<0.05$). Neither 21% [O_2] or 60% [O_2] storage report a significant difference in pH over storage duration (7.1±0.14 vs 7.27±0.09, P=0.2142; 7.1±0.14 vs 6.83±0.17, P=0.1559, respectively).

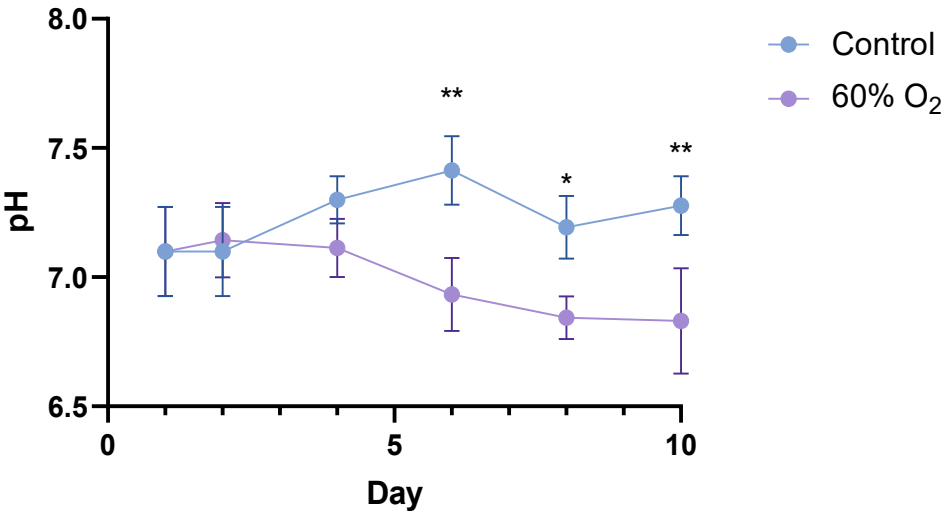

Figure 6.13 – **pH Level of PCs.** QC measures of PCs throughout the 10-day storage period to ensure units do not drop below the 6.4 cut-off value. *p<0.05, **p<0.01. Error bars denote ±SD, N= 3.

6.4.2.8 CD62P

CD62P% expression measured by flow cytometry was significantly higher in 60% [O_2] from day 7 onwards (day 7 p<0.01, day 10 p<0.0001). Comparing day 2 vs day 10, 21% [O_2] and 60% [O_2] had a significant increase of CD62P% expression (9.88±4.71% vs 39.9±6.56%, P=0.0149; 17.53±5.92% vs 87.4±7.95%, P=0.0006; respectively).

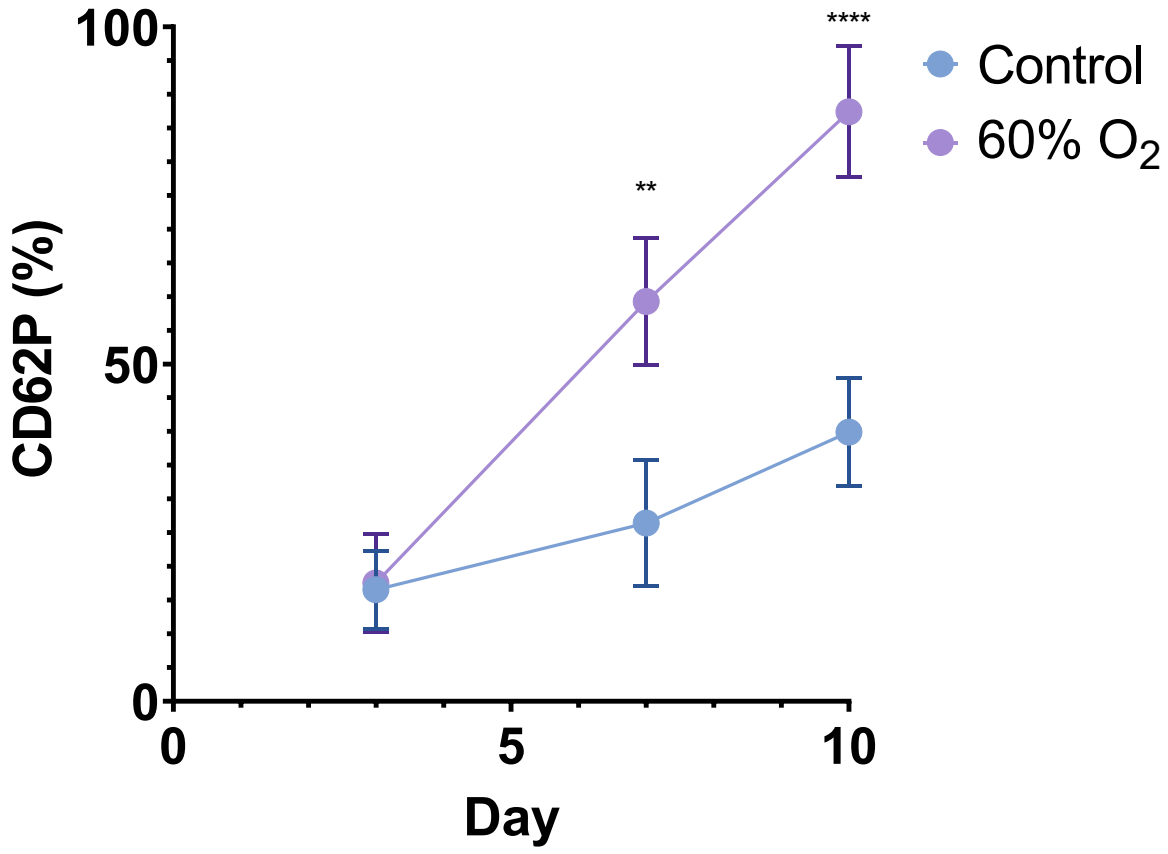

Figure 6.14 – **CD62P% expression on PLTs.** CD62P% surface expression on PLTs isolated throughout storage measured by flow cytometry. **p<0.01, ****p<0.0001. Error bars denote ±SD, N= 3.

6.4.2.9 ORAC

ORAC was utilised to assess the total antioxidant capacity of PLT supernatant and respective PLT lysate by calculating the sample induced protection against radical induced decrease in fluorescence in a widely applied assay. Where radical induced fluorescence was maintained, this was taken to reflect low total antioxidant capacity. AAPH was used as a radical generator. There was a significant increase in total antioxidant capacity as reflected by a decrease fluorescence decline in 21% and 60% [O_2] PLT lysates on all storage days, except day 6 for 21% [O_2], compared to AAPH ($p<0.0001$, Fig 6.15A). When assessing PC supernatant, total antioxidant capacity was lower at 60% [O_2] compared to 21% [O_2] on day 8 ($p<0.5$, Fig 6.15B). AAPH alone induced a greater fluorescence decline on day all days compared to 21% [O_2] supernatant ($p<0.05$), implying a greater antioxidant capacity (Fig 6.15B)

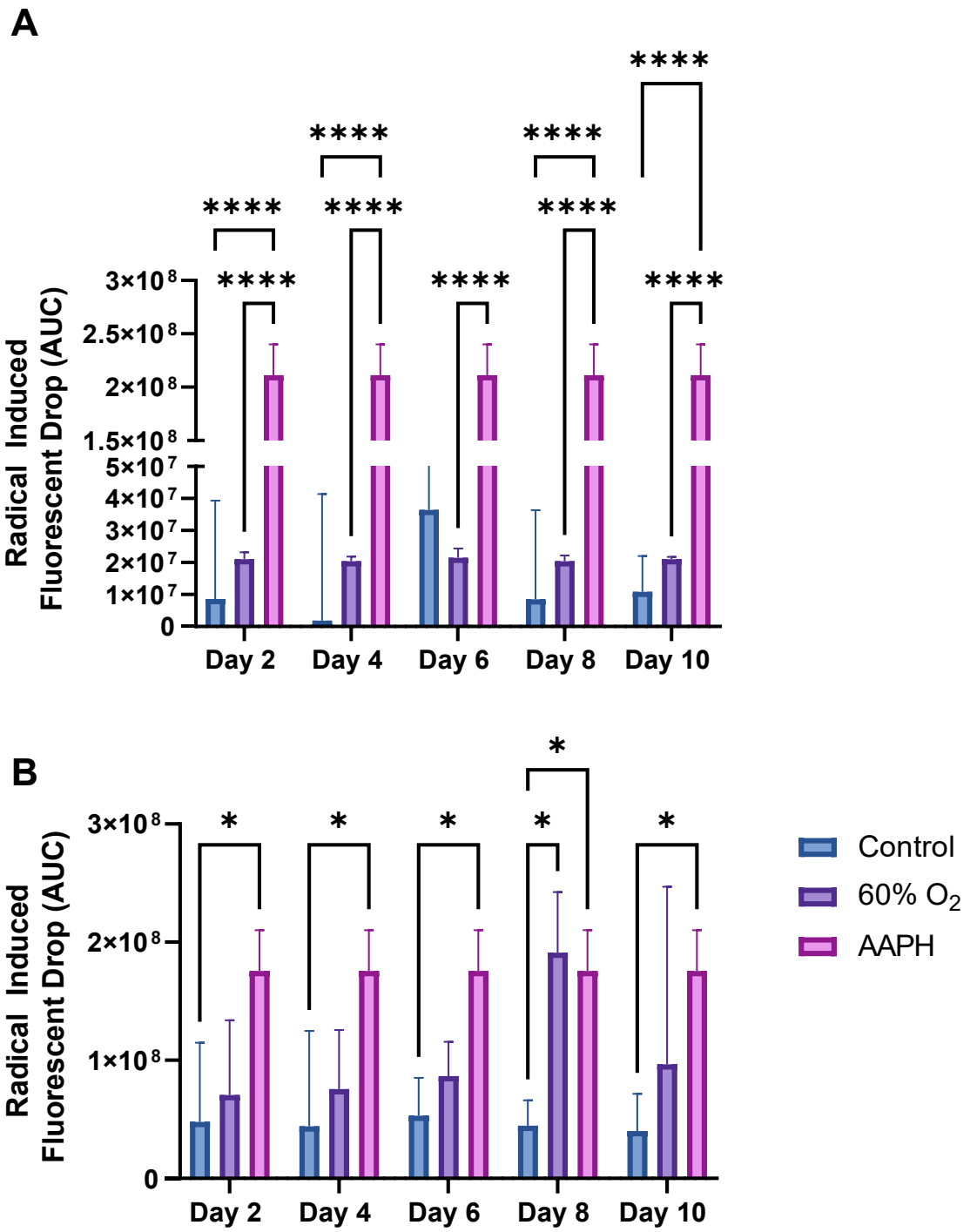

Figure 6.15 – **ORAC assay on PLT lysates and supernatants.** Total antioxidant capacity determined by the radical induced fluorescent decrease from baseline, compared to a radical generator AAPH. A) Platelet Lysate diluted 1in1000 (control data has been scaled x10 to ensure visibility). B) Neat PC Supernatant samples. *p<0.05, ****p<0.0001. Error bars denote ±SD, N= 3.

6.5 Discussion

6.5.1 Key Findings

- Reducing the PLT concentration by 50% improves PLT aggregation compared to the control when normalised for overall PLT number, which is not apparent at 25% PLT concentration.
- Increasing the external O_2 corrects the heterogeneity of O_2 within the container but decreases the PC quality determined by a drop in pH and significantly reduced aggregation compared to the control.
- The decrease in PC quality at 60% [O_2] is likely due to an increased level of OS, demonstrated by an increase in cyanide resistant O_2 consumption and reduced antioxidant capacity.

6.5.2 Main Discussion

These results present new findings into improving the O_2 availability within PC containers. Applying the mathematical model introduced in chapter 5.3, this chapter demonstrates that by altering OCR (by decreasing PLT concentration), or by increasing the external [O_2], does significantly improve O_2 availability across the container, therefore demonstrating the robustness of the model. When normalised for PLT number, a 50% reduction in PLT concentration improves Trap-6 responsiveness over the early days of storage compared to the control. The Ristocetin function is also retained over the 10-day storage period. However, this effect was not reported at 25% PLT concentration. When increasing the [O_2] to 60%, O2 heterogeneity within the container was corrected but high levels of O_2 lead to high OS and rapidly diminished PLT quality and function.

6.5.2.1 Reducing PLT Concentration

A prediction resulting from the model calculations for the reduction in PLT concentration was that the OCR would decrease by 50% and 75% respectively for the 50% PLT concentration and 25% PLT concentrations. Therefore, when corrected for PLT number, all units in study arm 1 should demonstrate the same OCR, which was confirmed (Fig 6.1). The 25% PLT concentration was

significantly higher on day 4, but this is likely due to error of normalisation as the measured OCR was so small with low PLT concentration. As PLT number is decreased, [O_2] in the bag is correspondingly increased (Fig 6.2), which again aligns with the predicted model (section 5.3). This agrees with the report by Torres et al 2016 suggesting a reduction in PLT concentration would have the largest effect on increasing O_2 availability (400).

EV concentration was not significantly different with altered PLT concentration. However, considering that the lower concentration of PLTs produce the same level of EVs, the results are suggestive that more EVs per PLT are produced (401). Therefore, increasing [O_2] appears to influence PLT EV production. This data does correlate with increase in CD62P expression at 25% and 50% PLT concentration compared to the control, which is significant by day 10 (Fig 6.7) and confirms increased PLT activation is associated significantly with EV production. The increased PLT activation is however surprising, based on the hypothesis that increased O_2 availability should improve PLT quality. One possible explanation could be linked to the significant increase in pH in the reduced concentration units, which is significantly higher than the control from day 4 onwards (Fig 6.6). A 2007 study showed pH above 7.44 was correlated to more CD62P expression, a greater rate of glycolysis and more PS compared to pH 7 (401). The current guidelines don't suggest a high pH cut-off for QC; therefore, pH range should be more specific if used as a true measure of PC quality. Another potential reason is increased sheer stress from agitation. Flatbed agitation has been the method of choice in the UK for decades. However, with a decreased PLT concentration, there is a possibility that sheer rates could be increased due to more movement within the PC. A previous report demonstrated that compared to circular agitation, flatbed agitation induced the highest sheer rate, above that which PLTs would experience in the veins (402, 403). At lower concentrations of PLTs in the same volume, this sheer rate could be exacerbated and result in a higher level of PLT activation and consequent PLT degranulation. The method of agitation was applied as standard throughout this thesis and therefore needs further investigation for solid conclusions to be drawn.

When assessing the procoagulant capability of the PC derived EVs, when normalised to $1x10^{10}$p/ml, the same effect of reducing the time taken to maximum clot formation was reported. This effect has been reported in both Chapter 4 and 5, suggesting EVs isolated from PCs will reduce the time to maximal clot formation. The pro-coagulant potential of EV is therefore not altered by the varying conditions applied throughout this thesis. However, due to the fact the number of EV changes under different storage conditions, it follows that the total pro-coagulant potential per PC unit is effectively increased and may have important implications for transfusion therapy.

PLT aggregation data was normalised to PLT number allowing a direct comparison of the PLT quality under the various conditions applied. Trap-6 responsiveness (Fig6.5A) shows a significantly increased response in 50% PLT concentration on day 4 of storage compared to the control, suggesting that the PLT quality is superior. This could be a potential explanation as to why studies looking at lower PLT concentrations showed no significant risk in bleeding times in transfused patients (392-394). The storage time of the units were not classified in these studies. This may explain why from day 6, inconsistencies are seen as the control trap-6 aggregation is equal to the 50% PLT concentration. 25% PLT concentration does not follow the trend of the 50% PLT concentration. The potential reasons for this are either due to an increased level of OS or a PLT number too low for optimal aggregation measurements using the multiplate assay. When comparing Ristocetin, 25% PLT concentration is significantly higher than the control on day 4. Although the 50% PLT concentration is not significantly better than the control, over storage, Ristocetin response does not significantly decline, whereby the control does decline over the 10 days. This is also apparent in other studies (404). Taken as a whole, the presented data suggests that the quality of PLT when stored at 50% PLT concentration in the initial days of storage is improved compared to the control. This could potentially lead to a corresponding decrease in the number of BCs required to form a PC, therefore, reducing waste and/or improving the PC stock levels.

6.5.2.2 Increasing external [O_2]

By applying an increased external [O_2], the OCR is not significantly different to the control at any time point. However, the OCR does significantly decrease over the 10-day storage duration, which is not apparent in the control (Fig6.8). This data suggests that the PLTs stored at increased [O_2] are overall less metabolically active, and therefore, are consuming less O_2 overtime. To investigate this further, cyanide was added during OCR experiments to block oxidative phosphorylation and therefore assess non-ATP linked O_2 usage. Previous research has shown that increases in non-mitochondrial/ATP-linked OCR occurs in the presence of ROS and reactive nitrogen species (405-407). The control on day 2 has no-cyanide resistant O_2 consumption, suggesting that -radical forming oxygen consumption by PLTs represents a very low proportion of overall O_2 usage, approximately 1%. From day 4 onwards, there is no significant differences between mitochondrial and cyanide resistant OCR in 60% O_2 stored PC, suggesting a high proportion of O_2 consumption by PLTs under this condition is the result of radical production or other O_2 utilising processes (Fig 6.9). Normal oxidative phosphorylation does decrease in 60% O_2; possibly reflecting the number of PLTs displaying cyanide resistant OCR has not increased. To further confirm that high [O_2] had caused excessive OS in PLTs, the total antioxidant capacity was assessed in supernatant and PLT lysate samples (Fig 6.15). ORAC assesses the antioxidant capacity of a sample, which for cell-based samples reflects the major eliminators of ROS (399). The results detailed that PC at 21% and 60% [O_2] exhibited an antioxidant protection against AAPH generated radical, however the trend suggests less protection in 60% [O_2] when assessing lysates. In the supernatant, there was no significant difference between AAPH and 60% [O_2], suggesting little antioxidant protection (Fig 15). This data suggests ROS had overwhelmed the PLTs very early on leading to severe OS over the storage period.

As reported with reducing the PLT concentration, increasing the external [O_2] significantly increases the [O_2] measured directly within the PC (Fig6.10). This again demonstrates the robustness of the mathematical model (section 5.3) and proves the prediction and assumptions made were correct. This agrees with a previous modelling study that investigated O_2 theoretical modelling for

reduced agitation of PCs (400), different from the current study. However, increasing the external [O_2] to such a high level caused a high level of OS, as shown for other cell types (396) and suggests 60% [O_2] is not a suitable storage condition for PC units. It is important to point out that what is measured represents average [O_2] as it is not possible to measure [O_2] at specific points within the container. It was reasonable to assume that given the container is agitated and constantly mixed, O_2 will distribute maximally within the contain. However, this data shows PLTs at the outer edge are likely experiencing more than the predicted average O_2 within the container (shown in Fig 6.10).

EV concentration is not significantly different in 60% [O_2] compared to the 21% [O_2] (Fig 6.11). This is contradictory to the previous results within this thesis that suggests EV production is associated with increased CD62P, this is significantly increased in 60% [O_2] is compared to the 21% [O_2] from day 7 onwards (Fig6.14). PLTs express CD62P after irreversible activation, which usually involves the release of EVs (described in detail in section 1.3.6). The change seen in CD62P production in this model is related to the increase in OS, present at 60% [O_2]. However, OS has been demonstrated to increase the release of EV (408), therefore disagreeing with the current findings. Increased ROS, in particular superoxide, has been shown to augment platelet aggregation responses (409, 410), possibly activating PLTs in the PC. However, if the PLTs become overwhelmed by ROS and OS and the mitochondrial function becomes critical, the PLTs may induce apoptosis. Apoptosis in PLTs is controlled by the mitochondria, and during times of high OS, caspase-3 activity has been shown to increase leading to PLT death (411). However, even in this situation, the influx of Ca^{2+} in apoptosis would lead to an increase in EV release, demonstrated previously (411). It is important to point out these investigators used flow cytometry, and as a result the measurements could be reflective of apoptotic bodies (Section 1.3) and not the EV population (as measured within this thesis). This warrants further investigation.

Although EV did not cause a significant decrease in time to maximum clot formation, there was a significant increase in time to 50% lysis when comparing the EVs isolated from the PC versus the control plasma (Fig 6.12). This implies EV cause the formation of a clot that is more resistant to lysis

and is in agreement with data in other chapters reporting the pro-coagulant function of EV. Interestingly, 60% [O_2] stored PC EVs appeared to demonstrate a different haemostatic character. On days 4 and 6, the EVs isolated from 60% [O_2] did significantly decrease the lag time, inducing a quicker clot initiation. However, the EVs also induced a long time to maximum clot formation compared to the plasma control, likely due to the clot being much larger (Fig 6.12). Taking this data together it suggests the overall clot formation is likely not to be significantly different, therefore suggesting that the EVs isolated from PC under various conditions are not different.

PLT aggregation response to Trap-6 is significantly reduced in 60% O_2 stored PC from day 4 onwards, reaching a point of no aggregation by day 6 (Fig 6.13A). Ristocetin shows a similar trend, whereby 60% O_2 stored PCs have a reduced response by day 8, reaching no response by day 10 (Fig 6.13B). ROS generation by non-phagocytic NADPH oxidase is important in relation to reactivity to thrombin or collagen (412, 413), an increase in ROS generation prior to activation has been shown in CVD patients, leading to increased aggregation responses. ROS are also involved in platelet receptor activation, therefore suggests ROS would cause PLT activation to be enhanced (414). Conversely, ROS are involved in receptor shedding, GP1bα and GPVI (415), important for the agonists used within this study. A reduction in these receptors would therefore lead to a decrease in aggregation. An alternative explanation could be due to PLTs already being pre-activated within the container. This is a recognised limitation of in vitro assays whereby pre-activated PLTs are unable to re-activate when stimulated by an agonist in the assay. Increased intracellular ROS can lead to hyperpolarisation of the mitochondrial membrane potential causing subsequent PLT activation (415). This concept of activation of PLT in the PC is evident when assessing the level of CD62P% on the cell surface, which is significantly increased compared to the control (Fig 6.14). A final plausible explanation is the increased PLT senescence caused by OS. OS is a major cause of senescence and dysfunction during PC storage. With the increase of OS caused by a high [O_2], the increase in senescence will result in poor aggregation responses (416). Interestingly, the results of poor PLT quality and function in 60% [O_2] reflects the results of 25% PLT concentration in terms of TRAP response, possibly suggesting trap-6 response is highly sensitive to OS.

The average [O_2] measured in the container when stored at an external O_2 of 60% is ~50% [O_2]. This confirms adequate oxygenation throughout the container and therefore PLTs at any position are unlikely to experience anaerobic conditions (chapter 5). Despite this adequate O_2, the pH in 60% [O_2] is significantly lower than the control from day 6. This suggests even with adequate oxygen the PLTs are still undertaking anaerobic metabolism. This agrees with the majority of O_2 consumption being due to OS and not ATP generation (Fig 6.9).

6.5.3 Limitations

A limitation is the ORAC assay. Firstly, it would have been better to compare the protective effect of the sample to that of a standard antioxidant, such as TROLOX. Fluorescein has a relatively low reactivity towards $ROO^{\cdot}$ radicals, which may lead to over-representation of the results (398). The assay also uses AUC and does not specifically measure the efficacy or amount of antioxidant present. This assay also does not directly measure ROS. However, this is a well-documented assay used in multiple model systems and across different cell types to analyse antioxidant capacity (398, 399).

Secondly, the cyanide-based OCR was only tested i) in the 60% [O_2] study arm and ii) a low sample number (N=2). Although an ANOVA and SD is valid on N=2, it is as a result underpowered. Due to the unexpected drop in function and pH observed in initial experiments applying 60% [O_2], this led to further investigations into the reasoning behind this finding and the CN resistant OCR was applied in the latter testing undertaken N=2. The SD on average would be underestimated compared to the true population, and the SD is not known with any great accuracy. This can lead to inaccurate p values and uncertainty in the results. This assay should be repeated to collect a higher N and tested in the lower PLT concentration arm to determine if the increase in O_2 availability has a similar effect regarding OS. It is reasonable to predict this will not be the case given that the maximum O_2 experienced by PLTs at 50% and 25% O_2 would be no greater than 21% but this needs to be tested.

6.5.4 Conclusion

The mathematical model presented (section 5.3 and throughout chapter 6) can accurately predict the conditions required to improve the O_2 availability within the PC. This has been demonstrated by two independent methods which test the model and confirm its validity. A consequence of applying high external [O_2] is that the PC experienced high OS and damage associated with ROS production led to poor PC quality and function, in contradiction to the original hypothesis. Reducing the PLT concentration to 50%, which in turn doubles the availability of O_2 seems more promising and led to an initial increase in PLT aggregation, suggesting that halving the PLT concentration within a PC unit will have equal if not improved efficacy when transfused before day 6. This needs to be confirmed by studies investigating the effectiveness of reducing PLT concentration within PC stored under standard O_2 conditions and whether these PC maintain bleeding times and correct thrombocytopenia up to standard.

7.0 General Discussion

7.1 Overview and Conclusions

The primary aims of this thesis were to optimise PC storage, to improve PLT quality throughout storage, and utilise this new knowledge to propose ways to extend the current shelf life beyond 7-days. There was particular focus on PC derived EV character and concentration and how this changed throughout storage. It was demonstrated that PEVs were the predominant EV within the PC. Applying standardised storage conditions as set up at WBS, PLT aggregation over storage decreases from day 2 and throughout storage in comparison to fresh WB, suggesting PC PLT function is an important area to address in the context of the recipient patient. Studies carried out applying CS showed PLT aggregation was not improved, and EV concentration was significantly increased by the end of storage, when compared to RT control. These PEVs when taken at the higher concentration produced in CS were shown to exhibit an increased procoagulant effect when applied to the turbidometric model. The conclusion drawn from this suggests that CS unit may have specific utility when applied to trauma patients as a direct result of increased concentration of procoagulant EVs. In further studies, the storage condition of PC for incubation was reduced to 10% and 5% [O_2] to test the hypothesis that OS is a primary mechanism of impacting on PC quality. Direct measurement of [O_2] sampled within PC storage containers showed a significant limitation by demonstrating that large regions of hypoxia exist within the PC container even when stored at air (21% [O_2]). To improve O_2 distribution and availability, the storage conditions were modified for incubation at 60% [O_2]. In agreement with the predictions of a theoretical model that was applied, this resulted in improved distribution of O_2 within the container and had a positive effect on PLT functionality and a modest effect on PC quality for a short incubation period. However, increasing [O_2] to this level was shown to exacerbate OS and cause a subsequent decrease in both PLT function and PLT quality.

PC have the shortest shelf-life of all blood products, at 7-days (56). Due to the extensive WBS manufacturing and testing protocols, PCs are not released until day 2, leaving only 5-days for PC to be available for use. This leads to high PC waste and significant stress on donor supply. The storage

conditions of PC have not been updated since the late 80s-90s, despite a massive investment in research on donated PLTs. As PLT half-life *in vivo* is 10 days, there is obvious indications that PC storage could be improved by at least 3 days. Manipulating calculations from a Canadian market research (report not available) and an inventory saving report (417), projected savings to the WBS for extending the storage by 1, 2 or 3 days is £87,626, £160,696, and £222,357 per annum respectively (Appendix 1). These savings would be 5-10x larger in England due to the supply required for the population served and given the current climate experienced by the UK's health boards post pandemic, changes in PLT storage should be a current and future priority.

As expected, the EVs isolated from fresh PC preparation are predominantly of PLT origin (chapter 3) and increased significantly over storage time. This EV increase over time can be correlated with the increase of CD62P% expression on PLTs, suggesting EVs as a marker of PLT activation. PEVs are highly pro-coagulant as previously described (section 1.3.6), and as suggested by Price et al 2021 (418), this raises the possibility that EV isolated from out-of-date PC could be used as an additional blood product.

PLT aggregation as measured by ex vivo assays, despite a large increase in pro-coagulant EV concentration, was not improved in CS. Throughout the thesis, EVs derived from a PCs when normalised for EV concentration have been shown to have the same procoagulant character, as reflected by a reduction in time to clot formation. An increase in EV concentration in CS PCs may play a pivotal role in the function of a PC in regard to bleeding time reduction. The move in the USA to application of CS PCs for trauma treatment is largely based on apheresis derived PCs, which is an important difference to the data shown within Chapter 4.0. The use of BC derived PCs within this thesis means that due to the overnight resting step, they cannot be stored within 2 hours of collection, instead were stored in CS by a maximum of 30 hours post collection. The results reported here suggest that BC derived PCs do not react positively to CS but do generate a significant number of EVs compared to conventional storage. The difference in production methods has been assessed in RT, reporting no significant difference with *in vitro* function testing and metabolic measures (303). The difference in CS

is hypothesis generating and should be investigated as this could have large ramifications when applying for process approval.

When taking the data as a whole, a consistency seen throughout is the unreliability of pH as a quality control marker of PC quality for PAS only. Currently the globally accepted quality control cut-off value for pH is 6.4. At no point do any of the PCs tested reach this value. Importantly, even when stored at low [O_2] which caused a severely hypoxic storage environment with poor functionality, the pH never dropped below 6.8, which was surprising based on lactate being the main driver of pH reduction and the assumed anaerobic environment created at 5% [O_2]. The reason for this is the successful buffering capacity of the PAS. But with this buffering capacity, a question is raised as to whether the 6.4 pH cut off is redundant for confirming the PC quality. The reason pH falls in PCs is due to the build-up of lactate which depletes the bicarbonate buffering mechanism, whereby lactate levels of up to 20mmol can be buffered in plasma before pH begins to drop (419). The acetate in additive solutions such as SSP+ (section 2.1) can generate bicarbonate by accepting a H+ from the dissociation of carbonic acid, thereby maintaining pH levels above 7.0 (361). A suggestion from the results reported could be to increase this cut off value to 6.8, as when the majority of units dropped to this level, Trap-6 and Ristocetin functionality significantly decreased, suggesting the quality of the PC had diminished. Perhaps a more predictive yet still easily measurable parameter in a transfusion setting would be lactate or glucose (as lactate will not increase once glucose is exhausted) levels in PC suspended in PAS (420), and ought to be reviewed.

The data in this thesis has demonstrated the importance of O_2 availability within the bag, and this may be important given the need for transfusion treatment options for trauma patients. A shift of returning to the use of WB transfusion has begun in USA, with the ideology of using WB instead of a 1:1:1 ratio of the individual components (421, 422). Storage of WB would be similar to that of RBCs, where units are stored at 4^{o}C with no agitation. With this, a number of questions have been raised. RBCs, as previously alluded to, show a better quality when stored in anoxic conditions (373), but data from this and other studies demonstrate hypoxia is detrimental to PLT lifespan (100). Therefore, the

O_2 saturation at which the viability of each cell type is maintained could be key to storing a quality, long lasting product. The second issue is the storage duration, which will be determined by the PLT lifespan, which when stored at 4^{o}C is still a largely debated subject. A final question would be the interplay of EVs within a WB unit when transfused. RBCs release EVs during storage as they age (423), and PLT release a significant amount of EVs when storage in the cold (chapter 4). Although PEVs are pro-coagulant, the data surrounding RBC EVs is conflicted, with some showing procoagulant potential, inflammatory and immune regulatory effects (424). How a high level of RBC EVs and PEVs would interact when transfused is not currently understood and would need to be investigated.

Overall, the studies presented herein provide new insights to factors affecting PLT storage within PC. Importantly, they have applied direct measures to inform the condition and environment within the PC container which when applied to a theoretical model align with predicted outcomes. These studies point the way forward to important future studies.

7.2 Future Direction

Future research should aim to build on the themes presented within this thesis and explore in detail the relationship between O_2 availability and PC quality. When O_2 availability was increased so that the hypoxic region was corrected to give homogeneity of O_2 distribution (chapter 6), contrary to our expectation overall PC quality and PLT function diminished rapidly. There was evidence that double the O_2 availability could also be achieved in a different way, as precited by the theoretical model, by reducing PLT concentration in PC. Applying 50% PLT concentration, (Chapter 6) did somewhat improve PC quality for half the amount of PLTs. These results suggest a possible "sweet-spot" of PC O_2 availability. An interesting future study based on this work would be to utilise PC and 50% PLT to evaluate whether a reduced dose of PLTs transfused within a PC unit to trauma and/or thrombocytopenic patients would yield similar or superior results to a normal PC unit. This would be based on a better PLT functionality explained by the increased O_2 availability. The literature suggests there will be no difference (392-394). This has the added benefit of doubling the PC stock, reducing recipient-donor exposure and donor demand.

To alleviate the OS demonstrated in the high O_2 environment, antioxidants could be supplemented to PAS which have been shown to be successful in normal storage conditions. A previous study in 2019 supplemented PCs with resveratrol, a natural antioxidant found in grape skins and peanuts, and has little toxicity even at high doses (AO-37). Supplementing with 50µM of resveratrol decreased OS, senescence levels and reduced spontaneous PLT activation compared to the control (416). Studies in agreement with this utilising L-carnitine as an antioxidant reported a significant decrease in lipid peroxidation, therefore less OS (425). They also reported ROS generation plays a pivotal role in PLT senescence and therefore decreased PC quality. N-acetyl-l-cysteine which scavenges ROS led to a decrease in PLT senescence (416). Others have reported N-acetyl-l-cysteine supplementation in CS prevents PLT clearance upon reinfusion due to decreased ROS (341). The use of N-acetyl-l-cysteine however should be approached with caution, due to a recent report in 2022 demonstrating that it can inhibit PLT aggregation through regeneration of the non-oxidative from of

albumin (426), although it is unknown how this will interplay with the PAS. Addition of an antioxidant or ROS scavenger to 60% O_2 may reduce the OS potential of the high O_2 availability but reserve the positive effects of no hypoxic region.

An issue with the implementation of CS PC into blood establishments is the timing of when to put PC into the CS after donation. Currently, as mentioned, the FDA guidelines on CS of PCs state the PCs need to be at 4^{o}C within 2 hours post collection (335), which is achievable for apheresis. However, in Wales, and the majority of Europe, the main PC component derives from BCs. Therefore more investigations are needed on the effect of delaying CS of PC quality. Along with this, the issue of two inventories adds complexity to already stretched blood establishments (427). To mitigate this, few studies have investigated delayed CS. One recent study investigated PC stored at 4^{o}C immediately or after 4 days of RT life (428). Although delayed CS had similar PLT count, due to being stored at RT, delayed CS PC had lower pH, glucose and a higher lactate compared to conventional CS. This study showed better HSR response in delayed CS, suggesting a benefit (428) however a second study using delayed CS apheresis after 7 days showed worse aggregation and clot dynamics in delayed CS compared to conventional CS (429). Delayed CS idea could solve the dual inventory problem, but more studies evaluating the quality and usability of these products, especially clinical, are required.

Although the EV field has exponentially accelerated in the past 5 years, there remains a large discrepancy within the transfusion field on importance of EVs as possible QC markers for blood products and the role EVs have upon transfusion. Research has suggested that EVs alone could stimulate coagulation factors and reduce bleeding times in mice (430), but others have demonstrated rapid clearance of EVs upon re-infusion, up to 90% within an hour (431), therefore this should be investigated in regard to PC derived EVs. With this, there is a possibility of an EV only product. EVs are significantly higher at the end of storage, reported throughout this thesis and by others (83). The PC, once expired, could then be utilised to isolate procoagulant EVs which could be tested in an animal based trauma model to be used alongside current treatments. This is similar to previous research by Paul Harrison in Birmingham University where the group reported lysing PCs lead to a PLT enhanced

plasma which was shown to cause more thrombin generation than standard plasma, which could be used in traumatic treatments and utilising an otherwise wasted product (418).

Studies should look to investigate the "true" procoagulant capability of EVs with a PC transfusion, which is currently debated within transfusion. With the CS PC data reported within this thesis (Chapter 4.0), this further adds to the question as to whether EVs play a significant role in the haemostatic effect of PCs. Washed PCs do not contain EVs due to all supernatant of the PC being replaced (432). Therefore, a suitable animal study would be to look at the differences of CS PC in a traumatic bleeding model using washed and unwashed PCs to determine if there is a synergistic effect of EVs and PLTs. A possible study that would follow on from the procoagulant results of EVs in cold storage would be to investigate the negative effects, such as pro-inflammatory responses of EVs isolated from PC (433). A unit high in EVs may be suitable for transfusion in the context of trauma, but for patients with inflammatory or pro-inflammatory conditions could exacerbate the patient's condition.

Finally, it has been reported by several authors that *in vitro* measures of PLT functionality do not always correlate with *in vivo* measures (discussed in section 1.2.3.4). More *in vivo* like measurement systems and models have been developed using microfluidics (434). Methods like impedance aggregometry do not capture the vessel characteristics, therefore prevents the assessment of PLTs within the true in vivo microenvironment. Microfluidics can be customised to mimic different vascular anatomies (435, 436), allowing different clinical presentations to be studied. Microfluidics can also stimulate and assess the effects of shear stress and synergistic effects of chemicals released by activated PLTs (437). With the development of bleeding models that more reliably mimic in vivo conditions after transfusion, the assessment of PC quality would be improved (438). These microfluidic set-ups should be compared to *in vitro* and *in vivo* measures to review the suitability of the assay in PC research as a research tool for investigating new products and possibly a QC assay in the future.

8.0 References

1. Ribatti D, Crivellato E. Giulio Bizzozero and the discovery of platelets. Leuk Res. 2007;31(10):1339-41.
2. Webber AJ, Johnson SA. Platelet participation in blood coagulation aspects of hemostasis. Am J Pathol. 1970;60(1):19-42.
3. Clemetson KJ. Platelets and primary haemostasis. Thromb Res. 2012;129(3):220-4.
4. Siedlecki CA, Lestini BJ, Kottke-Marchant KK, Eppell SJ, Wilson DL, Marchant RE. Shear-dependent changes in the three-dimensional structure of human von Willebrand factor. Blood. 1996;88(8):2939-50.
5. Clemetson JM, Polgar J, Magnenat E, Wells TN, Clemetson KJ. The platelet collagen receptor glycoprotein VI is a member of the immunoglobulin superfamily closely related to FcalphaR and the natural killer receptors. J Biol Chem. 1999;274(41):29019-24.
6. Nieswandt B, Brakebusch C, Bergmeier W, Schulte V, Bouvard D, Mokhtari-Nejad R, et al. Glycoprotein VI but not alpha2beta1 integrin is essential for platelet interaction with collagen. EMBO J. 2001;20(9):2120-30.
7. Sharda A, Flaumenhaft R. The life cycle of platelet granules. F1000Res. 2018;7:236.
8. Bennett JS. Structure and function of the platelet integrin alphaIIbbeta3. J Clin Invest. 2005;115(12):3363-9.
9. Gale AJ. Current understanding of hemostasis. Toxicol Pathol. 2011;39(1):273-80.
10. Yun SH, Sim EH, Goh RY, Park JI, Han JY. Platelet Activation: The Mechanisms and Potential Biomarkers. Biomed Res Int. 2016;2016:9060143.
11. Stegner D, Nieswandt B. Platelet receptor signaling in thrombus formation. J Mol Med (Berl). 2011;89(2):109-21.
12. Kamae T, Shiraga M, Kashiwagi H, Kato H, Tadokoro S, Kurata Y, et al. Critical role of ADP interaction with P2Y12 receptor in the maintenance of alpha(IIb)beta3 activation: association with Rap1B activation. J Thromb Haemost. 2006;4(6):1379-87.
13. Daniel JL, Dangelmaier C, Jin J, Ashby B, Smith JB, Kunapuli SP. Molecular basis for ADP-induced platelet activation. I. Evidence for three distinct ADP receptors on human platelets. J Biol Chem. 1998;273(4):2024-9.
14. Herbert JM, Savi P. P2Y12, a new platelet ADP receptor, target of clopidogrel. Semin Vasc Med. 2003;3(2):113-22.
15. Berndt MC, Metharom P, Andrews RK. Primary haemostasis: newer insights. Haemophilia. 2014;20 Suppl 4:15-22.
16. Morrell CN, Maggirwar SB. Recently recognized platelet agonists. Curr Opin Hematol. 2011;18(5):309-14.
17. Pignone M, Williams CD. Aspirin for primary prevention of cardiovascular disease in diabetes mellitus. Nat Rev Endocrinol. 2010;6(11):619-28.
18. Owens AP, Mackman N. Tissue factor and thrombosis: The clot starts here. Thromb Haemost. 2010;104(3):432-9.
19. Bach RR. Initiation of coagulation by tissue factor. CRC Crit Rev Biochem. 1988;23(4):339-68.
20. Mackman N. Role of tissue factor in hemostasis and thrombosis. Blood Cells Mol Dis. 2006;36(2):104-7.
21. Wheeler AP, Gailani D. The Intrinsic Pathway of Coagulation as a Target for Antithrombotic Therapy. Hematol Oncol Clin North Am. 2016;30(5):1099-114.

22. Rumbaut R, Thiagarajan P. Platelet-Vessel Wall Interactions in Haemostasis and Thrombosis. Platelet Recruitment and Blood Coagulation: San Rafael (CA): Morgan & Claypool Life Sciences; 2010.
23. Kalafatis M, Swords NA, Rand MD, Mann KG. Membrane-dependent reactions in blood coagulation: role of the vitamin K-dependent enzyme complexes. Biochim Biophys Acta. 1994;1227(3):113-29.
24. Rucińska M, Gacko M, Skrzydlewski Z. Tissue factor pathway inhibitor (TFPI). Roczniki Akademii Medycznej w Bialymstoku (1995). 1997;42 Suppl 1:118-22.
25. Gu J-M, Patel C, Kauser K. Plasma Tissue Factor Pathway Inhibitor (TFPI) Levels in Healthy Subjects and Patients with Hemophilia A and B. Blood. 2015;126(23):4672-.
26. Wood JP, Ellery PE, Maroney SA, Mast AE. Biology of tissue factor pathway inhibitor. Blood. 2014;123(19):2934-43.
27. Wypasek E, Undas A. Protein C and protein S deficiency - practical diagnostic issues. Advances in clinical and experimental medicine : official organ Wroclaw Medical University. 2013;22(4):459-67.
28. Dahlbäck B, Villoutreix BO. Regulation of Blood Coagulation by the Protein C Anticoagulant Pathway. 2005;25(7):1311-20.
29. Longstaff C, Kolev K. Basic mechanisms and regulation of fibrinolysis. J Thromb Haemost. 2015;13 Suppl 1:S98-105.
30. Sakharov DV, Nagelkerke JF, Rijken DC. Rearrangements of the fibrin network and spatial distribution of fibrinolytic components during plasma clot lysis. Study with confocal microscopy. J Biol Chem. 1996;271(4):2133-8.
31. Sakharov DV, Rijken DC. Superficial accumulation of plasminogen during plasma clot lysis. Circulation. 1995;92(7):1883-90.
32. Bu G, Warshawsky I, Schwartz AL. Cellular receptors for the plasminogen activators. Blood. 1994;83(12):3427-36.
33. Hoylaerts M, Rijken DC, Lijnen HR, Collen D. Kinetics of the activation of plasminogen by human tissue plasminogen activator. Role of fibrin. J Biol Chem. 1982;257(6):2912-9.
34. Marder VJ, Shulman NR, Carroll WR. High molecular weight derivatives of human fibrinogen produced by plasmin. I. Physicochemical and immunological characterization. J Biol Chem. 1969;244(8):2111-9.
35. Walker JB, Nesheim ME. The molecular weights, mass distribution, chain composition, and structure of soluble fibrin degradation products released from a fibrin clot perfused with plasmin. J Biol Chem. 1999;274(8):5201-12.
36. Jeanneau C, Sultan Y. Tissue plasminogen activator in human megakaryocytes and platelets: immunocytochemical localization, immunoblotting and zymographic analysis. Thromb Haemost. 1988;59(3):529-34.
37. Brisson-Jeanneau C, Nelles L, Rouer E, Sultan Y, Benarous R. Tissue-plasminogen activator RNA detected in megakaryocytes by in situ hybridization and biotinylated probe. Histochemistry. 1990;95(1):23-6.
38. Veljkovic DK, Rivard GE, Diamandis M, Blavignac J, Cramer-Bordé EM, Hayward CP. Increased expression of urokinase plasminogen activator in Quebec platelet disorder is linked to megakaryocyte differentiation. Blood. 2009;113(7):1535-42.
39. Horne MK, Merryman PK, Cullinane AM. Plasminogen interaction with platelets: the importance of carboxyterminal lysines. Thromb Res. 2005;116(6):499-507.
40. Miles LA, Plow EF. Binding and activation of plasminogen on the platelet surface. J Biol Chem. 1985;260(7):4303-11.
41. Miles LA, Parmer RJ. Plasminogen receptors: the first quarter century. Semin Thromb Hemost. 2013;39(4):329-37.
42. Brzoska T, Tanaka-Murakami A, Suzuki Y, Sano H, Kanayama N, Urano T. Endogenously generated plasmin at the vascular wall injury site amplifies lysine binding site-dependent plasminogen accumulation in microthrombi. PLoS One. 2015;10(3):e0122196.

43. Loscalzo J, Pasche B, Ouimet H, Freedman JE. Platelets and plasminogen activation. Thromb Haemost. 1995;74(1):291-3.
44. Whyte CS, Mitchell JL, Mutch NJ. Platelet-Mediated Modulation of Fibrinolysis. Semin Thromb Hemost. 2017;43(2):115-28.
45. Schneider M, Nesheim M. A study of the protection of plasmin from antiplasmin inhibition within an intact fibrin clot during the course of clot lysis. J Biol Chem. 2004;279(14):13333-9.
46. Silva MM, Thelwell C, Williams SC, Longstaff C. Regulation of fibrinolysis by C-terminal lysines operates through plasminogen and plasmin but not tissue-type plasminogen activator. J Thromb Haemost. 2012;10(11):2354-60.
47. Murphy S. Platelets from pooled buffy coats: an update. Transfusion. 2005;45(4):634-9.
48. Siddon AJ, Tormey CA, Snyder EL. 64 - Platelet Transfusion Medicine. In: Michelson AD, editor. Platelets (Fourth Edition): Academic Press; 2019. p. 1137-59.
49. Schrezenmeier H, Seifried E. Buffy-coat-derived pooled platelet concentrates and apheresis platelet concentrates: which product type should be preferred? Vox Sang. 2010;99(1):1-15.
50. Murphy S, Gardner FH. Platelet storage at 22 degrees C; metabolic, morphologic, and functional studies. J Clin Invest. 1971;50(2):370-7.
51. Murphy S, Kahn RA, Holme S, Phillips GL, Sherwood W, Davisson W, et al. Improved storage of platelets for transfusion in a new container. Blood. 1982;60(1):194-200.
52. Murphy S, Sayar SN, Gardner FH. Storage of platelet concentrates at 22 degrees C. Blood. 1970;35(4):549-57.
53. Murphy S, Gardner FH. Platelet storage at 22 degrees C: role of gas transport across plastic containers in maintenance of viability. Blood. 1975;46(2):209-18.
54. Wallvik J, Akerblom O. The platelet storage capability of different plastic containers. Vox Sang. 1990;58(1):40-4.
55. Kakaiya RM, Katz AJ. Platelet preservation in large containers. Vox Sang. 1984;46(2):111-8.
56. Britain G. Guidelines for the blood transfusion services in the United Kingdom: Stationery Office; 2013.
57. Kuehnert MJ, Roth VR, Haley NR, Gregory KR, Elder KV, Schreiber GB, et al. Transfusion-transmitted bacterial infection in the United States, 1998 through 2000. Transfusion. 2001;41(12):1493-9.
58. Ketter PM, Kamucheka R, Arulanandam B, Akers K, Cap AP. Platelet enhancement of bacterial growth during room temperature storage: mitigation through refrigeration. Transfusion. 2019;59(S2):1479-89.
59. Reddoch KM, Pidcoke HF, Montgomery RK, Fedyk CG, Aden JK, Ramasubramanian AK, et al. Hemostatic function of apheresis platelets stored at 4°C and 22°C. Shock. 2014;41 Suppl 1:54-61.
60. Yang J, Yin W, Zhang Y, Sun Y, Ma T, Gu S, et al. Evaluation of the advantages of platelet concentrates stored at 4°C versus 22°C. Transfusion. 2018;58(3):736-47.
61. Filip DJ, Aster RH. Relative hemostatic effectiveness of human platelets stored at 4 degrees and 22 degrees C. J Lab Clin Med. 1978;91(4):618-24.
62. Hoffmeister KM, Felbinger TW, Falet H, Denis CV, Bergmeier W, Mayadas TN, et al. The clearance mechanism of chilled blood platelets. Cell. 2003;112(1):87-97.
63. Montgomery RK, Reddoch KM, Evani SJ, Cap AP, Ramasubramanian AK. Enhanced shear-induced platelet aggregation due to low-temperature storage. Transfusion. 2013;53(7):1520-30.
64. Estcourt LJ, Birchall J, Allard S, Bassey SJ, Hersey P, Kerr JP, et al. Guidelines for the use of platelet transfusions. Br J Haematol. 2017;176(3):365-94.
65. Stubbs JR, Tran SA, Emery RL, Hammel SA, Haugen AL, Zielinski MD, et al. Cold platelets for trauma-associated bleeding: regulatory approval, accreditation approval, and practice implementation-just the "tip of the iceberg". Transfusion. 2017;57(12):2836-44.
66. Six KR, Devloo R, Compernolle V, Feys HB. Impact of cold storage on platelets treated with Intercept pathogen inactivation. Transfusion. 2019;59(8):2662-71.

67. Holme S, Heaton A. In vitro platelet ageing at 22 degrees C is reduced compared to in vivo ageing at 37 degrees C. Br J Haematol. 1995;91(1):212-8.
68. Bertino AM, Qi XQ, Li J, Xia Y, Kuter DJ. Apoptotic markers are increased in platelets stored at 37 degrees C. Transfusion. 2003;43(7):857-66.
69. Snyder EL, Koerner TA, Kakaiya R, Moore P, Kiraly T. Effect of mode of agitation on storage of platelet concentrates in PL-732 containers for 5 days. Vox Sang. 1983;44(5):300-4.
70. van der Meer PF, de Korte D. Platelet preservation: agitation and containers. Transfus Apher Sci. 2011;44(3):297-304.
71. van der Meer PF, Liefting LA, Pietersz RN. The effect of interruption of agitation on in vitro measures of platelet concentrates in additive solution. Transfusion. 2007;47(6):955-9.
72. Blajchman MA, Goldman M, Baeza F. Improving the bacteriological safety of platelet transfusions. Transfus Med Rev. 2004;18(1):11-24.
73. Pietersz RN. Pooled platelet concentrates: an alternative to single donor apheresis platelets? Transfus Apher Sci. 2009;41(2):115-9.
74. Bolton-Maggs PH, Cohen H. Serious Hazards of Transfusion (SHOT) haemovigilance and progress is improving transfusion safety. Br J Haematol. 2013;163(3):303-14.
75. Organs AcotSoBTa. Pathogen inactivation of platelets report of the SaBTO working group. SaBTO Reports; 2014.
76. van der Meer PF, Pietersz RN. Sterilization method of platelet storage containers affects in vitro parameters. Vox Sang. 2007;92(1):32-6.
77. Devine DV, Serrano K. The platelet storage lesion. Clin Lab Med. 2010;30(2):475-87.
78. Perrotta P, Snyder E. Platelet Storage and Transfusion. Platelets. 2007;2:1265-95.
79. Dumont LJ, VandenBroeke T. Seven-day storage of apheresis platelets: report of an in vitro study. Transfusion. 2003;43(2):143-50.
80. Picker SM. In-vitro assessment of platelet function. Transfus Apher Sci. 2011;44(3):305-19.
81. Shams Hakimi C, Hesse C, Wallén H, Boulund F, Grahn A, Jeppsson A. In vitro assessment of platelet concentrates with multiple electrode aggregometry. Platelets. 2015;26(2):132-7.
82. Labrie A, Marshall A, Bedi H, Maurer-Spurej E. Characterization of platelet concentrates using dynamic light scattering. Transfus Med Hemother. 2013;40(2):93-100.
83. Black A, Pienimaeki-Roemer A, Kenyon O, Orsó E, Schmitz G. Platelet-derived extracellular vesicles in plateletpheresis concentrates as a quality control approach. Transfusion. 2015;55(9):2184-96.
84. Vetlesen A, Mirlashari MR, Ezligini F, Kjeldsen-Kragh J. Evaluation of platelet activation and cytokine release during storage of platelet concentrates processed from buffy coats either manually or by the automated OrbiSac system. Transfusion. 2007;47(1):126-32.
85. Leytin V, Allen DJ, Mutlu A, Mykhaylov S, Lyubimov E, Freedman J. Platelet activation and apoptosis are different phenomena: evidence from the sequential dynamics and the magnitude of responses during platelet storage. Br J Haematol. 2008;142(3):494-7.
86. Gutensohn K, Geidel K, Brockmann M, Siemensen M, Krueger W, Kroeger N, et al. Binding of activated platelets to WBCs in vivo after transfusion. Transfusion. 2002;42(10):1373-80.
87. Perseghin P, Mascaretti L, Speranza T, Belotti D, Baldini V, Dassi M, et al. Platelet activation during plasma-reduced multicomponent PLT collection: a comparison between COBE Trima and Spectra LRS turbo cell separators. Transfusion. 2004;44(1):125-30.
88. Berger G, Hartwell DW, Wagner DD. P-Selectin and platelet clearance. Blood. 1998;92(11):4446-52.
89. Cardigan R, Sutherland J, Garwood M, Bashir S, Turner C, Smith K, et al. In vitro function of buffy coat-derived platelet concentrates stored for 9 days in CompoSol, PASII or 100% plasma in three different storage bags. Vox Sang. 2008;94(2):103-12.
90. Turner CP, Sutherland J, Wadhwa M, Dilger P, Cardigan R. In vitro function of platelet concentrates prepared after filtration of whole blood or buffy coat pools. Vox Sang. 2005;88(3):164-71.

91. Maurer-Spurej E, Chipperfield K. Past and future approaches to assess the quality of platelets for transfusion. Transfus Med Rev. 2007;21(4):295-306.
92. Goodrich RP, Li J, Pieters H, Crookes R, Roodt J, Heyns AuP. Correlation of in vitro platelet quality measurements with in vivo platelet viability in human subjects. Vox Sang. 2006;90(4):279-85.
93. Murphy S, Rebulla P, Bertolini F, Holme S, Moroff G, Snyder E, et al. In vitro assessment of the quality of stored platelet concentrates. The BEST (Biomedical Excellence for Safer Transfusion) Task Force of the International Society of Blood Transfusion. Transfus Med Rev. 1994;8(1):29-36.
94. Cardigan R, Williamson LM. The quality of platelets after storage for 7 days. Transfus Med. 2003;13(4):173-87.
95. Brecher ME, Hay SN. Transfusion medicine illustrated. Platelet swirling. Transfusion. 2004;44(5):627.
96. Rothwell SW, Maglasang P, Reid TJ, Gorogias M, Krishnamurti C. Correlation of in vivo and in vitro functions of fresh and stored human platelets. Transfusion. 2000;40(8):988-93.
97. Italiano JE, Bergmeier W, Tiwari S, Falet H, Hartwig JH, Hoffmeister KM, et al. Mechanisms and implications of platelet discoid shape. Blood. 2003;101(12):4789-96.
98. Gulliksson H, AuBuchon JP, Cardigan R, van der Meer PF, Murphy S, Prowse C, et al. Storage of platelets in additive solutions: a multicentre study of the in vitro effects of potassium and magnesium. Vox Sang. 2003;85(3):199-205.
99. Bordbar A, Yurkovich JT, Paglia G, Rolfsson O, Sigurjónsson Ó, Palsson BO. Elucidating dynamic metabolic physiology through network integration of quantitative time-course metabolomics. Sci Rep. 2017;7:46249.
100. Kilkson H, Holme S, Murphy S. Platelet metabolism during storage of platelet concentrates at 22 degrees C. Blood. 1984;64(2):406-14.
101. Picker SM, Schneider V, Oustianskaia L, Gathof BS. Cell viability during platelet storage in correlation to cellular metabolism after different pathogen reduction technologies. Transfusion. 2009;49(11):2311-8.
102. Zhang JG, Carter CJ, Culibrk B, Devine DV, Levin E, Scammell K, et al. Buffy-coat platelet variables and metabolism during storage in additive solutions or plasma. Transfusion. 2008;48(5):847-56.
103. Sjövall F, Ehinger JK, Marelsson SE, Morota S, Frostner EA, Uchino H, et al. Mitochondrial respiration in human viable platelets--methodology and influence of gender, age and storage. Mitochondrion. 2013;13(1):7-14.
104. Ravi S, Chacko B, Kramer PA, Sawada H, Johnson MS, Zhi D, et al. Defining the effects of storage on platelet bioenergetics: The role of increased proton leak. Biochim Biophys Acta. 2015;1852(11):2525-34.
105. Holme S, Moroff G, Murphy S. A multi-laboratory evaluation of in vitro platelet assays: the tests for extent of shape change and response to hypotonic shock. Biomedical Excellence for Safer Transfusion Working Party of the International Society of Blood Transfusion. Transfusion. 1998;38(1):31-40.
106. Maurer-Spurej E, Devine DV. Platelet aggregation is not initiated by platelet shape change. Lab Invest. 2001;81(11):1517-25.
107. Okada Y, Maeno E, Shimizu T, Dezaki K, Wang J, Morishima S. Receptor-mediated control of regulatory volume decrease (RVD) and apoptotic volume decrease (AVD). J Physiol. 2001;532(Pt 1):3-16.
108. BORN GV. Aggregation of blood platelets by adenosine diphosphate and its reversal. Nature. 1962;194:927-9.
109. Keuren JF, Cauwenberghs S, Heeremans J, de Kort W, Heemskerk JW, Curvers J. Platelet ADP response deteriorates in synthetic storage media. Transfusion. 2006;46(2):204-12.
110. Murphy S, Gardner FH. Platelet storage at 22 degrees C; metabolic, morphologic, and functional studies. The Journal of clinical investigation. 1971;50(2):370-7.

111. van der Meer PF, Tomson B, Brand A. In vivo tracking of transfused platelets for recovery and survival studies: an appraisal of labeling methods. Transfus Apher Sci. 2010;42(1):53-61.
112. Holme S. In vitro assays used in the evaluation of the quality of stored platelets: correlation with in vivo assays. Transfus Apher Sci. 2008;39(2):161-5.
113. Murphy S. What's so bad about old platelets? Transfusion. 2002;42(7):809-11.
114. Norfolk DR, Ancliffe PJ, Contreras M, Hunt BJ, Machin SJ, Murphy WG, et al. Consensus Conference on Platelet Transfusion, Royal College of Physicians of Edinburgh, 27-28 November 1997. Synopsis of background papers. Br J Haematol. 1998;101(4):609-17.
115. Collaborative TBEfST. Platelet radiolabeling procedure. 2006;46(s3):59S-66S.
116. Murphy S. Radiolabeling of PLTs to assess viability: a proposal for a standard. Transfusion. 2004;44(1):131-3.
117. Strandenes G, Sivertsen J, Bjerkvig CK, Fosse TK, Cap AP, del Junco DJ, et al. A Pilot Trial of Platelets Stored Cold versus at Room Temperature for Complex Cardiothoracic Surgery. Anesthesiology. 2020;133(6):1173-83.
118. Shimizu T, Murphy S. Roles of acetate and phosphate in the successful storage of platelet concentrates prepared with an acetate-containing additive solution. Transfusion. 1993;33(4):304-10.
119. van der Meer PF, de Korte D. Platelet Additive Solutions: A Review of the Latest Developments and Their Clinical Implications. Transfus Med Hemother. 2018;45(2):98-102.
120. CHARGAFF E, WEST R. The biological significance of the thromboplastic protein of blood. J Biol Chem. 1946;166(1):189-97.
121. Wolf P. The nature and significance of platelet products in human plasma. Br J Haematol. 1967;13(3):269-88.
122. Johnstone RM, Adam M, Hammond JR, Orr L, Turbide C. Vesicle formation during reticulocyte maturation. Association of plasma membrane activities with released vesicles (exosomes). J Biol Chem. 1987;262(19):9412-20.
123. Johnstone RM. The Jeanne Manery-Fisher Memorial Lecture 1991. Maturation of reticulocytes: formation of exosomes as a mechanism for shedding membrane proteins. Biochem Cell Biol. 1992;70(3-4):179-90.
124. Raposo G, Nijman HW, Stoorvogel W, Liejendekker R, Harding CV, Melief CJ, et al. B lymphocytes secrete antigen-presenting vesicles. J Exp Med. 1996;183(3):1161-72.
125. Lötvall J, Hill AF, Hochberg F, Buzás EI, Di Vizio D, Gardiner C, et al. Minimal experimental requirements for definition of extracellular vesicles and their functions: a position statement from the International Society for Extracellular Vesicles. J Extracell Vesicles. 2014;3:26913.
126. Witwer KW, Soekmadji C, Hill AF, Wauben MH, Buzás EI, Di Vizio D, et al. Updating the MISEV minimal requirements for extracellular vesicle studies: building bridges to reproducibility. J Extracell Vesicles. 2017;6(1):1396823.
127. Karlsson M, Lundin S, Dahlgren U, Kahu H, Pettersson I, Telemo E. "Tolerosomes" are produced by intestinal epithelial cells. Eur J Immunol. 2001;31(10):2892-900.
128. Stegmayr B, Ronquist G. Promotive effect on human sperm progressive motility by prostasomes. Urol Res. 1982;10(5):253-7.
129. Di Vizio D, Morello M, Dudley AC, Schow PW, Adam RM, Morley S, et al. Large oncosomes in human prostate cancer tissues and in the circulation of mice with metastatic disease. Am J Pathol. 2012;181(5):1573-84.
130. Gould SJ, Raposo G. As we wait: coping with an imperfect nomenclature for extracellular vesicles. J Extracell Vesicles. 2013;2.
131. Morelli AE, Larregina AT, Shufesky WJ, Sullivan ML, Stolz DB, Papworth GD, et al. Endocytosis, intracellular sorting, and processing of exosomes by dendritic cells. Blood. 2004;104(10):3257-66.
132. Stoorvogel W, Strous GJ, Geuze HJ, Oorschot V, Schwartz AL. Late endosomes derive from early endosomes by maturation. Cell. 1991;65(3):417-27.

133. Théry C, Zitvogel L, Amigorena S. Exosomes: composition, biogenesis and function. Nat Rev Immunol. 2002;2(8):569-79.
134. Yellon DM, Davidson SM. Exosomes: nanoparticles involved in cardioprotection? Circ Res. 2014;114(2):325-32.
135. Henne WM, Buchkovich NJ, Emr SD. The ESCRT pathway. Dev Cell. 2011;21(1):77-91.
136. Hurley JH. ESCRTs are everywhere. EMBO J. 2015;34(19):2398-407.
137. Villarroya-Beltri C, Baixauli F, Gutiérrez-Vázquez C, Sánchez-Madrid F, Mittelbrunn M. Sorting it out: regulation of exosome loading. Semin Cancer Biol. 2014;28:3-13.
138. Colombo M, Moita C, van Niel G, Kowal J, Vigneron J, Benaroch P, et al. Analysis of ESCRT functions in exosome biogenesis, composition and secretion highlights the heterogeneity of extracellular vesicles. J Cell Sci. 2013;126(Pt 24):5553-65.
139. Airola MV, Hannun YA. Sphingolipid metabolism and neutral sphingomyelinases. Handb Exp Pharmacol. 2013(215):57-76.
140. Castro BM, Prieto M, Silva LC. Ceramide: a simple sphingolipid with unique biophysical properties. Prog Lipid Res. 2014;54:53-67.
141. Perez-Hernandez D, Gutiérrez-Vázquez C, Jorge I, López-Martín S, Ursa A, Sánchez-Madrid F, et al. The intracellular interactome of tetraspanin-enriched microdomains reveals their function as sorting machineries toward exosomes. J Biol Chem. 2013;288(17):11649-61.
142. Linares R, Tan S, Gounou C, Arraud N, Brisson AR. High-speed centrifugation induces aggregation of extracellular vesicles. J Extracell Vesicles. 2015;4:29509.
143. van den Boorn JG, Dassler J, Coch C, Schlee M, Hartmann G. Exosomes as nucleic acid nanocarriers. Adv Drug Deliv Rev. 2013;65(3):331-5.
144. Edgar JR, Eden ER, Futter CE. Hrs- and CD63-dependent competing mechanisms make different sized endosomal intraluminal vesicles. Traffic. 2014;15(2):197-211.
145. Tschuschke M, Kocherova I, Bryja A, Mozdziak P, Angelova Volponi A, Janowicz K, et al. Inclusion Biogenesis, Methods of Isolation and Clinical Application of Human Cellular Exosomes. J Clin Med. 2020;9(2).
146. Hsu C, Morohashi Y, Yoshimura S, Manrique-Hoyos N, Jung S, Lauterbach MA, et al. Regulation of exosome secretion by Rab35 and its GTPase-activating proteins TBC1D10A-C. J Cell Biol. 2010;189(2):223-32.
147. Ostrowski M, Carmo NB, Krumeich S, Fanget I, Raposo G, Savina A, et al. Rab27a and Rab27b control different steps of the exosome secretion pathway. Nat Cell Biol. 2010;12(1):19-30; sup pp 1-13.
148. Webber JP, Spary LK, Sanders AJ, Chowdhury R, Jiang WG, Steadman R, et al. Differentiation of tumour-promoting stromal myofibroblasts by cancer exosomes. Oncogene. 2015;34(3):290-302.
149. Baietti MF, Zhang Z, Mortier E, Melchior A, Degeest G, Geeraerts A, et al. Syndecan-syntenin-ALIX regulates the biogenesis of exosomes. Nat Cell Biol. 2012;14(7):677-85.
150. Pfeffer SR. Unsolved mysteries in membrane traffic. Annu Rev Biochem. 2007;76:629-45.
151. Fader CM, Sánchez DG, Mestre MB, Colombo MI. TI-VAMP/VAMP7 and VAMP3/cellubrevin: two v-SNARE proteins involved in specific steps of the autophagy/multivesicular body pathways. Biochim Biophys Acta. 2009;1793(12):1901-16.
152. Savina A, Furlán M, Vidal M, Colombo MI. Exosome release is regulated by a calcium-dependent mechanism in K562 cells. J Biol Chem. 2003;278(22):20083-90.
153. Lehmann BD, Paine MS, Brooks AM, McCubrey JA, Renegar RH, Wang R, et al. Senescence-associated exosome release from human prostate cancer cells. Cancer Res. 2008;68(19):7864-71.
154. Beer L, Zimmermann M, Mitterbauer A, Ellinger A, Gruber F, Narzt MS, et al. Analysis of the Secretome of Apoptotic Peripheral Blood Mononuclear Cells: Impact of Released Proteins and Exosomes for Tissue Regeneration. Sci Rep. 2015;5:16662.
155. Xiao X, Yu S, Li S, Wu J, Ma R, Cao H, et al. Exosomes: decreased sensitivity of lung cancer A549 cells to cisplatin. PLoS One. 2014;9(2):e89534.

156. Kanemoto S, Nitani R, Murakami T, Kaneko M, Asada R, Matsuhisa K, et al. Multivesicular body formation enhancement and exosome release during endoplasmic reticulum stress. Biochem Biophys Res Commun. 2016;480(2):166-72.
157. Boya P, Reggiori F, Codogno P. Emerging regulation and functions of autophagy. Nat Cell Biol. 2013;15(7):713-20.
158. Clark MR. Flippin' lipids. Nat Immunol. 2011;12(5):373-5.
159. Hankins HM, Baldridge RD, Xu P, Graham TR. Role of flippases, scramblases and transfer proteins in phosphatidylserine subcellular distribution. Traffic. 2015;16(1):35-47.
160. Manno S, Takakuwa Y, Mohandas N. Identification of a functional role for lipid asymmetry in biological membranes: Phosphatidylserine-skeletal protein interactions modulate membrane stability. Proc Natl Acad Sci U S A. 2002;99(4):1943-8.
161. Fox JE, Austin CD, Boyles JK, Steffen PK. Role of the membrane skeleton in preventing the shedding of procoagulant-rich microvesicles from the platelet plasma membrane. J Cell Biol. 1990;111(2):483-93.
162. Midura EF, Prakash PS, Johnson BL, Rice TC, Kunz N, Caldwell CC. Impact of caspase-8 and PKA in regulating neutrophil-derived microparticle generation. Biochem Biophys Res Commun. 2016;469(4):917-22.
163. Akers JC, Gonda D, Kim R, Carter BS, Chen CC. Biogenesis of extracellular vesicles (EV): exosomes, microvesicles, retrovirus-like vesicles, and apoptotic bodies. J Neurooncol. 2013;113(1):1-11.
164. He C, Zheng S, Luo Y, Wang B. Exosome Theranostics: Biology and Translational Medicine. Theranostics. 2018;8(1):237-55.
165. Aatonen MT, Ohman T, Nyman TA, Laitinen S, Grönholm M, Siljander PR. Isolation and characterization of platelet-derived extracellular vesicles. J Extracell Vesicles. 2014;3.
166. Curtis AM, Edelberg J, Jonas R, Rogers WT, Moore JS, Syed W, et al. Endothelial microparticles: sophisticated vesicles modulating vascular function. Vasc Med. 2013;18(4):204-14.
167. Turiák L, Misják P, Szabó TG, Aradi B, Pálóczi K, Ozohanics O, et al. Proteomic characterization of thymocyte-derived microvesicles and apoptotic bodies in BALB/c mice. J Proteomics. 2011;74(10):2025-33.
168. de Jong OG, Verhaar MC, Chen Y, Vader P, Gremmels H, Posthuma G, et al. Cellular stress conditions are reflected in the protein and RNA content of endothelial cell-derived exosomes. J Extracell Vesicles. 2012;1.
169. Kalra H, Simpson RJ, Ji H, Aikawa E, Altevogt P, Askenase P, et al. Vesiclepedia: a compendium for extracellular vesicles with continuous community annotation. PLoS Biol. 2012;10(12):e1001450.
170. Théry C, Boussac M, Véron P, Ricciardi-Castagnoli P, Raposo G, Garin J, et al. Proteomic analysis of dendritic cell-derived exosomes: a secreted subcellular compartment distinct from apoptotic vesicles. J Immunol. 2001;166(12):7309-18.
171. Valadi H, Ekström K, Bossios A, Sjöstrand M, Lee JJ, Lötvall JO. Exosome-mediated transfer of mRNAs and microRNAs is a novel mechanism of genetic exchange between cells. Nat Cell Biol. 2007;9(6):654-9.
172. Bobrie A, Colombo M, Raposo G, Théry C. Exosome secretion: molecular mechanisms and roles in immune responses. Traffic. 2011;12(12):1659-68.
173. Nolte-'t Hoen EN, Buermans HP, Waasdorp M, Stoorvogel W, Wauben MH, 't Hoen PA. Deep sequencing of RNA from immune cell-derived vesicles uncovers the selective incorporation of small non-coding RNA biotypes with potential regulatory functions. Nucleic Acids Res. 2012;40(18):9272-85.
174. Needham D, Nunn RS. Elastic deformation and failure of lipid bilayer membranes containing cholesterol. Biophys J. 1990;58(4):997-1009.

175. Subra C, Grand D, Laulagnier K, Stella A, Lambeau G, Paillasse M, et al. Exosomes account for vesicle-mediated transcellular transport of activatable phospholipases and prostaglandins. J Lipid Res. 2010;51(8):2105-20.
176. Pienimaeki-Roemer A, Kuhlmann K, Böttcher A, Konovalova T, Black A, Orsó E, et al. Lipidomic and proteomic characterization of platelet extracellular vesicle subfractions from senescent platelets. Transfusion. 2015;55(3):507-21.
177. Deregibus MC, Cantaluppi V, Calogero R, Lo Iacono M, Tetta C, Biancone L, et al. Endothelial progenitor cell derived microvesicles activate an angiogenic program in endothelial cells by a horizontal transfer of mRNA. Blood. 2007;110(7):2440-8.
178. Kirchhausen T. Clathrin. Annu Rev Biochem. 2000;69:699-727.
179. Escrevente C, Keller S, Altevogt P, Costa J. Interaction and uptake of exosomes by ovarian cancer cells. BMC Cancer. 2011;11:108.
180. Mulcahy LA, Pink RC, Carter DR. Routes and mechanisms of extracellular vesicle uptake. J Extracell Vesicles. 2014;3.
181. Nanbo A, Kawanishi E, Yoshida R, Yoshiyama H. Exosomes derived from Epstein-Barr virus-infected cells are internalized via caveola-dependent endocytosis and promote phenotypic modulation in target cells. J Virol. 2013;87(18):10334-47.
182. Izquierdo-Useros N, Naranjo-Gómez M, Archer J, Hatch SC, Erkizia I, Blanco J, et al. Capture and transfer of HIV-1 particles by mature dendritic cells converges with the exosome-dissemination pathway. Blood. 2009;113(12):2732-41.
183. Colombo M, Raposo G, Théry C. Biogenesis, secretion, and intercellular interactions of exosomes and other extracellular vesicles. Annu Rev Cell Dev Biol. 2014;30:255-89.
184. Feng D, Zhao WL, Ye YY, Bai XC, Liu RQ, Chang LF, et al. Cellular internalization of exosomes occurs through phagocytosis. Traffic. 2010;11(5):675-87.
185. Yuyama K, Sun H, Mitsutake S, Igarashi Y. Sphingolipid-modulated exosome secretion promotes clearance of amyloid-β by microglia. J Biol Chem. 2012;287(14):10977-89.
186. Del Conde I, Shrimpton CN, Thiagarajan P, López JA. Tissue-factor-bearing microvesicles arise from lipid rafts and fuse with activated platelets to initiate coagulation. Blood. 2005;106(5):1604-11.
187. Diehl P, Fricke A, Sander L, Stamm J, Bassler N, Htun N, et al. Microparticles: major transport vehicles for distinct microRNAs in circulation. Cardiovasc Res. 2012;93(4):633-44.
188. Terrisse AD, Puech N, Allart S, Gourdy P, Xuereb JM, Payrastre B, et al. Internalization of microparticles by endothelial cells promotes platelet/endothelial cell interaction under flow. J Thromb Haemost. 2010;8(12):2810-9.
189. Lawson C, Vicencio JM, Yellon DM, Davidson SM. Microvesicles and exosomes: new players in metabolic and cardiovascular disease. J Endocrinol. 2016;228(2):R57-71.
190. Witwer KW, Buzás EI, Bemis LT, Bora A, Lässer C, Lötvall J, et al. Standardization of sample collection, isolation and analysis methods in extracellular vesicle research. J Extracell Vesicles. 2013;2.
191. Lippi G, Fontana R, Avanzini P, Aloe R, Ippolito L, Sandei F, et al. Influence of mechanical trauma of blood and hemolysis on PFA-100 testing. Blood Coagul Fibrinolysis. 2012;23(1):82-6.
192. Breddin HK, Harder S. [The value of platelet function tests]. Vasa. 2003;32(3):123-9.
193. Jayachandran M, Miller VM, Heit JA, Owen WG. Methodology for isolation, identification and characterization of microvesicles in peripheral blood. J Immunol Methods. 2012;375(1-2):207-14.
194. Shah MD, Bergeron AL, Dong JF, López JA. Flow cytometric measurement of microparticles: pitfalls and protocol modifications. Platelets. 2008;19(5):365-72.
195. Kim DJ, Linnstaedt S, Palma J, Park JC, Ntrivalas E, Kwak-Kim JY, et al. Plasma components affect accuracy of circulating cancer-related microRNA quantitation. The Journal of molecular diagnostics : JMD. 2012;14(1):71-80.
196. Lacroix R, Judicone C, Mooberry M, Boucekine M, Key NS, Dignat-George F. Standardization of pre-analytical variables in plasma microparticle determination: results of the International Society on Thrombosis and Haemostasis SSC Collaborative workshop. J Thromb Haemost. 2013.

197. Ismail N, Wang Y, Dakhlallah D, Moldovan L, Agarwal K, Batte K, et al. Macrophage microvesicles induce macrophage differentiation and miR-223 transfer. Blood. 2013;121(6):984-95.
198. Kessler RJ, Fanestil DD. Interference by lipids in the determination of protein using bicinchoninic acid. Anal Biochem. 1986;159(1):138-42.
199. György B, Módos K, Pállinger E, Pálóczi K, Pásztói M, Misják P, et al. Detection and isolation of cell-derived microparticles are compromised by protein complexes resulting from shared biophysical parameters. Blood. 2011;117(4):e39-48.
200. van der Pol E, Böing AN, Harrison P, Sturk A, Nieuwland R. Classification, functions, and clinical relevance of extracellular vesicles. Pharmacol Rev. 2012;64(3):676-705.
201. Théry C, Amigorena S, Raposo G, Clayton A. Isolation and characterization of exosomes from cell culture supernatants and biological fluids. Curr Protoc Cell Biol. 2006;Chapter 3:Unit 3.22.
202. Böing AN, van der Pol E, Grootemaat AE, Coumans FA, Sturk A, Nieuwland R. Single-step isolation of extracellular vesicles by size-exclusion chromatography. J Extracell Vesicles. 2014;3.
203. Welton JL, Webber JP, Botos LA, Jones M, Clayton A. Ready-made chromatography columns for extracellular vesicle isolation from plasma. J Extracell Vesicles. 2015;4:27269.
204. Yuana Y, Levels J, Grootemaat A, Sturk A, Nieuwland R. Co-isolation of extracellular vesicles and high-density lipoproteins using density gradient ultracentrifugation. J Extracell Vesicles. 2014;3.
205. Clayton A, Court J, Navabi H, Adams M, Mason MD, Hobot JA, et al. Analysis of antigen presenting cell derived exosomes, based on immuno-magnetic isolation and flow cytometry. J Immunol Methods. 2001;247(1-2):163-74.
206. Rabesandratana H, Toutant JP, Reggio H, Vidal M. Decay-accelerating factor (CD55) and membrane inhibitor of reactive lysis (CD59) are released within exosomes during In vitro maturation of reticulocytes. Blood. 1998;91(7):2573-80.
207. Chen S, Shiesh SC, Lee GB, Chen C. Two-step magnetic bead-based (2MBB) techniques for immunocapture of extracellular vesicles and quantification of microRNAs for cardiovascular diseases: A pilot study. PLoS One. 2020;15(2):e0229610.
208. Chen C, Skog J, Hsu CH, Lessard RT, Balaj L, Wurdinger T, et al. Microfluidic isolation and transcriptome analysis of serum microvesicles. Lab Chip. 2010;10(4):505-11.
209. Wu M, Ouyang Y, Wang Z, Zhang R, Huang PH, Chen C, et al. Isolation of exosomes from whole blood by integrating acoustics and microfluidics. Proc Natl Acad Sci U S A. 2017;114(40):10584-9.
210. Van Deun J, Mestdagh P, Agostinis P, Akay Ö, Anand S, Anckaert J, et al. EV-TRACK: transparent reporting and centralizing knowledge in extracellular vesicle research. Nat Methods. 2017;14(3):228-32.
211. Hartjes TA, Mytnyk S, Jenster GW, van Steijn V, van Royen ME. Extracellular Vesicle Quantification and Characterization: Common Methods and Emerging Approaches. Bioengineering (Basel). 2019;6(1).
212. Filipe V, Hawe A, Jiskoot W. Critical evaluation of Nanoparticle Tracking Analysis (NTA) by NanoSight for the measurement of nanoparticles and protein aggregates. Pharmaceutical research. 2010;27(5):796-810.
213. Erdbrügger U, Lannigan J. Analytical challenges of extracellular vesicle detection: A comparison of different techniques. Cytometry Part A. 2016;89(2):123-34.
214. van der Pol E, Coumans FA, Grootemaat AE, Gardiner C, Sargent IL, Harrison P, et al. Particle size distribution of exosomes and microvesicles determined by transmission electron microscopy, flow cytometry, nanoparticle tracking analysis, and resistive pulse sensing. J Thromb Haemost. 2014;12(7):1182-92.
215. Kubota S, Chiba M, Watanabe M, Sakamoto M, Watanabe N. Secretion of small/microRNAs including miR-638 into extracellular spaces by sphingomyelin phosphodiesterase 3. Oncol Rep. 2015;33(1):67-73.
216. Flaumenhaft R. Formation and fate of platelet microparticles. Blood Cells Mol Dis. 2006;36(2):182-7.

217. Boudreau LH, Duchez AC, Cloutier N, Soulet D, Martin N, Bollinger J, et al. Platelets release mitochondria serving as substrate for bactericidal group IIA-secreted phospholipase A2 to promote inflammation. Blood. 2014;124(14):2173-83.
218. Horstman LL, Ahn YS. Platelet microparticles: a wide-angle perspective. Crit Rev Oncol Hematol. 1999;30(2):111-42.
219. Baj-Krzyworzeka M, Majka M, Pratico D, Ratajczak J, Vilaire G, Kijowski J, et al. Platelet-derived microparticles stimulate proliferation, survival, adhesion, and chemotaxis of hematopoietic cells. Exp Hematol. 2002;30(5):450-9.
220. Antwi-Baffour S, Adjei J, Aryeh C, Kyeremeh R, Kyei F, Seidu MA. Understanding the biosynthesis of platelets-derived extracellular vesicles. Immun Inflamm Dis. 2015;3(3):133-40.
221. Heijnen HF, Schiel AE, Fijnheer R, Geuze HJ, Sixma JJ. Activated platelets release two types of membrane vesicles: microvesicles by surface shedding and exosomes derived from exocytosis of multivesicular bodies and alpha-granules. Blood. 1999;94(11):3791-9.
222. Seiki M. Membrane-type 1 matrix metalloproteinase: a key enzyme for tumor invasion. Cancer Lett. 2003;194(1):1-11.
223. Chen YW, Chen YC, Wang JS. Absolute hypoxic exercise training enhances in vitro thrombin generation by increasing procoagulant platelet-derived microparticles under high shear stress in sedentary men. Clin Sci (Lond). 2013;124(10):639-49.
224. Owens AP, Mackman N. Microparticles in hemostasis and thrombosis. Circ Res. 2011;108(10):1284-97.
225. Connor DE, Exner T, Ma DD, Joseph JE. The majority of circulating platelet-derived microparticles fail to bind annexin V, lack phospholipid-dependent procoagulant activity and demonstrate greater expression of glycoprotein Ib. Thromb Haemost. 2010;103(5):1044-52.
226. Zubairova LD, Nabiullina RM, Nagaswami C, Zuev YF, Mustafin IG, Litvinov RI, et al. Circulating Microparticles Alter Formation, Structure, and Properties of Fibrin Clots. Sci Rep. 2015;5:17611.
227. Yáñez-Mó M, Siljander PR, Andreu Z, Zavec AB, Borràs FE, Buzas EI, et al. Biological properties of extracellular vesicles and their physiological functions. J Extracell Vesicles. 2015;4:27066.
228. Castaman G, Yu-Feng L, Rodeghiero F. A bleeding disorder characterised by isolated deficiency of platelet microvesicle generation. Lancet. 1996;347(9002):700-1.
229. Rhee JS, Black M, Schubert U, Fischer S, Morgenstern E, Hammes HP, et al. The functional role of blood platelet components in angiogenesis. Thromb Haemost. 2004;92(2):394-402.
230. Barry OP, Praticò D, Savani RC, FitzGerald GA. Modulation of monocyte-endothelial cell interactions by platelet microparticles. J Clin Invest. 1998;102(1):136-44.
231. Barry OP, Pratico D, Lawson JA, FitzGerald GA. Transcellular activation of platelets and endothelial cells by bioactive lipids in platelet microparticles. J Clin Invest. 1997;99(9):2118-27.
232. Preston RA, Jy W, Jimenez JJ, Mauro LM, Horstman LL, Valle M, et al. Effects of severe hypertension on endothelial and platelet microparticles. Hypertension. 2003;41(2):211-7.
233. Forlow SB, McEver RP, Nollert MU. Leukocyte-leukocyte interactions mediated by platelet microparticles under flow. Blood. 2000;95(4):1317-23.
234. World Heath Organisation. Cardiovasular Diseases WHO database2021 [Available from: Cardiovascular diseases (who.int).
235. Stepanian A, Bourguignat L, Hennou S, Coupaye M, Hajage D, Salomon L, et al. Microparticle increase in severe obesity: not related to metabolic syndrome and unchanged after massive weight loss. Obesity (Silver Spring). 2013;21(11):2236-43.
236. Murakami T, Horigome H, Tanaka K, Nakata Y, Ohkawara K, Katayama Y, et al. Impact of weight reduction on production of platelet-derived microparticles and fibrinolytic parameters in obesity. Thromb Res. 2007;119(1):45-53.

237. Gündüz Z, Dursun İ, Tülpar S, Başтuğ F, Baykan A, Yıkılmaz A, et al. Increased endothelial microparticles in obese and overweight children. J Pediatr Endocrinol Metab. 2012;25(11-12):1111-7.
238. Campello E, Zabeo E, Radu CM, Spiezia L, Gavasso S, Fadin M, et al. Hypercoagulability in overweight and obese subjects who are asymptomatic for thrombotic events. Thromb Haemost. 2015;113(1):85-96.
239. Morel O, Luca F, Grunebaum L, Jesel L, Meyer N, Desprez D, et al. Short-term very low-calorie diet in obese females improves the haemostatic balance through the reduction of leptin levels, PAI-1 concentrations and a diminished release of platelet and leukocyte-derived microparticles. Int J Obes (Lond). 2011;35(12):1479-86.
240. Sabatier F, Darmon P, Hugel B, Combes V, Sanmarco M, Velut JG, et al. Type 1 and type 2 diabetic patients display different patterns of cellular microparticles. Diabetes. 2002;51(9):2840-5.
241. Nomura S, Suzuki M, Katsura K, Xie GL, Miyazaki Y, Miyake T, et al. Platelet-derived microparticles may influence the development of atherosclerosis in diabetes mellitus. Atherosclerosis. 1995;116(2):235-40.
242. Benjamin EJ, Muntner P, Alonso A, Bittencourt MS, Callaway CW, Carson AP, et al. Heart Disease and Stroke Statistics-2019 Update: A Report From the American Heart Association. Circulation. 2019;139(10):e56-e528.
243. Müller G. Microvesicles/exosomes as potential novel biomarkers of metabolic diseases. Diabetes Metab Syndr Obes. 2012;5:247-82.
244. Cherian P, Hankey GJ, Eikelboom JW, Thom J, Baker RI, McQuillan A, et al. Endothelial and platelet activation in acute ischemic stroke and its etiological subtypes. Stroke. 2003;34(9):2132-7.
245. Chen Y, Xiao Y, Lin Z, Xiao X, He C, Bihl JC, et al. The Role of Circulating Platelets Microparticles and Platelet Parameters in Acute Ischemic Stroke Patients. J Stroke Cerebrovasc Dis. 2015;24(10):2313-20.
246. Kuriyama N, Nagakane Y, Hosomi A, Ohara T, Kasai T, Harada S, et al. Evaluation of factors associated with elevated levels of platelet-derived microparticles in the acute phase of cerebral infarction. Clinical and applied thrombosis/hemostasis : official journal of the International Academy of Clinical and Applied Thrombosis/Hemostasis. 2010;16(1):26-32.
247. Tripisciano C, Weiss R, Eichhorn T, Spittler A, Heuser T, Fischer MB, et al. Different Potential of Extracellular Vesicles to Support Thrombin Generation: Contributions of Phosphatidylserine, Tissue Factor, and Cellular Origin. Sci Rep. 2017;7(1):6522.
248. Tripisciano C, Weiss R, Karuthedom George S, Fischer MB, Weber V. Extracellular Vesicles Derived From Platelets, Red Blood Cells, and Monocyte-Like Cells Differ Regarding Their Ability to Induce Factor XII-Dependent Thrombin Generation. Front Cell Dev Biol. 2020;8:298.
249. Couch Y, Akbar N, Davis S, Fischer R, Dickens AM, Neuhaus AA, et al. Inflammatory Stroke Extracellular Vesicles Induce Macrophage Activation. Stroke. 2017;48(8):2292-6.
250. Simak J, Gelderman MP, Yu H, Wright V, Baird AE. Circulating endothelial microparticles in acute ischemic stroke: a link to severity, lesion volume and outcome. J Thromb Haemost. 2006;4(6):1296-302.
251. Knijff-Dutmer EA, Koerts J, Nieuwland R, Kalsbeek-Batenburg EM, van de Laar MA. Elevated levels of platelet microparticles are associated with disease activity in rheumatoid arthritis. Arthritis Rheum. 2002;46(6):1498-503.
252. Berckmans RJ, Nieuwland R, Tak PP, Böing AN, Romijn FP, Kraan MC, et al. Cell-derived microparticles in synovial fluid from inflamed arthritic joints support coagulation exclusively via a factor VII-dependent mechanism. Arthritis Rheum. 2002;46(11):2857-66.
253. Berckmans RJ, Nieuwland R, Kraan MC, Schaap MC, Pots D, Smeets TJ, et al. Synovial microparticles from arthritic patients modulate chemokine and cytokine release by synoviocytes. Arthritis Res Ther. 2005;7(3):R536-44.

254. Mastronardi ML, Mostefai HA, Meziani F, Martínez MC, Asfar P, Andriantsitohaina R. Circulating microparticles from septic shock patients exert differential tissue expression of enzymes related to inflammation and oxidative stress. Crit Care Med. 2011;39(7):1739-48.
255. Ochs HD, Notarangelo LD. Structure and function of the Wiskott-Aldrich syndrome protein. Curr Opin Hematol. 2005;12(4):284-91.
256. Shcherbina A, Rosen FS, Remold-O'Donnell E. Pathological events in platelets of Wiskott-Aldrich syndrome patients. Br J Haematol. 1999;106(4):875-83.
257. Maurer-Spurej E, Chipperfield K. Could Microparticles Be the Universal Quality Indicator for Platelet Viability and Function? J Blood Transfus. 2016;2016:6140239.
258. Maurer-Spurej E, Larsen R, Labrie A, Heaton A, Chipperfield K. Microparticle content of platelet concentrates is predicted by donor microparticles and is altered by production methods and stress. Transfus Apher Sci. 2016;55(1):35-43.
259. Millar D, Murphy L, Labrie A, Maurer-Spurej E. Routine Screening Method for Microparticles in Platelet Transfusions. J Vis Exp. 2018(131).
260. Sossdorf M, Otto GP, Claus RA, Gabriel HH, Lösche W. Cell-derived microparticles promote coagulation after moderate exercise. Med Sci Sports Exerc. 2011;43(7):1169-76.
261. Burnouf T, Chou ML, Goubran H, Cognasse F, Garraud O, Seghatchian J. An overview of the role of microparticles/microvesicles in blood components: Are they clinically beneficial or harmful? Transfus Apher Sci. 2015;53(2):137-45.
262. Flaumenhaft R, Dilks JR, Richardson J, Alden E, Patel-Hett SR, Battinelli E, et al. Megakaryocyte-derived microparticles: direct visualization and distinction from platelet-derived microparticles. Blood. 2009;113(5):1112-21.
263. Noulsri E, Udomwinijsilp P, Lerdwana S, Chongkolwatana V, Permpikul P. Differences in levels of platelet-derived microparticles in platelet components prepared using the platelet rich plasma, buffy coat, and apheresis procedures. Transfus Apher Sci. 2017;56(2):135-40.
264. Federici AB, Vanelli C, Arrigoni L. Transfusion issues in cancer patients. Thromb Res. 2012;129 Suppl 1:S60-5.
265. Wysoczynski M, Ratajczak MZ. Lung cancer secreted microvesicles: underappreciated modulators of microenvironment in expanding tumors. Int J Cancer. 2009;125(7):1595-603.
266. Marcoux G, Duchez AC, Rousseau M, Lévesque T, Boudreau LH, Thibault L, et al. Microparticle and mitochondrial release during extended storage of different types of platelet concentrates. Platelets. 2017;28(3):272-80.
267. Chen Z, Schubert P, Bakkour S, Culibrk B, Busch MP, Devine DV. p38 mitogen-activated protein kinase regulates mitochondrial function and microvesicle release in riboflavin- and ultraviolet light-treated apheresis platelet concentrates. Transfusion. 2017;57(5):1199-207.
268. Marcoux G, Magron A, Sut C, Laroche A, Laradi S, Hamzeh-Cognasse H, et al. Platelet-derived extracellular vesicles convey mitochondrial DAMPs in platelet concentrates and their levels are associated with adverse reactions. Transfusion. 2019;59(7):2403-14.
269. Khorana AA, Francis CW, Blumberg N, Culakova E, Refaai MA, Lyman GH. Blood transfusions, thrombosis, and mortality in hospitalized patients with cancer. Arch Intern Med. 2008;168(21):2377-81.
270. Blajchman MA. Substitutes and alternatives to platelet transfusions in thrombocytopenic patients. J Thromb Haemost. 2003;1(7):1637-41.
271. Nasiri S. Infusible platelet membrane as a platelet substitute for transfusion: an overview. Blood Transfus. 2013;11(3):337-42.
272. Chao FC, Kim BK, Houranieh AM, Liang FH, Konrad MW, Swisher SN, et al. Infusible platelet membrane microvesicles: a potential transfusion substitute for platelets. Transfusion. 1996;36(6):536-42.
273. McGill M, Fugman DA, Vittorio N, Darrow C. Platelet membrane vesicles reduced microvascular bleeding times in thrombocytopenic rabbits. J Lab Clin Med. 1987;109(2):127-33.
274. Nasiri S, Mousavi Hosseini K. Infusible Platelet Membrane versus Conventional

Platelet Concentrate: Benefits and Disadvantages. Iranian Journal of Blood and Cancer. 2013;6(2):87-93.
275. Services UKB. H**andbook of Transfusion Medicine** Joint United Kingdom (UK) Blood Transfusion and Tissue Transplantation Services Professional Advisory Committee: TSO; 2014.
276. Saunders C, Rowe G, Wilkins K, Collins P. Impact of glucose and acetate on the characteristics of the platelet storage lesion in platelets suspended in additive solutions with minimal plasma. Vox Sang. 2013;105(1):1-10.
277. Saunders C, Rowe G, Wilkins K, Holme S, Collins P. In vitro storage characteristics of platelet concentrates suspended in 70% SSP+(TM) additive solution versus plasma over a 14-day storage period. Vox Sang. 2011;101(2):112-21.
278. Cardinal DC, Flower RJ. The electronic aggregometer: a novel device for assessing platelet behavior in blood. Journal of pharmacological methods. 1980;3(2):135-58.
279. Schmidt DE, Bruzelius M, Majeed A, Odeberg J, Holmström M, Ågren A. Whole blood ristocetin-activated platelet impedance aggregometry (Multiplate) for the rapid detection of Von Willebrand disease. Thromb Haemost. 2017;117(8):1528-33.
280. Lucchetti D, Battaglia A, Ricciardi-Tenore C, Colella F, Perelli L, De Maria R, et al. Measuring Extracellular Vesicles by Conventional Flow Cytometry: Dream or Reality? Int J Mol Sci. 2020;21(17).
281. Bohren CF, Hoffmann DR. Particles Small Compared with the Wavelength. Absorption and Scattering of Light by Small Particles1998. p. 130-57.
282. Newton I. Opticks: or, A Treatise of the Reflexions, Refractions, Inflexions and Colours of Light 1704.
283. Gardiner C, Shaw M, Hole P, Smith J, Tannetta D, Redman CW, et al. Measurement of refractive index by nanoparticle tracking analysis reveals heterogeneity in extracellular vesicles. J Extracell Vesicles. 2014;3:25361.
284. Presley T, Kuppusamy P, Zweier JL, Ilangovan G. Electron paramagnetic resonance oximetry as a quantitative method to measure cellular respiration: a consideration of oxygen diffusion interference. Biophysical journal. 2006;91(12):4623-31.
285. Weaver JM, Liu KJ. In vivo electron paramagnetic resonance oximetry and applications in the brain. Med Gas Res. 2017;7(1):56-67.
286. Ahmad R, Kuppusamy P. Theory, instrumentation, and applications of electron paramagnetic resonance oximetry. Chem Rev. 2010;110(5):3212-36.
287. Belkin S, Mehlhorn RJ, Packer L. Determination of dissolved oxygen in photosynthetic systems by nitroxide spin-probe broadening. Arch Biochem Biophys. 1987;252(2):487-95.
288. Sarna T, Duleba A, Korytowski W, Swartz H. Interaction of melanin with oxygen. Arch Biochem Biophys. 1980;200(1):140-8.
289. Connolly KD, Guschina IA, Yeung V, Clayton A, Draman MS, Von Ruhland C, et al. Characterisation of adipocyte-derived extracellular vesicles released pre- and post-adipogenesis. J Extracell Vesicles. 2015;4:29159.
290. Dragovic RA, Gardiner C, Brooks AS, Tannetta DS, Ferguson DJ, Hole P, et al. Sizing and phenotyping of cellular vesicles using Nanoparticle Tracking Analysis. Nanomedicine : nanotechnology, biology, and medicine. 2011;7(6):780-8.
291. Saveyn H, De Baets B, Thas O, Hole P, Smith J, Van der Meeren P. Accurate particle size distribution determination by nanoparticle tracking analysis based on 2-D Brownian dynamics simulation. Journal of Colloid and Interface Science. 2010;352(2):593-600.
292. Carter AM, Cymbalista CM, Spector TD, Grant PJ, Investigators E. Heritability of clot formation, morphology, and lysis: the EuroCLOT study. Arterioscler Thromb Vasc Biol. 2007;27(12):2783-9.
293. J. O. Williams, C Whelan, J Nash, James. PE. Extracellular Vesicles in Atherosclerosis Research. Atherosclerosis. Atherosclerosis,In Press - 2021.
294. Chaudhary R, Dubey A, Sonker A. Techniques used for the screening of hemoglobin levels in blood donors: current insights and future directions. J Blood Med. 2017;8:75-88.

295. Deng ZB, Poliakov A, Hardy RW, Clements R, Liu C, Liu Y, et al. Adipose tissue exosome-like vesicles mediate activation of macrophage-induced insulin resistance. Diabetes. 2009;58(11):2498-505.
296. Zaldivia MTK, McFadyen JD, Lim B, Wang X, Peter K. Platelet-Derived Microvesicles in Cardiovascular Diseases. 2017;4(74).
297. Thangaraju K, Neerukonda SN, Katneni U, Buehler PW. Extracellular Vesicles from Red Blood Cells and Their Evolving Roles in Health, Coagulopathy and Therapy. International journal of molecular sciences. 2020;22(1):153.
298. Matsumoto A, Takahashi Y, Ogata K, Kitamura S, Nakagawa N, Yamamoto A, et al. Phosphatidylserine-deficient small extracellular vesicle is a major somatic cell-derived sEV subpopulation in blood. iScience. 2021;24(8):102839.
299. Kolonics F, Kajdácsi E, Farkas VJ, Veres DS, Khamari D, Kittel Á, et al. Neutrophils produce proinflammatory or anti-inflammatory extracellular vesicles depending on the environmental conditions. 2021;109(4):793-806.
300. Mörtberg J, Lundwall K, Mobarrez F, Wallén H, Jacobson SH, Spaak J. Increased concentrations of platelet- and endothelial-derived microparticles in patients with myocardial infarction and reduced renal function- a descriptive study. BMC Nephrology. 2019;20(1):71.
301. Williams JO, Watkeys L, Nash J, Whelan C, Davies AJ, Evans J, et al. A Two-Phase, Single Cohort Study of COVID-19 Antibody Sera-Surveillance. . A Epidemiol Public Health.2021.
302. NHS. Haematology Reference Ranges Gloucestershire NHS Foundation Trust 2022 [updated 2021. Available from: https://www.gloshospitals.nhs.uk/our-services/services-we-offer/pathology/haematology/haematology-reference-ranges/.
303. Fiedler SA, Boller K, Junker AC, Kamp C, Hilger A, Schwarz W, et al. Evaluation of the in vitro Function of Platelet Concentrates from Pooled Buffy Coats or Apheresis. Transfusion Medicine and Hemotherapy. 2020;47(4):314-25.
304. Reddoch KM, Pidcoke HF, Montgomery RK, Fedyk CG, Aden JK, Ramasubramanian AK, et al. Hemostatic function of apheresis platelets stored at 4°C and 22°C. Shock (Augusta, Ga). 2014;41 Suppl 1(0 1):54-61.
305. Schlagenhauf A, Kozma N, Leschnik B, Wagner T, Muntean W. Thrombin receptor levels in platelet concentrates during storage and their impact on platelet functionality. Transfusion. 2012;52(6):1253-9.
306. Jin J, Kunapuli SP. Coactivation of two different G protein-coupled receptors is essential for ADP-induced platelet aggregation. Proc Natl Acad Sci U S A. 1998;95(14):8070-4.
307. Baurand A, Eckly A, Bari N, Léon C, Hechler B, Cazenave JP, et al. Desensitization of the platelet aggregation response to ADP: differential down-regulation of the P2Y1 and P2cyc receptors. Thromb Haemost. 2000;84(3):484-91.
308. de Korte D, Gouwerok CW, Fijnheer R, Pietersz RN, Roos D. Depletion of dense granule nucleotides during storage of human platelets. Thromb Haemost. 1990;63(2):275-8.
309. Fisk J, Pisciotto P, Snyder E, Perrotta P. Blood Banking and Transfusion Medicine. 2007.
310. Koessler J, Hermann S, Weber K, Koessler A, Kuhn S, Boeck M, et al. Role of Purinergic Receptor Expression and Function for Reduced Responsiveness to Adenosine Diphosphate in Washed Human Platelets. PLOS ONE. 2016;11(1):e0147370.
311. Keuren JFW, Cauwenberghs S, Heeremans J, De Kort W, Heemskerk JWM, Curvers J. Platelet ADP response deteriorates in synthetic storage media. 2006;46(2):204-12.
312. Prudova A, Serrano K, Eckhard U, Fortelny N, Devine DV, Overall CM. TAILS N-terminomics of human platelets reveals pervasive metalloproteinase-dependent proteolytic processing in storage. Blood. 2014;124(26):e49-60.
313. Michelson AD, Adelman B, Barnard MR, Carroll E, Handin RI. Platelet storage results in a redistribution of glycoprotein Ib molecules. Evidence for a large intraplatelet pool of glycoprotein Ib. J Clin Invest. 1988;81(6):1734-40.

314. Prudova A, Serrano K, Eckhard U, Fortelny N, Devine DV, Overall CM. TAILS N-terminomics of human platelets reveals pervasive metalloproteinase-dependent proteolytic processing in storage. Blood. 2014;124(26):e49-e60.
315. Shen L, Yang T, Xia K, Yan Z, Tan J, Li L, et al. P-selectin (CD62P) and soluble TREM-like transcript-1 (sTLT-1) are associated with coronary artery disease: a case control study. BMC Cardiovascular Disorders. 2020;20(1):387.
316. Morel A, Rywaniak J, Bijak M, Miller E, Niwald M, Saluk J. Flow cytometric analysis reveals the high levels of platelet activation parameters in circulation of multiple sclerosis patients. Mol Cell Biochem. 2017;430(1-2):69-80.
317. Griesshammer M, Beneke H, Nussbaumer B, Grünewald M, Bangerter M, Bergmann L. Increased platelet surface expression of P-selectin and thrombospondin as markers of platelet activation in essential thrombocythaemia. Thromb Res. 1999;96(3):191-6.
318. Choudhury A, Chung I, Blann AD, Lip GYH. Platelet Surface CD62P and CD63, Mean Platelet Volume, and Soluble/Platelet P-Selectin as Indexes of Platelet Function in Atrial Fibrillation: A Comparison of “Healthy Control Subjects” and “Disease Control Subjects” in Sinus Rhythm. Journal of the American College of Cardiology. 2007;49(19):1957-64.
319. Lu Q, Malinauskas RA. Comparison of two platelet activation markers using flow cytometry after in vitro shear stress exposure of whole human blood. Artificial organs. 2011;35(2):137-44.
320. Holcar M, Ferdin J, Sitar S, Tušek-Žnidarič M, Dolžan V, Plemenitaš A, et al. Enrichment of plasma extracellular vesicles for reliable quantification of their size and concentration for biomarker discovery. Scientific Reports. 2020;10(1):21346.
321. Palviainen M, Saraswat M, Varga Z, Kitka D, Neuvonen M, Puhka M, et al. Extracellular vesicles from human plasma and serum are carriers of extravesicular cargo—Implications for biomarker discovery. PLOS ONE. 2020;15(8):e0236439.
322. Coumans FAW, Brisson AR, Buzas EI, Dignat-George F, Drees EEE, El-Andaloussi S, et al. Methodological Guidelines to Study Extracellular Vesicles. 2017;120(10):1632-48.
323. Johnsen KB, Gudbergsson JM, Andresen TL, Simonsen JB. What is the blood concentration of extracellular vesicles? Implications for the use of extracellular vesicles as blood-borne biomarkers of cancer. Biochimica et Biophysica Acta (BBA) - Reviews on Cancer. 2019;1871(1):109-16.
324. Ali SF. Platelet Activation in Stored Platelet Concentrates: Comparison of Two Methods Preparation2012.
325. Wagner SJ, Hapip CA, Turgeon A, Abel L, Kaelber N. Influence of apheresis collection device and container on the storage properties of platelets in 90% PAS-5/10% plasma. Blood transfusion = Trasfusione del sangue. 2019;17(3):210-6.
326. Tripisciano C, Weiss R, Karuthedom George S, Fischer MB, Weber V. Extracellular Vesicles Derived From Platelets, Red Blood Cells, and Monocyte-Like Cells Differ Regarding Their Ability to Induce Factor XII-Dependent Thrombin Generation. 2020;8.
327. Tripisciano C, Weiss R, Karuthedom George S, Fischer MB, Weber V. Extracellular Vesicles Derived From Platelets, Red Blood Cells, and Monocyte-Like Cells Differ Regarding Their Ability to Induce Factor XII-Dependent Thrombin Generation. Frontiers in cell and developmental biology. 2020;8:298-.
328. Whelan C, Burnley-Hall N, Morris K, Rees DA, James PE. The procoagulant effects of extracellular vesicles derived from hypoxic endothelial cells can be selectively inhibited by inorganic nitrite. Nitric Oxide. 2022;122-123:6-18.
329. Jayasena T, Poljak A, Braidy N, Zhong L, Rowlands B, Muenchhoff J, et al. Application of Targeted Mass Spectrometry for the Quantification of Sirtuins in the Central Nervous System. Scientific Reports. 2016;6(1):35391.
330. Italiano JE, Jr., Mairuhu ATA, Flaumenhaft R. Clinical relevance of microparticles from platelets and megakaryocytes. Current opinion in hematology. 2010;17(6):578-84.
331. Giacomazzi A, Degan M, Calabria S, Meneguzzi A, Minuz P. Antiplatelet Agents Inhibit the Generation of Platelet-Derived Microparticles. Frontiers in pharmacology. 2016;7:314.

332. Catalano M, O'Driscoll L. Inhibiting extracellular vesicles formation and release: a review of EV inhibitors. Journal of extracellular vesicles. 2019;9(1):1703244-.
333. Kosgodage US, Trindade RP, Thompson PR, Inal JM, Lange S. Chloramidine/Bisindolylmaleimide-I-Mediated Inhibition of Exosome and Microvesicle Release and Enhanced Efficacy of Cancer Chemotherapy. International journal of molecular sciences. 2017;18(5):1007.
334. Valeri CR. Circulation and Hemostatic Effectiveness of Platelets Stored at 4 C or 22 C. 1976;16(1):20-3.
335. Exceptions and Alternative Procedures Approved Under 21 CFR 640.120(a), (2022).
336. Braathen H, Sivertsen J, Lunde THF, Kristoffersen EK, Assmus J, Hervig TA, et al. In vitro quality and platelet function of cold and delayed cold storage of apheresis platelet concentrates in platelet additive solution for 21 days. 2019;59(8):2652-61.
337. Lee JH, Jung H, Song J, Choi ES, You G, Mok H. Activated Platelet-Derived Vesicles for Efficient Hemostatic Activity. Macromolecular bioscience. 2020;20(3):e1900338.
338. Lopez E, Srivastava AK, Burchfield J, Wang YW, Cardenas JC, Togarrati PP, et al. Platelet-derived- Extracellular Vesicles Promote Hemostasis and Prevent the Development of Hemorrhagic Shock. Sci Rep. 2019;9(1):17676.
339. Miyazawa B, Trivedi A, Togarrati PP, Potter D, Baimukanova G, Vivona L, et al. Regulation of endothelial cell permeability by platelet-derived extracellular vesicles. J Trauma Acute Care Surg. 2019;86(6):931-42.
340. Hegde S, Akbar H, Zheng Y, Cancelas JA. Towards increasing shelf life and haemostatic potency of stored platelet concentrates. Curr Opin Hematol. 2018;25(6):500-8.
341. Hegde S, Wellendorf AM, Zheng Y, Cancelas JA. Antioxidant prevents clearance of hemostatically competent platelets after long-term cold storage. Transfusion. 2021;61(2):557-67.
342. NasrEldin E. Effect of cold storage on platelets quality stored in a small containers: Implications for pediatric transfusion. Pediatric Hematology Oncology Journal. 2017;2(2):29-34.
343. Sandgren P, Hansson M, Gulliksson H, Shanwell A. Storage of buffy-coat-derived platelets in additive solutions at 4 degrees C and 22 degrees C: flow cytometry analysis of platelet glycoprotein expression. Vox Sang. 2007;93(1):27-36.
344. Kerris EWJ, Hoptay C, Calderon T, Freishtat RJ. Platelets and platelet extracellular vesicles in hemostasis and sepsis. 2020;68(4):813-20.
345. White JG, Krivit W. An ultrastructural basis for the shape changes induced in platelets by chilling. Blood. 1967;30(5):625-35.
346. White JG. Effects of colchicine and Vinca alkaloids on human platelets. I. Influence on platelet microtubules and contractile function. Am J Pathol. 1968;53(2):281-91.
347. Tolias KF, Hartwig JH, Ishihara H, Shibasaki Y, Cantley LC, Carpenter CL. Type Iα phosphatidylinositol-4-phosphate 5-kinase mediates Rac-dependent actin assembly. Current Biology. 2000;10(3):153-6.
348. Hoffmeister KM, Falet H, Toker A, Barkalow KL, Stossel TP, Hartwig JH. Mechanisms of Cold-induced Platelet Actin Assembly*. Journal of Biological Chemistry. 2001;276(27):24751-9.
349. Xiang B, Zhang G, Zhang Y, Wu C, Joshi S, Morris AJ, et al. Calcium Ion Chelation Preserves Platelet Function During Cold Storage. Arteriosclerosis, Thrombosis, and Vascular Biology. 2021;41(1):234-49.
350. Sinauridze EI, Kireev DA, Popenko NY, Pichugin AV, Panteleev MA, Krymskaya OV, et al. Platelet microparticle membranes have 50- to 100-fold higher specific procoagulant activity than activated platelets. Thromb Haemost. 2007;97(3):425-34.
351. Zhao H, Devine DV. The Missing Pieces to the Cold-Stored Platelet Puzzle. 2022;23(3):1100.
352. Stolla M, Bailey SL, Fang L, Fitzpatrick L, Gettinger I, Pellham E, et al. Effects of storage time prolongation on in vivo and in vitro characteristics of 4°C-stored platelets. Transfusion. 2020;60(3):613-21.

353. Six KR, Devloo R, Compernolle V, Feys HB. Impact of cold storage on platelets treated with Intercept pathogen inactivation. 2019;59(8):2662-71.
354. Six KR, Compernolle V, Feys HBJAoB. When platelets are left in the cold. 2020. 2020;5.
355. ZUCKER MB, BORRELLI J. Reversible alterations in platelet morphology produced by anticoagulants and by cold. Blood. 1954;9(6):602-8.
356. Kornblith LZ, Robles AJ, Conroy AS, Hendrickson CM, Calfee CS, Fields AT, et al. Perhaps it's not the platelet: Ristocetin uncovers the potential role of von Willebrand factor in impaired platelet aggregation following traumatic brain injury. J Trauma Acute Care Surg. 2018;85(5):873-80.
357. Montgomery RK, Reddoch KM, Evani SJ, Cap AP, Ramasubramanian AK. Enhanced shear-induced platelet aggregation due to low-temperature storage. Transfusion. 2013;53(7):1520-30.
358. Jansen AJ, Josefsson EC, Rumjantseva V, Liu QP, Falet H, Bergmeier W, et al. Desialylation accelerates platelet clearance after refrigeration and initiates GPIbα metalloproteinase-mediated cleavage in mice. Blood. 2012;119(5):1263-73.
359. Sandgren P, Shanwell A, Gulliksson H. Storage of buffy coat–derived platelets in additive solutions: in vitro effects of storage at 4°C. 2006;46(5):828-34.
360. Gulliksson H. Defining the optimal storage conditions for the long-term storage of platelets. Transfus Med Rev. 2003;17(3):209-15.
361. Vinay P, Cardoso M, Tejedor A, Prud'homme M, Levelillee M, Vinet B, et al. Acetate metabolism during hemodialysis: metabolic considerations. Am J Nephrol. 1987;7(5):337-54.
362. Richards RH, Vreman HJ, Zager P, Feldman C, Blaschke T, Weiner MW. Acetate Metabolism in Normal Human Subjects. American Journal of Kidney Diseases. 1982;2(1):47-57.
363. Wallvik J, Akerblom O. Platelet concentrates stored at 22 degrees C need oxygen. The significance of plastics in platelet preservation. Vox Sang. 1983;45(4):303-11.
364. McKeown SR. Defining normoxia, physoxia and hypoxia in tumours-implications for treatment response. Br J Radiol. 2014;87(1035):20130676.
365. Höckel M, Vaupel P. Tumor hypoxia: definitions and current clinical, biologic, and molecular aspects. J Natl Cancer Inst. 2001;93(4):266-76.
366. Parrinello S, Samper E, Krtolica A, Goldstein J, Melov S, Campisi J. Oxygen sensitivity severely limits the replicative lifespan of murine fibroblasts. Nat Cell Biol. 2003;5(8):741-7.
367. Eliasson P, Rehn M, Hammar P, Larsson P, Sirenko O, Flippin LA, et al. Hypoxia mediates low cell-cycle activity and increases the proportion of long-term-reconstituting hematopoietic stem cells during in vitro culture. Exp Hematol. 2010;38(4):301-10.e2.
368. Kanias T, Acker JP. Biopreservation of red blood cells--the struggle with hemoglobin oxidation. The FEBS journal. 2010;277(2):343-56.
369. Bosman GJ, Lasonder E, Luten M, Roerdinkholder-Stoelwinder B, Novotný VM, Bos H, et al. The proteome of red cell membranes and vesicles during storage in blood bank conditions. Transfusion. 2008;48(5):827-35.
370. D'Alessandro A, D'Amici GM, Vaglio S, Zolla L. Time-course investigation of SAGM-stored leukocyte-filtered red bood cell concentrates: from metabolism to proteomics. Haematologica. 2012;97(1):107-15.
371. Roussel C, Dussiot M, Marin M, Morel A, Ndour PA, Duez J, et al. Spherocytic shift of red blood cells during storage provides a quantitative whole cell-based marker of the storage lesion. Transfusion. 2017;57(4):1007-18.
372. Yoshida T, Prudent M, D'Alessandro A. Red blood cell storage lesion: causes and potential clinical consequences. Blood Transfus. 2019;17(1):27-52.
373. Yoshida T, Shevkoplyas SS. Anaerobic storage of red blood cells. Blood Transfus. 2010;8(4):220-36.
374. Dumont LJ, D'Alessandro A, Szczepiorkowski ZM, Yoshida T. CO2 -dependent metabolic modulation in red blood cells stored under anaerobic conditions. Transfusion. 2016;56(2):392-403.

375. D'Alessandro A, Yoshida T, Nestheide S, Nemkov T, Stocker S, Stefanoni D, et al. Hypoxic storage of red blood cells improves metabolism and post-transfusion recovery. Transfusion. 2020;60(4):786-98.
376. Steinlechner-Maran R, Eberl T, Kunc M, Margreiter R, Gnaiger E. Oxygen dependence of respiration in coupled and uncoupled endothelial cells. The American journal of physiology. 1996;271(6 Pt 1):C2053-61.
377. Torres R, Tormey C. Modeling Gas Exchange During Platelet Storage. American Journal of Clinical Pathology. 2014;142(suppl_1):A006-A.
378. Wilson DF, Erecińska M, Drown C, Silver IA. Effect of oxygen tension on cellular energetics. The American journal of physiology. 1977;233(5):C135-40.
379. Baccarelli AA, Byun H-M. Platelet mitochondrial DNA methylation: a potential new marker of cardiovascular disease. Clinical Epigenetics. 2015;7(1):44.
380. Melchinger H, Jain K, Tyagi T, Hwa J. Role of Platelet Mitochondria: Life in a Nucleus-Free Zone. 2019;6.
381. Diab YA, Thomas A, Luban NLC, Wong ECC, Wagner SJ, Levy RJ. Acquired cytochrome C oxidase impairment in apheresis platelets during storage: a possible mechanism for depletion of metabolic adenosine triphosphate. 2012;52(5):1024-30.
382. Tripisciano C, Weiss R, Karuthedom George S, Fischer MB, Weber V. Extracellular Vesicles Derived From Platelets, Red Blood Cells, and Monocyte-Like Cells Differ Regarding Their Ability to Induce Factor XII-Dependent Thrombin Generation. 2020;8(298).
383. Spakova T, Janockova J, Rosocha J. Characterization and Therapeutic Use of Extracellular Vesicles Derived from Platelets. 2021;22(18):9701.
384. Keeley TP, Mann GE. Defining Physiological Normoxia for Improved Translation of Cell Physiology to Animal Models and Humans. 2019;99(1):161-234.
385. Kiouptsi K, Gambaryan S, Walter E, Walter U, Jurk K, Reinhardt C. Hypoxia impairs agonist-induced integrin αIIbβ3 activation and platelet aggregation. Scientific Reports. 2017;7(1):7621.
386. Al-Ani A, Toms D, Kondro D, Thundathil J, Yu Y, Ungrin M. Oxygenation in cell culture: Critical parameters for reproducibility are routinely not reported. PLOS ONE. 2018;13(10):e0204269.
387. Randers-Eichhorn L, Bartlett RA, Frey DD, Rao G. Noninvasive oxygen measurements and mass transfer considerations in tissue culture flasks. Biotechnology and bioengineering. 1996;51(4):466-78.
388. Hayashi T, Tanaka S, Hori Y, Hirayama F, Sato EF, Inoue M. Role of mitochondria in the maintenance of platelet function during in vitro storage. 2011;21(3):166-74.
389. Levitt DG. Capillary-tissue exchange kinetics: an analysis of the Krogh cylinder model. Journal of theoretical biology. 1972;34(1):103-24.
390. Hanson SR, Slichter SJ. Platelet kinetics in patients with bone marrow hypoplasia: evidence for a fixed platelet requirement. Blood. 1985;66(5):1105-9.
391. Tinmouth AT, Freedman J. Prophylactic platelet transfusions: which dose is the best dose? A review of the literature. Transfus Med Rev. 2003;17(3):181-93.
392. Tinmouth A, Tannock IF, Crump M, Tomlinson G, Brandwein J, Minden M, et al. Low-dose prophylactic platelet transfusions in recipients of an autologous peripheral blood progenitor cell transplant and patients with acute leukemia: a randomized controlled trial with a sequential Bayesian design. 2004;44(12):1711-9.
393. Heddle NM, Cook RJ, Tinmouth A, Kouroukis CT, Hervig T, Klapper E, et al. A randomized controlled trial comparing standard- and low-dose strategies for transfusion of platelets (SToP) to patients with thrombocytopenia. Blood. 2009;113(7):1564-73.
394. Slichter SJ, Kaufman RM, Assmann SF, McCullough J, Triulzi DJ, Strauss RG, et al. Dose of prophylactic platelet transfusions and prevention of hemorrhage. The New England journal of medicine. 2010;362(7):600-13.
395. Manasa K, Vani R. Influence of Oxidative Stress on Stored Platelets. Adv Hematol. 2016;2016:4091461.

396. Oller AR, Buser CW, Tyo MA, Thilly WG. Growth of mammalian cells at high oxygen concentrations. J Cell Sci. 1989;94 (Pt 1):43-9.
397. Freeman BA, Topolosky MK, Crapo JD. Hyperoxia increases oxygen radical production in rat lung homogenates. Arch Biochem Biophys. 1982;216(2):477-84.
398. Huang D, Ou B, Prior RL. The Chemistry behind Antioxidant Capacity Assays. Journal of agricultural and food chemistry. 2005;53(6):1841-56.
399. Huang D, Ou B, Hampsch-Woodill M, Flanagan JA, Prior RL. High-throughput assay of oxygen radical absorbance capacity (ORAC) using a multichannel liquid handling system coupled with a microplate fluorescence reader in 96-well format. Journal of agricultural and food chemistry. 2002;50(16):4437-44.
400. Torres R, Tormey CA. Modelling gas exchange during platelet storage without agitation. Vox Sanguinis. 2016;111(4):445-8.
401. Dekkers DW, De Cuyper IM, van der Meer PF, Verhoeven AJ, de Korte D. Influence of pH on stored human platelets. Transfusion. 2007;47(10):1889-95.
402. Torres R, Tormey CA, Stack G. Fluid motion and shear forces in platelet storage bags with different modes of agitation. Vox sanguinis. 2016;111(2):209-12.
403. Kroll MH, Hellums JD, McIntire LV, Schafer AI, Moake JL. Platelets and shear stress. Blood. 1996;88(5):1525-41.
404. van Hout FMA, Bontekoe IJ, de Laleijne LAE, Kerkhoffs JL, de Korte D, Eikenboom J, et al. Comparison of haemostatic function of PAS-C–platelets vs. plasma–platelets in reconstituted whole blood using impedance aggregometry and thromboelastography. Vox Sanguinis. 2017;112(6):549-56.
405. Chacko Balu K, Kramer Philip A, Ravi S, Benavides Gloria A, Mitchell T, Dranka Brian P, et al. The Bioenergetic Health Index: a new concept in mitochondrial translational research. Clinical Science. 2014;127(6):367-73.
406. Hill BG, Benavides GA, Lancaster JR, Jr., Ballinger S, Dell'Italia L, Jianhua Z, et al. Integration of cellular bioenergetics with mitochondrial quality control and autophagy. Biological chemistry. 2012;393(12):1485-512.
407. Dranka BP, Hill BG, Darley-Usmar VM. Mitochondrial reserve capacity in endothelial cells: The impact of nitric oxide and reactive oxygen species. Free Radic Biol Med. 2010;48(7):905-14.
408. Chiaradia E, Tancini B, Emiliani C, Delo F, Pellegrino RM, Tognoloni A, et al. Extracellular Vesicles under Oxidative Stress Conditions: Biological Properties and Physiological Roles. Cells. 2021;10(7):1763.
409. Handin RI, Karabin R, Boxer GJ. Enhancement of platelet function by superoxide anion. J Clin Invest. 1977;59(5):959-65.
410. Freedman JE. Oxidative Stress and Platelets. Arteriosclerosis, Thrombosis, and Vascular Biology. 2008;28(3):s11-s6.
411. Leytin V, Allen DJ, Mutlu A, Gyulkhandanyan AV, Mykhaylov S, Freedman J. Mitochondrial control of platelet apoptosis: effect of cyclosporin A, an inhibitor of the mitochondrial permeability transition pore. Laboratory Investigation. 2009;89(4):374-84.
412. Fuentes E, Moore-Carrasco R, de Andrade Paes AM, Trostchansky A. Role of Platelet Activation and Oxidative Stress in the Evolution of Myocardial Infarction. Journal of Cardiovascular Pharmacology and Therapeutics. 2019;24(6):509-20.
413. Schwaller J. Novel insights into the role of aberrantly expressed MNX1 (HLXB9) in infant acute myeloid leukemia. Haematologica. 2019;104(1):1-3.
414. Brill A, Chauhan AK, Canault M, Walsh MT, Bergmeier W, Wagner DD. Oxidative stress activates ADAM17/TACE and induces its target receptor shedding in platelets in a p38-dependent fashion. Cardiovascular research. 2009;84(1):137-44.
415. Masselli E, Pozzi G, Vaccarezza M, Mirandola P, Galli D, Vitale M, et al. ROS in Platelet Biology: Functional Aspects and Methodological Insights. International journal of molecular sciences. 2020;21(14):4866.

416. Wang L, Xie R, Fan Z, Yang J, Liang W, Wu Q, et al. The contribution of oxidative stress to platelet senescence during storage. Transfusion. 2019;59(7):2389-402.
417. Blake JT. Determining the inventory impact of extended-shelf-life platelets with a network simulation model. Transfusion. 2017;57(12):3001-8.
418. Price J, Gardiner C, Harrison P. Platelet-enhanced plasma: Characterization of a novel candidate resuscitation fluid's extracellular vesicle content, clotting parameters, and thrombin generation capacity. Transfusion. 2021;61(7):2179-94.
419. Sandgren P, Callaert M, Shanwell A, Gulliksson H. Storage of platelet concentrates from pooled buffy coats made of fresh and overnight-stored whole blood processed on the novel Atreus 2C+ system: in vitro study. Transfusion. 2008;48(4):688-96.
420. Saunders C, Rowe G, Wilkins K, Holme S, Collins P. In vitro storage characteristics of platelet concentrates suspended in 70% SSP+TM additive solution versus plasma over a 14-day storage period. Vox Sanguinis. 2011;101(2):112-21.
421. Hall S, Murphy MF. Limitations of component therapy for massive haemorrhage: is whole blood the whole solution? Anaesthesia. 2015;70(5):511-4.
422. Seheult JN, Stram MN, Sperry J, Spinella PC, Triulzi DJ, Yazer MH. In silico model of the dilutional effects of conventional component therapy versus whole blood in the management of massively bleeding adult trauma patients. Transfusion. 2019;59(1):146-58.
423. Straat M, Böing AN, Tuip-De Boer A, Nieuwland R, Juffermans NP. Extracellular Vesicles from Red Blood Cell Products Induce a Strong Pro-Inflammatory Host Response, Dependent on Both Numbers and Storage Duration. Transfusion Medicine and Hemotherapy. 2016;43(4):302-5.
424. Almizraq RJ, Holovati JL, Acker JP. Characteristics of Extracellular Vesicles in Red Blood Concentrates Change with Storage Time and Blood Manufacturing Method. Transfusion Medicine and Hemotherapy. 2018;45(3):185-93.
425. Helmi Siasi N, Deyhim MR, Amiri F, Amini Kafiabad S. The antioxidant impact of the L-carnitine (LC) in platelet concentrates during storage %J The Scientific Journal of Iranian Blood Transfusion Organization. 2017;14(3):175-87.
426. Eligini S, Porro B, Aldini G, Colli S, Banfi C. N-Acetylcysteine Inhibits Platelet Function through the Regeneration of the Non-Oxidative Form of Albumin. Antioxidants (Basel). 2022;11(3).
427. Lee HJ, Oh SH, Jo SY, Kim IS. Platelet Inventory Management Program: Development and Practical Experience. Annals of laboratory medicine. 2021;41(1):95-100.
428. Wood B, Johnson L, Hyland RA, Marks DC. Maximising platelet availability by delaying cold storage. 2018;113(5):403-11.
429. Braathen H, Sivertsen J, Lunde THF, Kristoffersen EK, Assmus J, Hervig TA, et al. In vitro quality and platelet function of cold and delayed cold storage of apheresis platelet concentrates in platelet additive solution for 21 days. Transfusion. 2019;59(8):2652-61.
430. Dyer MR, Alexander W, Hassoune A, Chen Q, Brzoska T, Alvikas J, et al. Platelet-derived extracellular vesicles released after trauma promote hemostasis and contribute to DVT in mice. Journal of thrombosis and haemostasis : JTH. 2019;17(10):1733-45.
431. Kang M, Jordan V, Blenkiron C, Chamley LW. Biodistribution of extracellular vesicles following administration into animals: A systematic review. Journal of Extracellular Vesicles. 2021;10(8):e12085.
432. Wirtz MR, Jurgens J, Zuurbier CJ, Roelofs JJTH, Spinella PC, Muszynski JA, et al. Washing or filtering of blood products does not improve outcome in a rat model of trauma and multiple transfusion. Transfusion. 2019;59(1):134-45.
433. Cognasse F, Hally K, Fauteux-Daniel S, Eyraud M-A, Arthaud C-A, Fagan J, et al. Effects and Side Effects of Platelet Transfusion. Hamostaseologie. 2021;41(02):128-35.
434. Zhang Y, Jiang F, Chen Y, Ju LA. Platelet Mechanobiology Inspired Microdevices: From Hematological Function Tests to Disease and Drug Screening. 2022;12.

435. Jain A, Graveline A, Waterhouse A, Vernet A, Flaumenhaft R, Ingber DE. A shear gradient-activated microfluidic device for automated monitoring of whole blood haemostasis and platelet function. Nature communications. 2016;7:10176.
436. Zhang C, Neelamegham S. Application of microfluidic devices in studies of thrombosis and hemostasis. Platelets. 2017;28(5):434-40.
437. Zhao YC, Vatankhah P, Goh T, Michelis R, Kyanian K, Zhang Y, et al. Hemodynamic analysis for stenosis microfluidic model of thrombosis with refined computational fluid dynamics simulation. Sci Rep. 2021;11(1):6875.
438. Hu X, Chen H, Li J, Meng K, Wang Y, Li Y. A microfluidic bleeding model to investigate the effects of blood flow shear on microvascular hemostasis. Friction. 2022;10(1):128-41.

9.0 Appendix 1 – Canadian Blood Market research report calculations.

	2016	2017	2018
Total PLTs	12990	11921	12416
Discard PLTs due to expiry	2319	3182	1752
Percentage	18%	27%	14%

Table 9.1 **– PCs produced and discarded by expiry by WBS.** Data obtained from 2016-2018.

Cost of Platelets by NICE (UK)	
2014*	£ 278.90
2.4% inflation p/a**	
2018	£ 306.84
2018 Cost of outdate	£ 537,583.68

Table 9.2 **– Cost per PC.** Based on the NICE Guidelines for costing of PC in 2014* and inflation calculated from Bank of England**.

8-day Shelf Life (1 day Increase)	
Wastage 2018 corrected for 8 days *	1466
Percentage	12%
Cost of 8 Day outdates	£ 449,958
Saving p/a	£ 87,626

Table 9.3 **– Corrected Costs and Savings of extended Storage.** Based on using a 16.3% decrease to wastage for every additional day (417). Calculations were provided via a Canadian market research report by Dave Norman Consulting (report not available).

9-day Shelf Life (2-day Increase)	
Wastage 2018 corrected for 9 days *	1227
Percentage	10%
Cost of 9 Day outdates	£ 376,614
Saving p/a	£ 160,969

Table 9.4 **– Corrected Costs and Savings of extended Storage.** Based on using a 16.3% decrease to wastage for every additional day (417). Calculations were provided via a Canadian market research report by Dave Norman Consulting (report not available).

10-day Shelf Life (3-day Increase)	
Wastage 2018 corrected for 10 days *	1027
Percentage	8%
Cost of 10 Day outdates	£ 315,226
Saving p/a	£ 222,357

Table 9.5 **– Corrected Costs and Savings of extended Storage.** Based on using a 16.3% decrease to wastage for every additional day (417). Calculations were provided via a Canadian market research report by Dave Norman Consulting (report not available).